


8-2012

Risk Analysis and Reliability Improvement of Mechanistic-Empirical Pavement Design

Xingqiang Danny Xiao
University of Arkansas, Fayetteville

Follow this and additional works at: <http://scholarworks.uark.edu/etd>

 Part of the [Civil Engineering Commons](#), and the [Transportation Engineering Commons](#)

Recommended Citation

Xiao, Xingqiang Danny, "Risk Analysis and Reliability Improvement of Mechanistic-Empirical Pavement Design" (2012). *Theses and Dissertations*. 536.
<http://scholarworks.uark.edu/etd/536>

This Dissertation is brought to you for free and open access by ScholarWorks@UARK. It has been accepted for inclusion in Theses and Dissertations by an authorized administrator of ScholarWorks@UARK. For more information, please contact scholar@uark.edu, ccmiddle@uark.edu.

RISK ANALYSIS AND RELIABILITY IMPROVEMENT OF MECHANISTIC-EMPIRICAL
PAVEMENT DESIGN

RISK ANALYSIS AND RELIABILITY IMPROVEMENT OF MECHANISTIC-EMPIRICAL
PAVEMENT DESIGN

A dissertation submitted in partial fulfillment
of the requirements for the degree of
Doctor of Philosophy in Engineering

By

Xingqiang Danny Xiao
Southwest Petroleum University
Bachelor of Science in Civil Engineering, 2004
Southwest Jiaotong University
Master of Science in Civil Engineering, 2007

August 2012
University of Arkansas

ABSTRACT

Reliability used in the Mechanistic Empirical Pavement Design Guide (MEPDG) is a congregated indicator defined as the probability that each of the key distress types and smoothness will be less than a selected critical level over the design period. For such a complex system as the MEPDG which does not have closed-form design equations, classic reliability methods are not applicable. A robust reliability analysis can rely on Monte Carlo Simulation (MCS). The ultimate goal of this study was to improve the reliability model of the MEPDG using surrogate modeling techniques and Monte Carlo simulation.

To achieve this goal, four tasks were accomplished in this research. First, local calibration using 38 pavement sections was completed to reduce the system bias and dispersion of the nationally calibrated MEPDG. Second, uncertainty and risk in the MEPDG were identified using Hierarchical Holographic Modeling (HHM). To determine the critical factors affecting pavement performance, this study applied not only the traditional sensitivity analysis method but also the risk assessment method using the Analytic Hierarchy Process (AHP). Third, response surface models were built to provide a rapid solution of distress prediction for alligator cracking, rutting and smoothness. Fourth, a new reliability model based on Monte Carlo Simulation was proposed. Using surrogate models, 10,000 Monte Carlo simulations were calculated in minutes to develop the output ensemble, on which the predicted distresses at any reliability level were readily available. The method including all data and algorithms was packed in a user friendly software tool named *ReliME*.

Comparison between the AASHTO 1993 Guide, the MEPDG and *ReliME* was presented in three case studies. It was found that the smoothness model in MEPDG had an extremely high level of variation. The product from this study was a consistent reliability model specific to local

conditions, construction practices and specifications. This framework also presented the feasibility of adopting Monte Carlo Simulation for reliability analysis in future mechanistic empirical pavement design software.

This dissertation is approved for recommendation
to the Graduate Council.

Dissertation Director:

Dr. Kevin D. Hall

Dissertation Committee:

Dr. Edward A. Pohl

Dr. Kelvin C.P. Wang

Dr. Stacy G. Williams

Dr. Robert P. Elliott

DISSERTATION DUPLICATION RELEASE

I hereby authorize the University of Arkansas Libraries to duplicate this dissertation when needed for research and/or scholarship.

Agreed _____
Xingqiang Danny Xiao

Refused _____
Xingqiang Danny Xiao

ACKNOWLEDGEMENTS

First and foremost, I am in debt for my advisor, Dr. Kevin D. Hall, for his motivation and guidance in helping me complete this dissertation. Without his leadership and patience, this study could not be completed. Special appreciation also belongs to Dr. Kelvin C.P. Wang, whose advice and constructive criticism are helpful during the period of this research. Besides technical knowledge, their engineering professionalism, passion and vision set two models for me to follow.

My thanks also go to Dr. Ed Pohl, Dr. Stacy Williams and Dr. Robert Elliott for serving on my dissertation committee. Especially I appreciate for Dr. Pohl, who introduced me the new field of Reliability Engineering. Other faculties and staff at the Department of Civil Engineering are appreciated as well. They are all wonderful people to follow and work with.

I would like to express my appreciation to Dr. Qiang Li, Dr. Vu Nguyen, Daniel Byram and Alan Nguyen for their wonderful collaboration, advice and friendship.

The friendship with Dr. Jennifer Retherford at Vanderbilt University should also be acknowledged. It has been a great experience to work with Jenny in a competitive and collaborative way to solve such a difficult topic using different methods.

I am grateful for the Arkansas State Highway and Transportation Department, whose support made this research possible. The internship at the Department was a pleasant learning experience thanks to the advice and encouragement from Elisha Wright-Kehner, Mark Evans, Jacqueline Hou, Alan Meadors, Sarah Tamayo, Mark Greenwood and Jared Wiley.

Special thanks are also given to Dr. Yanjun Qiu at Southwest Jiaotong University and Dr. Xingzheng Xiao at Sichuan University of Science and Engineering for their motivation and guidance.

I would like to thank my friends here and abroad for their friendship, encouragement and help in my daily life. Special appreciation belongs to Mr. Bill Moeller for his kindness and graciousness which gave hundreds of foreign students, including me, an easier settledown and transition to this new lovely community.

I am also in debt to my father and mother, who advocate the importance of education, admire knowledge, and support selflessly with all they have.

Last but not the least, I would like to thank my precious wife Tian Zuo for her sacrifice of a good career and her willingness to hold my hands on this rough road, to share joy and tears, to support the family both morally and materially, and to raise our lovely daughter Zoe L. Xiao.

DEDICATION

Love is patient, love is kind. It does not envy, it does not boast, it is not proud. It is not rude, it is not self-seeking, it is not easily angered, it keeps no record of wrongs. Love does not delight in evil but rejoices with the truth. It always protects, always trusts, always hopes, always perseveres.

Love never fails.

(1 Corinthians 13: 4-8)

TABLE OF CONTENTS

CHAPTER 1	INTRODUCTION.....	1
1.1	Background	1
1.2	Problem Statement	4
1.3	Research Objectives	5
1.4	Dissertation Organization.....	6
CHAPTER 2	LITERATURE REVIEW.....	8
2.1	Pavement Design Approaches.....	8
2.1.1	Empirical Methods.....	8
2.1.2	Mechanistic-Empirical Methods.....	10
2.1.3	The Mechanistic-Empirical Pavement Design Guide (MEPDG).....	11
2.2	Evolution of Reliability in Pavement Design.....	17
2.2.1	AASHTO 1986	17
2.2.2	AASHTO 1993	17
2.2.3	MEPDG 2002.....	25
2.3	Risk and Uncertainty in Pavement Design.....	31
2.3.1	Terminology.....	32
2.3.2	Uncertainty Taxonomy	33
2.3.3	Uncertainty Quantification.....	35
2.4	Reliability Analysis Methods.....	39
2.4.1	Factors of Safety	39
2.4.2	Reliability Index.....	41
2.4.3	Propagation of Uncertainty.....	42
2.4.4	Monte Carlo Simulation (MCS).....	43
2.5	Summary	47
CHAPTER 3	LOCAL CALIBRATION	48
3.1	Introduction	48
3.2	Methodology	50
3.3	Data Collection.....	53
3.3.1	Structure and Materials.....	55

3.3.2	Traffic	57
3.3.3	Performance	58
3.4	Verification and Calibration.....	63
3.4.1	Hierarchical Input	63
3.4.2	Alligator Cracking	65
3.4.3	Rutting.....	70
3.4.4	Longitudinal Cracking	75
3.4.5	Transverse Cracking	75
3.4.6	Smoothness (IRI)	77
3.5	Validation.....	77
3.6	Summary	78
CHAPTER 4	RISK ANALYSIS	80
4.1	Introduction	80
4.2	Risk Identification	86
4.3	Risk Assessment.....	97
4.4	Summary	107
CHAPTER 5	RISK MODELING	109
5.1	Introduction	109
5.1.1	NCHRP1-37A (Neural Network)	110
5.1.2	Response Surface Method.....	114
5.2	Design of Experiment.....	117
5.2.1	Global Pavement Structure	117
5.2.2	Importance Ranking.....	128
5.2.3	Screening of Climate Location	130
5.2.4	Screening of Operational Speed.....	135
5.2.5	Examples of Experimental Design.....	137
5.3	Model construction.....	144
5.3.1	Parameters Preparation	144
5.3.2	Outlier Test	150
5.3.3	Regression Analysis.....	158
5.4	Validation and Sensitivity Analysis	163

5.5	Summary	170
CHAPTER 6 RELIABILITY IMPROVEMENT.....		172
6.1	Introduction	172
6.2	Monte Carlo Simulation.....	173
6.2.1	Generation of Random Numbers	174
6.2.2	Simulation Numbers	179
6.2.3	Determine the Reliability.....	182
6.3	Development of <i>ReliME</i>	185
6.3.1	Procedures.....	186
6.3.2	Software Coding	188
6.3.3	Software Test	191
6.4	Case Studies	193
6.4.1	Bella Vista Bypass	195
6.4.2	Pleasant Plains Bypass.....	203
6.4.3	Sheridan Bypass.....	212
6.5	Summary	219
CHAPTER 7 CONCLUSIONS AND RECOMMENDATIONS		221
7.1	Conclusions	221
7.2	Recommendations	223
7.3	Byproducts	226
7.3.1	Distress Classification.....	226
7.3.2	Arkansas' Long Term Pavement Performance Program	227
7.3.3	Accuracy Requirement for Thickness Estimation	227
7.3.4	Integration of Pavement Management and Design.....	229
REFERENCES		232
Appendix A Screenshot of the AHP Pairwise Comparison Survey Sheet.....		241
Appendix B Overall Ranking of All Factors Influencing Flexible Pavement Design.....		246
Appendix C Design of Experiment for Importance Ranking		249
Appendix D Central Composite Design (CCD) for Model Construction.....		254
Appendix E Design of Experiment for Model Construction: Random Selection.....		264
Appendix F Design of Experiment for Model Validation		268

LIST OF FIGURES

Figure 1.1 Procedure of mechanistic-empirical pavement design (5)	2
Figure 2.1 Concept of mechanistic-empirical pavement design (9)	11
Figure 2.2 Definition of reliability and evaluation of reliability design factor F_R (7)	20
Figure 2.3 Screenshot of the AASHTOWare DARWin [®] (credit of Trinity Smith)	23
Figure 2.4 Screenshot of the 1993 Design Guide being embedded into a spreadsheet (credit of Kevin D. Hall).....	24
Figure 2.5 Reliability concept in MEPDG (IRI) (5)	26
Figure 2.6 Screenshot of input reliability in MEPDG	27
Figure 2.7 Nationally calibrated predicted versus estimated measured asphalt rutting (14)	28
Figure 2.8 Predict standard error for AC rutting (14).....	30
Figure 2.9 Uncertainty in a pavement's life-cycle.....	32
Figure 2.10 Relationship between capacity and demand (33)	41
Figure 2.11 The three actors in the development of the Monte Carlo method: (a) John von Neumann (1903-1957), (b) Stanislaw Ulam (1909-1984), and (c) Nicholas Metropolis (1915-1999) (source: National Air and Space Museum and Los Alamos National Laboratory)	44
Figure 2.12 Incorporation of variation in <i>PerRoad</i>	46
Figure 3.1 LTPP sites for new flexible pavement calibration in MEPDG (13).....	48
Figure 3.2 Concept of MEPDG calibration (adapted from FHWA).....	49
Figure 3.3 Steps of local calibration (adjusted from (16)).....	51
Figure 3.4 Pavement sections used to calibrate new flexible pavement models in Arkansas.	55
Figure 3.5 Measured alligator cracking	60
Figure 3.6 Measured longitudinal cracking	60
Figure 3.7 Measured transverse cracking	61
Figure 3.8 Measured total rutting.....	62
Figure 3.9 Measured IRI.....	62
Figure 3.10 Verification of the alligator cracking model	66
Figure 3.11 Calibrated alligator cracking	67
Figure 3.12 Manual distress survey record of the R80065 Good section (2009).	69

Figure 3.13 Verification of rutting model.....	71
Figure 3.14 Composition of total rutting (AC).....	72
Figure 3.15 Composition of total rutting (Base).....	72
Figure 3.16 Composition of total rutting (Subgrade).....	73
Figure 3.17 Calibration of rutting model.....	74
Figure 3.18 Verification of national calibrated longitudinal cracking model.....	75
Figure 3.19 Verification of national calibrated longitudinal cracking model.....	76
Figure 3.20 Verification of national calibrated IRI model.....	77
Figure 3.21 Validation of calibrated (a) alligator cracking and (b) rutting models.....	78
Figure 4.1 Perspectives to Analyze Flexible Pavement Design.....	90
Figure 4.2 Flexible Pavement Design in the Perspective of Different People.....	91
Figure 4.3 Flexible Pavement Design in Temporal Perspective.....	92
Figure 4.4 Flexible Pavement Design in the Perspective of Components.....	93
Figure 4.5 Flexible Pavement Design in the Perspective of Cost Allocation.....	94
Figure 4.6 Flexible Pavement Design using MEPDG Version 1.1 Software.....	95
Figure 4.7 Flexible Pavement Design using General Mechanistic Empirical Methods.....	96
Figure 4.8 A screenshot of the AHP pairwise comparison survey sheet (Level 2).....	99
Figure 4.9 Importance ranking of Level 2 factors.....	100
Figure 4.10 Top 15 Factors Influencing Flexible Pavement Design.....	101
Figure 5.1 Steps to build a surrogate model.....	110
Figure 5.2 Flowchart of Neural Network development for JPCP in NCHRP1-37A.....	111
Figure 5.3 A three-dimensional response surface showing the expected yield (η) as a function of temperature (x_1) and pressure (x_2) (75).....	115
Figure 5.4 Concept of the response surface method for MEPDG.....	116
Figure 5.5 The global structure and factors considered in this study.....	118
Figure 5.6 Vehicle class distribution.....	122
Figure 5.7 Hourly distribution.....	122
Figure 5.8 Single axle load spectra for Class 9 vehicle.....	126
Figure 5.9 Tandem axle load spectra for Class 9 vehicle.....	126
Figure 5.10 Tandem axle load spectra for Class 7 vehicle.....	127
Figure 5.11 Tandem axle load spectra for Class 10 vehicle.....	127

Figure 5.12 Results of screening analysis.....	129
Figure 5.13 Map of Arkansas sites (Google Maps 2011).....	130
Figure 5.14 Longitudinal cracking predicted for Arkansas sites.....	131
Figure 5.15 Alligator cracking predicted for Arkansas sites.....	132
Figure 5.16 Total rutting predicted for Arkansas sites.....	132
Figure 5.17 IRI predicted for Arkansas sites.....	133
Figure 5.18 Normalized difference for Arkansas sites.....	134
Figure 5.19 Influence of speed on alligator cracking.....	136
Figure 5.20 Influence of speed on total rutting.....	136
Figure 5.21 Influence of speed on IRI.....	137
Figure 5.22 (a) Full factorial design; (b) Box-Behnken design.....	139
Figure 5.23 Central composite design (a) faced, (b) circumscribed.....	140
Figure 5.24 Example of random and Latin Hypercube sampling.....	143
Figure 5.25 Traffic levels considered in the experimental design.....	144
Figure 5.26 Relationship between initial AADTT and ESALs.....	147
Figure 5.27 Growth ratio of ESALs.....	149
Figure 5.28 An example of predicting time series ESALs using AADTT.....	149
Figure 5.29 Box plot of alligator cracking (a) before and (b) after outliers are removed.....	152
Figure 5.30 Alligator cracking (a) before and (b) after outliers are excluded.....	153
Figure 5.31 Box plot of rutting shows possible outliers.....	154
Figure 5.32 Total rutting (a) before and (b) after outliers are excluded.....	155
Figure 5.33 Box plot of IRI shows (a) before and (b) after outliers are removed.....	156
Figure 5.34 IRI (a) before and (b) after outliers are excluded.....	157
Figure 5.35 Response surface models for: (a) $\text{Log}N_f$, (b) alligator cracking, (c) total rutting, and (d) IRI.....	161
Figure 5.36 Validation of response surface models: (a) $\text{Log}N_f$, (b) alligator cracking, (c) total rutting, and (d) IRI.....	164
Figure 5.37 Sensitivity analysis of AADTT and AC thickness (3D mesh plot).....	165
Figure 5.38 Sensitivity analysis of AADTT and AC thickness (contour plot).....	166
Figure 5.39 Sensitivity analysis VFA and base thickness (3D mesh plot).....	167
Figure 5.40 Sensitivity analysis of VFA and base thickness (contour plot).....	168

Figure 5.41 Sensitivity analysis of resilient modulus of base and subgrade (mesh plot)	169
Figure 5.42 Sensitivity analysis of resilient modulus of base and subgrade (contour plot)	170
Figure 6.1 Flowchart of the proposed reliability improvement procedure	172
Figure 6.2 Determination of random number x with desired distribution from uniformly distributed random number r . (88).....	175
Figure 6.3 Histogram of generated random samples	177
Figure 6.4 Histogram of generated random samples (covariance=0.49).....	178
Figure 6.5 Histogram of generated random samples (covariance=0.30).....	179
Figure 6.6 Test of simulation numbers ($h_{ac}=11''$)	181
Figure 6.7 Test of simulation numbers ($h_{ac}=8''$)	181
Figure 6.8 Example of estimating the reliability level in a histogram plot.....	184
Figure 6.9 Example of estimating the reliability level in a CDF plot.....	184
Figure 6.10 Steps to develop <i>ReliME</i>	186
Figure 6.11 Screenshot of <i>ReliME-AR</i>	188
Figure 6.12 Example of estimating the reliability level.....	189
Figure 6.13 Screenshot of <i>ReliME</i> with COV=1	192
Figure 6.14 Verification of <i>ReliME</i> using 100 random samples: (a) alligator cracking, (b) total rutting, and (c) IRI.	193
Figure 6.15 Location of Bella Vista Bypass	197
Figure 6.16 Recommended pavement structures	199
Figure 6.17 Reliability of alligator cracking for Bella Vista Bypass.....	201
Figure 6.18 Reliability of total rutting for Bella Vista Bypass	202
Figure 6.19 Reliability of IRI for Bella Vista Bypass	203
Figure 6.20 Location of Job R50084	204
Figure 6.21 Aerial map of Pleasant Plains by Google Earth (a) 1994, (b) 2001	204
Figure 6.22 ROW of R50084 when first constructed in 2001	205
Figure 6.23 ROW of R50084 in April 2010	205
Figure 6.24 ROW of R50084 after resurfacing in September 2010	206
Figure 6.25 Measured and predicted ADT of R50084	207
Figure 6.26 Truck percentage of AADTT of R50084	207
Figure 6.27 Recommended pavement structures for job R50084.....	209

Figure 6.28 Reliability of alligator cracking for Pleasant Plain Bypass	210
Figure 6.29 Reliability of total rutting for Pleasant Plain Bypass	211
Figure 6.30 Reliability of IRI for Pleasant Plain Bypass	211
Figure 6.31 Location of the Sheridan Bypass	213
Figure 6.32 Truck classification of station 270017 for Job 020464.	215
Figure 6.33 Proposed pavement structure by AASHTO 1993 and MEPDG (not to scale).	216
Figure 6.34 Reliability of alligator cracking for Sheridan Bypass	217
Figure 6.35 Reliability of total rutting for Sheridan Bypass.....	218
Figure 6.36 Reliability of IRI for Sheridan Bypass	218
Figure 7.1 Integration of management and design.....	230

LIST OF TABLES

Table 2.1 Reliability level in AASHTO 1993 (7).....	18
Table 2.2 Variables and variability estimates (7)	22
Table 2.3 Reliability level in MEPDG (13)	26
Table 2.4 Definition of groups for AC rutting data (14).....	29
Table 2.5 Variation of materials (15).....	35
Table 2.6 Variation of modulus and thickness used in <i>PerRoad</i>	36
Table 2.7 Variation of concrete materials (22)	37
Table 2.8 Variation of traffic (15).....	37
Table 3.1 Recommended calibration coefficients to be adjusted for flexible pavement (16)	52
Table 3.2 Experimental Matrix	54
Table 3.3 Pavement structure of calibration sections	56
Table 3.4 Traffic data of calibration sites	57
Table 3.5 Summary of Measured Distress	59
Table 3.6 Input levels used in this study.....	63
Table 3.7 Summary of paired Z-Test for alligator cracking model	68
Table 3.8 Summary of z-Test for rutting models.....	74
Table 3.9 Summary of calibration coefficients.....	79
Table 4.1 Ranking of new HMA design inputs (reprint of Table 5.1 in (64)).....	85
Table 4.2 Qualitative and quantitative guidelines for pairwise comparison (52).....	98
Table 4.3 Pairwise comparison of Level 2 categories	99
Table 4.4 Statistics of pairwise comparison of Level 2 categories.....	100
Table 4.5 Critical factors of MEPDG from literature.....	103
Table 4.6 Top 15 factors of MEPDG from this study and NCHRP 1-47	104
Table 4.7 Risk assessment of the top 10 parameters	105
Table 4.8 Risk matrix of traffic.....	106
Table 5.1 Number of simulations to develop neural networks for rigid pavement design in NCHRP1-37A.....	113
Table 5.2 Experimental design for initial interests	119
Table 5.3 Gradations for asphalt mixture	120

Table 5.4 Input for deterministic variables	121
Table 5.5 Statewide Single Axle Load Spectra (78).....	123
Table 5.6 Statewide Tandem Axle Load Spectra (78).....	124
Table 5.7 Statewide Tridem Axle Load Spectra (78)	125
Table 5.8 Results (Lenth's <i>t</i> -ratio) of influence ranking.....	129
Table 5.9 Matrix of MEPDG simulations.....	138
Table 5.10 Example of experimental design for three factors with three levels.....	141
Table 5.11 Viscosity parameters for binders	145
Table 5.12 Model Coefficients for Alligator Cracking.....	160
Table 5.13 Model Coefficients for Total Rutting	162
Table 5.14 Model Coefficients for Smoothness (IRI)	162
Table 6.1 Example of variable distributions	176
Table 6.2 Coefficient of variance simulated in <i>ReliME</i>	195
Table 6.3 Inputs for flexible pavement design.....	198
Table 6.4 Inputs for MEPDG analysis	199
Table 6.5 Inputs for flexible pavement design.....	208
Table 6.6 Inputs for MEPDG analysis	209
Table 6.7 Main Design Information for Job 020464	212
Table 6.8 Mix Design for Job 020464	214
Table 6.9 Summary of Variance Comparison.....	220
Table 7.1 Summary of Findings/Observations for layer thickness accuracy requirement	229

LIST OF ABBREVIATIONS

AADT	Annual Average Daily Traffic
AADTT	Annual Average Daily Truck Traffic
AASHO	American Association of State Highway Officials
AASHTO	American Association of State Highway and Transportation Officials
ADT	Annual Daily Traffic
AHP	Analytic Hierarchy Process
AHTD	Arkansas State Highway and Transportation Department
ATB	Asphalt Treated Base
BVB	Bella Vista Bypass
Caltrans	California Department of Transportation
CCD	Central Composite Design
COV	Coefficient of Variation
CRCP	Continuous Reinforced Concrete Pavement
CTB	Cement Treated Base
CTE	Coefficient of Thermal Expansion
DARWin	Pavement Design, Analysis and Rehabilitation for Windows
DARWin-ME	Mechanistic-Empirical based Pavement Design, Analysis and Rehabilitation for Windows
DCP	Dynamic Cone Penetrometer
DOT	Department of Transportation
EICM	Enhanced Integrated Climate Model
ENIAC	Electronic Numerical Integrator And Computer
ESAL	Equivalent Single Axle Load
FC	Fatigue cracking
FHWA	Federal Highway Administration
FOSM	First Order Second Moment
FS	Factor of Safety
FWD	Falling Weight Deflectometer
GPR	Ground Penetrating Radar
GPS	General Pavement Studies (in LTPP)
GPS	Global Positioning System
HHM	Hierarchical Holographic Modeling
HMA	Hot Mixed Asphalt
IRI	International Roughness Index
JPCP	Jointed Plain Concrete Pavement
JULEA	Jacob Uzan Layered Elastic Analysis
LANL	Los Alamos National Laboratory
LCCA	Life-Cycle Cost Analysis

LTPP	Long-Term Pavement Performance
MAAT	Mean Annual Air Temperature
MATLAB	Matrix Laboratory
MBTC	Mark-Blackwell Rural Transportation Center
MCS	Monte Carlo Simulation
MEPDG	Mechanistic Empirical Pavement Design Guide
NCAT	National Center for Asphalt Technology
NCHRP	National Cooperative Highway Research Program
NDT	Nondestructive Testing
NN	Neural Network
PATB	Permeable Asphalt Treated Base
PCC	Portland Cement Concrete
PEM	Point Estimate Method
PG	Performance Grade
PMS	Pavement Management System
PSI	Pavement Serviceability Index
ROW	Right of Way
RSM	Response Surface Methodology
SHA	State Highway Agency
SHRP	Strategic Highway Research Program
SN	Structural Number
SPS	Specific Pavement Studies
SSE	Sum of Standard Error
TRB	Transportation Research Board
TRC	Transportation Research Committee
TTC	Truck Traffic Classification
TWLTL	Two Way Left Turn Lane
UofA	University of Arkansas
USGS	United States Geological Survey
VFA	Voids Filled with Asphalt
VMA	Voids between Mineral Aggregates
WIM	Weigh-In-Motion
WSDOT	Washington State Department of Transportation

CHAPTER 1 INTRODUCTION

1.1 Background

Mechanistic-Empirical pavement design is being widely used and implemented by many highway agencies around the world (1) (2) (3) (4). For one reason, the traditional empirical design method can only be safely used for locations that have similar subgrade, traffic, climate and materials as the sites where the empirical tests were conducted. The application of empirical design method is limited, because any extrapolation from the testing sites may produce systematic error. For the other reason, mechanistic pavement design is limited that only maximum pavement responses (i.e. stress, strain and deflection) are predicted. Since pavement is evaluated by performance such as smoothness, rideability, distresses and rutting, pavement responses alone are implicit to understand not only for end users but also for engineers. Mechanistic-empirical design method fills the gap.

Mechanistic-empirical pavement design is composed of three stages, shown in Figure 1.1. First, a trial structure is proposed and the corresponding design parameters including traffic, climate and material properties are input into a mechanistic model, which analyzes structural responses of the trial design. This is the mechanistic part. The second step is predicting the performance of the trial design using transfer functions, which convert stress and strain into distresses such as cracking, rutting and smoothness. If the performance passes the design criteria, the trial design is considered to be appropriate; otherwise, it is modified, and step 1 and step 2 are repeated until the predicted performance fulfills the requirements. This is the empirical part because transfer functions are empirical relationships developed using historical measurements of different pavements. Finally, more trial designs are proposed so that the best strategy could be selected based on life cycle cost analysis and other considerations.

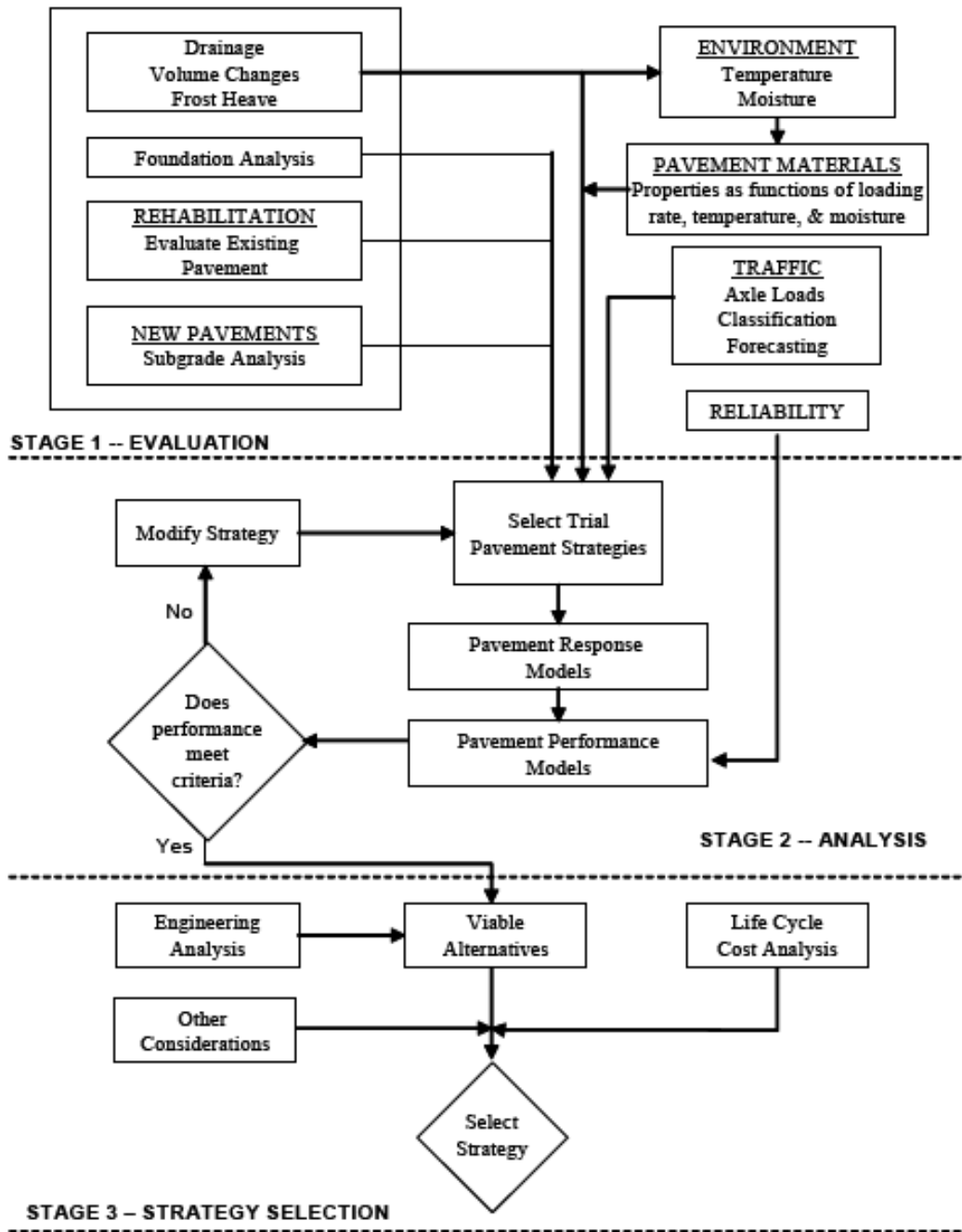


Figure 1.1 Procedure of mechanistic-empirical pavement design (5)

The Mechanistic-Empirical Design Guide for New and Rehabilitated Pavement

Structures (5), known as the MEPDG, was released in 2004 under the NCHRP Project 1-37A.

MEPDG is the latest mechanistic empirical pavement design method which incorporates the

latest researches in traffic, material, climate, structural analysis, and other related areas. MEPDG provides significant potential benefits over empirical methods. The current MEPDG has been calibrated using data from the Long Term Pavement Performance (LTPP) program, which contains pavement sections located throughout United States and Canada. By matching predicted pavement performances from the new design procedure with measured pavement performances in field, MEPDG is validated, modified and, therefore, reliable for routine use. However, national calibration could not cover all conditions of local roads. Local calibration is therefore recommended to reduce potential bias and variation of national calibrated models.

There is no doubt that variability is a nature of fact for input parameters in pavement design. For instance, the material property tested in laboratory is only a nominal value representing the overall property. That is, materials paved on road may vary from the representative value in the design. The extent of variation is assumed to be curbed by specifications and quality control. Furthermore, it is well understood that layer thickness is different between as-designed and as-constructed. The difference may be reduced as much as possible by good construction equipment, appropriate techniques, quality control and quality assurance. Apparently these uncertainties should be considered in the design process. This is called a probability-based design.

Reliability was first introduced to pavement design in the AASHTO 1986 Guide, which added two new variables into the design equation: standard deviate Z_R and standard error S_θ . This concept was continuously adopted in the AASHTO 1993 Guide and the MEPDG. In general, it was a congregated definition that contains all sources of uncertainty. It was assumed that the difference between the predicted and the measured pavement performance came from all uncertainties.

1.2 Problem Statement

Ideally, the ultimate goal of engineering modeling is to be able to predict the same performance as measured in field. With such an accurate model, cost-effective designs would be achievable. However, the following limitations and challenges were identified in current mechanistic-empirical pavement design methods.

First, the current MEPDG was calibrated using national wide data from the LTPP program. Because of the difference between national conditions and local conditions such as climate, material properties, traffic patterns, construction and management techniques, bias may exist in those models. Moreover, the diversity of materials and construction specifications in a whole nation may lead to a larger variation than a local agency does. Therefore, MEPDG needs to be validated and calibrated for local conditions.

Second, the reliability approach incorporated in the current MEPDG is a simplified method comparing to other reliability methods such as the Monte Carlo Simulation (MCS). The congregated definition of reliability is based on the assumption that the difference between the predicted and the measured performance is a result of all variations and uncertainties. Hence, this approach is not able to show the impact of variation in each variable. For example, inputs in Level 1 uses the same reliability model with them in Level 3, although the hierarchal input assumes that Level 1 would have lower level of uncertainty than Level 3 (5). Meanwhile, this approach does not account for the effect of design input variability on the design reliability, which could be accomplished easily by using Monte Carlo simulation (6).

Third, comparing to old design methods, MEPDG is a complicated procedure that hundreds of inputs are required to run a simulation. Not only are the tests and procedures to collect these data difficult, but also the preparation and quality control of these data are not an

easy work. Furthermore, MEPDG is not an explicit mathematic equation but a combination of models and equations. This makes the application of traditional reliability methods such as First Order Second Moment (FOSM) and Rosenbluth on MEPDG a big challenge, if not impossible.

Fourth, MEPDG takes a lot of computing time and resource, especially for flexible pavement designs. In fact, reliability analysis based on MCS was successfully combined with MEPDG rigid pavement distress models. But the application in flexible pavements was considered to be computationally demanding, and therefore, the current reliability approach was adopted in MEPDG (6). Darter et al. (6) recommended that

Therefore, it is important to improve the computational efficiency of the flexible design and implement the MC-based reliability analysis in future versions of the M-E PDG. Local calibration of the models is one way to improve on the estimate of error of the models for use in a local area (e.g., within a state or given climatic region of a state).

1.3 Research Objectives

The ultimate goal of this dissertation is to improve the reliability model of MEPDG. A robust reliability analysis can rely on Monte Carlo Simulation (MCS). The hinder of computation time for MCS is eliminated by developing surrogate models of MEPDG to represent the comprehensive modeling capability in a computing efficient manner. In detail, objectives of this dissertation include:

- To reduce bias and variation of national-calibrated models by local calibration.
- To identify risks and uncertainties in mechanistic-empirical pavement design methods.
- To develop surrogate models of performance prediction models.

- To propose a new procedure for reliability analysis in MEPDG based on Monte Carlo simulation.

1.4 Dissertation Organization

This chapter is the introduction that states the problem and objectives of this study.

Chapter 2 documents the literature review on the topic pertinent to this dissertation, such as pavement design approaches, risk and uncertainty in pavement, evaluation of reliability in pavement design methods, and some common reliability analysis methods.

Chapter 3 is to reduce the possible bias and variation of the nationally calibrated models through local calibration. The concept, data source, calibration procedures, results and validation are discussed in detail.

Chapter 4 analyzes the mechanistic empirical pavement design method in a general scope using the risk assessment methods which are widely used in Reliability Engineering. Details of how the Hierarchical Holographic Modeling (HHM) method and the analytic hierarchy process (AHP) method are used in pavement are documented. The result from Chapter 4 is the most significant factors (derived from a new method different from sensitivity analysis) which should be included in surrogate models.

Chapter 5 develops all of the surrogate models that will be used in Chapter 6. Neural network and Response Surface Methodology (RSM) are introduced. Experiment design that reduces the simulations numbers is explained, followed by model construction and validation.

Chapter 6 addresses the proposed method which relies on Monte Carlo Simulation (MCS) and surrogate models to improve the reliability method in MEPDG. The process of developing a software tool named *ReliME* is presented in detail. Comparison of the existing method and the new method is presented, ending with three case studies of real world projects.

Chapter 7 summarizes the conclusions and recommendations from this study.

CHAPTER 2 LITERATURE REVIEW

2.1 Pavement Design Approaches

In general, pavement design approaches can be divided to two categories: empirical based methods and mechanistic-empirical based methods.

2.1.1 Empirical Methods

Many pavement design procedures have adopted an empirical approach. The relationships among design inputs, such as loads, materials, layer configurations and environment, and pavement failure were obtained through engineering experience, experimental observations, or a combination of both.

The *American Association of State Highway and Transportation Officials (AASHTO) Guide for Design of Pavement Structures (7)* was the primary document used to design new and rehabilitated highway pavements in the United States today. The Federal Highway Administration's (FHWA) 1995-1997 National Pavement Design Review found that more than 80% of states use the 1972, 1986, or 1993 AASHTO Guides (8). All versions of the AASHTO design guide were based on empirical models drawn from field performance data measured at the AASHO road test in the late 1950s located at Ottawa, Illinois, about 80 miles southwest of Chicago, along with some theoretical support for layer coefficients and drainage factors. The overall serviceability of the pavement was quantified by the present serviceability index (*PSI*), a composite performance measure combining cracking, patching, rutting, and other distresses. Roughness was the dominant factor governing *PSI* and was therefore the principal component of the pavement performance.

Empirical pavement design methods literally were all based on empirical equations derived from historical data. For example, equation 2.1 and 2.3 are the equations for flexible and rigid pavement design in the *AASHTO 1993 Guide*, respectively.

$$\log_{10}(W_{18}) = Z_R \times S_0 + 9.36 \times \log_{10}(SN + 1) - 0.20 + \frac{\log_{10}\left(\frac{\Delta PSI}{4.2 - 1.5}\right)}{0.40 + \frac{1094}{(SN + 1)^{5.19}}} + 2.32 \times \log_{10}(M_R) - 8.07 \quad (2.1)$$

where: W_{18} = predicted traffic in the design life represented by the number of 18,000 lb Equivalent Single Axle Load (ESAL)

Z_R = standard normal deviate

S_0 = combined standard error of the traffic prediction and performance prediction

SN = structural number, and

$$SN = a_1 D_1 + a_2 D_2 m_2 + a_3 D_3 m_3 + \dots \quad (2.2)$$

a_i = layer coefficient of the i^{th} layer

D_i = thickness of the i^{th} layer

m_i = drainage coefficient of the i^{th} layer

ΔPSI = difference of the initial PSI and the terminal PSI

M_R = subgrade resilient modulus

$$\log_{10}(W_{18}) = Z_R \times S_0 + 7.35 \times \log_{10}(D + 1) - 0.06 + \frac{\log_{10}\left(\frac{\Delta PSI}{4.5 - 1.5}\right)}{1 + \frac{1.624 \times 10^7}{(D + 1)^{8.46}}} + (4.22 - 0.32 p_t) \times \log_{10} \left[\frac{(S'_c)(C_d)(D^{0.75} - 1.132)}{215.63(J) \left[D^{0.75} - \frac{18.42}{\left(\frac{E_c}{k}\right)^{0.25}} \right]} \right] \quad (2.3)$$

With closed-form equations, empirical methods can be easily adopted in routine pavement designs by using spreadsheet or design software. As long as design inputs are ready, the output (either SN or D in this example) can be solved in a fraction of seconds.

The various versions of the AASHTO guide had served the industry well, but had deficiencies due to some of the limitations of the AASHO Road Test (5):

- Today's traffic loads are much higher than they were six decades ago;
- Rehabilitated pavements were not monitored;
- Only one climatic condition and one subgrade type were included in the road test;
- Only one hot-mix asphalt and one PCC mixture were studied;
- Test pavements did not include drainage;
- Only 2 years of monitoring were conducted, rather than the entire pavement life of every section (some sections did, however, fail within 2 years).

2.1.2 Mechanistic-Empirical Methods

Right after the development of the *1986 AASHTO Design Guide*, the need to develop mechanistic pavement analysis and design procedures suitable for use in future versions of the AASHTO guide was initiated by AASHTO. NCHRP Project 1-26, *Calibrated Mechanistic Structural Analysis Procedures for Pavements*, was initiated to provide the basic framework for future development of a mechanistic-empirical pavement design method (9).

In a pavement design, the responses can be stresses, strains and deflections within a pavement structure, and the physical causes are loads (both environmental and traffic) and material properties. The relationships among these phenomena and their physical causes are typically described using mathematical models. Along with this mechanistic approach, empirical models are used when defining the relationships among the calculated stresses, strains and

deflections, and pavement failure. As a result, the number of loading cycles to failure is derived. This approach is called a mechanistic-empirical based design method, as shown in Figure 2.1.

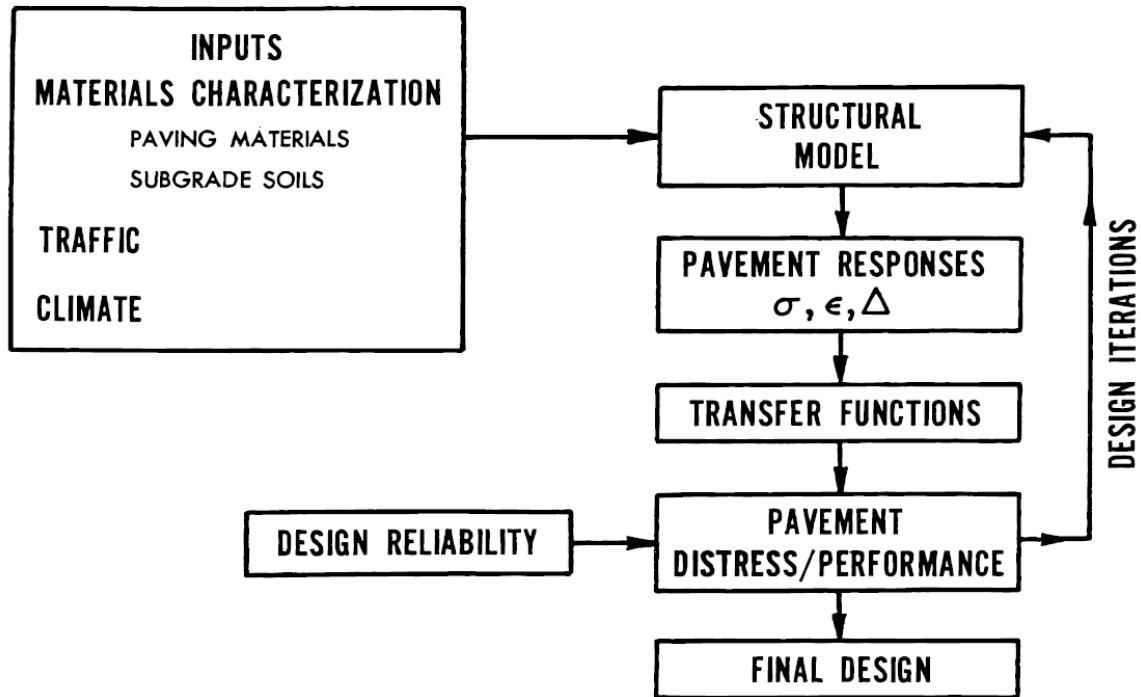


Figure 2.1 Concept of mechanistic-empirical pavement design (9)

Since NCHRP 1-26 was completed, several typical mechanistic-empirical based design approaches were developed, including the Illinois Department of Transportation Design Manual (10), the Washington State Department of Transportation (WSDOT) Pavement Guide (11), the MnPAVE computer program developed in Minnesota Department of Transportation (Mn/DOT) (12), and the MEPDG (13).

2.1.3 The Mechanistic-Empirical Pavement Design Guide (MEPDG)

The *Mechanistic-Empirical Design Guide for New and Rehabilitated Pavement Structures* (13), known as the MEPDG, was released in 2004 under the NCHRP Project 1-37A. MEPDG provided significant potential benefits over the *1993 AASHTO Guide*. This approach provided

more realistic characterization of in-service pavements and provided uniform guidelines for designing the in-common features of flexible, rigid, and composite pavements. It also offered procedures for evaluating existing pavements and recommendations for rehabilitation treatments, drainage, and foundation improvements. Most importantly, its computational software: (1) implemented an integrated analysis approach for predicting pavement condition over time (including fatigue, rutting, and thermal cracking in asphalt pavements, and cracking and faulting in concrete pavements) that accounted for the interaction of traffic, climate, and pavement structure; (2) allowed consideration of special loadings with multiple tires or axles; and (3) provided a means for evaluating design variability and reliability. MEPDG allowed pavement designers to make better informed decisions and to take cost-effective advantages of new materials and features. The software could also serve as a forensic tool for analyzing the condition of existing pavements and pinpointing deficiencies in past designs.

The main distress models in MEPDG are briefly explained here. Details on the assumptions, development procedures, and sensitivity analysis can be found in several MEPDG documents (13).

Rutting Model

The overall permanent deformation (total rutting) is the sum of permanent deformation for each individual layer and is mathematically expressed as:

$$RD = \sum_{i=1}^{nsublayers} \varepsilon_p^i h^i \quad (2. 4)$$

where RD = pavement total permanent deformation

$N_{sublayers}$ = number of sublayers

ε_p^i = total plastic strain in sublayer i

h^i = thickness of sublayer i.

The total rutting in asphalt mixture layers is given by

$$\frac{\varepsilon_p}{\varepsilon_r} = k_1 * 10^{-3.4488} T^{1.5606} N^{0.479244} \quad (2.5)$$

where ε_p = accumulated plastic strain at N repetitions of load (in/in)

ε_r = resilient strain of the asphalt material as a function of mix properties, temperature and time rate of loading (in/in)

N = number of load repetitions

T = temperature (degree F)

K_I = a depth parameter to correct for the confining pressure at different depths

$$k_1 = (C_1 + C_2 * depth) * 0.328196^{depth} \quad (2.6)$$

$$C_1 = -0.1039 * h_{ac}^2 + 2.4868 * h_{ac} - 17.342 \quad (2.7)$$

$$C_2 = 0.0172 * h_{ac}^2 - 1.7331 * h_{ac} + 27.428 \quad (2.8)$$

where h_{ac} = the total AC thickness (in)

The model statistics are

$$R^2 = 0.644$$

$$N = 3476 \text{ observations}$$

$$Se = 0.321$$

$$Se/Sy = 0.597$$

The rutting for unbound layers (including base and subgrade) is:

$$\delta_a(N) = \beta_1 \left(\frac{\varepsilon_0}{\varepsilon_r} \right) e^{-\left(\frac{\rho}{N}\right)^\beta} \varepsilon_v h \quad (2.9)$$

where δ_a = permanent deformation for the layer/sublayer (in)

N = number of traffic repetitions

ε_0 , β , and ρ = material properties

ε_r = resilient strain imposed in laboratory test to obtain the above listed material properties (in/in)

ε_v = average vertical resilient strain in the layer/sublayer as obtained from the primary response model (in/in)

h = thickness of the layer/sublayer (in)

β_1 = calibration factor

Fatigue Cracking Model

Miner's Law is utilized in MEPGD to predict fatigue cracking.

$$D = \sum_{i=1}^T \frac{n_i}{N_i} \quad (2.10)$$

where D = damage

T = total number of periods

n_i = actual traffic period i

N_i = traffic allowed under conditions prevailing in i .

Fatigue cracking in asphalt mixtures in MEPGD includes bottom-up alligator cracking and top-down longitudinal cracking. The both have a common basic structure which is a function of the tensile strain and asphalt mixture strength. The final model built in MEPGD is

$$N_f = 0.00432C \left(\frac{1}{\varepsilon_t} \right)^{3.291} \left(\frac{1}{E} \right)^{0.854}$$

$$C = 10^M$$

$$M = 4.84 \left(\frac{V_b}{V_a + V_b} - 0.69 \right) \quad (2.11)$$

where N_f = number of repetitions to fatigue cracking

ε_t = tensile strain at the critical location

E = stiffness of the material

C = laboratory to field adjustment factor

V_b = effective binder content (%)

V_a = air voids (%)

After damage is obtained, transfer functions are applied to convert damage to visible distresses such as bottom-up alligator cracking and top-down longitudinal cracking.

$$F.C.bottom_up = \left(\frac{6000}{1 + e^{(C_1 * C_1' + C_2 * C_2' * \log_{10}(D * 100))}} \right) * \left(\frac{1}{60} \right) \quad (2.12)$$

where D = bottom-up damage

$$C_1 = 1.0$$

$$C_2 = 1.0$$

$$C_2' = -2.40874 - 39.748 * (1 + h_{ac}) - 2.856$$

$$C_1' = -2 * C_2'$$

h_{ac} = AC thickness

The statistics for bottom-up cracking model are

$$N = 461 \text{ observations}$$

$$Se = 6.2\%$$

$$Se/Sy = 0.947$$

Top-down (longitudinal) cracking is given by:

$$F.C.top_down = \left(\frac{1000}{1 + e^{(C_1 - C_2 * \log D)}} \right) * (10.56) \quad (2.13)$$

where D = top-down damage,

$$C_1 = 7,$$

$$C_2 = 3.5.$$

The statistics for top-down cracking model are

$$N = 414 \text{ observations}$$

$$Se = 1242.25 \text{ ft/mi}$$

$$Se/Sy = 0.977$$

Smoothness Models (IRI)

The International Roughness Index (IRI) is the widely accepted standard for measuring road roughness. Research has found that IRI is significantly affected by other distresses such as rutting, fatigue cracking, potholes, depressions and swelling. Different IRI models are used in MEPDG for different types of base materials.

Unbound Aggregate Bases and Subbases

$$\begin{aligned} IRI = IRI_0 + 0.0463 \left[SF \left(e^{\frac{age}{20}} - 1 \right) \right] + 0.00119(TC_L)_T + 0.1834(COV_{RD}) + 0.00384(FC)_T \\ + 0.00736(BC)_T + 0.00115(LC_{SNWP})_{MH} \end{aligned} \quad (2.14)$$

where IRI = IRI at any given time, m/km

IRI_0 = initial IRI, m/km

SF = site factor

COV_{RD} = coefficient of variation of the rut depths

$(TC_L)_T$ = total length of transverse cracking, m/km

$(FC)_T$ = fatigue cracking in wheel path, percent

$(BC)_T$ = area of block cracking as a percent of total lane area

$(LC_{SNWP})_{MH}$ = length of moderate and high severity sealed longitudinal cracks outside wheelpath, m/km

Asphalt Treated Bases

$$IRI = IRI_0 + 0.0099947(Age) + 0.0005183(FI) + 0.00235(FC)_T + 18.36 \left[\frac{1}{(TC_S)_H} \right] + 0.9694(P)_H \quad (2.15)$$

where $(TC_S)_H$ = average spacing of high severity transverse cracking, m

$(P)_H$ = area of high severity patches, percent of total lane area, %

Chemically Stabilized Bases

$$IRI = IRI_0 + 0.00732(FC)_T + 0.07647(SD_{RD}) + 0.0001449(TC_L)_T + 0.00842(BC)_T + 0.002115(LC_{NWP})_{MH} \quad (2.16)$$

where $(LC_{NWP})_{MH}$ = medium and high severity sealed longitudinal cracking outside the wheel path, m/km.

SD_{RD} = standard deviation of the rut depth, mm

2.2 Evolution of Reliability in Pavement Design

2.2.1 AASHTO 1986

Reliability was first introduced into pavement design in the 1986 AASHTO Guide. Since the major difference between 1993 Guide and 1986 Guide was the overlay design procedure and the accompanying appendices (7), the reliability part was exactly the same. Therefore, 1993 Guide is closely reviewed in the next part for up to date information.

2.2.2 AASHTO 1993

First of all, it is worthwhile noting that AASHTO 1993 Guide was an empirical design method based on AASHO Road Test. Traffic was simplified with equivalent single axle load (*ESAL*), and the design output was structural number (*SN*) for flexible pavement and slab thickness for

rigid pavement. Moreover, the design criteria was the pavement serviceability index (*PSI*), ranging from 0 to 5.

The reliability of a pavement design-performance process was the probability that a pavement section designed using the process would perform satisfactorily over the traffic and environmental conditions for the design period (7). Mathematically, reliability was considered using standard normal deviate, Z_R , and combined standard error of the traffic prediction and performance prediction, S_0 , as shown in equation 2.1 and 2.3. Z_R was correlated to the level of reliability determined by designers according to Table 2.1. It was clear that important roads such as interstate and urban road should be designed with higher reliability, because interruption or close of traffic for maintenance in these roads is prohibitive.

Table 2.1 Reliability level in AASHTO 1993 (7)

Functional Classification	Recommended Level of Reliability	
	Urban	Rural
Interstate and Other Freeways	85-99.9	80-99.9
Principal Arterials	80-99	75-95
Collectors	80-95	75-95
Local	50-80	50-80

S_0 accounted for both the chance variation in traffic predictions and the normal variation in pavement performance predictions. The suggested values were 0.40-0.50 for flexible pavement, and 0.30-0.40 for rigid pavement.

The reliability method in AASHTO 1993 Guide was indeed a Factor of Safety method. The Design Guide (7) documented the detail of the development of this method. Figure 2.2 is a reprint of the definition and evaluation of the reliability design factor, F_R . The overall design-performance deviation (δ_0) was assumed to be normally distributed with a variance of S_0^2 . The

stippled area above the range $\delta_0 \geq 0$ means that a pavement section will survive the design period traffic ($N_t \geq N_T$, or design traffic is more than the actual traffic). This is also the reliability of the design R . By converting the normal curve to a Z-scale standard normal curve, the reliability design factor was derived as

$$F_R = 10^{-Z_R \times S_0} \quad (2.17)$$

Input equation 2.17 to the basic design equation

$$\log F_R = (\log W_t - \log w_T) \geq 0 \quad (2.18)$$

where W_t = the predicted total traffic that the section can withstand,

w_T = the actual number of design period traffic.

The logarithm was used to induce normality in the probability distributions. The two design equations 2.1 and 2.3 were then developed by replacing w_T with empirical relationships between traffic load and design variables.

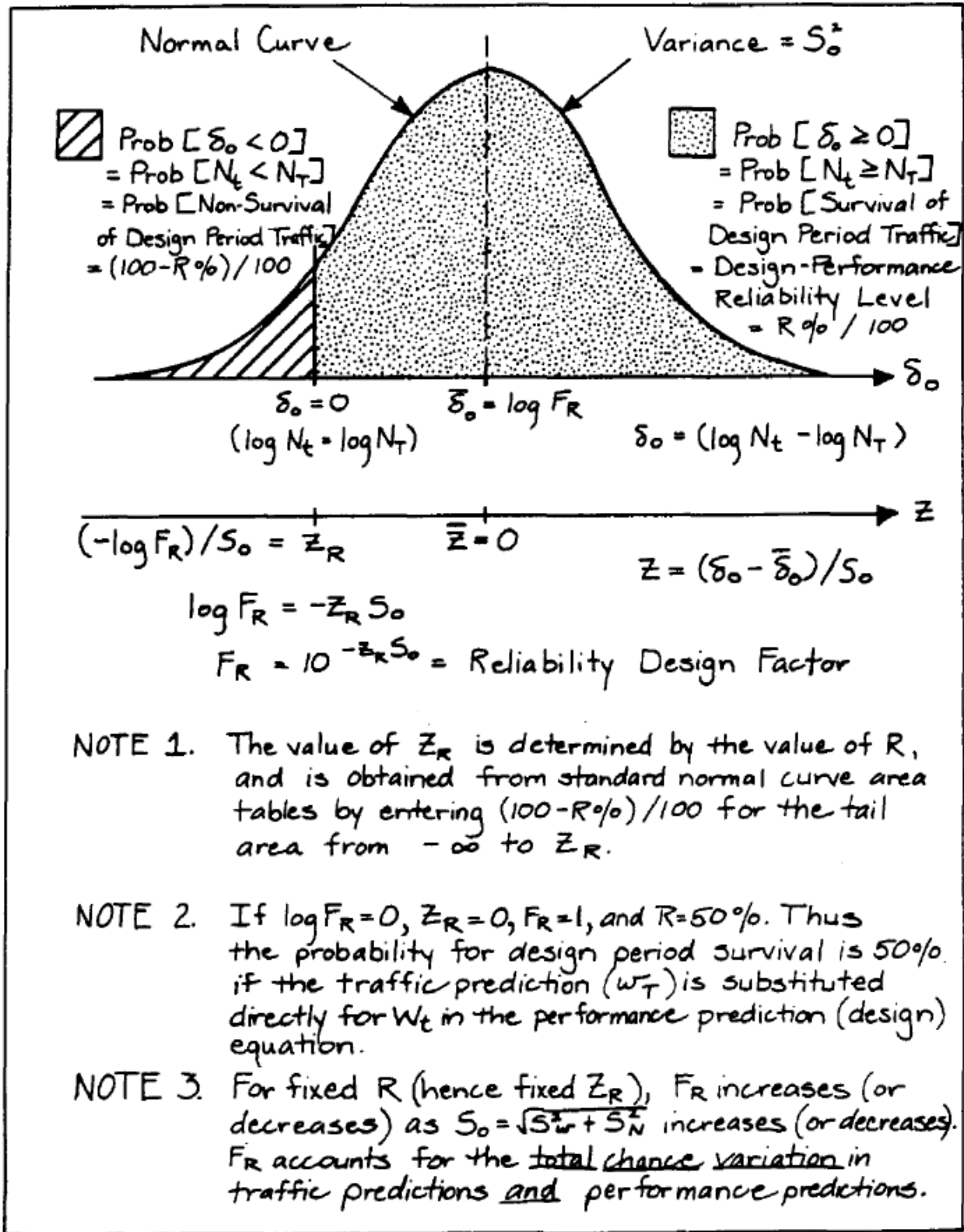


Figure 2.2 Definition of reliability and evaluation of reliability design factor F_R (7)

The detail of how national value of variance S_0^2 was estimated is presented in Appendix EE of the Design Guide (7). Table 2.2 reprints some critical values that were used in this research. This table is a reduction of Table EE.4 and EE.6 from the Appendix. Note that any cell may be solely located by its column letter (A-R) and row number (1-30). Columns F-I denote the class and name of design variables used in the design equation. Columns P-R are the estimated design mean value and standard deviation. By definition, Column Q equals to Column P divided by Column R, or vice versa. Code letters (i.e. c, g) behind some values correspond to the Appendix reference which is not included here. A major source for the estimation was from NCHRP Project 20-7, “*Revision of AASHTO Interim Guide for Design of Pavement Structures*”.

Note that the coefficient of variance for surface and base thickness is 10%. The strength factor and subgrade resilient modulus has about 15% coefficient of variance. Number of axle loads is 10% but the axle-load equivalence has 35% variance.

Table 2.2 Variables and variability estimates (7)

Variables sub-class	Name	Symbol	Units	Standard deviation of df	Coefficient of variance CVdf	Design level of df	Row No.
F	G	H	I	P	Q	R	Col.
Pavement Service-ability Level	Initial serviceability index	Pi		.36c .28g	6.7g	4.6	1
	Terminal serviceability index	Pt				2.5	2
Pavement structure above subgrade	Surfacing strength factor	a ₁		.044	10g	0.42	3
	Surfacing thickness	D ₁	in	.400	10	8.0	4
	Base strength factor	a ₂		.02g	14.3	0.14	5
	Base drainage factor	m ₂		.10	10g	1.20	6
	Base thickness	D ₂		.80	10g	7.0	7
	Subbase strength factor	a ₃		.02g	18.2	0.08	8
	Subbase drainage factor	m ₃		.10	10g	1.20	9
	Subbase thickness	D ₃		1.00	10g	11.0	10
	Structural number	SN		.41	10.4	5.60	11
Pavement structure at/below subgrade	Effective subgrade resilient modulus	M _R	psi	450	15g	5700	12
Axle-Load Equivalence	Summation of ESAL over % axle distrib.	$\Sigma P_i E_i$	ESAL	.1128 (flex)	35	.3225 (flex)	19
Number of Axle Loads	Initial average daily traffic	ADTi	Vehicles	750	15c	5,000	20
	Traffic growth factor			.006	10c	.06	21
	Avg. No. trucks in ADT	T	Trucks/1000ADT	.02	10c	.20	22
	Avg. No. axles per truck	A	Axles/Truck	.25	10c	2.50	23

Practically the 1993 Design Guide was easy to use, especially after the design equation being coded to software named DARWin[®] or embedded into a spreadsheet in Excel[®]. Take Arkansas as an example, pavements were mainly designed by engineers in the Roadway Design Division in the Arkansas State Highway and Transportation Department (AHTD). For an engineer, he/she only needed to input (1) the design traffic in ESALs provided by the Technical Services Section which handles all the traffic count and report to FHWA, (2) Reliability according to Table 2.1, (3) Standard deviation, $S_o=0.44$ for flexible pavement and $S_o=0.34$ for rigid pavement, (4) Subgrade modulus provided by the Materials Division which deals with every aspect of materials involved in pavement construction, and (5) the $\Delta PSI=2$ for Arkansas. The final result was a required Structural Number (SN). The design engineer then proposed different pavement structures and materials to meet the required SN .

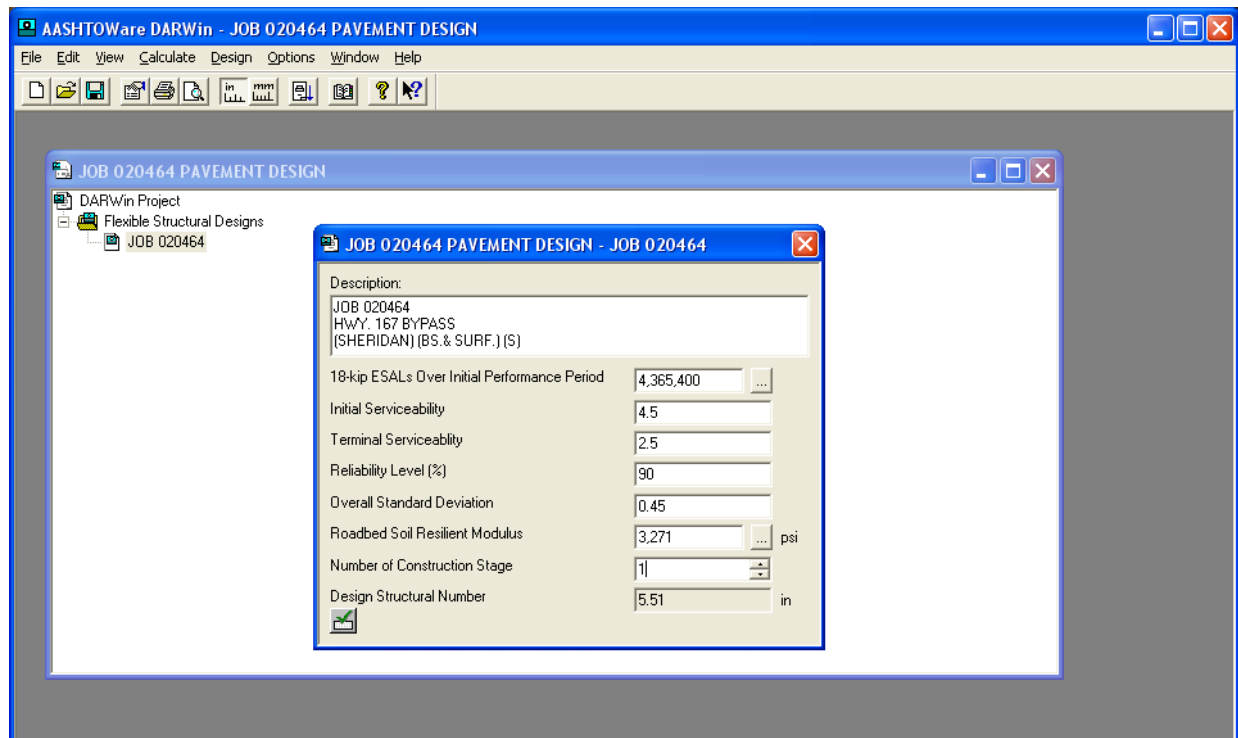


Figure 2.3 Screenshot of the AASHTOWare DARWin[®] (credit of Trinity Smith)

A	B	C	D	E	F
	AASHTO SN Program	CVEG 4433	Spring 2009		1 1
	AASHTO Flexible Pavement Design STRUCTURAL NUMBER ANALYSIS				
	INPUTS				
	Design Traffic, w18 (ESAL)	10000000	Do not use this space		
	Reliability, R (%)	90			
	Standard Deviation, S_o	0.44			
	Subgrade Modulus, MR (psi)	10000			
	Performance, ΔPSI	2			
	Calculate				
	Design Structural Number, SN	3.40			

Figure 2.4 Screenshot of the 1993 Design Guide being embedded into a spreadsheet (credit of Kevin D. Hall)

Credits should be given to the 1993 Guide that by treating design uncertainty as a separate factor, designers did not use “conservative” estimates for design inputs. Instead, designers inputted the mean or average value for each parameter, and considered reliability by selecting appropriate standard deviate Z_R and standard error S_0 .

However, there were many limitations of reliability design in 1993 Guide. First, the fact of Z_R and S_0 was to multiply a reliability design factor, FR , with the predicted total traffic, represented by *ESALs*. This multiplication could produce a large number of traffic loads that were far beyond the range applied at the AASHTO Road Test, on which the Guide was based (5). Therefore, large extrapolation out of the known range was needed for many pavement designs. Furthermore, it was shown by sensitivity analysis of equation 2.1 and 2.3 that the two equations were mathematically not sensitive at S_0 and standard deviate Z_R when the reliability was lower than 95%. The third limitation was that the wide range of reliability levels recommended in

Table 2.1 did not give designers any specific value for their design. In some extent, selecting a higher reliability only made designers felt safer, not really the design was safer.

It is also worth noting that, by investigating equation 2.1 and 2.3, a higher level of reliability requires a larger SN or D . That is, thicker pavement is required to build a safer road. This is reasonable. However, the limitation is that making pavement thicker is usually the only effective way to fulfill the reliability requirement. 1993 Guide cannot consider other techniques. For example, reduce the possibility of pavement rutting by subgrade reinforcement. There is important information lost by combining variability from different sources into the combined standard error, S_0 .

2.2.3 MEPDG 2002

In 2002 Design Guide (or widely called MEPDG), reliability was considered more specifically. Design reliability was defined as the probability that each of the key distress types and smoothness would be less than a selected critical level over the design period (5).

$$R = P [\text{Distress over design period} < \text{Critical distress level}] \quad (2.19)$$

By doing this, specific distresses such as cracking, rutting, faulting and smoothness of pavement was taken into consideration separately. For instance, a trial flexible pavement design may pass the thermal cracking, fatigue cracking and smoothness criteria, but fail the rutting criteria at the desired reliability level. It is possible then to revise the design to pass the rutting requirement by increasing surface thickness, increasing base thickness, changing the HMA mixture design, or strengthening the subgrade by lime or cement.

The procedure for designers was the same as previous Guides. Designers made the best estimation of all inputs and the design software predicts the distresses at the end of the design life. This is the mean prediction, or 50% reliability. By assuming normal distributions of all

variations and regression models calibrated from LTPP and other historical records, the mean prediction was exaggerated to a certain level of reliability, which was decided by designers according to the importance of the project (i.e. 90%). The recommended level of reliability is shown in Table 2.3. Comparing to the recommendation in 1993 Guide (Table 2.1), it was found that the level of reliability was generally lower in MEPDG than it was in 1993 Guide.

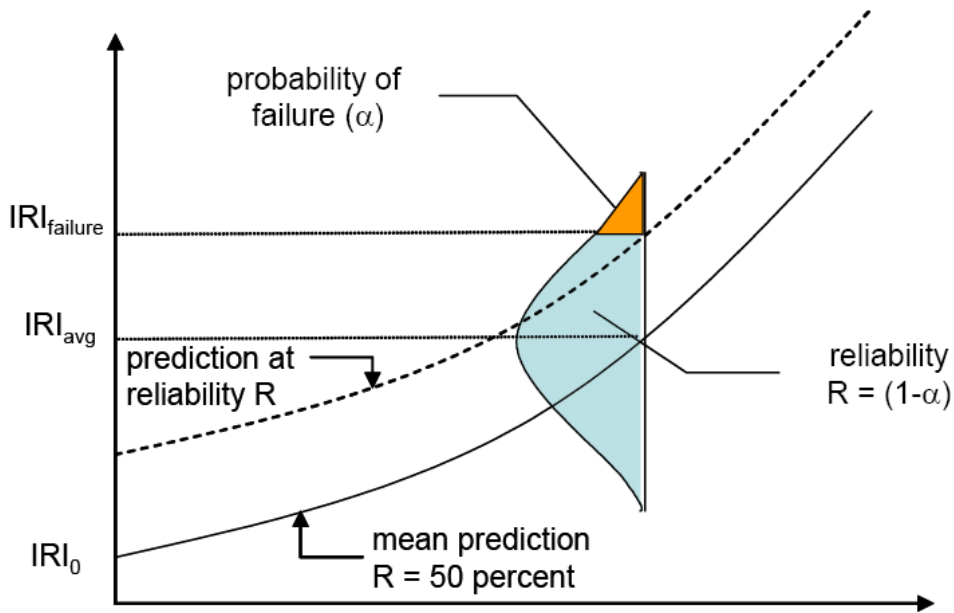


Figure 2.5 Reliability concept in MEPDG (IRI) (5)

Table 2.3 Reliability level in MEPDG (13)

Functional Classification	Recommended Level of Reliability	
	Urban	Rural
Interstate and Other Freeways	85-97	80-95
Principal Arterials	80-95	75-90
Collectors	75-85	70-80
Local	50-75	50-75

From user's perspective, the reliability in MEPDG was the same as in the AASHTO 1993 Guide. The only difference was that MEPDG broke down the reliability of the overall performance (*PSI*) into several distresses, as shown in Figure 2.6. A designer only needed to refer to Table 2.3 or a similar table in the specification and inputted the appropriate reliability level to MEPDG. Reliability level was usually selected in the interval of 5, such as 75, 80, 85 and 90. Other levels such as 73, 82 and 91 were rarely, if not ever, used.

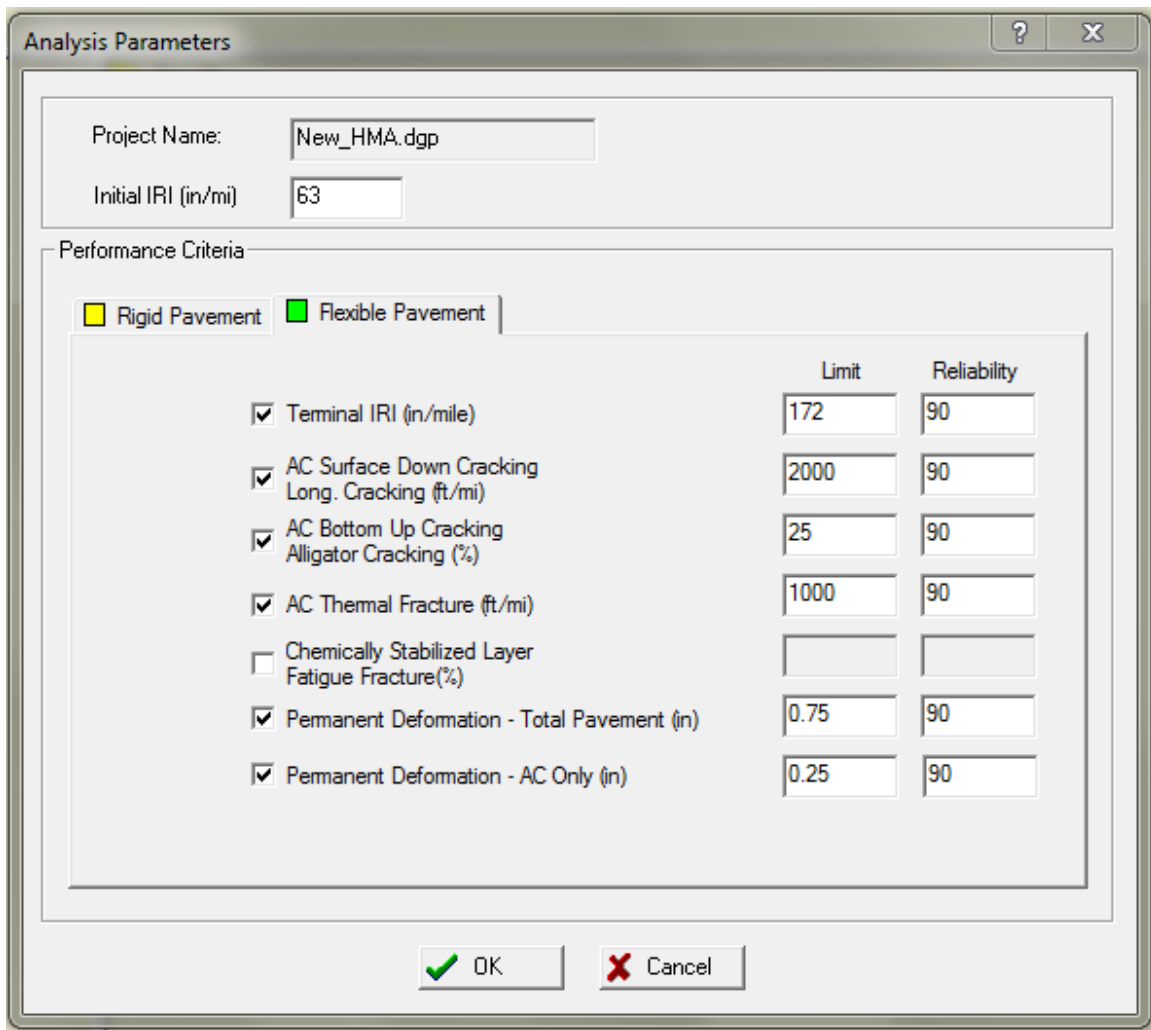


Figure 2.6 Screenshot of input reliability in MEPDG

For the purpose of this research, it is worth understanding how the reliability method in the MEPDG was developed. Appendix BB in the MEPDG documents was devoted to this topic (14). The rutting in asphalt layer is presented here as an example.

It was assumed that the expected permanent deformation (rutting) was approximately normally distributed with a predicted mean and a standard deviation. The standard deviation was a function of the error associated with the predicted rutting and the measured rutting in the national calibration database. In addition, the standard deviation was directly related to the level of predicted rutting. That is, the higher the rutting was, the larger the standard deviation was. This was reasonable considering extensive rutting would occur in a late time of the design life; hence more uncertainties were involved. The development of reliability estimation for AC rutting contained four steps.

Step 1. Compare the average measured AC rutting with the average predicted rutting (reliability level is 50%). Figure 2.7 shows the national calibration database.

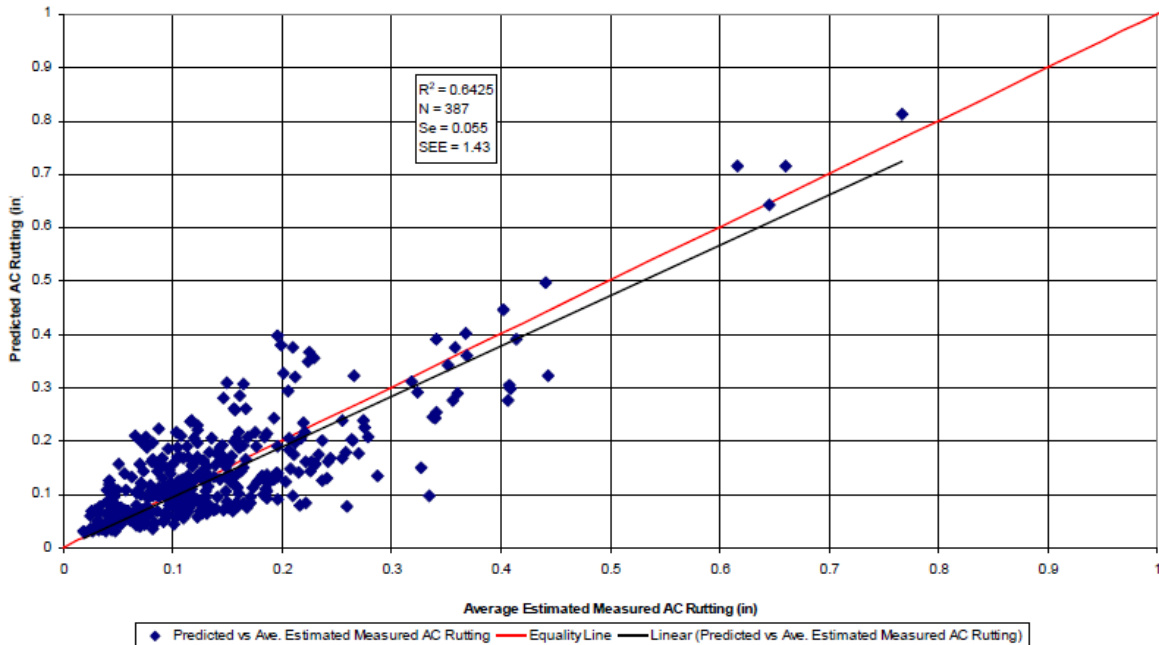


Figure 2.7 Nationally calibrated predicted versus measured asphalt rutting (14)

Step 2. Group all data points by the level of predicted rutting. The database was divided to six groups from 0 to above 0.5'' as shown in Table 2.4.

Step 3. Compute descriptive statistics for each group data. Average predicted rutting, average measured rutting and standard error of predicted rutting were calculated.

Table 2.4 Definition of groups for AC rutting data (14)

Group	Range of predicted AC rutting, inches	Number of data points	Avg. Predicted	Avg. Measured	Standard error of predicted
1	0-0.1	219	0.0457	0.0597	0.0337
2	0.1-0.2	153	0.1438	0.1465	0.0627
3	0.2-0.3	61	0.2392	0.1196	0.0883
4	0.3-0.4	20	0.3465	0.2998	0.1272
5	0.4-0.5	11	0.4342	0.3186	0.1498
6	0.5 and above	6	0.7356	0.6711	0.0853
Total		470			

Step 4. Determine relationship for the standard error. Standard error was tied to the predicted AC rutting, as shown in Figure 2.8. The relationship was

$$Se_{PDAC} = 0.1587PD_{ac}^{0.4579} \quad (2.20)$$

where Se_{PDAC} = standard error for AC permanent deformation from calibration

PD_{AC} = predicted AC permanent deformation, inches

$$R^2 = 69.8\%$$

$$N = 6$$

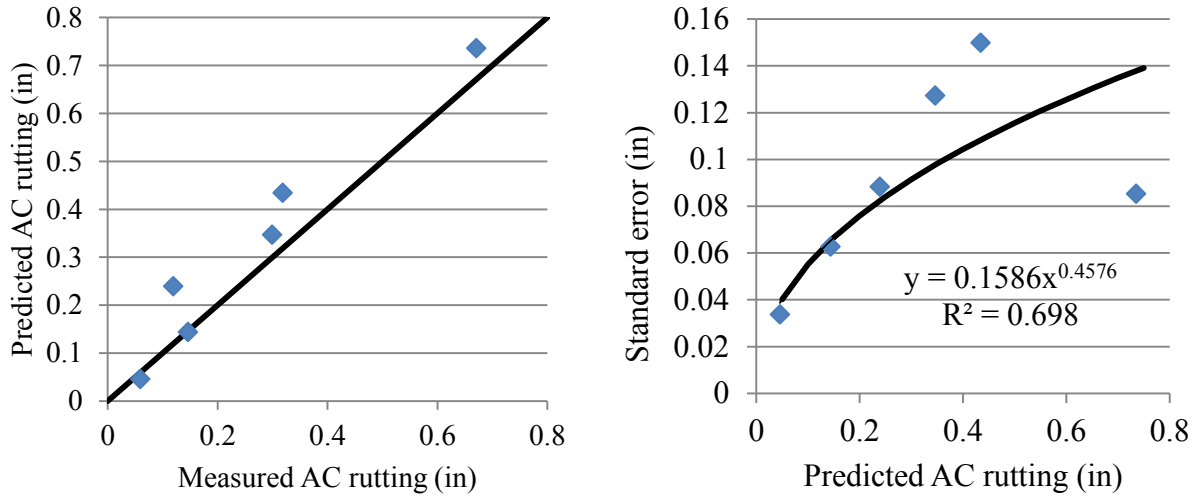


Figure 2.8 Predict standard error for AC rutting (14)

With the standard error of AC rutting available, the rutting at any user-defined reliability level could be calculated using

$$Rutting_{AC}^R = \overline{Rutting_{AC}} + Se_{AC} * Z_R \quad (2.21)$$

where $Rutting_{AC}^R$ = AC rutting corresponding to the reliability level R.

$\overline{Rutting_{AC}}$ = expected AC rutting estimated using mean input values (corresponds to a 50% reliability level).

Se_{AC} = standard error for AC rutting.

Z_R = standard normal deviate for the selected reliability level R.

The same procedure was applied to develop reliability estimation for other distresses including alligator cracking, longitudinal cracking, thermal cracking and IRI. The standard error and reliability for bottom-up alligator cracking were given by

$$Se_{FC} = 0.5 + \frac{12}{1 + e^{1.308 - 2.949 * \log D}} \quad (2.22)$$

where Se_{FC} = standard error of estimate for bottom up fatigue cracking.

D = predicted damage for bottom up fatigue cracking

$$Crack_{BottomUp}^R = \overline{Crack_{BottomUp}} + Se_{FC} * Z_R \quad (2.23)$$

where $Crack_{BottomUp}^R$ = AC rutting corresponding to the reliability level R .

$\overline{Crack_{BottomUp}}$ = expected AC rutting estimated using mean input values (corresponds to a 50% reliability level).

In summary, the reliability method in MEPDG was an empirical approach which assumed that all errors were “packed” together and led to the difference between predicted performance and measured performance. No estimation or assumption was made on the variance of each variable in the design equation. This was different from the AASHTO 1993 Guide. One could also realize that this method heavily relied on the national calibration database, on which the standard error was estimated.

2.3 Risk and Uncertainty in Pavement Design

It is well known that uncertainty exists almost everywhere. This is true for pavement design. It is convenient to decompose uncertainty in a pavement according to its life cycle, as shown in Figure 2.9. There are variations related to most of the inputs, categorized as traffic, climate and materials. The design uncertainty comes from the simplification of modeling and the truncation in computing. Variability occurs due to construction process and machine functioning. Finally, the variability in performance evaluation is brought back to the design model through model calibration.

Uncertainty should be carefully investigated and quantified to develop a better pavement design procedure.

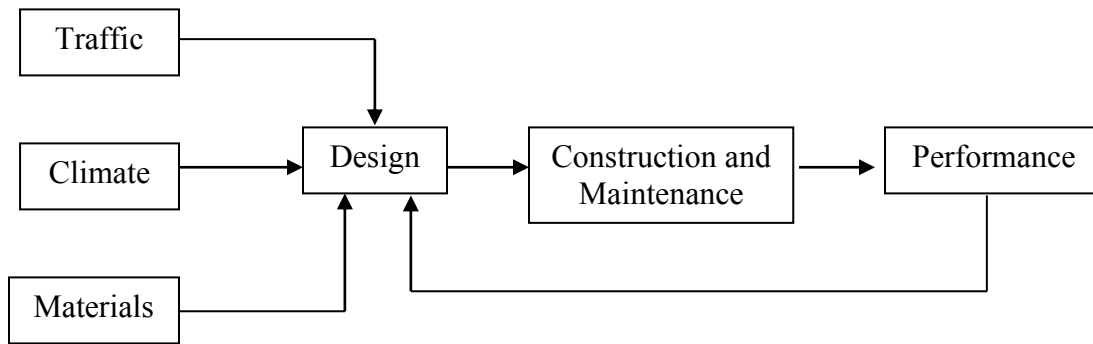


Figure 2.9 Uncertainty in a pavement's life-cycle

2.3.1 Terminology

First, some important terms deserve a close investigation. The following definitions were based on the Merriam-Webster dictionary and Von Quintus et al. (16).

Accuracy: The exactness of a prediction to the observed or “actual” value. The concept of accuracy encompasses both precision and bias.

Bias: An effect that deprives predictions of simulating “real world” observations by systematically distorting it, as distinct from a random error that may distort on any one occasion but balances out on the average. A prediction model that is “biased” is significantly over or under predicting observed distress or roughness.

Precision: The ability of a model to give repeated estimates that correlate strongly with the observed values. They may be consistently higher or lower but they correlate strongly with observed values.

Risk: noun, someone or something that creates or suggests a hazard.

Reliability: noun, the extent to which an experiment, test, or measuring procedure yields the same results on repeated trials.

Uncertainty: noun, the quality or state of being uncertain.

Variation: noun, the extent to which or the range in which a thing varies.

Variance: noun, 1. change in something. 2. (in statistics) square of standard deviation.

Variability: noun, the state or characteristic of being variable.

2.3.2 *Uncertainty Taxonomy*

The sources of uncertainty for pavement design were categorized into three kinds by Huang (15): variance due to design factors, lack of fit of design equation, and unexplained variance. Von Quintus (16) described four components for the uncertainty: measurement error, input error, model error and pure error. In this study, the sources of variability were divided into the following four types.

Reducible uncertainty of tests and construction. This includes the statistical variation related to the number of samples for material characterization tests and pavement performance measurement. For example, the aggregates mixed from different quarries vary from the designed gradation, because sieve analysis is done only on limited samples from quarries. Inputs in Level 1 require site specific testing, but Level 3 uses data from catalogs or common values, which bring more uncertainty into the design process. There are also quality variations in the asphalt mixture plant. The construction process is the most explicit part when people talk about pavement quality and performance, since it has been complained for a long time that poor pavement is due to poor construction. It is possible to reduce this type of uncertainty by increase the sample size, if time and cost are necessary. The development of equipment also reduces some uncertainty. For example, layer thickness is estimated by drilling cores in pavement. The application of Ground Penetrating Radar (GPR), which can provide continuous profile of pavement structure, makes layer thickness more reliable. This is the same for construction. By

using new technology and equipment, such as intelligent compaction and material transfer vehicles, the uncertainty related to construction will be decreased.

Reducible uncertainty of simplification and assumptions. Due to the complexity of the system and/or the impractical employment using current technology, pavement design guides are a simplified model of the real world. In other words, a perfect model cannot be done right now, although we know how to do it. For instance, tire pressure on pavement is not uniform; however, uniform distribution has been widely used for pavement design. In addition, most material properties are nonlinear; nevertheless, linear elastic model was embedded in current design guide, even nonlinear analysis could be done using complex finite element analysis. The assumptions of homogeneous layers and full contact between layers were also considered as a simplified truth. It is expected that the uncertainty caused by these simplifications and assumptions would be reduced in the future when computer technology enters a new era.

Irreducible uncertainty of materials per se. There are inherent irregularities in the properties and behavior of materials and the pavement as a whole system. In particular, pavement structures are unique that a design section is constructed across a long distance. Variability along the distance is unavoidable. Therefore, a probabilistic design is required as an improvement of deterministic design.

Unknown uncertainty due to the lack of knowledge. This means, sadly, that a simple question had not been fully understood: why some pavement sections perform better than others? A pavement is a complicated system. For instance, a well-defined relationship between roughness and dynamic impact of tires on pavement is yet achieved. It is still a debate on the mechanism of top-down cracking. How to transfer damage in micro-level to distress in macro-

level is another challenge. For a probability-base design, all these deficiencies should be considered.

2.3.3 *Uncertainty Quantification*

Thickness

Layer thickness varies from point to point in one project because of the variability of materials and construction. Table 2.5 shows the thickness variation for flexible pavement and rigid pavement (15) (17; 18).

Table 2.5 Variation of materials (15)

Material	Standard deviation
Concrete (9 in)	0.29 in
Hot mix asphalt	0.41 in
Cement treated base	0.68 in
Aggregate base	0.79 in
Aggregate subbase	1.25 in

It shows that concrete has the smallest variation, and lower layers (base and subbase) vary more than surface layers.

The thickness data in the Long-Term Pavement Performance (LTPP) program were analyzed to find out how as-constructed layers differ from as-designed layer (19). It was verified that thickness variations within a layer was normally distributed. In addition, the mean difference of layer thickness between as-constructed and as-designed was within 0.5 in for 74% of the data and within 1 in for 92% of the data.

Modulus

Modulus of pavement materials, including HMA, PCC, base and subgrade, are more complicated than thickness, because modulus is determined either by laboratory testing or backcalculation from deflection testing. Furthermore, modulus per se is dramatically influenced by temperature and moisture content.

Timm (20) developed a probability-based pavement design software named *PerRoad* in which modulus variation and thickness variation were considered using Monte Carlo Simulation. The default values of variation for some materials are listed in Table 2.6. It was found that the variation of modulus was much larger than the variation of layer thickness. The minimum Coefficient of Variation (COV) of modulus was twice than the maximum COV of thickness.

Table 2.6 Variation of modulus and thickness used in *PerRoad*

Layer	Material	Modulus		Thickness	
		Distribution	COV	Distribution	COV
1	AC	log-normal	30	normal	5
2	AC binder	log-normal	30	normal	8
3	AC base	log-normal	30	normal	15
4	Granular base	log-normal	40	normal	8
5	Soil	log-normal	50	N/A	N/A

Note: COV is Coefficient of Variation. N/A is Not Available.

It was also clear that the lower layer varied more than the upper layer. This could be due to quality of the lower layer material, the effects of thickness variations, geophone sensor errors, and back-analysis errors, if backcalculation method was used to estimate modulus (21). It was also found that the COV of AC layer and aggregate base was 20.5 to 36.2 and 19.4 to 89.5, respectively.

For concrete materials, Tayabji and Vu (22) analyzed the variation in LTPP and recommended COV for pavement design, showing Table 2.7. Comparing to Table 2.6, it was noted that variation of concrete modulus was lower than that of asphalt mixture. This could be due to the sensitivity of asphalt mixture's property to temperature.

Table 2.7 Variation of concrete materials (22)

Parameter	COV (%)
Compressive strength (cylinders or cores)	15
Flexural strength (beams)	12
Split tensile strength (cylinders or cores)	15
Modulus of elasticity (cores)	15

Traffic

A report about the variation of traffic parameters for AASHTO Guide was found in the literature, as shown in Table 2.8 (15). However, very little research has been done on the variability of load spectra or weigh-in-motion data. This may be due to the complexity of the load matrix.

Table 2.8 Variation of traffic (15)

Description	Coefficient of variation (%)
Equivalent Load Factor	35
Initial average daily traffic	15
Traffic growth factor	10
Percentage of trucks	10
Average no. of axles per truck	10
Overall traffic prediction	42

Current MEPDG calculated pavement stress and strain every month during the design life.

The average values of traffic classification and axle load distribution were determined from the

continuous traffic record of WIM stations. Turochy et al. analyzed the spatial and temporal variation of axle load spectrum using statistical methods (23). It was concluded that, from a statistical perspective, the distribution of observed axle loads differ significantly between each month and the annual average, between directions at a given site, and between each site and the combination of all sites, However, from a practical perspective (using AASHTO 1993 Method), the impacts of axle load distribution differences on pavement design were not so spectacular.

In the development of national default traffic values, Von Quintus noticed the existence of traffic variability (24). Because no definite pattern was found across US, it was determined to keep the monthly distribution factor at 1.0 for each month. For the initial development, this assumption was acceptable. But more research is demanded for probability-based design in the future.

Climate

MEPDG calculates stress and strain each month during the design life. Since climate data is continuously recorded, monthly average climate is input into MEPDG. In addition, MEPDG simply repeats the available historical climate data as the prediction for future. Minnesota (25) studied the influence of climate on MEPDG by modeling 610 stations across the United States, but the variation of climate data was not the focus. Another research at Delaware investigated the impact of climate change on pavement performance (26). The uncertainty of climate change was presented, but not the variation of the climate data in the current MEPDG. Therefore, a study is highly recommended to address this topic.

Performance

The variability of performance measurement has long been noticed by engineers because it is strongly subjective. For example, manual distress surveys provide different values by different raters, and in different time of the same rater.

In 1998, Rada et al. (27) found that the COV of total distress for AC pavements ranged from 9% to 38%, and COV of cracking related distresses for PCC pavement ranged from 8% to 22%. The transverse cracking spacing for continuous reinforced concrete pavement (CRCP) was found not normally distributed but skewed with a long right tail, which could be described using a Weibull distribution (28). Later, it was found that the cracking width could also be a Weibull distribution, rather than normal distribution (29).

2.4 Reliability Analysis Methods

The concept of reliability was first introduced in the aircraft industry during 1930s (30). It was then increasingly used in the design of nuclear power plants and their control system during 1950s. Nowadays, reliability is being applied almost everywhere, such as aircraft, chemical plants, communication system, bridge design, computer network, and financial market.

Many reliability analysis methods were developed accordingly. Harr (31) divided them into three categories, exact methods, first-order, second-moment method (FOSM), and the point estimate method (PEM). A brief introduction of some important methods follows.

2.4.1 Factors of Safety

In general, structures are designed with appropriate capacity (C) to fulfill the demand (D) of structural requirements. For example, a pavement is designed with enough thickness and stiffness to withstand the traffic in the expected life. The capacity can be defined as the traffic

that the designed pavement could endure. The demand is the real traffic traveled on the pavement after its construction. The factor of safety (FS) is then defined:

$$FS = \frac{\text{Capacity}}{\text{Demand}} = \frac{\text{ESAL capacity}}{\text{ESAL demand}} \quad (2.24)$$

For example, if a pavement for a rural primary road requires 8,000,000 ESALs in the 20 years design period, and the designed pavement could withstand 14,000,000 ESALs, the FS is $14,000,000/8,000,000=1.75$. However, if the same structure is designed for an urban arterial road, which demands 20,000,000 ESALs, the design will be not safe because the FS is $14,000,000/20,000,000=0.7$.

The reliability of design, R , is defined by

$$R=P(\text{ESAL capacity} > \text{ESAL demand}) \quad (2.25)$$

Factor of safety is simple in concept and easy to be applied. Since the demand of a structure is a known value, designers can use the FS to estimate the capacity. The FS is usually a standard based on engineering experience and judgment.

However, there are many disadvantages that come from the simplification. First of all, individual inputs of the design model are not taken into consideration. No matter what input is changed, the factor of safety is the ratio of the system's capacity and the demand. Another limitation is that the selection of safety factors is subjective in many cases. As stated by Carter (32):

“As a person who was brought up on factors of safety and used them all his professional life, their simplicity appeals to me. However, if we are to make any progress the bundle has to be unbundled, and each of the constituents correctly modeled...”

2.4.2 Reliability Index

Factor of safety is easy to understand and use; however, it assumes that C and D are uniformly distributed, which is not correct. When the variability of C and D is taken into consideration, there are chances that the two distributions will overlap, as shown in Figure 2.10.

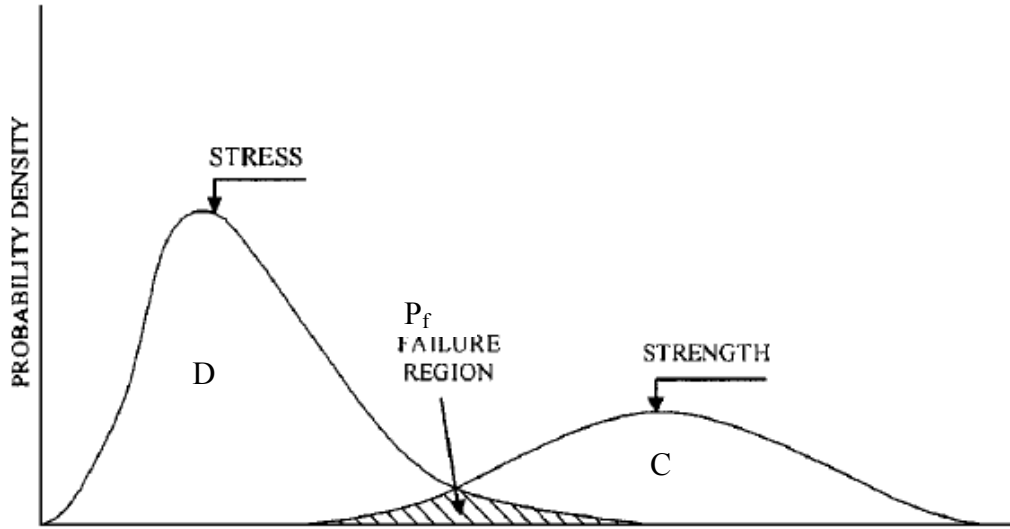


Figure 2.10 Relationship between capacity and demand (33)

Define the safety margin as

$$S=C-D \quad (2.26)$$

In a limit state design, it is also as the limit state function:

$$G(X,t) = C-D \quad (2.27)$$

Then the probability of failure could be defined as

$$P(f) = P [(C-D) \leq 0] = P[S \leq 0] \quad (2.28)$$

and the reliability index is given by

$$\beta = \frac{\bar{S}}{\sigma(S)} \quad (2.29)$$

where \bar{S} is the mean of the safety margin and $\sigma(S)$ is its standard deviation.

Note that reliability index is in fact the reciprocal of the coefficient of variation of the safety margin.

$$COV = \frac{\sigma(s)}{S} = \frac{1}{\beta} \quad (2.30)$$

Zhang (33) proposed a methodology to develop the reliability function for AASHTO 1993 design equations. By determining the mean and standard deviation, the reliability index and the failure probability could be calculated using the method of moments.

$$G(SN, \Delta PSI, Mr, ESAL, r, t) = \log W_{18} - \log N(t) \quad (2.31)$$

$$\beta_{2M}(t) = \frac{\mu_{G(SN, Mr, ESAL_0, r, t)}}{\sigma_{G(SN, Mr, ESAL_0, r, t)}} \quad (2.32)$$

$$F_{2M}(t) = \Phi(-\beta_{2M}(t)) \quad (2.33)$$

It is worth noting that an explicit function is required to apply the reliability index method.

2.4.3 Propagation of Uncertainty

An engineering system is a relationship between inputs and outputs. Theoretically, no matter how complex the system is, it can be simplified as

$$y=g(x) \quad (2.34)$$

where x = input variable,

y = output variable, and

g = a function that relates input and output.

When x is considered as a random variable, engineers are interested in how the output is influenced by the uncertainty of the input. In other words, reversely, how the uncertainty

propagates from the input to the output. Therefore, this method is called propagation of uncertainty.

For simple relationships which can be expressed as an explicit function, analytic procedures are available. For instance, if

$$Y=g(\mathbf{X})=a_0+a_1X_1+a_2 X_2 \quad (2.35)$$

where a_0 , a_1 and a_2 are real numbers,

then the mean and the variance of Y are

$$E(Y)=a_0+a_1E(X_1)+a_2E(X_2) \quad (2.36)$$

$$Var(Y) = a_0^2 + a_1^2Var(X_1) + a_2^2Var(X_2) \quad (2.37)$$

For other cases that involve a more complicated function or a mixture of distribution types, approximate methods based on Taylor series expansion can be used. Details can be referred in many textbooks such as Ayyub and Klir (34).

2.4.4 Monte Carlo Simulation (MCS)

Monte Carlo simulation is a technique developed in 1940s to test engineering systems by imitating their real behavior. Since this research heavily relies on Monte Carlo simulation, it is worthwhile tracking the origin and the development of this method.

The story as told by Nicholas Metropolis, one of the key inventors in the development of MCS, is as following (35):

The first electronic computer-the ENIAC- at the University of Pennsylvania in Philadelphia, developed in 1945 and widely credited to John von Neumann, provided a great leap forward on computation speed. The review of the ENIAC results at Los Alamos excited many scientists, among which was Stan Ulam with an extensive mathematical background. Stan was aware that statistical sampling techniques had fallen into desuetude because of the length and

tediousness of the calculations. But with the miraculous development of the ENIAC, it occurred to him that statistical techniques should be resuscitated. Stan discussed this idea with von Neumann. Then John von Neumann saw the relevance of Ulam's suggestion and, on March 11, 1947, sent a handwritten letter to Robert Richtmyer, the Theoretical Division leader at Los Alamos National Lab. His letter included a detailed outline of a possible statistical approach to solving the problem of neutron diffusion in fissionable material. This letter carries the spirit of the now-known Monte Carlo method. The name, however, was coined by Nick Metropolis. For one reason, it was obvious that the new statistical method has the same spirit as the roulette in the Monte Carlo Casino in Monaco. For the other reason, it was a fact that Stan had an uncle who would borrow money from relatives because he just had to go to Monte Carlo. The new method was first published by Nicholas Metropolis and Stan Ulam in 1949 (36).



(a)



(b)



(c)

Figure 2.11 The three actors in the development of the Monte Carlo method: (a) John von Neumann (1903-1957), (b) Stanislaw Ulam (1909-1984), and (c) Nicholas Metropolis (1915-1999) (source: National Air and Space Museum and Los Alamos National Laboratory)

Monte Carlo method was first applied to problems related to the atomic bomb, then to evaluate complex multidimensional integrals and to solve certain integral equations, occurring in physics, that were not amenable to analytic solution (37). After more than 60 years development, Monte Carlo method is now being used in physics, engineering, biology, statistics, mathematics, and many other fields of applications.

Six steps are needed for a Monte Carlo simulation (34) :

1. Definition of the system using an input-output numerical model.
2. Generation of random numbers.
3. Generation of random variables using transformation methods from random numbers to random variables.
4. Evaluation of the model multiple times (N simulation cycles).
5. Statistical analysis of the resulting behavior.
6. Study of simulation efficiency and convergence.

Monte Carlo simulation can be used in a pavement design as following. Suppose the variability of pavement design inputs were known, it would be possible to pick up a random number from the distribution of each input, and then run the design procedure, which finally predicts a pavement performance. This is called one simulation. Using the same concept, another random number can be selected and another design can be run. This process repeats until all possible numbers of all inputs are simulated. The result of the simulation is many predicted pavement performances that represent the variability of all inputs. If a performance criterion is defined, the reliability of the design can be determined as the number of predicted performance passed the criteria out of the total number of the simulation. This is how Monte Carlo simulation works for reliability analysis of a pavement design.

In fact, Monte Carlo simulation has been applied in pavement designs (20). A software named *PerRoad* was developed to design flexible perpetual pavements considering layer thickness variability and modulus variability. Figure 2.12 is a screenshot of the software. Note that the distribution type and coefficient of variation were input parameters, which were used for random sampling in Monte Carlo simulation. Also note that the mechanistic modeling in *PerRoad* was the AASHTO 1993 design equations, and only two variations were considered.

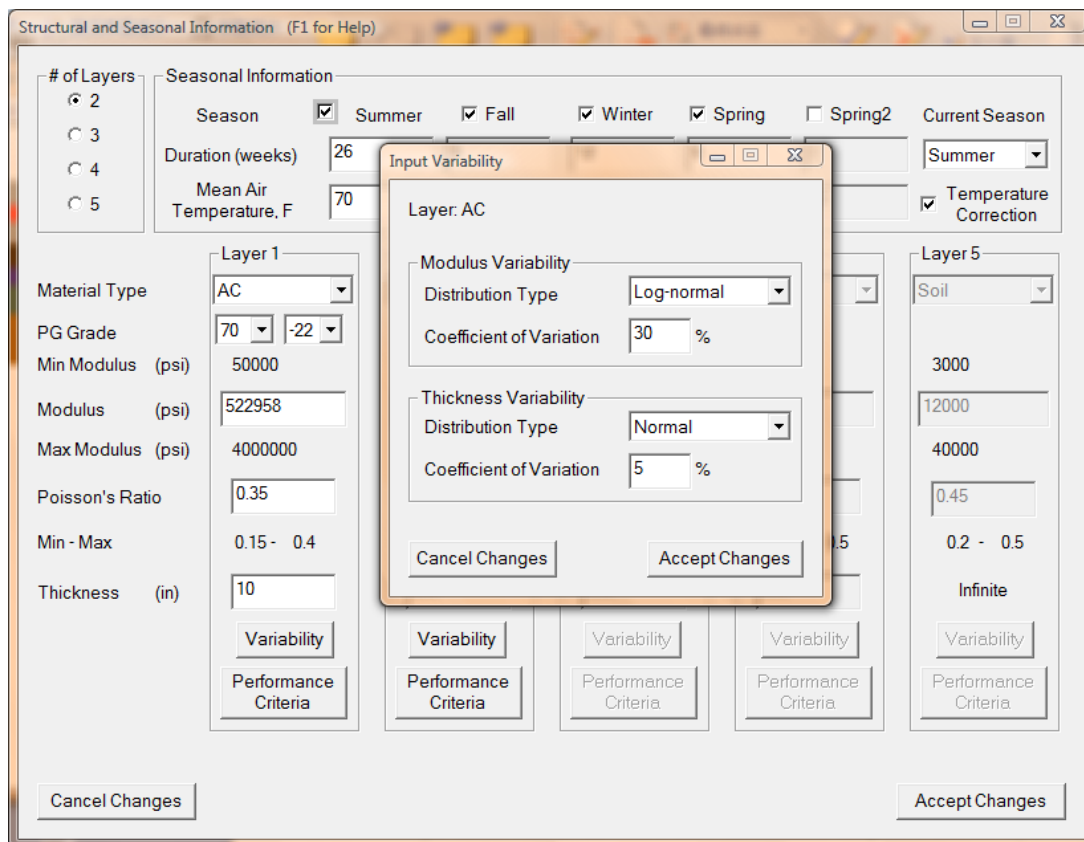


Figure 2.12 Incorporation of variation in *PerRoad*

However, Monte Carlo simulation needs a very large number of trials to achieve a stable reliability (i.e. 5000 times in *PerRoad*). This process may take a long time to run, especially for the following situations. First, when finite element analyses are used for structural modeling, such as the flexible pavement design in MEPDG (5). Second, when the number of inputs and

variations are so many that the random selection of all inputs becomes impossible. Unfortunately, MEPDG has hundreds of inputs that Monte Carlo simulation is prohibitive to be conducted (6).

2.5 Summary

Some major subjects in this research were reviewed in this chapter. Evolution of pavement design approaches, from empirical to mechanistic-empirical, was explained, along with the evolution of the method how uncertainty and reliability were considered. This section also included a literature view of historical and recent studies on “reliability or uncertainty of pavement design”. Sources of uncertainty, or risk, in pavement design were presented. Finally, this chapter ended with some widely used reliability analysis methods, especially Monte Carlo Simulation which will be applied in Chapter 6.

CHAPTER 3 LOCAL CALIBRATION

3.1 Introduction

The currently available MEPDG was calibrated using national wide data from the Long-Term Pavement Performance (LTPP) program. Figure 3.1 shows 94 LTPP sites used to calibrate new constructed flexible pavement. Initially, 80% of LTPP data were used for calibration and the left 20% data were used for verification. Because a reasonable verification was found, all LTPP data were combined to obtain a comprehensive national model.

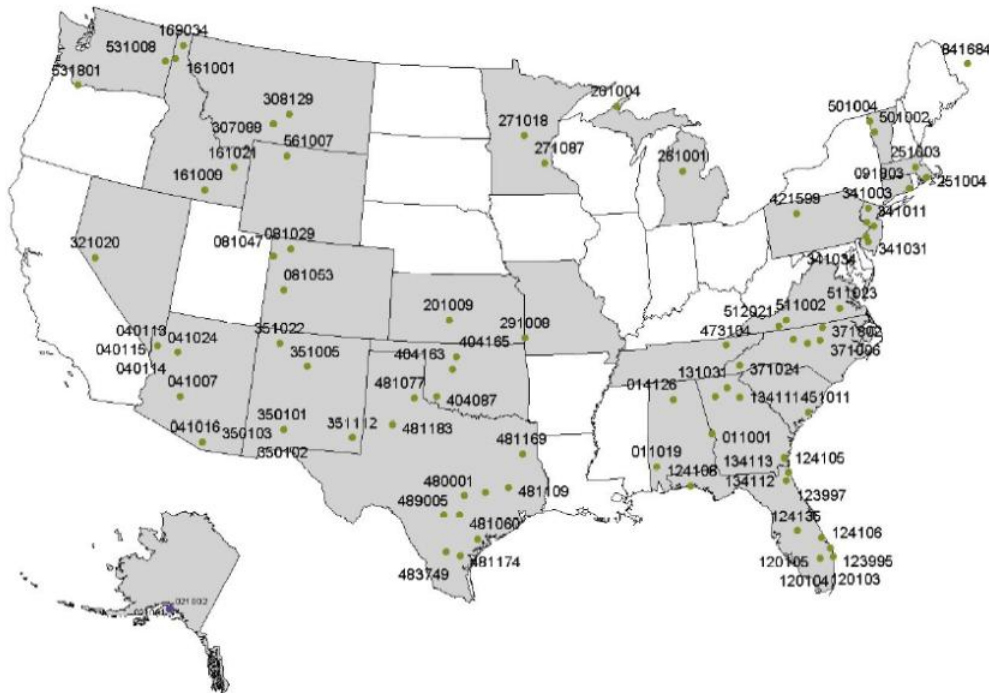


Figure 3.1 LTPP sites for new flexible pavement calibration in MEPDG (13)

However, because of the difference between national conditions and local conditions such as climate, material properties, traffic patterns, construction and management techniques, a statewide or regional calibration was recommended for any agency who wants to implement MEPDG with good confidence (13). In addition, one may notice that there was no LTPP stations in some states (i.e. Arkansas) being used in the national calibration. Therefore, local calibration

became not only a recommendation but also a mandatory procedure. Figure 3.2 illustrates the concept of MEPDG and what role calibration plays in the system.

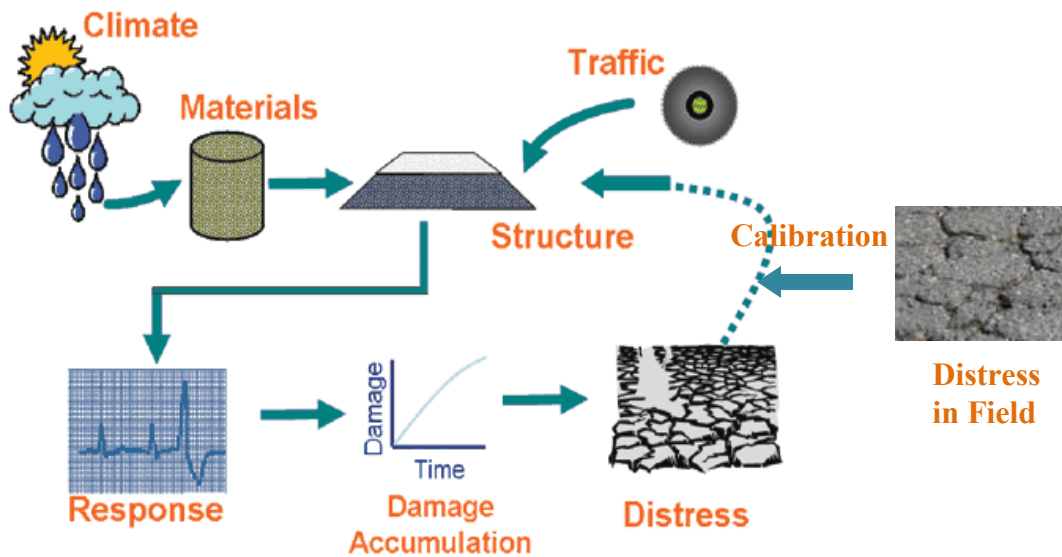


Figure 3.2 Concept of MEPDG calibration (adapted from FHWA)

Calibration projects were completed or are undergoing in many states such as Wisconsin (38), Montana (4), Florida (39), North Carolina (40), Texas (41), Minnesota (42), and Ohio (43). The calibration in Montana made use of 89 LTPP sections and 13 non-LTPP sites located both inside Montana and in the adjacent states. It was found that MEPDG significantly over predicted the total rut depth, primarily because higher levels of rutting were predicted in the unbound layers and embankment soils. The project also reduced the bias of bottom-up alligator cracking and longitudinal cracking model. A good correlation was found for non-load related transverse cracking (thermal cracking).

Minnesota conducted the local calibration using field performance data obtained from MnROAD pavement sections and other pavement sections located in Minnesota and neighboring states (42). For flexible pavement, rutting model, alligator cracking model and thermal cracking model were calibrated successfully to match Minnesota's condition. However, the longitudinal

cracking model, rutting model for base and subgrade, and IRI model were not able to be calibrated.

A national guideline on local calibration was also developed in NCHRP Project 1-40B (16). The report explained the component of variations in MEPDG, the difference between calibration and validation, and most importantly, a step-by-step procedure for local calibration. The methodology was adopted and changed slightly for this research.

Overall, the objective of local calibration was to reduce the bias and dispersion of the nationally-calibrated model through comparing the predicted performance with state specific performance.

3.2 Methodology

The procedure of local calibration is illustrated in Figure 3.3.

Step 1. Developed a detailed, statistically sound experimental plan or sampling template based on local conditions, such as the type of major materials, structures, climate regions and other policies.

Step 2. Calibration sites from all possible database and projects were selected. The philosophy was to make the best use of existing data and reduce the cost for additional field investigation and testing. Fortunately, Arkansas had a project named the TOP 25, which was initiated in March 2002 to validate the SuperPave[®] mix design method in Arkansas. In total, the performance of 25 roadways across the state (each location contains three 100-ft-long sections) had been monitoring since then. The database was used as the backbone to conduct the local calibration. In addition, LTPP sections located in Arkansas were also included in the local calibration database.

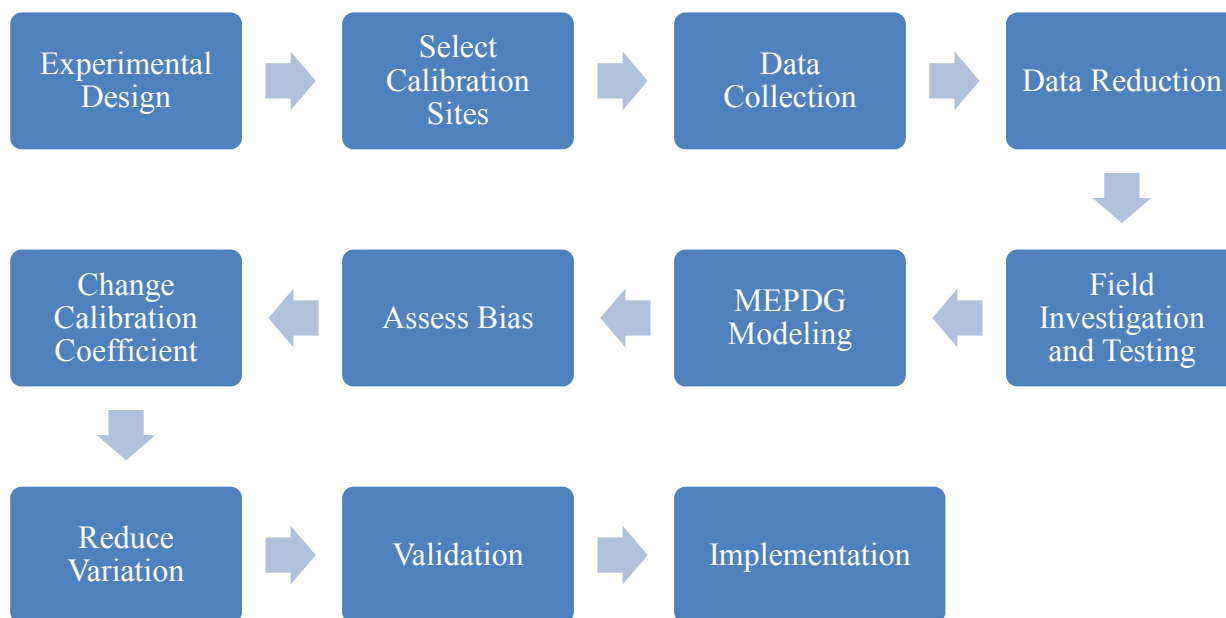


Figure 3.3 Steps of local calibration (adjusted from (16))

Step 3. Collected data from different locations and sections. Although most of the required input to MEPDG were available somewhere, there was no such an integrated database warehouse. Pavement design data were retrieved from design records. Material data were from construction records. Maintenance data were not included because the focus here was only for new flexible pavement models. Traffic data were from the Technical Services Section at AHTD. Historical performance data such as distress survey, rutting, IRI, and FWD test were collected from pavement management system, along with data stored in the Research Section under the TOP 25 project. Details about data collection will be presented in the next section.

Step 4. All data were synthesized together and data reduction was conducted. This included identifying missing data, checking the reasonableness and converting to the required format or unit.

Step 5. Conducted field investigation and testing to fill the gap of missing data. Although forensic testing was recommended to verify the assumption in MEPDG, such as the rutting composition in different layers, and where cracking initiates (bottom-up or top-down) (16), no forensic testing was conducted in this study due to budget limit.

Step 6. Each calibration section was simulated in MEPDG.

Step 7. Compared the predicted performance from MEPDG and the measured performance from field to assess the bias of the national-calibrated model. If no significant bias was observed, the scatter plot of performance from the two sources should match at the line of equality. Otherwise, calibration coefficients in MEPDG should be optimized to reduce or eliminate the bias. Step 7 is also called verification.

Step 8. Calibration coefficients were changed and MEPDG simulation was conducted again. The NCHRP Local Calibration Guide (16) provided recommendations on what coefficients should be adjusted to eliminate bias or reduce variation for different models, as shown in Table 3.1.

Table 3.1 Recommended calibration coefficients to be adjusted for flexible pavement (16)

Distress		Eliminate bias	Reduce standard error
Total rutting	Unbound materials and HMA layers	$k_{r1}, \beta_{s1}, \text{ or } \beta_{r1}$	$k_{r2}, k_{r3}, \text{ and } \beta_{r2}, \beta_{r3}$
Load related cracking	Alligator cracking	$C_2 \text{ or } k_{f1}$	$k_{f2}, k_{f3} \text{ and } C_1$
	Longitudinal cracking	$C_2 \text{ or } k_{f1}$	$k_{f2}, k_{f3} \text{ and } C_1$
	Semi-rigid pavements	$C_2 \text{ or } k_{f1}$	$k_{f2}, k_{f3} \text{ and } C_1$
Non-load related cracking	Transverse cracking	β_{r3}	β_{r3}
IRI		C_4	C_1, C_2, C_3

Step 9. Compared the predicted performance after coefficients were adjusted with the measured performance again. Step 8 and 9 together was the core process of local calibration. It could be an iterative process depends on the model requirement. For alligator cracking and longitudinal cracking model, the calibration coefficients could be optimized using a mathematical process because empirical functions were available. But the rutting and IRI model could not be completed in this way.

Step 10. The calibrated model was validated using a different set of data. In this research, 80% of the total available data were used for calibration and 20% of them were set aside for validation.

Step 11. A model which was calibrated and validated should be ready for implementation. In this study, the local calibrated MEPDG served as the basis for further analysis to improve the overall reliability of pavement designs.

3.3 Data Collection

Two data sources were available for local calibration: the Long Term Pavement Performance (LTPP) database from Federal Highway Administration (FHWA) and the local Pavement Management System (PMS) from AHTD. Table 3.2 lists the 38 sections available from both LTPP and PMS sources, categorized by HMA thickness and base types. Eighty percent of the sections (30 sections) were randomly selected for calibration efforts; twenty percent (8 sections) were preserved for subsequent validation. It was also noted that there was no section with thin HMA over unbound base and no section with thick HMA over asphalt treated base (ATB) and cement treated base (CTB). This was reasonable considering the low strength of unbound base and high strength of ATB and CTB. As shown in Figure 3.4, these 38 sections were located across Arkansas. Note that SPS-1 in Jonesboro contained 12 sections. Each site of

TOP25 had three 100-ft sections identified as Good, Average and Poor based on the pavement condition at the time when the TOP 25 project was initiated.

Table 3.2 Experimental Matrix

HMA thickness	Thin (≤ 4 in.)	Intermediate	Thick (≥ 8 in.)	No. of sections
Unbound base		<u>0113</u> ,0114,0804, 070079G,070079A, 070079P	R20149G,R20149P,090001G, 090001A,090001P, <u>090048G</u> , <u>090048A</u> ,090048P,070018G, 070018A,070018P	17
ATB	0803	0115,0116,0117,0118,0119 <u>0120</u> ,0121,0122,0123,0124 R80065G,R80065A, R80065P, <u>R50067G</u> , R50067A,R50067P		17
CTB		2042, <u>3048</u> , 3058,3071		4
No. of sections	1	26	11	38

Note: 1. Underlined sections are randomly selected for validation.

2. ATB: Asphalt Treated Base; CTB: Cement Treated Base; G is Good; A is Average; P is Poor.

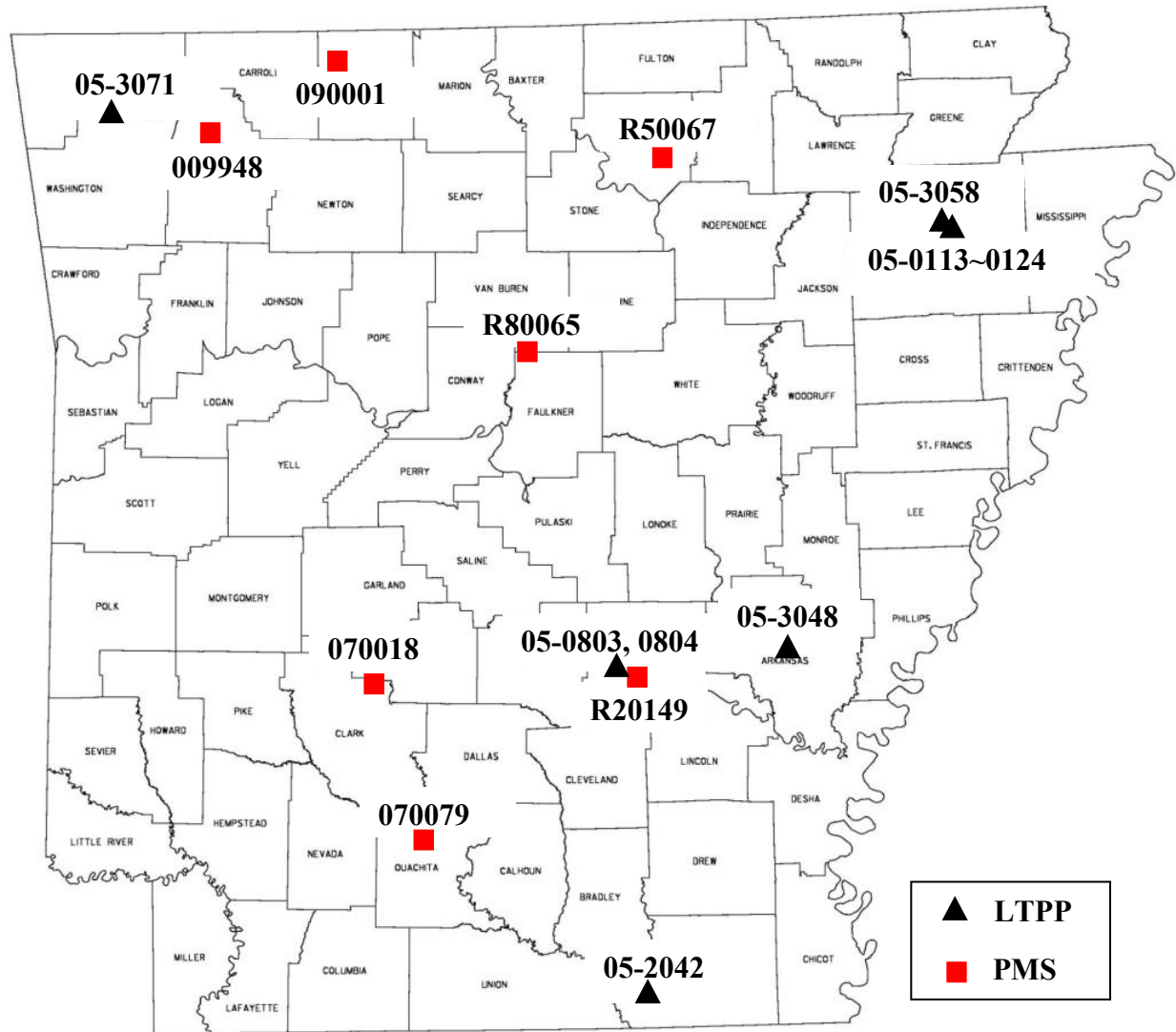


Figure 3.4 Pavement sections used to calibrate new flexible pavement models in Arkansas.

3.3.1 Structure and Materials

Data of LTPP sections were retrieved from the Standard Data Release 24 which was released on January 2010. Data of the TOP25 sections were prepared from raw data provided by AHTD.

Table 3.3 shows the pavement structure. Half amount of the sections had 4 inch to 8 inch HMA surface. Base materials included uncrushed gravel, crushed stone, asphalt treated base, permeable asphalt treated base, and cement treated base. There were also six full-depth sections.

Table 3.3 Pavement structure of calibration sections

Program	Site ID	Thickness (in.)		Subgrade Type
		AC	Base	
SPS-2	0113	4	8.1 Uncrushed Gravel	A-2-4
SPS-2	0114	6.9	11 Uncrushed Gravel	A-2-4
SPS-2	0115	7	7.4 ATB	A-2-4
SPS-2	0116	4.1	11.8 ATB	A-2-4
SPS-2	0117	6.9	3.8 ATB/4.2 Crushed stone	A-2-4
SPS-2	0118	4.1	7.9 ATB/3.5 Crushed stone	A-2-4
SPS-2	0119	6.8	3.4 PATB/4.1 Crushed stone	A-2-4
SPS-2	0120	4.3	3.2 PATB/8.1 Crushed stone	A-2-4
SPS-2	0121	4.4	3.1 PATB/12.1 Crushed stone	A-2-4
SPS-2	0122	4.4	4.1 ATB/3.5PATB/Geotextile	A-2-4
SPS-2	0123	7.2	8.2 ATB/3.5PATB/Geotextile	A-2-4
SPS-2	0124	6.9	11.1 ATB/3.7PATB/Geotextile	A-2-4
SPS-8	0803	3.7	7.3 Crushed stone	A-6
SPS-8	0804	7.3	12.7 Crushed stone	A-6
GPS-2	2042	5.2	6.6 CTB	A-4
GPS-2	3048	5.2	7.4 CTB	A-2-4
GPS-2	3058	6	7.3 ATB	A-3
GPS-2	3071	5.9	10.5 ATB	A-6
TOP25	R20149Good	13.5	12 Class 5	A-7-6
TOP25	R20149Poor	13	13 Class 7	A-4
TOP25	090001Good	8.75	7.25 Class 7	A-4
TOP25	090001Avg	10.25	7.75 Class 7	A-4
TOP25	090001Poor	9.5	6.5 Class 7	A-4
TOP25	009948Good	10	6.5 Class 7	A-4
TOP25	009948Avg	9.25	6.75 Class 7	A-4
TOP25	009948Poor	9	7 Class 7	A-4
TOP25	R80065Good	13.25	NO BASE	A-2-7
TOP25	R80065Avg	14.75	NO BASE	A-2-7
TOP25	R80065Poor	16.5	NO BASE	A-2-7
TOP25	070079Good	6.25	8 Class 7	A-4
TOP25	070079Avg	5.5	8 Class 7	A-4
TOP25	070079Poor	6	8 Class 7	A-4
TOP25	070018Good	11.5	13 Class 5	A-4
TOP25	070018Avg	10.5	13 Class 5	A-4
TOP25	070018Poor	11.5	9 Class 5	A-4
TOP25	R50067Good	13	NO BASE	A-4
TOP25	R50067Avg	12.75	NO BASE	A-4
TOP25	R50067Poor	13.75	NO BASE	A-4

Note: ATB is asphalt treated base; CTB is cement treated base; PATB is permeable asphalt treated base; Class 5 and Class 7 are two types of aggregate base used in Arkansas.

3.3.2 Traffic

All sections in SPS-1 site were considered as the same location; therefore, the same climate state and traffic data could be used. Traffic data are listed in Table 3.4. It was found that LTPP sections were older than TOP25 sections. The old age of LTPP sections drew a concern on the HMA materials. Since the Superpave mix design method was not implemented in Arkansas until the end of 1990s, HMA mixtures in the LTPP projects were most likely designed using the Marshall method. Data in Table 3.4 also indicated that traffic volume covered different levels of road from 10 vehicles per day to 25,000 vehicles per day.

Table 3.4 Traffic data of calibration sites

Site ID	Traffic Open Date	Age, year	AADT	AADTT	Growth Rate, %	Truck Percent, %	Functional Class
01**	9/1/1994	16	8200	1695	2.8	0.0	2
08**	12/1/1997	13	10	10	0	0	17
2042	12/1/1972	38	3400	646	4.2	19.0	2
3048	12/1/1981	29	900	162	2.4	18.0	2
3058	2/1/1990	20	3860	810	6.9	21.0	12
3071	7/1/1987	23	10840	1897	2.8	17.5	2
R20149	5/1/2001	9	5300	848	1.2	16.0	2
090001	6/1/2000	10	6800	884	2.1	13.0	2
009948	5/1/2000	10	3400	377	4.2	11.1	2
R80065	11/1/2000	10	7000	1134	2.7	16.2	2
070079	11/1/1999	11	1500	80	0	5.3	7
070018	11/1/2000	10	25000	10475	2.2	41.9	1
R50067	7/1/2002	8	5100	270	1.2	5.3	6

Note: 01** contains section 0113 to 0124; 08** contains section 0803 and 0804.

3.3.3 Performance

For calibration purpose, historical performance data are required. The LTPP database contains monitored data which were collected by experienced technicians according to the *LTPP Distress Identification Manual*. The pavement performance parameters are alligator cracking, longitudinal cracking, transverse cracking, rutting and IRI.

LTPP contains two types of cracking data for flexible pavements. One is manual inspection in the field (MON_DIS_AC_REV); the other is interpreted from 35 mm black and white photographs using PADIAS software (MON_DIS_PADIAS42_AC). Most of cracking data available for Arkansas were manual inspected; therefore, the difference between manual and automatic methods was ignored in this study. Paper record of manual distress survey on TOP25 sections were provided by AHTD. Two engineers manually interpreted the distress according to the *LTPP Distress Identification Manual*. Therefore, distress data of LTPP sections and TOP 25 sections were analyzed together.

Although it has been noted that the variability of distress measurement influences the accuracy of model calibration, all measurements from LTPP and TOP25 were considered as the best data available fulfilling distress measurement specifications. Table 3.5 shows the average and standard deviation of measured distresses. It was noted that the overall (average) performance was relatively low comparing to the design criteria. For instance, the average total rutting was 0.19'' and the design criterion of total rutting was 0.75''. In addition, the variation of longitudinal cracking and transverse cracking was extremely large, which could be converted to coefficient of variation as 200% and 250%, respectively. One could also notice that there were more than 50% zeros in the measured cracking data.

Figures 3.5 through 3.9 show the measured performance for each distress respectively. They are time series data grouped by LTPP and TOP25. Generally speaking, the increasing trend of alligator cracking was not distinctive as either linear or exponential. On the contrary, longitudinal cracking grow quickly (could be exponential) from the 6th year to the 10th year.

Table 3.5 Summary of Measured Distress

Distress	Design Criteria	Average	Std. Dev.	Min.	Max.	Zero Measurement, %
Total Rutting, in	0.75	0.19	0.07	0.02	0.45	0
Alligator Cracking, %	25	2.1	4.9	0.0	37.3	57.2
Long. Cracking, ft/mi	2000	860	1735	0	10243	54.8
Trans. Cracking, ft/mi	1000	131	328	0	2429	53.2
IRI, in/mi	172	72.9	19.3	36.6	128.6	0

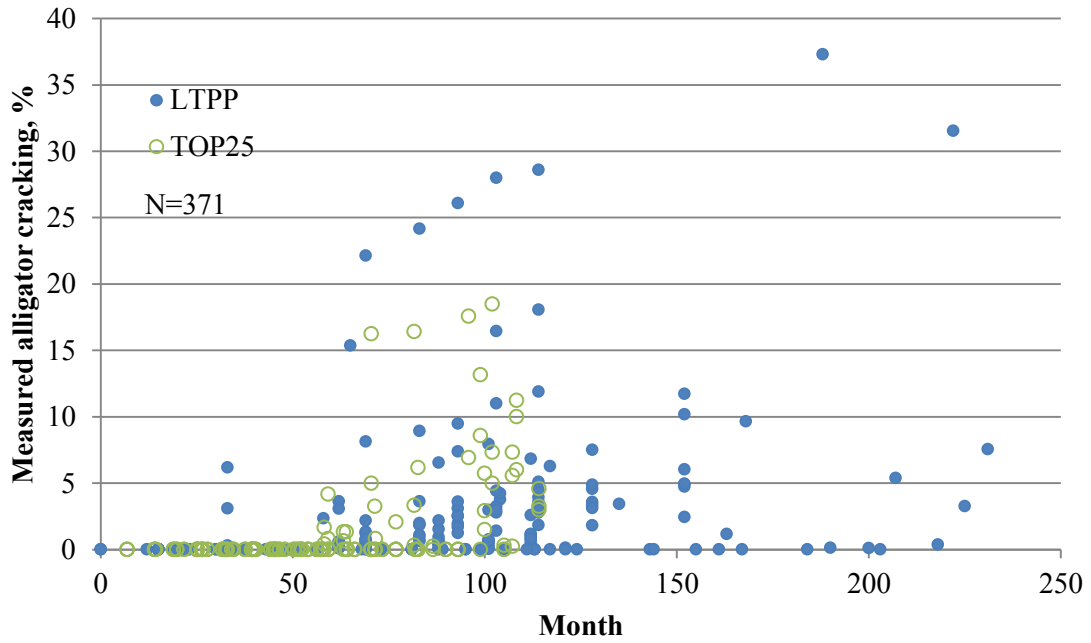


Figure 3.5 Measured alligator cracking

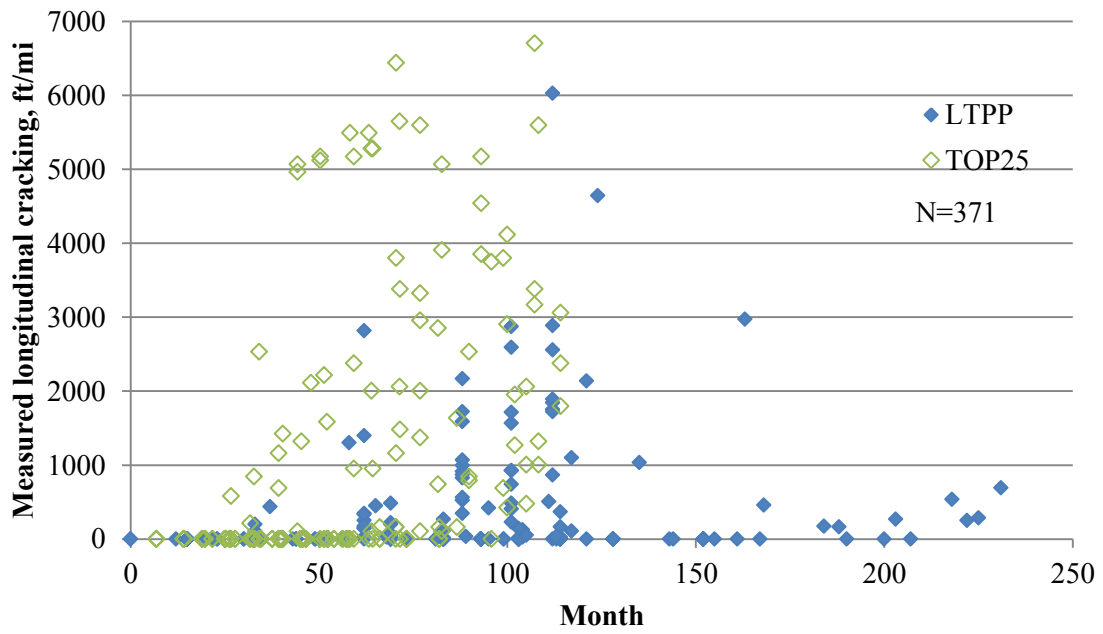


Figure 3.6 Measured longitudinal cracking

Very few transverse cracking were observed in LTPP sections, but TOP25 projects had some transverse cracking recorded. This led to two speculations: (1) different asphalt binders were used in the two systems LTPP and TOP25, considering that LTPP sections were built before Superpave was implemented in Arkansas while TOP25 projects were all Superpave mixtures (Table 3.4); (2) transverse cracking could have been defined and surveyed differently, considering that LTPP sections were surveyed by contractors and certified distress raters while TOP25 sections were surveyed by staff at AHTD. Further investigation is needed to justify these speculations.

The overall trend for total rutting and IRI was distinctive, but the variance was large. Eighty percent of the pavement sections had 0.1 to 0.3 inches of rutting, even for the sites older than 15 years. This suggested either: (a) rutting reached a maximum of 0.3 inches by consolidation under traffic, without plastic failure; or (b) rutting measurements (typically by straightedge) were recorded as a maximum of 0.3 inches regardless of the actual measurement.

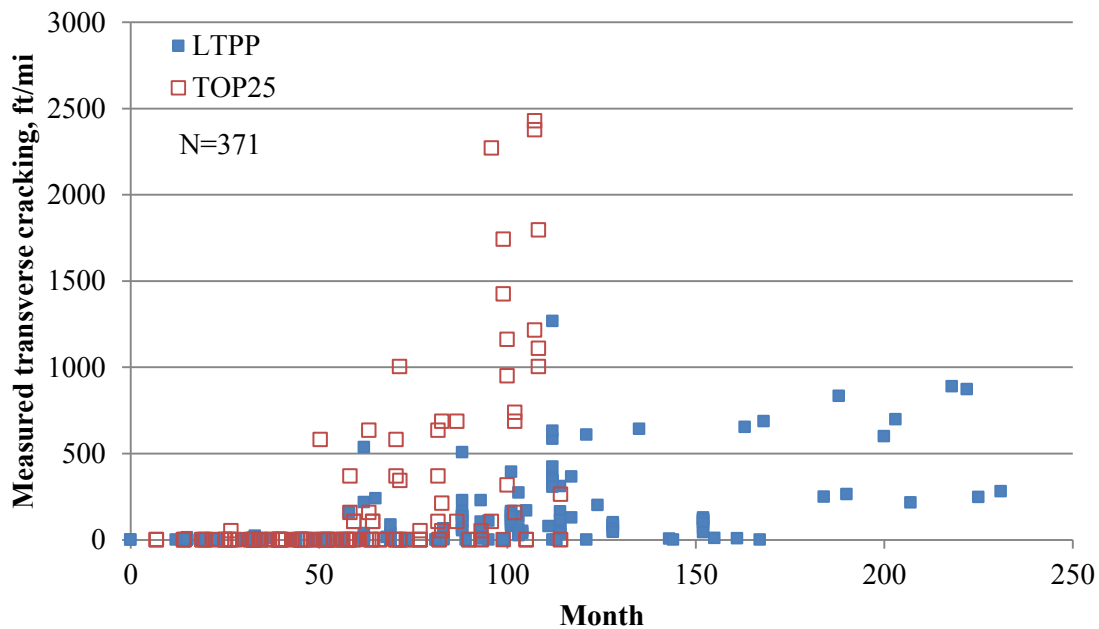


Figure 3.7 Measured transverse cracking

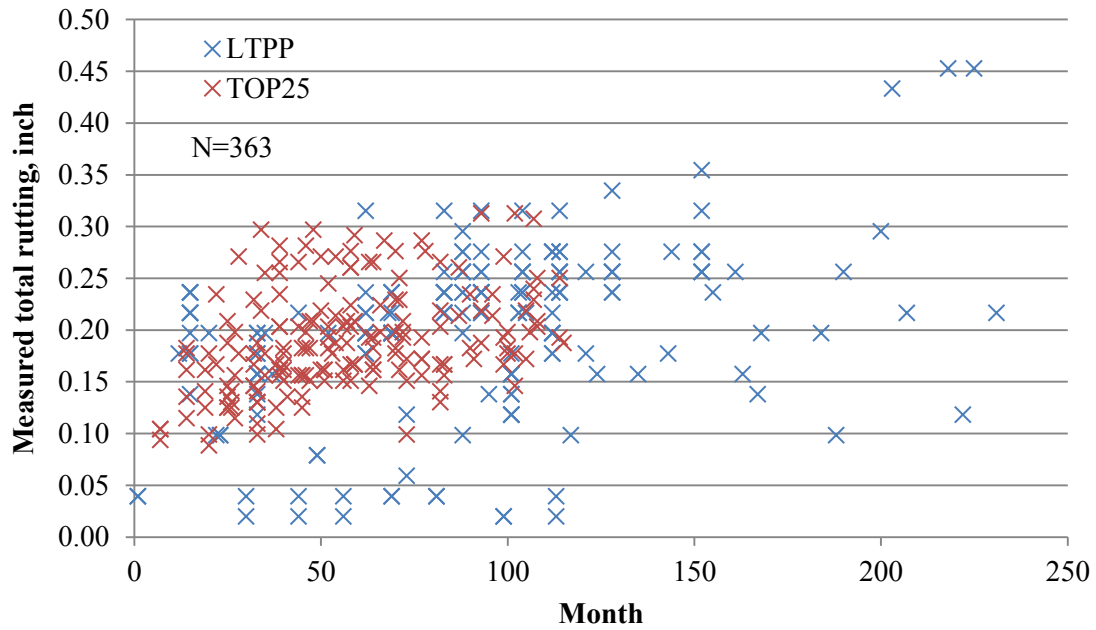


Figure 3.8 Measured total rutting

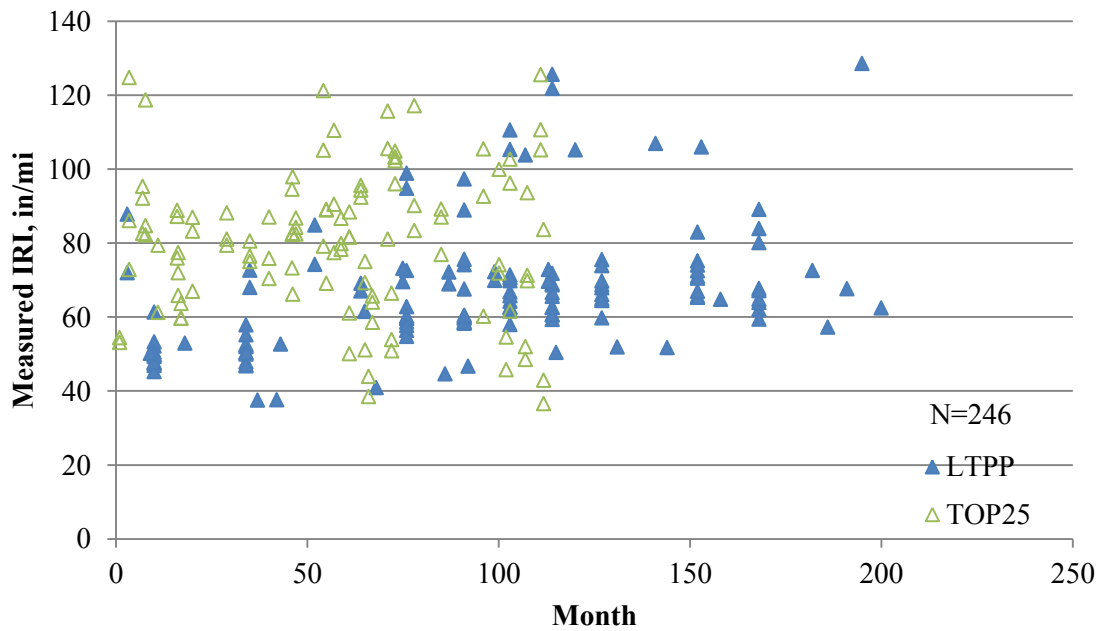


Figure 3.9 Measured IRI

3.4 Verification and Calibration

3.4.1 Hierarchical Input

MEPDG defined three levels of input. Level 1 was the most accurate input normally involving comprehensive laboratory or field tests. In contrast, Level 3 used national default values or engineering judgment based on experience with little or no testing. Inputs at Level 2 were estimated through correlations with other material properties that were measured in the laboratory or field. Statewide inputs were also considered as Level 2 input (13).

In this study, all available data were retrieved from LTPP and TOP25 database. In case of missing data, statewide default (Level 2) or national default values (Level 3) were used. In summary, Table 3.6 shows the input level for all parameters.

Table 3.6 Input levels used in this study

Data needed for MEPDG		Input Level	Data Source
General Information	Design life	2	Arkansas specification
	Base construction time	1	Assumed to be one month before pavement construction time
	Pavement construction time	1	Assumed to be the same as open to traffic time
	Open to traffic time	1	
	Site location	1	
	Route	1	
	Section	1	
	Log mile	1	
	Traffic direction	1	
Analysis parameters	3		
Traffic	Initial AADTT	1	
	Number of lanes	1	
	Truck percentage	1	
	Direction distribution	2	According to TRC-0402
	Lane distribution	2	According to TRC-0402
	Operational speed	1	Posted truck speed
	Monthly adjustment	3	

Data needed for MEPDG	Input Level	Data Source
Hourly adjustment	3	
Vehicle class distribution	2	According to TRC-0402, TTC
Traffic growth factor	1	
Axle load distribution factors	2	According to TRC-0402, statewide input
General traffic inputs	3	
Number axle/truck	3	
Design lane width	1	
Climate		
GPS coordination	1	
Elevation	1	
Water table depth	1	USGS
Weather station	3	Use MEPDG to generate climate files
Structure		
Material types	1	
Thickness of each layer	1	
Thermal properties	3	
HMA surface		
Aggregate gradation	1	Testing data or design record
Binder grade	1	
Effective binder content	1	Based on volumetric properties
As-built air voids	2	Arkansas specification
Total unit weight	2	Based on volumetric properties
Poisson's ratio	3	
Dynamic modulus	3	Global model
Bound Base		
Strength	3	
Unit weight	3	
Poisson's ratio	3	
Unbound Base		
Resilient modulus	3	Default value to the material type
Poisson's ratio	3	
Sieve analysis	1	
Atterberg Limit	1	
Maximum dry unit weight	1	
Optimum water content	1	
Subgrade		
Resilient modulus	3	Default value to the subgrade type
Poisson's ratio	3	
Sieve analysis	1	
Atterberg Limit	1	
Maximum dry unit weight	1	
Optimum water content	1	

Some important assumptions are listed below.

- If the construction time was unknown, it was assumed that surface was completed one month later of base completion, and the open-to-traffic data was the same as the surface completion date.
- Default values were accepted for analysis parameters, i.e., initial IRI=63 in/mi and terminal IRI = 172 in/mi.
- Recommendations about traffic input from project TRC0402 were used. Therefore, it was statewide Level 2 input. The posted truck speed limit was considered as the operational speed. Compound growth rate was calculated from AADT records.
- The latitude and longitude were used to generate a virtual weather station for each site. The water table depth was from the ground water sites retrieved from the National Water Information System provided by United States Geological Survey (USGS). The closest site to the calibration section with available data was used.
- Level 3 defaults were used for resilient modulus of granular base and subgrade in TOP25 sites. Geotextile was not modeled in MEPDG.

3.4.2 Alligator Cracking

Figure 3.10 shows the comparison of measured alligator cracking with predicted alligator cracking using the national calibrated model. It was found that the national model underestimated alligator cracking for the most cases. Especially for TOP25 sections, no alligator was predicted from MEPDG. But there was alligator cracking surveyed from the field.

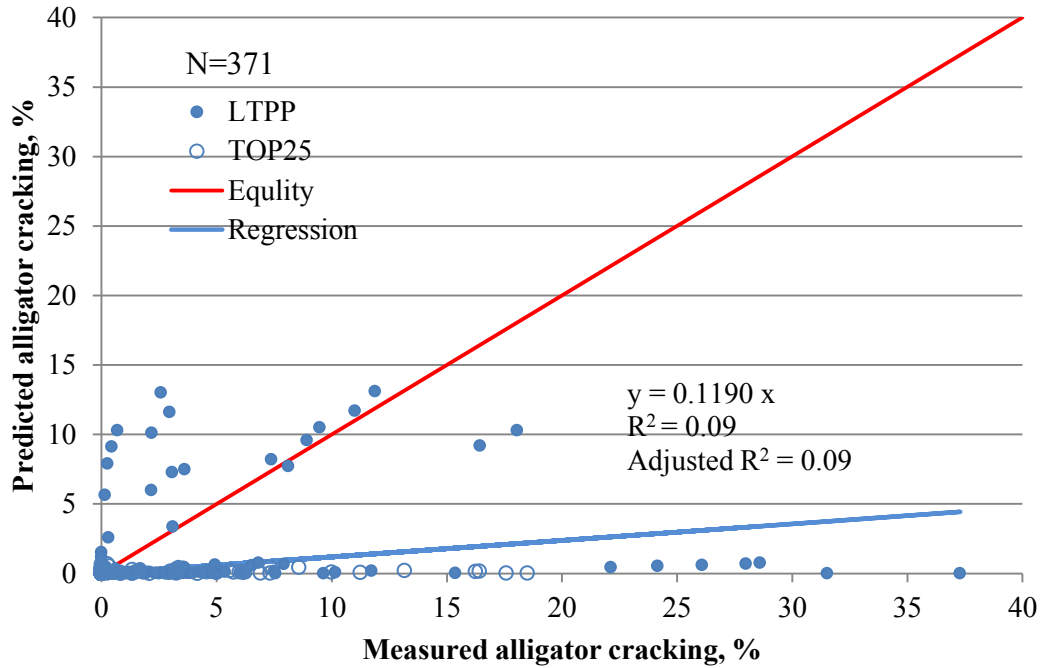


Figure 3.10 Verification of the alligator cracking model

Equation 3.1 is the bottom-up cracking model in MEPDG:

$$F.C.bottom_up = \left(\frac{6000}{1 + e^{(C_1 * C_1' + C_2 * C_2' * \log_{10}(D * 100))}} \right) * \left(\frac{1}{60} \right) \quad (3.1)$$

where D = bottom_up damage

$$C_1 = 1.0$$

$$C_2 = 1.0$$

$$C_1' = -2 * C_2'$$

$$C_2' = -2.40874 - 39.748 * (1 + h_{ac}) - 2.856$$

h_{ac} = AC thickness

To reduce the bias and variation, Excel Solver was used to reduce the Sum of Standard

Error (SSE) by adjusting C_1 and C_2 .

$$SSE = \sum_{i=1}^N (\text{predicted} - \text{measured})^2 \quad (3.2)$$

The calibrated alligator cracking is shown in Figure 3.11.

To statistically test the existence of bias, the Z-Test was conducted on the national model and calibrated model. The hypothesis was H_0 : the difference between the mean of measured and predicted alligator cracking is zero. It was found in Table 3.7 that the alligator cracking model was significantly improved by calibration process. However, the regression coefficient between prediction and measurement was still very poor. The alligator cracking model needed further calibration, or maybe the alligator cracking model in MEPDG needed further improvement (44).

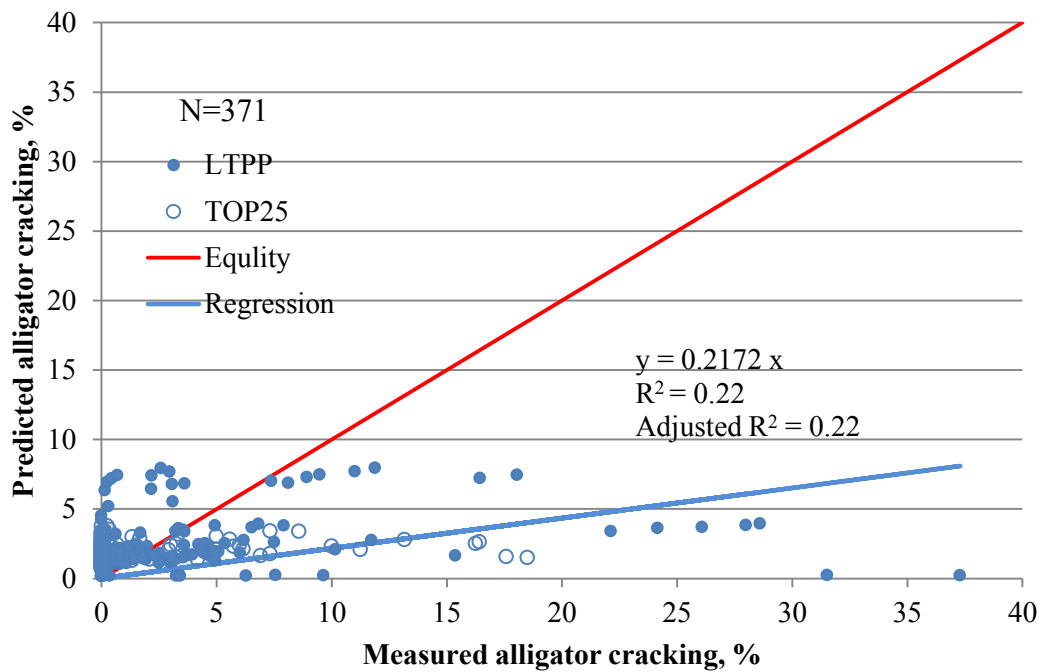


Figure 3.11 Calibrated alligator cracking

Table 3.7 Summary of paired Z-Test for alligator cracking model

Parameters	Verification		Calibration	
	Measured	Predicted	Measured	Predicted
Mean	2.07	0.55	2.07	2.01
Known Variance	24.04	4.27	24.04	2.09
Observations	371	371	371	371
Hypothesized Mean Difference	0		0	
z	5.49401		0.232773	
P(Z<=z) one-tail	1.96E-08		0.407969	
z Critical one-tail	1.644854	Reject	1.644854	Accept
P(Z<=z) two-tail	3.93E-08		0.815938	
z Critical two-tail	1.959964	Reject	1.959964	Accept

It was worth noting that MEPDG underestimated alligator cracking for these calibration sections. This seemed reasonable considering that most of these sections had thick pavement structures (Table 3.1). Another reason could come from the cracking survey and interpretation. The difficulty of cracking interpretation had been realized by many researchers (45) (46) (47). In MEPDG, alligator cracking is a type of load related fatigue cracking that starts at the bottom of pavement layers and propagates to the surface. Bottom-up fatigue cracking first shows up as short longitudinal cracks in the wheelpath then quickly spreads and becomes interconnected to form a chicken wire/alligator cracking pattern. The distinction between alligator cracking and longitudinal cracking is very subjective. In this study, it had been tried to consider longitudinal cracking in wheelpath as alligator cracking (area = length * 1 ft). But no improvement was achieved.

Interpreting cracking from the *Manual Distress Survey Form* was another concern. As shown in Figure 3.12, the location, length and width of cracks in the 100 ft long pavement were recorded in a letter size (8.5 by 11 inches) paper. The accuracy would be better if cracks were

measured and classified in the field, or in-house interpretation based on digital pictures. Automatic distress survey and interpretation could be another alternative.

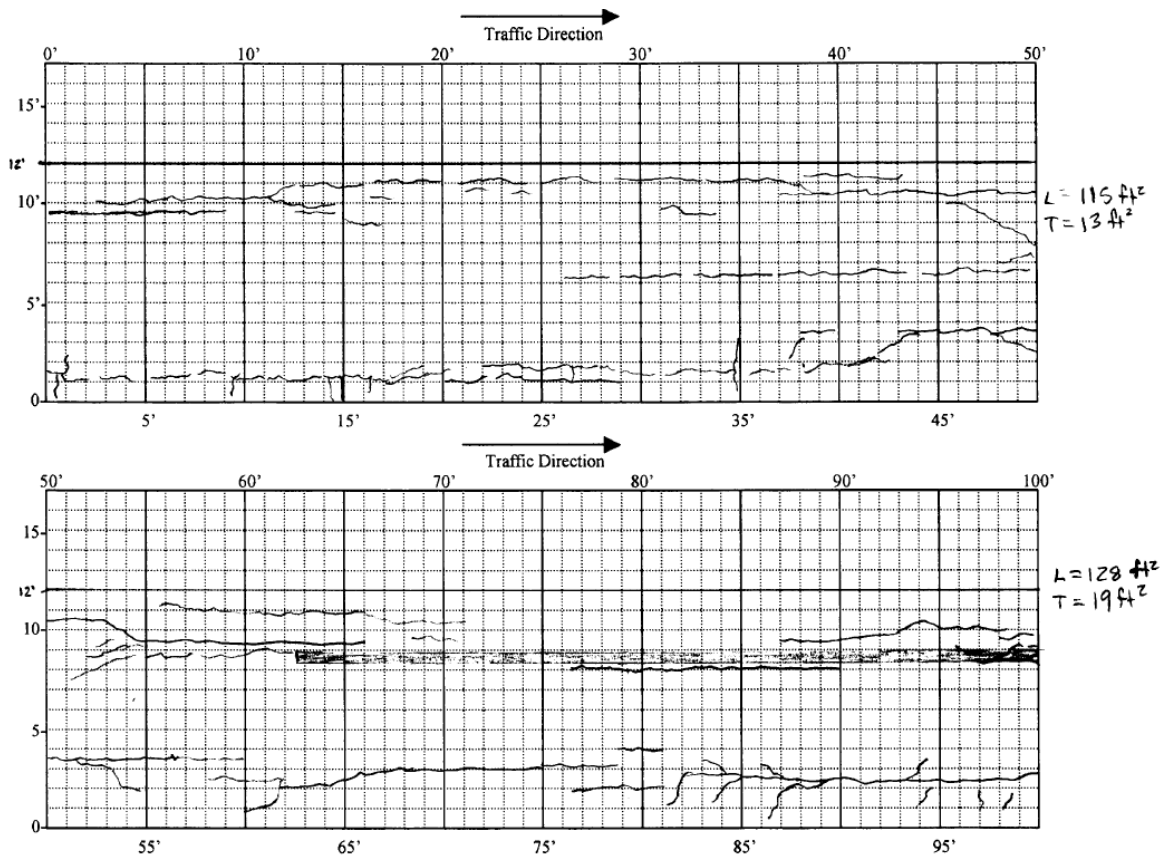


Figure 3.12 Manual distress survey record of the R80065 Good section (2009).

Two more observations should also be pointed out:

- Fatigue Cracking: Both alligator cracking and longitudinal cracking predicted by MEPDG were forms of fatigue cracking. Transfer functions were used to predict visual cracking from mechanistic “damage” at the bottom and top of HMA layers. This made the HMA layer thickness to be an extremely significant factor affecting performance predictions.
- Asphalt Treated Base (ATB): Although ATB is a type of stabilized base, it was not modeled as “Stabilized Base” but as “Asphalt” (albeit with a reduced

stiffness). Therefore, the HMA layer in the sections with asphalt treated base became very thick in the MEPDG, which reduced the stress and strain at the bottom and top of the HMA layer, in turn reduced the predicted alligator cracking and longitudinal cracking. The other method to model ATB conservatively can be by considering it as “Granular Base” with an increased stiffness, which is moisture sensitive instead of temperature sensitive. However, both methods could induce errors into predicted distresses.

3.4.3 Rutting

Permanent deformation in MEPDG is modeled on all layers, HMA surface, unbound base, and subgrade. The sum of deformation in each layer is the total rutting, which is the measured rutting in field. Although the composition of rutting could be measured by coring and trenching, only the total rutting was validated in this study. Figure 3.13 shows the comparison of measured total rutting and predicted total rutting from national models. In general, national rutting models performed better than cracking models. The R square was 0.88, although MEPDG over predicted rutting.

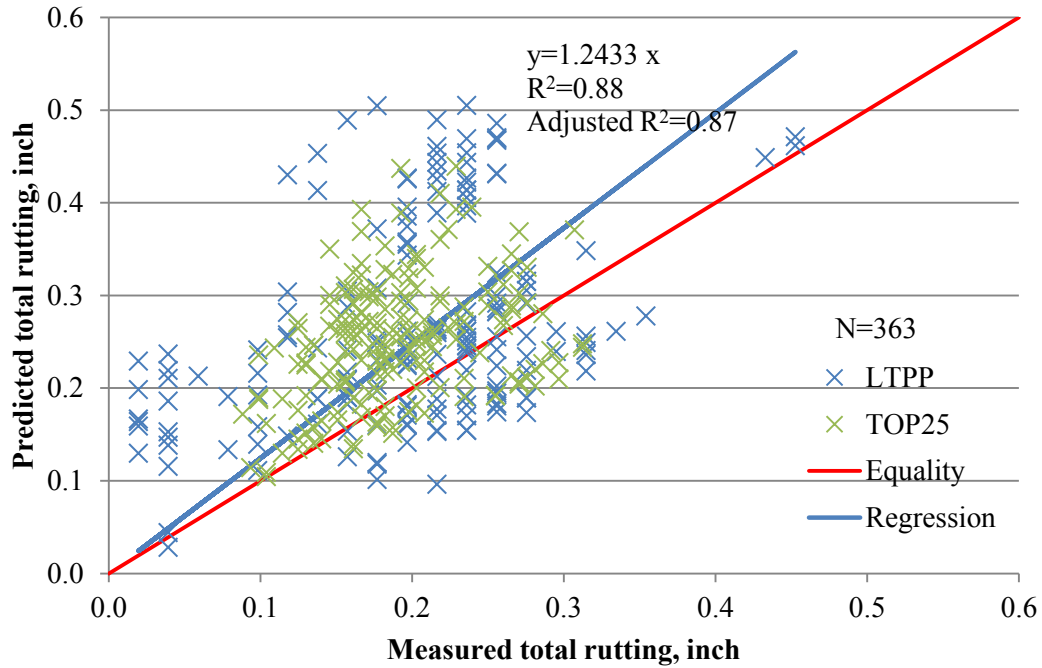


Figure 3.13 Verification of rutting model

To further understand the composition of the total rutting, rutting in HMA layer, base and subgrade as predicted by MEPDG were compared with the total rutting in Figure 3.14, 3.15 and 3.16, respectively. It was found that most of the rutting in base was less than 0.05 inch. Therefore, the calibration coefficient of rutting in base ($\beta_{sI}=1.0$) was not calibrated in this study, because it had little influence on the total rutting.

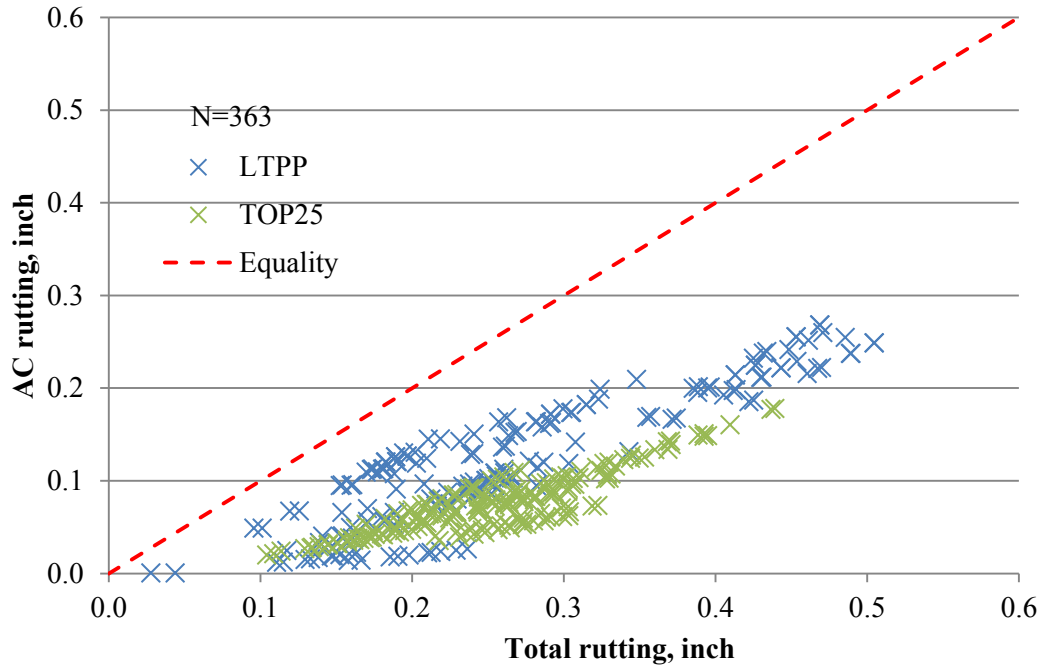


Figure 3.14 Composition of total rutting (AC)

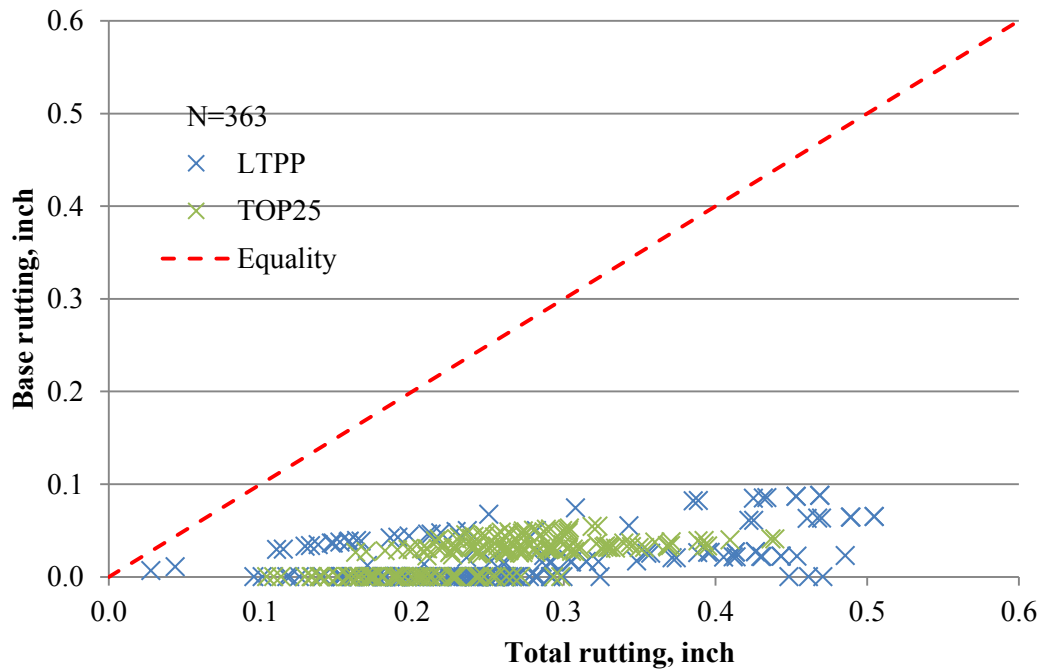


Figure 3.15 Composition of total rutting (Base)

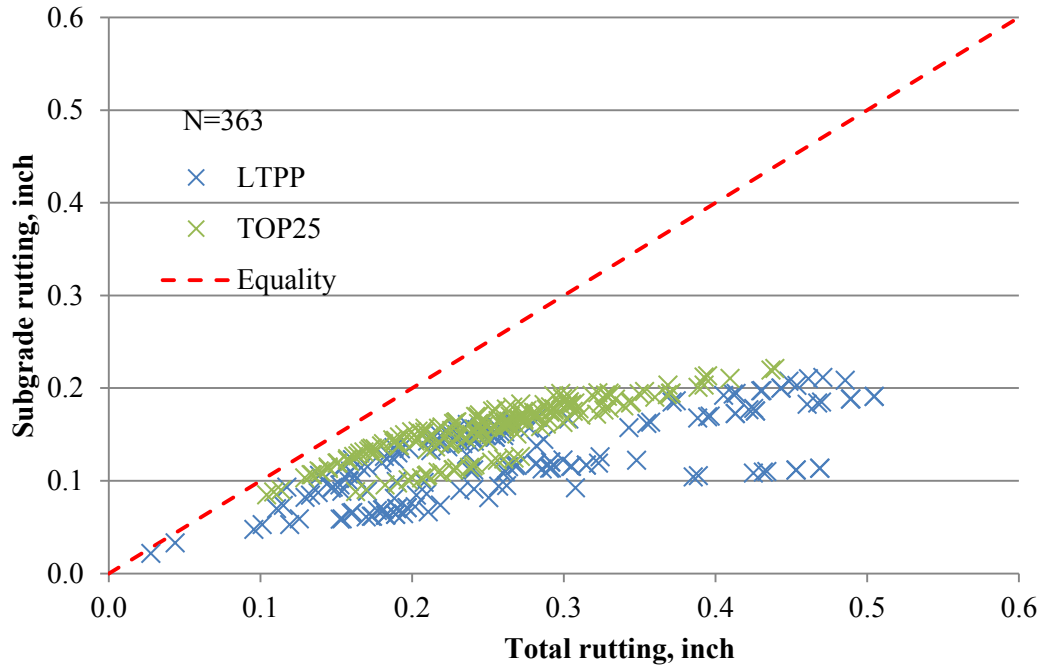


Figure 3.16 Composition of total rutting (Subgrade)

Calibration of the rutting model was conducted by adjusting coefficient β_{r1} for HMA and β_{s2} for subgrade. The following model was obtained:

$$TRUT = 0.68 * ACRUT + 1.0 * BASERUT + 0.85 * SUBRUT \quad (3.3)$$

where $TRUT$ = Total rutting.

$ACRUT$ = Rutting in HMA layers.

$BASERUT$ = Rutting in base layers.

$SUBRUT$ = Rutting in the subgrade.

Figure 3.17 shows the comparison of calibrated models. Note that the slope was 0.9843 with a R square of 0.87. The improvement was also proved by statistical testing as shown in Table 3.8. With $\alpha=0.05$, the rutting model was statistically improved. However, further improvement/calibration could still be necessary to increase the accuracy and reduce the dispersion of the rutting model.

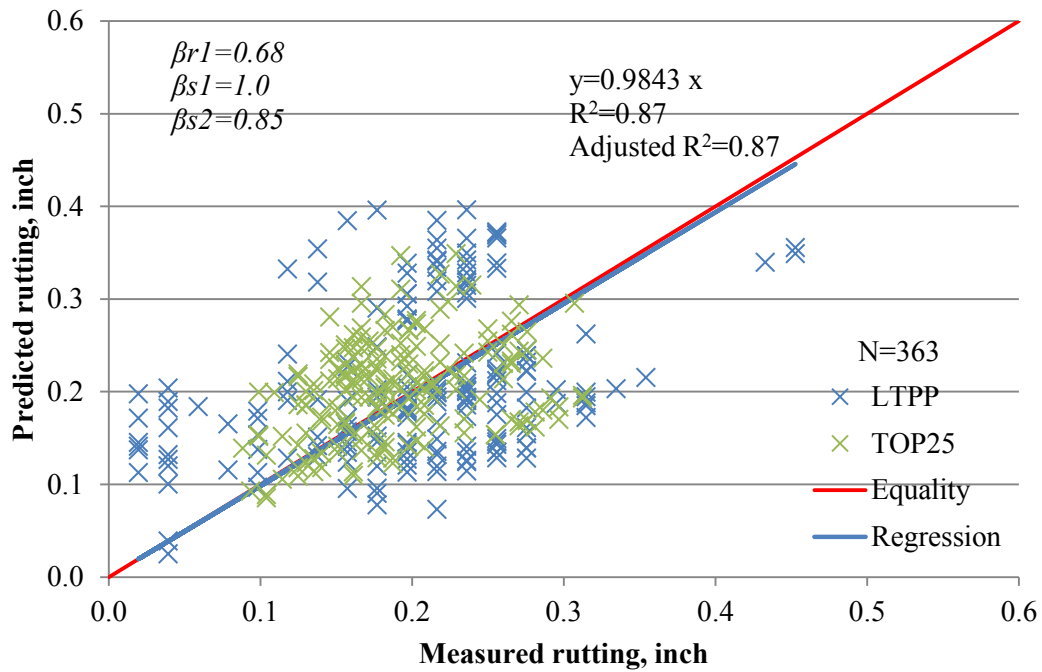


Figure 3.17 Calibration of rutting model

Table 3.8 Summary of Z-test for rutting models

Parameters	Validation		Calibration	
	Measured	Predicted	Measured	Predicted
Mean	0.194	0.259	0.194	0.186
Known Variance	0.00449	0.00784	0.00449	0.00339
Observations	363	363	363	363
Hypothesized Mean Difference	0		0	
z	-11.008		1.909343	
P(Z<=z) one-tail	0		0.028109	
z Critical one-tail	1.644854	Reject	1.644854	Reject
P(Z<=z) two-tail	0		0.056218	
z Critical two-tail	1.959964	Reject	1.959964	Accept

3.4.4 Longitudinal Cracking

Figure 3.18 shows the comparison of predicted and measured longitudinal cracking. It was found that MEPDG did not predict many longitudinal cracking for all calibration sections used in this research. For one reason, as stated above, the distress survey of top-down cracking is debatable, especially when the mechanism of top-down cracking is considered. For another reason, the mechanism of top-down cracking has not been well understood yet; hence the model in MEPDG needs future improvement. Due to the nature of the data, the longitudinal cracking model was not calibrated in this study.

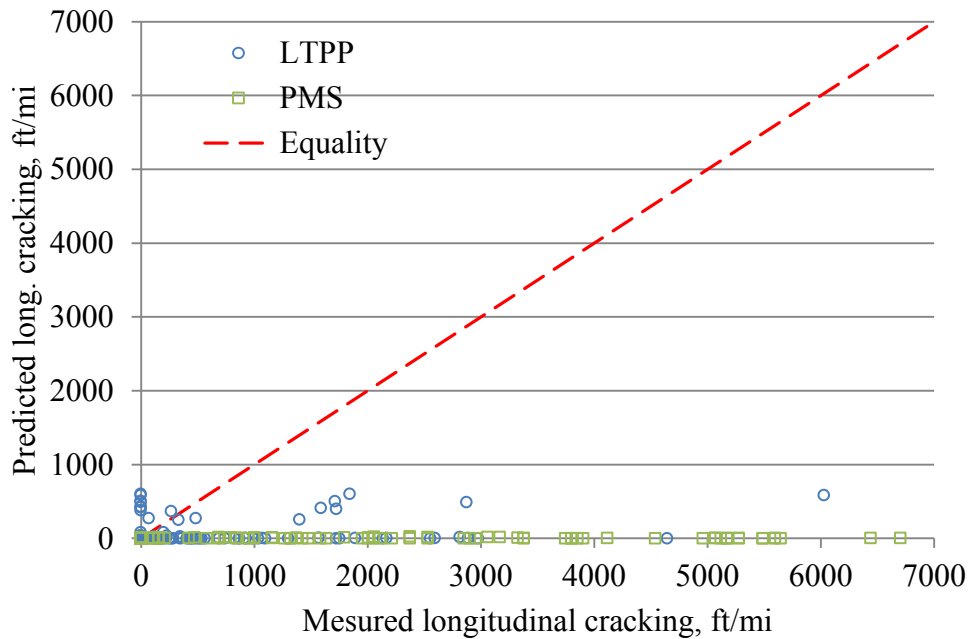


Figure 3.18 Verification of national calibrated longitudinal cracking model

3.4.5 Transverse Cracking

The transverse cracking is presented in Figure 3.19. One would not expect there to be any transverse cracking in Arkansas pavements with the advent of Performance Graded binders and the proper selection of those binders. As shown in Figure 3.19, MEPDG did not predict any thermal cracking when the right binder grade (PG64-22, 70-22 and 76-22) was used in Arkansas.

But this did not agree with the observation. It had been noticed that transverse cracking in the MEPDG was primarily related to thermal cracking, caused by thermal stress in pavement. However, transverse cracking in LTPP database and PMS were measured according to the *LTPP Distress Identification Manual*, in which transverse cracking was defined as *cracks that are predominately perpendicular to pavement centerline* (48). The implementation of Performance-Graded (PG) binders for HMA in Arkansas had all-but eliminated thermal cracking in flexible pavements; accordingly the MEPDG predicted no thermal cracking for Arkansas climate and a properly selected PG binder. However, transverse cracking was recorded in distress surveys, suggesting that (1) additional cracking mechanisms could be predominate in Arkansas, or (2) the PG grading was not the complete answer to transverse cracking, or (3) the wrong PG grade was used, or (4) some of the asphalt did not actually comply with the grading. At the very least, this showed that transverse cracking needed to be studied further. Due to the nature of the data, transverse cracking model was not calibrated in this research.

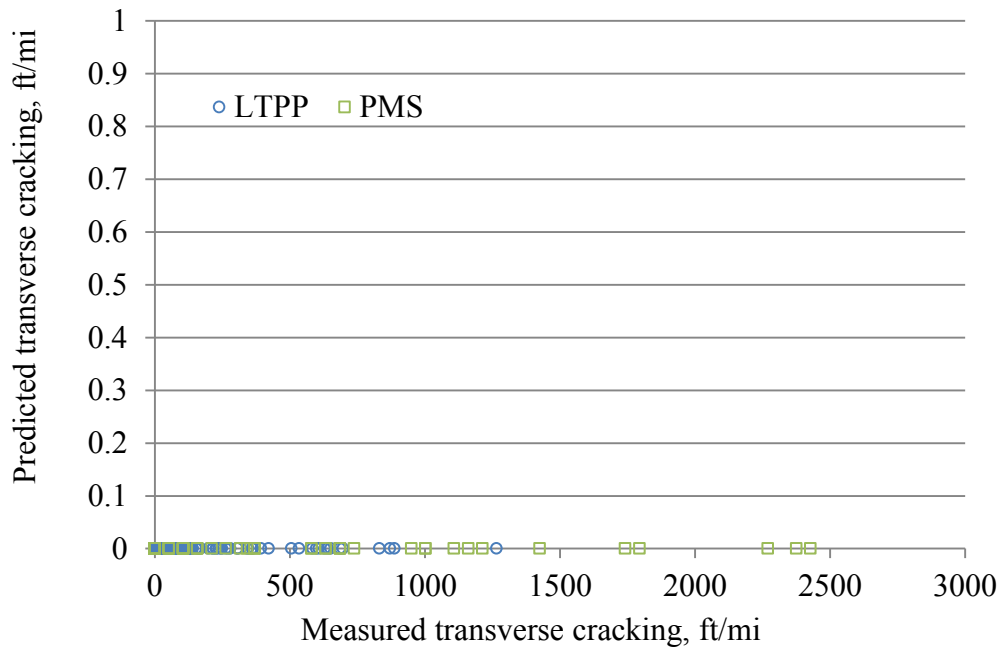


Figure 3.19 Verification of national calibrated longitudinal cracking model

3.4.6 Smoothness (IRI)

Figure 3.20 shows the comparison of predicted and measure IRI. This model apparently performed better than the longitudinal cracking and transverse cracking. But it seemed that MEPDG prediction had smaller variation (range from 60 to 100 in/mi) than the variance of measurement from field (range from 40 to 120 in/mi). Since the predicted IRI was a function of other predicted distresses (alligator cracking, longitudinal cracking and rutting), the smoothness (IRI) model was not calibrated.

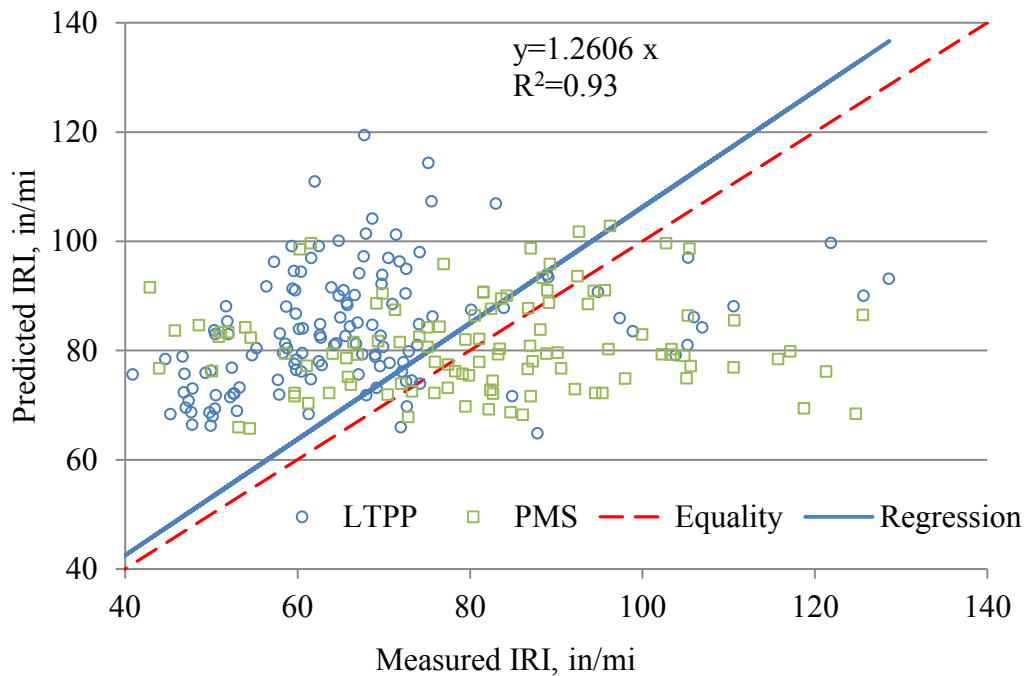


Figure 3.20 Verification of national calibrated IRI model

3.5 Validation

The calibrated models were validated by running the MEPDG on the remaining eight sections (Table 3.1) using adjusted calibration coefficients. The predicted and measured performance was compared and shown in Figure 3.21. It was clear that local calibration reduced the difference

between predicted and measured distresses; but additional efforts (sites, data) would be necessary to further reduce this difference.

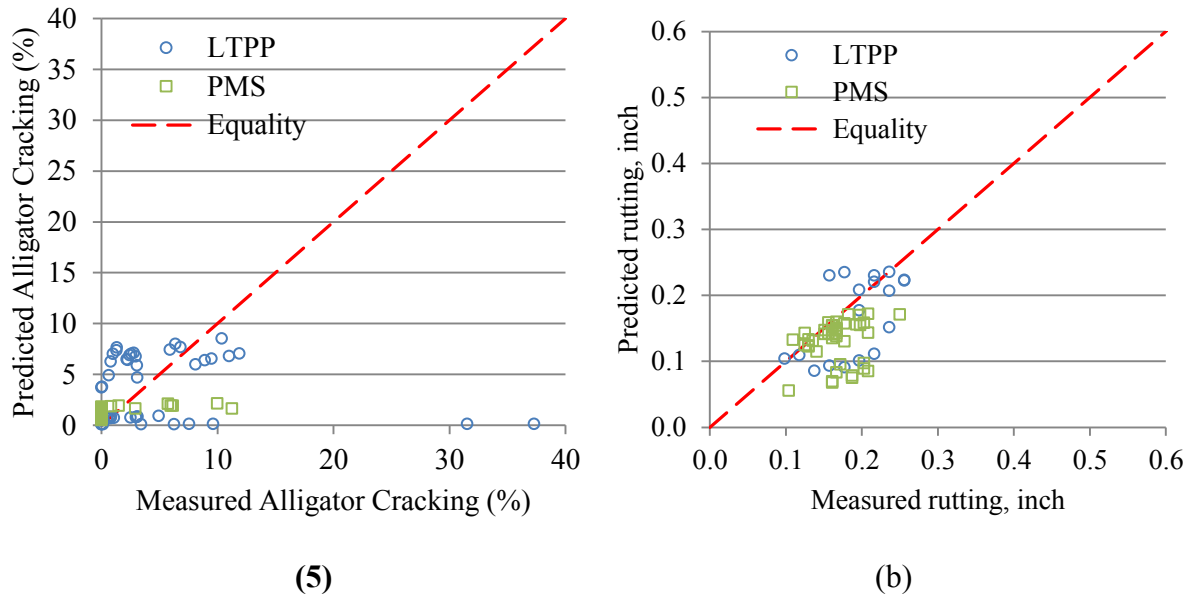


Figure 3.21 Validation of calibrated (a) alligator cracking and (b) rutting models.

3.6 Summary

In summary, the objective of local calibration was to reduce the possible bias and variation from the national calibrated models. All performance models of new flexible pavement were verified. MEPDG seemed to underestimate all types of cracking and overestimate rutting. However, issues of cracking measurement and interpretation were big concerns that influence the verification and calibration of MEPDG. According to MEPDG, Arkansas had no problem with thermal cracking. Longitudinal cracking and transverse cracking models were not recommended for calibration at this time due to the limitation of the models and the difficulty of distress measurement. IRI model was not calibrated due to its empirical nature with other models. Alligator cracking and rutting models were calibrated. Table 3.9 lists the recommended

calibration coefficients for Arkansas. The correlation between measured and predicted performance was improved through local calibration.

Table 3.9 Summary of calibration coefficients

Calibration Factor	National Default	Arkansas
Alligator cracking		
C_1	1.0	0.654
C_2	1.0	0.263
C_3	6000	6000
AC rutting		
β_{r1}	1.0	0.68
B_{r2}	1.0	1.0
B_{r3}	1.0	1.0
Base rutting		
β_{s1}	1.0	1.0
Subgrade rutting		
β_{s2}	1.0	0.85

CHAPTER 4 RISK ANALYSIS

Risk can be defined as someone or something that creates or suggests a hazard according to the Webster dictionary. In this perspective, uncertainty and variation in pavement design as discussed in Chapter 2.3 are risks that could jeopardize a successful pavement design. This chapter is to conduct a risk assessment of the pavement design process.

4.1 Introduction

Pavement is an important part of public asset that need to be well designed, constructed and maintained. The challenge of building better and cheaper pavements has driven the pavement engineering moving forward. According to the Federal Highway Administration (FHWA), the percentage of pavements with good ride quality had risen sharply over time, from approximately 39% in 1997 to about 57% in 2006 (49).

However, there are new challenges to be addressed. First, cost escalation is a serious problem for state highway agencies (SHAs), especially in a time of economic downturn. A study by Flyvbjerg et. Al (50) found that project costs were underestimated for approximately 90% of the 258 projects examined and their actual costs were in average 28% higher than the estimated cost. If a SHA fails to deliver individual projects and programs within established budgets there is a detrimental effect on later programs and a loss of faith in the agency's ability to wisely use the public's money (51).

Second, the importance of life-cycle cost analysis (LCCA) is growing. It has been realized that initial construction cost and later-on maintenance cost should be balanced. Otherwise, pavements would expect premature failure, reduced serviceability and increased maintenance cost. Nevertheless, uncertainty exists in forecasting. Hence, new techniques are needed to consider uncertainty and improve the reliability of pavement design.

Third, pavement design is moving from empirical method to mechanistic-empirical method. The new Mechanistic-Empirical Pavement Design Guide (MEPDG) has been adopted by American Association of State Highway and Transportation Officials (AASHTO) and becomes the official design guide named DARWin-ME. Comparing to the old AASHTO 1993 Guide, MEPDG has much more inputs including traffic, climate and materials. Furthermore, MEPDG is a comprehensive design and modeling package rather than an empirical equation. Due to the uncertainty nature of design inputs as well as the complexity of the new method, there is a need to conduct a risk analysis on pavement design using MEPDG.

In general, risk is a measure of the potential loss occurring due to natural or human activities. Risk analysis has been developed to design engineering systems to avoid risk. Risk analysis has three core elements: risk assessment, risk management and risk communication. Risk assessment answers three questions: (1) what can go wrong? (2) how likely is it? and (3) what are the consequences? Risk management is to identify the critical risks and employ strategies to minimize risks (52).

So far, risk analysis has been mainly applied in transportation safety, cost analysis, and performance related specifications. Using risk analysis, Monte Carlo simulations were used to estimate risk factors of work zone safety (53). With the model, the author was able to optimize the length and duration of closures for highway reconstruction and rehabilitation projects. Risk analysis approach was incorporated in life cycle cost analysis to account for the uncertainty associated with LCCA (54). California Department of Transportation (Caltrans) used risk management to minimize adverse impacts to project scope, cost and schedule, and to maximize opportunities to improve the project's objectives with lower cost, shorter schedules and higher quality (55). To consider the uncertainty in performance related specifications, risk analysis method was incorporated in pavement performance models and maintenance models, on which a contract price model was developed (56). In response to the problem of project cost escalation, NCHRP conducted a project introducing risk analysis tools and management practices to control transportation project costs (51). In the guidebook, risk analysis tools were adapted to the unique needs of highway project development. The framework was consisted of five steps: risk identification, risk assessment, risk mitigation, risk allocation, and risk monitoring. These five steps were then applied to the three project phases: planning, programming and designing.

After the release of the first version of MEPDG, engineers were interested in what the most significant variables were. Sensitivity analysis mainly using One-factor-At-a-Time (OAT) method was conducted by many researchers. Sensitivity analysis of the fatigue cracking and

rutting model found that subgrade stiffness and traffic were consistently significant (13). Kim (57) studied the influence on separate distress models based on two real pavement sections in Iowa. It was found that binder PG grade, volumetric properties, climate, AADTT, and type of base generally influenced most of the predicted performance measures. Graves and Mahboub (58) used a global approach to do sensitivity analysis and found that only AADTT, HMA thickness and subgrade strength were sensitive to all distresses. Tran and Hall (59) found that axle load spectra were significant for MEPDG prediction. This finding was also found in North Carolina (60). In addition, the research found that monthly adjustment factors and vehicle class distributions were also significant. However, axle load spectra were found to be moderate sensitive for typical WSDOT pavement designs (61). Evaluation of MEPDG in Michigan (62) showed that eleven design and material variables were significant in affecting performance. These include AC layer thickness, AC mix characteristics, base, subbase and subgrade moduli, and base and subbase thickness. Binder grade was found to be the most critical parameter affecting transverse cracking. A specific research on Poisson's ratio found that the Poisson's ratio of HMA had a clear influence of the MEPDG predictions (63). As Poisson's ratio increased, longitudinal cracking, total rutting and alligator cracking decreased. However, the Poisson's ratio of unbound materials was found not significant.

Considering the limitation of the OAT method (also known as local sensitivity analysis), NCHRP supported the project 1-47 to investigate the relationship in a systematic manner and

consider the combined effects of variations in two or more input parameters (also known as global sensitivity analysis) (64). The results for new HMA models are shown in Table 18. The normalized sensitivity index (NSI) was the parameter that represents how sensitive a variable was to the predicted performance. The larger the NSI absolute value, the more important it was. Plus or negative means the direction of its influence (plus means the same direction). The top three most significant variables to each distress type are highlighted. All variables were categorized to four sensitivity levels: hypersensitive (HS), very sensitive (VS), sensitive (S) and non-sensitive (NS). Some notable findings include

- HMA dynamic modulus E^* and thickness were the most significant parameters for almost all distresses. Other important variables were base resilient modulus and thickness, HMA air voids, effective binder content, traffic volume (AADTT), subgrade resilient modulus. Overall, it agreed with past research and engineering experience.
- However, HMA Poisson's ratio was unexpectedly found as a very sensitive parameter. Poisson's ratio was conventionally thought to have only minor effect on pavement performance and consequently its value was usually assumed for design.
- Thermal cracking was dramatically different from other distresses. The main influence on thermal cracking came from the property of HMA, such as dynamic modulus, creep compliance and tensile strength at 14 °F. This was reasonable

considering that thermal cracking was exclusively environment-driven but other distresses were mostly load related.

- Details of subgrade such as plasticity index, liquid limit, unit weight and thermal conductivity had only minor impact on predicted performance. Even groundwater table depth was found not as significant as normally assumed.

Table 4.1 Ranking of new HMA design inputs (reprint of Table 5.1 in (64))

Design Input	Maximum NSI _{$\mu \pm 2\sigma$} Values (ANN RSMs) ¹							
	Long. Crack	Alligator Crack	Thermal Crack	AC Rut Depth	Total Rut Depth	IRI	Max	OAT ²
HMA E* Alpha Parameter ³	-29.52	-15.94	-0.58	-24.40	-8.98	-3.58	-29.52	HS
HMA E* Delta Parameter ³	-23.87	-13.18	2.41	-24.43	-8.99	-2.80	-24.43	HS
HMA Thickness	-10.31	-7.46	-0.86	-4.21	-1.58	-1.11	-10.31	HS
<i>HMA Creep Compliance m Exponent</i>	N.A.	N.A.	-4.85	N.A.	N.A.	N.A.	-4.85	VS
<i>Base Resilient Modulus</i>	-4.72	-2.73	-0.17	0.14	-0.15	-0.36	-4.72	VS
<i>Surface Shortwave Absorptivity</i>	4.32	1.28	-0.20	4.65	1.67	0.67	4.65	VS
<i>HMA Air Voids</i>	4.47	3.39	1.33	-0.05	0.03	0.29	4.47	VS
<i>HMA Poisson's Ratio</i>	-2.38	-1.01	0.23	-4.33	-1.46	-0.43	-4.33	VS
<i>Traffic Volume (AADTT)</i>	3.72	3.94	0.02	1.87	0.66	0.51	3.94	VS
<i>HMA Effective Binder Volume</i>	-3.88	-2.93	-0.17	0.05	0.06	-0.24	-3.88	VS
<i>Subgrade Resilient Modulus</i>	-2.07	-3.41	0.15	0.08	-0.28	-0.44	-3.41	VS
<i>Base Thickness</i>	-2.40	-1.02	-0.03	0.22	0.04	-0.09	-2.40	VS
<i>Subgrade Percent Passing No. 200</i>	-1.71	-0.68	0.08	-0.10	-0.10	-0.12	-1.71	S
<i>HMA Tensile Strength at 14°F</i>	N.A.	N.A.	-1.59	N.A.	N.A.	N.A.	-1.59	S
<i>Operational Speed</i>	-1.26	-0.83	-0.04	-1.06	-0.39	-0.15	-1.26	S
<i>HMA Creep Compliance D Parameter</i>	N.A.	N.A.	-1.03	N.A.	N.A.	N.A.	-1.03	S
<i>HMA Unit Weight</i>	-0.88	0.97	-0.76	-0.88	-0.30	-0.08	0.97	S
<i>Base Poisson's Ratio</i>	0.91	0.90	0.18	-0.19	-0.05	0.09	0.91	S
<i>HMA Heat Capacity</i>	-0.76	-0.55	-0.77	-0.81	-0.28	-0.14	-0.81	S
<i>Subgrade Liquid Limit</i>	-0.67	-0.79	-0.10	-0.10	0.07	0.03	-0.79	S
<i>Binder Low Temperature PG</i>	0.56	0.09	-0.74	0.25	0.09	0.02	-0.74	S
<i>HMA Thermal Conductivity</i>	-0.53	-0.40	-0.67	0.20	0.04	0.02	-0.67	S
<i>Binder High Temperature PG</i>	-0.60	-0.48	0.00	-0.66	-0.25	-0.09	-0.66	S
<i>Subgrade Poisson's Ratio</i>	0.44	-0.59	0.16	0.08	0.07	0.04	-0.59	S
<i>Groundwater Depth</i>	0.20	-0.16	0.08	0.01	-0.02	-0.02	0.20	S
<i>Subgrade Plasticity Index</i>	-0.15	0.11	0.03	0.01	0.02	0.00	-0.15	S
<i>Aggregate Coef. Of Thermal Contraction</i>	N.A.	N.A.	-0.07	N.A.	N.A.	N.A.	-0.07	NS

In summary, the author did find any literature applying risk analysis method specifically on pavement design. All sensitivity analyses were based on MEPDG software to find out the key variables that had the most significant influence on MEPDG predictions. One shortcoming of

this method was that the limitation of the MEPDG software could be regarded as the truth of the real world mechanism. For instance, the NCHRP1-47 project found that the detail of subgrade was not significant to pavement performance; even the ground water table depth was not as significant as normally assumed. One should be aware that this finding was derived from, and valid only on, the software used in the study. It might not be the true relationship. The study only revealed that more efforts were needed to build the common sense (water is detrimental to pavement performance) into future design software.

This chapter was intended to investigate flexible pavement design using risk analysis methods. It did use the conventional sensitivity analysis method (changing inputs and observing the output). Instead, it stepped back from the design software and reviewed the mechanistic-empirical design process outside of the box. This chapter was composed of three parts: risk identification, risk assessment and risk management.

The criteria of flexible pavement design using MEPDG were to fulfill the accepted distresses of alligator cracking, longitudinal cracking, transverse cracking, rutting and IRI. However, this chapter will discuss pavement design in a more general perspective: pavement should be designed to be comfortable, cost affordable, safe and sustainable.

4.2 Risk Identification

To reduce the risk and increase the reliability of a system, the first task is to fully understand the structure and components of the system. Hierarchical Holographic Modeling (HHM) is a

powerful method for identifying risk (65). As most systems are hierarchical in nature, HHM gives a full picture of the system by viewing the system from different perspectives.

The goal of pavement design is to design a cost-efficient pavement that can provide a smooth and safe road surface for people to travel on. Considering a pavement design as a system, it is composed of many components such as design engineers, material testing technicians, design software, traffic prediction, climate change, construction and maintenance after the road is built. The system is also under many constraints such as site condition, material availability, budget, design time, construction ability, etc. Using HHM, flexible pavement design using MEPDG was investigated from six perspectives in this research: different people, temporal, components, cost allocation, using MEPDG, and using general mechanistic empirical methods, as shown in Figure 4.1 through 4.7.

Figure 4.1 shows the six perspectives applied in this study. Flexible pavement in the perspective of different people is presented in Figure 4.2. For example, end users may be interested in (1) the time that it takes to construct a road, (2) how smooth the road is, (3) whether noise from the pavement influence passengers and people living nearby the road, (4) whether the pavement is maintenance free or vice versa, (5) how much more or less users have to pay on fuel due to different pavement condition, (6) is it safe to use the road, and (7) is the road suitable for use under all types of weather condition. The same assessment was conducted to other categories.

Figure 4.3 presents the analysis from the temporal perspective, or the lifelong circle of a pavement. For instance, the following subjects are significant during the process of construction: (1) when is the best time for HMA paving, when is the last day for construction, (2) what is the budget limit, (3) how many equipment, engineers, technicians and staff are available to work on this project, (4) the location, cost and availability of materials, (5) what is the minimum quality requirement and how to achieve a higher level of quality, (6) the safety of construction crew and public travelers near the construction zone, and (7) how weather could influence the construction process. Risks may happen in any process and hinder the success of the goal.

Analysis of different components is shown in Figure 4.4. The success of a flexible pavement involves traffic, materials, climate, construction and reliability. Taking climate as an example, uncertainties may occur in (1) using one spot to represent a miles-long project, in which local condition (esp. water and moisture) may varies from section to section, (2) real temperature variation is usually simplified using mean temperature, (3) the difference between project level rainfall and the network level rainfall statistics, (4) number and extent of frost/thaw cycles, (5) material properties vary under different weather condition, (6) the correlation between load spectra and project level climate may be overlooked, and (7) the overall good construction quality may include some outliers due to unwelcomed climate condition (i.e. finish paving of the last truck materials when the rain starts).

Figure 4.5 decomposes flexible pavement according to how budget is allocated to different activities, from planning towards maintenance. For instance, maintenance considers equipment, workers, materials, traffic control, and environment protection.

Figure 4.6 and 4.7 are specifically for flexible pavement design using MEPDG and future mechanistic empirical methods in general. The difference between the two is that Figure 4.7 contains more comprehensive items than Figure 4.6 does. For example, geotextile is not an option in the current MEPDG software, but should be included in the future ME-based methods. Note that Figure 4.6 literally contains most of the major parameters in the MEPDG software because it is believed that all factors could be probabilistic and hence contains somewhat risk.

After analyzing flexible pavement design from six perspectives, it was possible to identify most, if not all, major factors which could introduce risks to a successful flexible pavement design. Finally, the perspective of general mechanistic empirical methods was believed to be the best framework representing flexible pavement design, because it incorporated the factors in MEPDG and other significant factors not considered in MEPDG. Hence, the rest of this study was based on the framework shown in Figure 4.7.

The framework is consisted of four levels. Level 1 is the goal. Level 2 is categories including traffic, climate, structure, material and reliability. Level 3 is factors of each category. Especially, material is divided into asphalt mixture, stabilized base, geotextile, unbound base and subgrade (Level 3), which are further decomposed into more factors (Level 4).

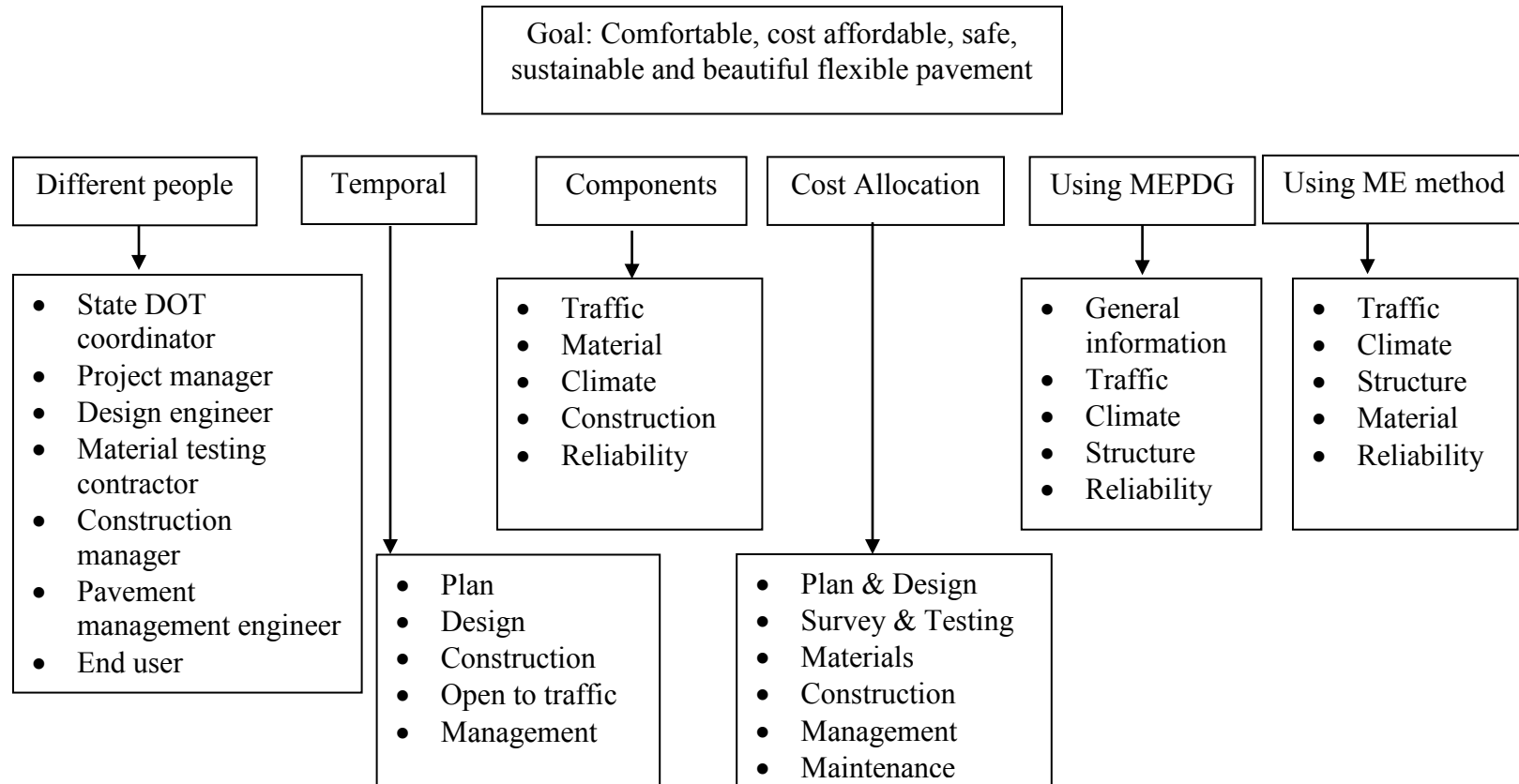


Figure 4.1 Perspectives to Analyze Flexible Pavement Design

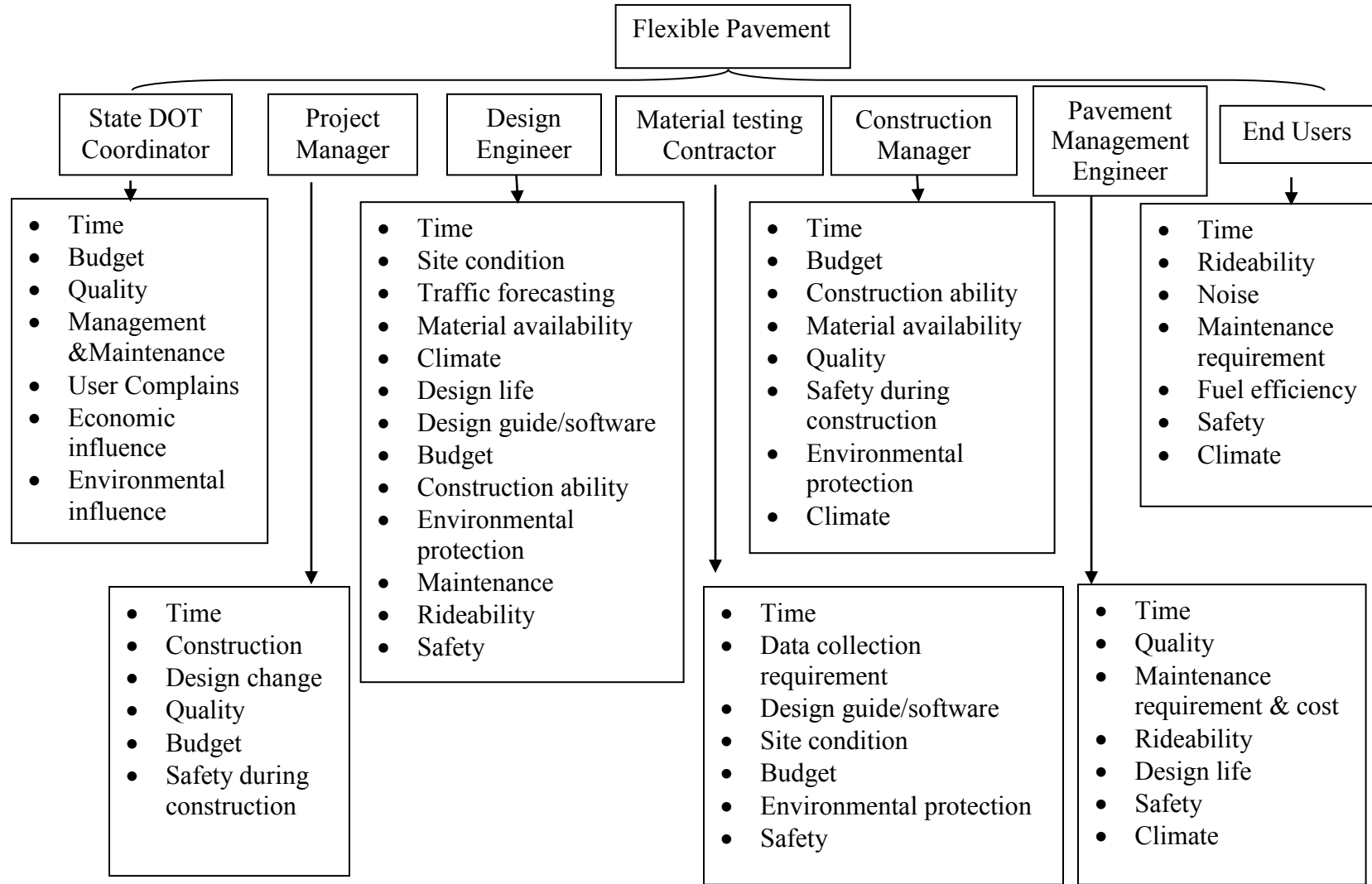


Figure 4.2 Flexible Pavement Design in the Perspective of Different People

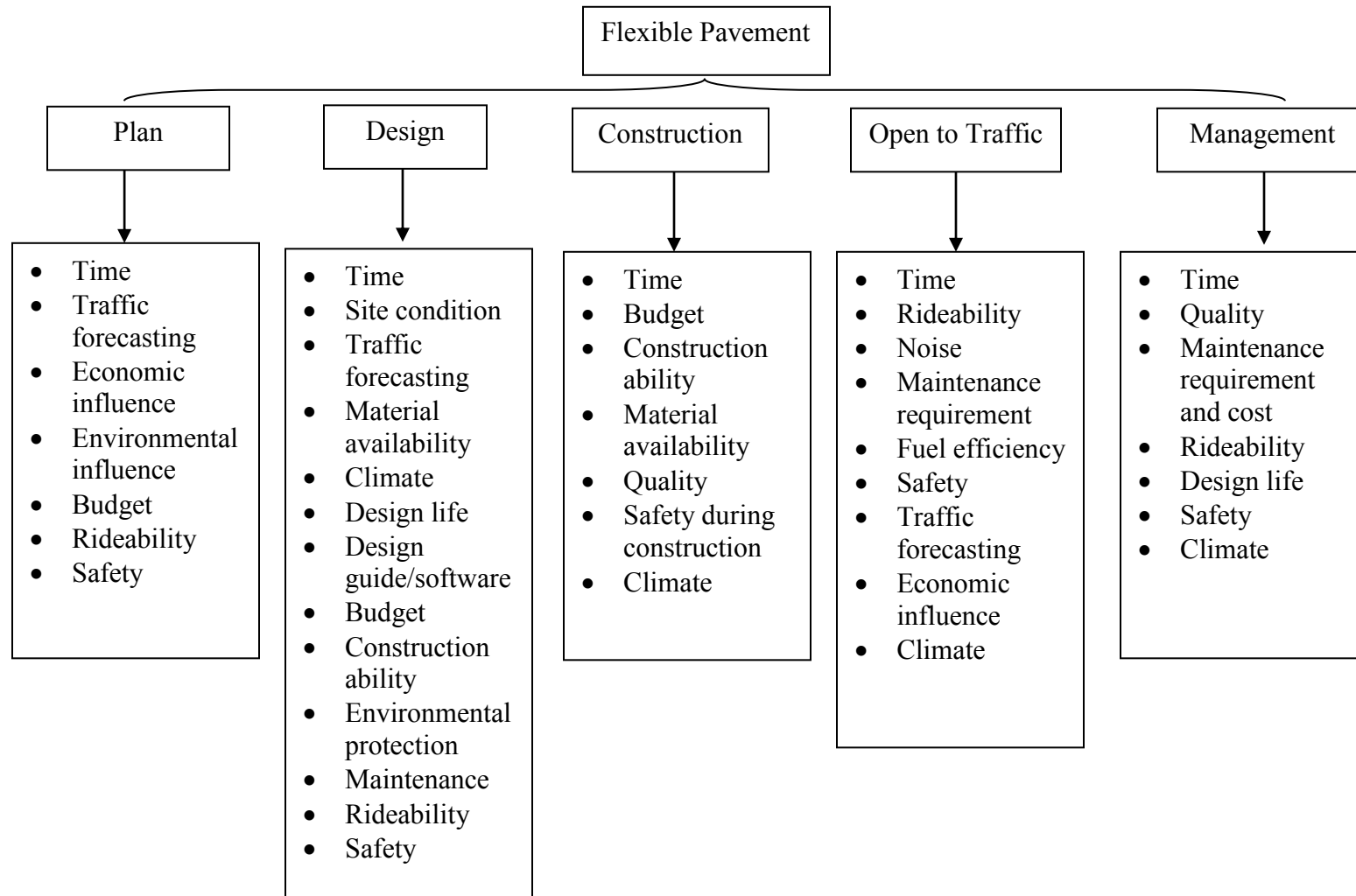


Figure 4.3 Flexible Pavement Design in Temporal Perspective

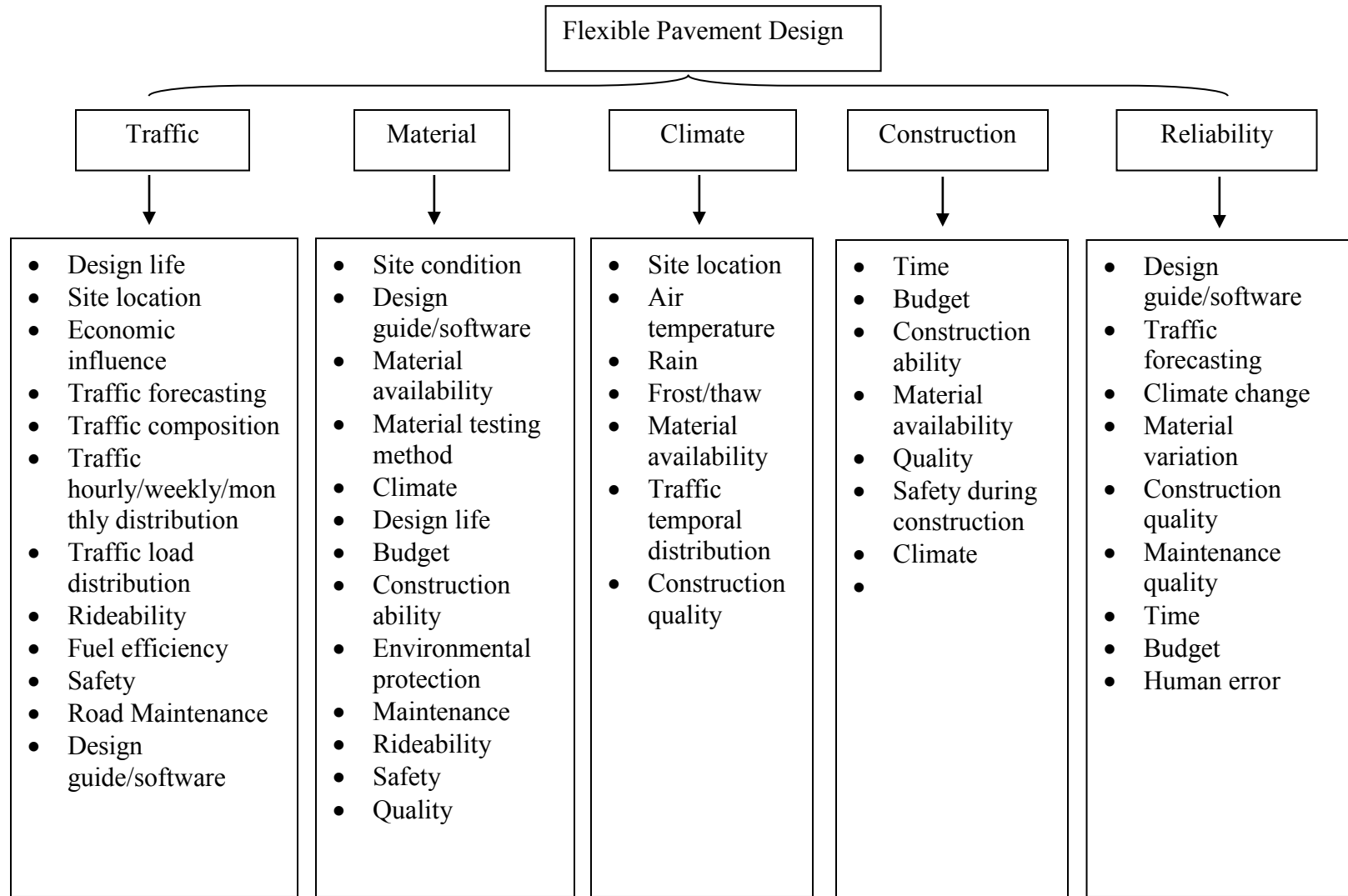


Figure 4.4 Flexible Pavement Design in the Perspective of Components

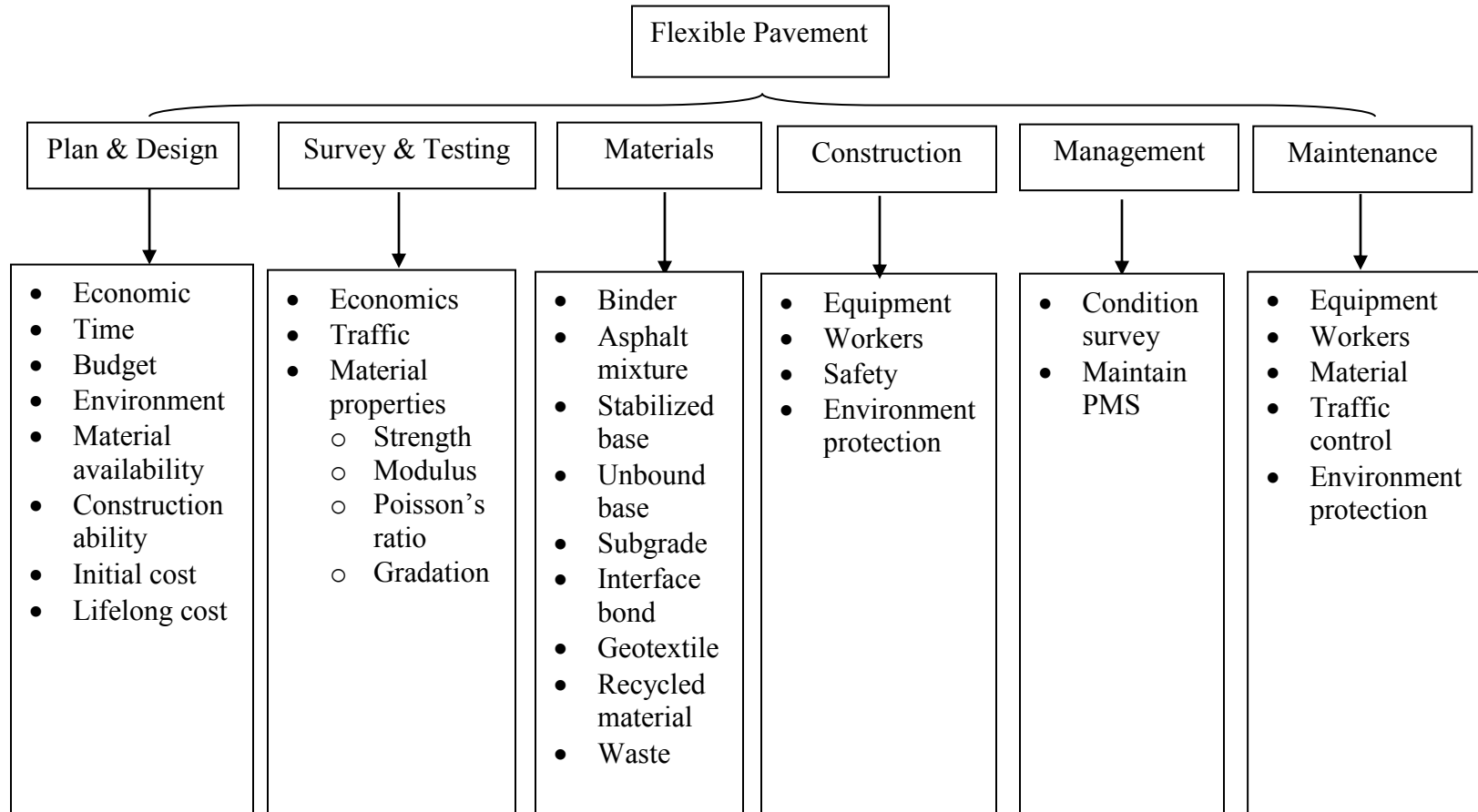


Figure 4.5 Flexible Pavement Design in the Perspective of Cost Allocation

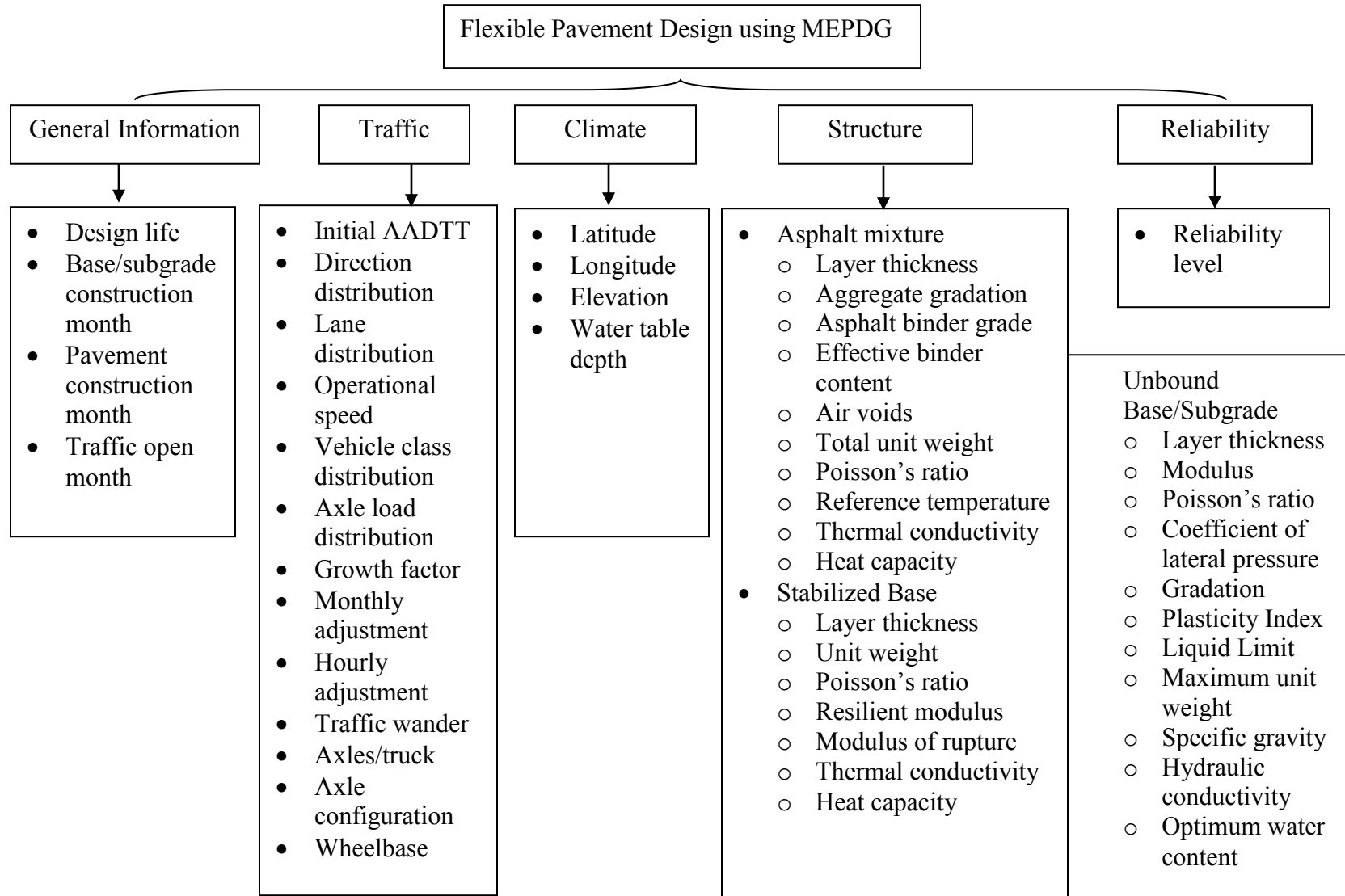


Figure 4.6 Flexible Pavement Design using MEPDG Version 1.1 Software

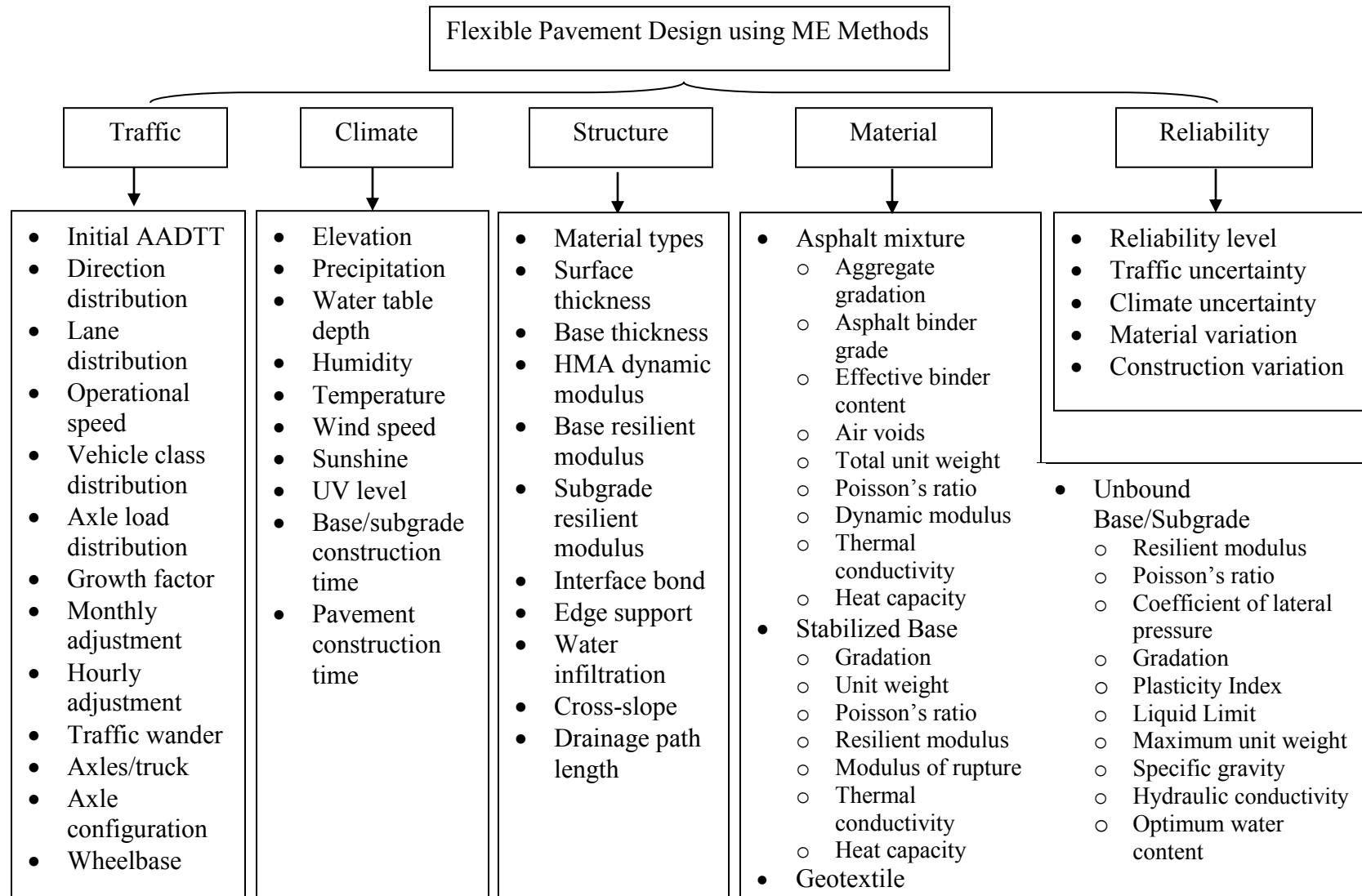


Figure 4.7 Flexible Pavement Design using General Mechanistic Empirical Methods

4.3 Risk Assessment

After the system was fully understood, the second task was risk assessment, which was mainly to address three very basic questions:

- What can go wrong?
- How likely is it?
- What are the consequences?

This chapter focused on identifying the most significant risks so that techniques could be applied to manage the risk with affordable cost. The analytic hierarchy process (AHP) was developed by Thomas L. Saaty (66). It was based on pairwise comparisons of the “properly identified components” of a system. Pairwise comparisons improved consistency by using as much information as possible (65). AHP was used as a tool for infrastructure management (67), pavement preservation prioritization and optimization (68) (69), and asphalt pavement construction quality control (70). In this paper, AHP was applied to prioritize significant factors that influence flexible pavement design, based on experience and knowledge of pavement engineers.

The principle of AHP is to construct the pairwise comparison matrix and then calculate its eigenvector which represents the relative weight of each factor.

$$\overline{A}\overline{W} = \lambda\overline{W} \quad (4.1)$$

where \overline{A} is the binary importance matrix, \overline{W} is the vector of weights of objectives, and λ is the eigenvalue.

The pairwise comparison matrix is a tool to convert qualitative knowledge to quantitative information according to the numerical rating listed in Table 4.2.

Table 4.2 Qualitative and quantitative guidelines for pairwise comparison (52)

Numerical Rating	Definition
9	Extremely preferred
7	Very strongly preferred
5	Strongly preferred
3	Moderately preferred
1	Equally preferred

Furthermore, the consistency of the pairwise comparison has to be checked by consistency index (C.I.) and consistency ratio (C.R.).

$$C.I. = \frac{\lambda_{\max} - n}{n - 1} \quad (4.2)$$

$$C.R. = \frac{C.I.}{R.I.} \quad (4.3)$$

where n is the number of factors in concern, and $R.I.$ is random index provided by Saaty (66). In general, $C.R.$ less than 0.1 is considered acceptable. Otherwise, the comparison has to be revised using more consistent judgment.

In this study, a survey sheet was created in Excel and sent to several graduate students working on projects related to pavements and transportation in the Department of Civil Engineering at the University of Arkansas. Figure 4.8 shows a screenshot of the survey sheet. The full survey sheet is presented in Appendix A.

	A	B	C	D	E	F
1		Traffic	Climate	Structure	Material	Reliability
2	Traffic	1				
3	Climate		1			
4	Structure			1		
5	Material				1	
6	Reliability					1
7						
8		Numerical Rating		Definition		
9		9		Extremely preferred		
10		7		Very strongly preferred		
11		5		Strongly preferred		
12		3		Moderately preferred		
13		1		Equally preferred		

Figure 4.8 A screenshot of the AHP pairwise comparison survey sheet (Level 2)

Data analysis was conducted in according to the following steps:

Step 1: Develop the pairwise comparison matrix of Level 2 categories. For example, the ratio of Traffic:Climate is 7:1 in Table 4.3. This means that this surveyor very strongly preferred the influence of traffic on flexible pavement performance than the climate influence is.

Table 4.3 Pairwise comparison of Level 2 categories

	Traffic	Climate	Structure	Material	Reliability
Traffic	1	7	3	3	9
Climate	0.14	1	0.14	0.20	3
Structure	0.33	7	1	1	5
Material	0.33	5	1	1	5
Reliability	0.11	0.33	0.20	0.20	1

Step 2: Calculate the eigenvalue and eigenvector using MATLAB, as shown in Table 4.4.

Step 3: Select the maximum eigenvalue and its corresponding eigenvector.

Step 4: Calculate and check the consistency ratio.

Table 4.4 Statistics of pairwise comparison of Level 2 categories

max. eigenvalue	5.2511	Factor	Eigenvector
n	5	Reliability	0.0650
Consistency Index	0.06	Climate	0.1033
Random Index	1.120	Material	0.3560
Consistency Ratio	0.056	Structure	0.3953
CR<0.1?	Yes	Traffic	0.8379

Step 5: Draw a bar chart to show the rank of factors according to the eigenvector from Step 3.

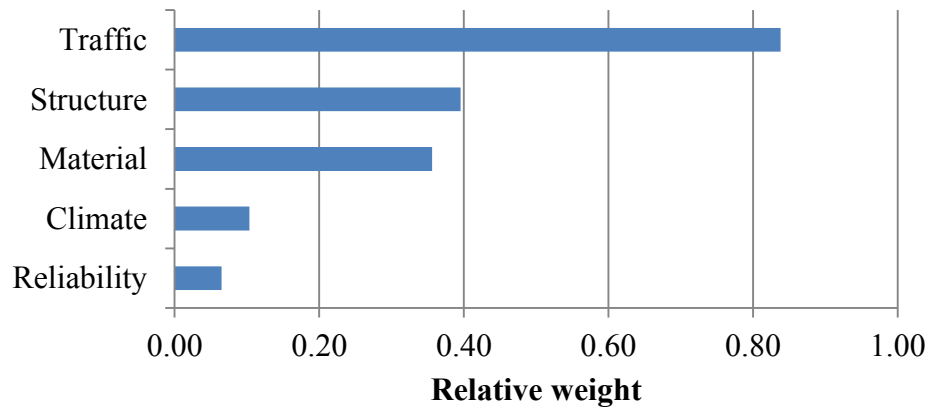


Figure 4.9 Importance ranking of Level 2 factors

Step 6: The same method from Step 1 to Step 5 was applied to Level 3 factors of each category.

Step 7: Specially, factors related to materials have two levels. The same method from Step 1 to Step 5 was applied.

Step 8: The overall ranking was conducted by multiplying Level 3 weight with its corresponding Level 2 weight.

In total 75 factors were compared. Traditionally, sensitivity analysis was conducted only within the same category, such as material factors or traffic factors. One advantage of AHP was it provided the comparison not only within each category but also between categories. For example, it was possible to assess the relative importance of traffic growth factor and the gradation of asphalt mixture using AHP. Appendix A shows the overall ranking of all 75 factors in respect of the final goal of flexible pavement design. The top 15 factors influencing flexible pavement design is listed in Figure 4.10.

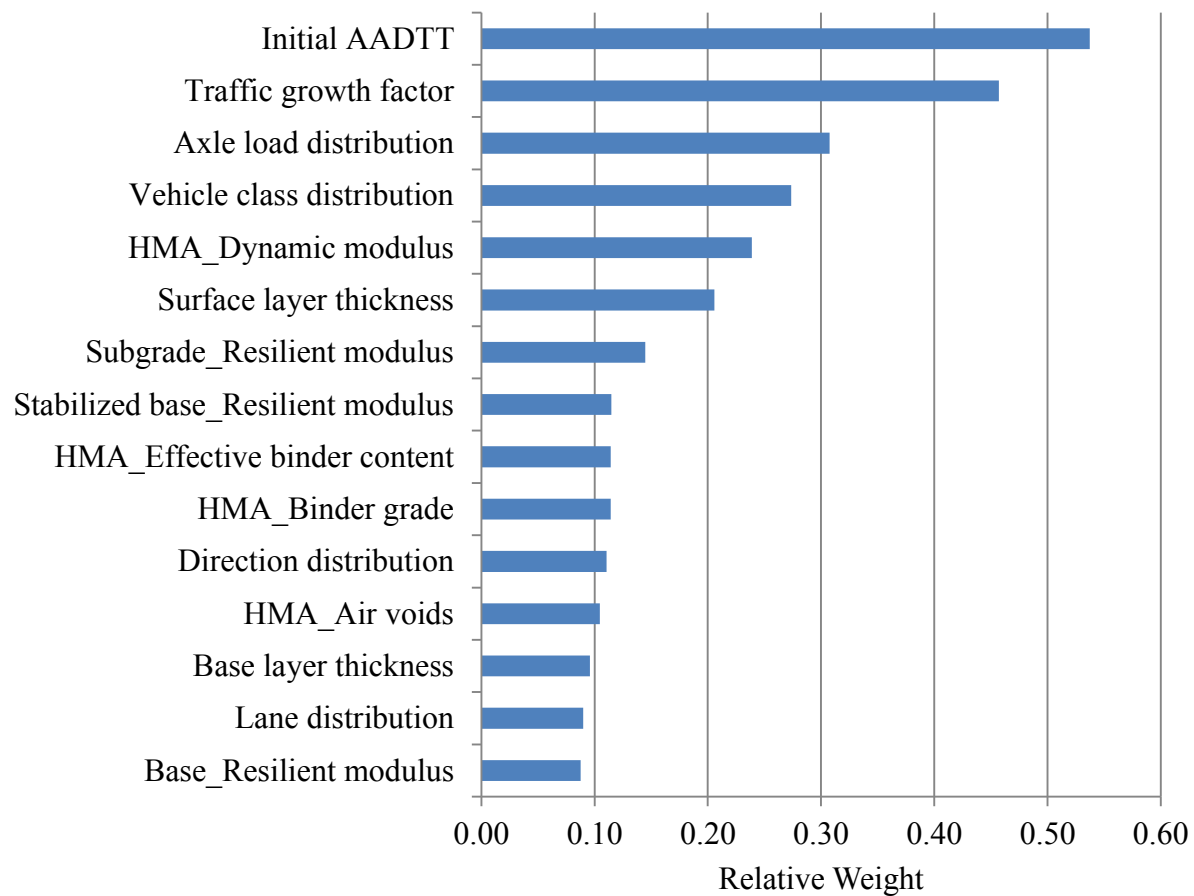


Figure 4.10 Top 15 Factors Influencing Flexible Pavement Design

It was found that traffic, structure and material were the most significant categories, while climate and reliability were not ranked in the top 15. Moreover, in general, traffic was the most important category, because top four factors were all belong to traffic. It should be noted that the Level 2 weight of traffic, structure and material in this study were assigned as 0.838, 0.395 and 0.356, respectively. In other words, traffic was considered more than twice important than structure and material. This might be assigned to a lower weight which would then change the rank of these factors.

Although factors were ranked reasonably in general, it was worthwhile comparing the result from AHP with the result from sensitivity analysis. Table 4.4 lists some critical factors in the literature. It was found that the critical factors using risk analysis matched well with former researches.

In addition, the Top 15 list was compared with the result from the NCHRP 1-47 study, which was a global sensitivity analysis on MEPDG. The list is presented in Table 4.6. It should be pointed out that the top 15 factors from NCHRP 1-47 was ranked based on the maximum of absolute value of the $NSI_{\mu \pm 2\sigma}$ among six distresses types. For instance, HMA creep compliance m exponent only impacted thermal cracking; but it was ranked as the 4th important factor because the absolute value was high (refer to Table 4.1). Also note that NCHRP 1-47 only considered the AADTT as a probabilistic variable in traffic. Keeping these in mind, it was found that this study matched well with the global sensitivity study:

- AADTT and traffic data was important.
- HMA thickness, modulus, air voids and effective binder content were critical.
- Base thickness and resilient modulus were important.

Table 4.5 Critical factors of MEPDG from literature

Literature	Critical parameters
Kim, Ceylan and Heitzman, 2005 (57)	HMA_binder grade HMA_volumetric properties Climate AADTT Type of base
Graves and Mahboub, 2006 (58)	AADTT HMA layer thickness Subgrade strength
Buch et al. 2008 (62)	HMA_Layer thickness HMA_aggregate gradation HMA_binder grade HMA_effective binder content HMA_air voids Base_Layer thickness Base_material Subgrade_material Climate regions
Sayyady et al. 2010 (60)	Axle load distribution Monthly adjustment factors Vehicle class distribution
Orobio, 2010 (71)	AADTT Traffic growth Direction distribution Lane distribution Resilient modulus of subgrade As-build air voids Poisson's ratio of HMA Effective binder content of HMA

Table 4.6 Top 15 factors of MEPDG from this study and NCHRP 1-47

Rank	Risk analysis (this study)	NCHRP 1-47 Global sensitivity analysis (64)
1	Initial AADTT	HMA E* Alpha Parameter
2	Traffic growth factor	HMA E* Delta Parameter
3	Axle load distribution	HMA Thickness
4	Vehicle class distribution	HMA Creep Compliance m Exponent
5	HMA_Dynamic modulus	Base Resilient Modulus
6	Surface layer thickness	Surface Shortwave Absorptivity
7	Subgrade_Resilient modulus	HMA Air Voids
8	Stabilized base_Resilient modulus	HMA Poisson's Ratio
9	HMA_Effective binder content	Traffic Volume (AADTT)
10	HMA_Binder grade	HMA Effective Binder Volume
11	Direction distribution	Subgrade Resilient Modulus
12	HMA_Air voids	Base Thickness
13	Base layer thickness	Subgrade Percent Passing No. 200
14	Lane distribution	HMA Tensile Strength at 14Of
15	Base_Resilient modulus	Operational Speed

With critical factors identified, further investigation was conducted to find out the possible risks, and the corresponding likelihood and consequences. Table 4.10 is an example of risk assessment on ten factors out of the Top 15 list.

In general, it was found that risks for flexible pavement were mainly related to the method of data collection and material testing. Factors belong to the same category could be influenced by same risks. For example, initial AADTT, growth factor, axle load distribution and vehicle class distribution were all influenced by risks of traffic data collection equipment and techniques. If a better equipment, which may cost more, could greatly reduce the risk of these parameters.

Table 4.7 Risk assessment of the top 10 parameters

Rank	Category	Factor and Risks
1	Traffic	Initial AADTT 1.1 Short term data recording 1.2 Malfunction of recording equipment 1.3 Miscalibration of equipment 1.4 Misclassify truck percentage 1.5 Misclassify road function level
2	Traffic	Growth factor 2.1 Error of historical ADT record 2.2 Simplification of growth function 2.3 Development due to road opening or road condition improvement
3	Traffic	Axle load distribution 3.1 Short term data recording 3.2 Malfunction of recording equipment 3.3 Miscalibration of equipment 3.4 Misclassify road function level
4	Traffic	Vehicle class distribution 4.1 Short term data recording 4.2 Malfunction of recording equipment 4.3 Miscalibration of equipment 4.4 Misclassify road function level
5	Structure	Dynamic modulus of HMA 5.1 Simplified testing method 5.2 Sampling error 5.3 Model error using Level 2 and 3 inputs 5.4 Change of gradation in construction 5.5 Air voids and compaction in construction
6	Structure	Surface layer thickness 6.1 Change of gradation in construction 6.2 Air voids and compaction in construction 6.3 Shortage of material during surface paving
7	Structure	Resilient modulus of subgrade 7.1 Simplified testing method 7.2 Sampling error 7.3 Model error using Level 2 inputs 7.4 Compaction in construction 7.5 Estimation error of water table depth
8	Material	SB_Resilient modulus 8.1 Simplified testing method 8.2 Sampling error

Rank	Category	Factor and Risks
		8.3 Model error using Level 2 inputs
		8.4 Compaction in construction
		8.5 Change of gradation in construction
9	Material	HMA_Binder grade
		9.1 Storage time
		9.2 Error in estimating annual temperature
10	Material	HMA_Effective binder content
		10.1 Change of gradation in construction
		10.2 Compaction in construction
		10.3 Weather during construction

In this study, traffic was selected as an example to illustrate the application of risk assessment and risk management. Based on qualitative judgment, risk matrix (Table 4.8) was developed in which the likelihood scale was *unlikely, seldom, occasional, likely, and frequent*, and the severity scale was *extremely high, high, moderate, and low*.

Table 4.8 Risk matrix of traffic

Effect	Likelihood				
	Unlikely	Seldom	Occasional	Likely	Frequent
Extremely high risk			Malfunction of recording equipment		
High risk		Miscalibration of equipment			Short term data collection
Moderate risk		Misclassify road function level	Misclassify truck percentage		Simplified equipment
Low risk					

Risks above the bold line mean either high risk or high likelihood, and thus should be managed. The same method could be applied to structure, materials and others. Because the

focus of this research was not risk management but the method of reliability design, only were examples provided to illustrate the risk analysis method. A comprehensive study on risk analysis of pavement was highly recommended.

4.4 Summary

Risk analysis method was applied to analyze flexible pavement design using mechanistic-empirical method. The goal was to assess risks in the system and provide methods to manage risks. Based on this research, the following conclusions were drawn:

- Risk analysis was illustrated to be helpful for pavement engineers. The steps of risk analysis included risk identification using Holographic Hierarchical Modeling (HHM), risk ranking using Analytical Hierarchical Process (AHP), risk assessment and risk management.
- AHP method made it possible to compare the importance of parameters not only within each category but also between categories. In total, 75 parameters were compared and the top 15 factors were recommended for further analysis.
- Comparing to traditional sensitivity analysis on the MEPDG software, risk assessment provided an “out-of-box” view of mechanistic-empirical pavement design methods in general. This could be very helpful revealing not only limits of a model but also some negligence and overlook of how the model was designed.
- The results presented in this study were based on a limited number of surveys completed by several graduate students at the University of Arkansas due to the extensive time needed to fill the survey. However, the method could be valid for a state level or national level research.

- Risks influencing flexible pavement design were mainly related to data collection and material testing.

CHAPTER 5 RISK MODELING

5.1 Introduction

The assessment of risk factors for a given system makes it possible to model the performance of the system in different possible scenarios in which one or many risks happen. In the context of probabilistic pavement design, risk modeling simulates the influence of uncertainties from various sources as identified in Chapters 2 and 4.

In general, risk modeling answers a series of *what-if* questions. Although the concept is straightforward, it may be prohibitive, if not impossible, for many real world problems which require several hours for a single simulation. For example, the flexible pavement design model in MEPDG needs about 20 minutes for one simulation using a normal desktop computer. Therefore, simulation on surrogate models has been widely used for a long time to alleviate the time and cost expense for complex systems.

Surrogate is explained as *one that serves as a substitute* in the Webster dictionary. Hence, a surrogate model is a (simple) model that serves as a substitute of a (complex) model. Surrogate models focus on the input-output behavior more than on the mechanism of the system. A surrogate model is developed by modeling the system based upon a limited number of runs of intelligently chosen data points. The challenge of surrogate modeling is how to develop a simplified model that can produce output as close as possible to the original complex model with as few simulations as possible.

Usually four steps are required to build a surrogate model as shown in Figure 5.1. First, samples from each variable are collected based on an experiment, which is designed to reduce the number of simulations while achieving the required accuracy. Second, a surrogate model is built using different techniques such as response surface method, regression analysis and

artificial neural networks. Third, another set of experimental designs is developed and more simulations on the complex model are conducted. The last step is to validate the surrogate model using the results from the third step. Note that this process can be iterative. In case the model does not reach the required accuracy or is not robust covering the full design space, step 1 to 4 are repeated: more simulations are required to improve the surrogate model.

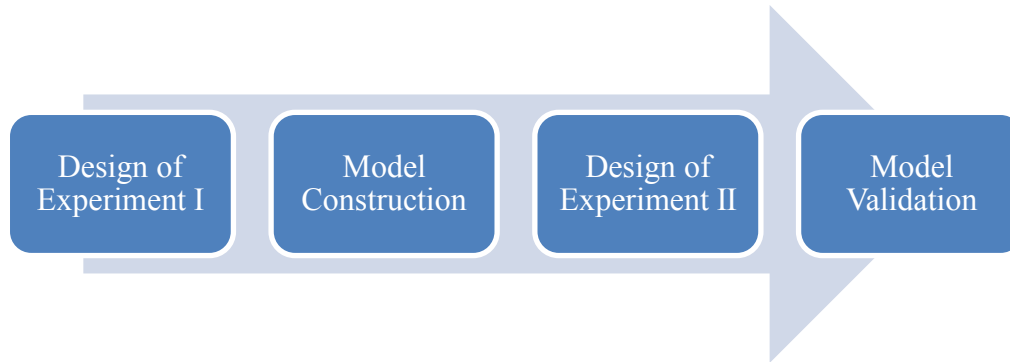


Figure 5.1 Steps to build a surrogate model

In fact, surrogate modeling has been used to develop the rigid pavement design models in MEPDG. The following section describes this in detail.

5.1.1 NCHRP1-37A (Neural Network)

Since MEPDG predicts pavement response and performance each month in the life time (esp. temperature data are calculated hourly for rigid pavement), the computing time of each run has been specifically addressed during the development of the software. For rigid pavement, neural networks were developed based on thousands of results from the 2-D finite element program, ISLAB2000 (72). Using these neural networks, MEPDG could provide accurate and virtually instantaneous predictions of pavement response and performance.

The development of neural networks for rigid pavement is illustrated in Figure 5.2.

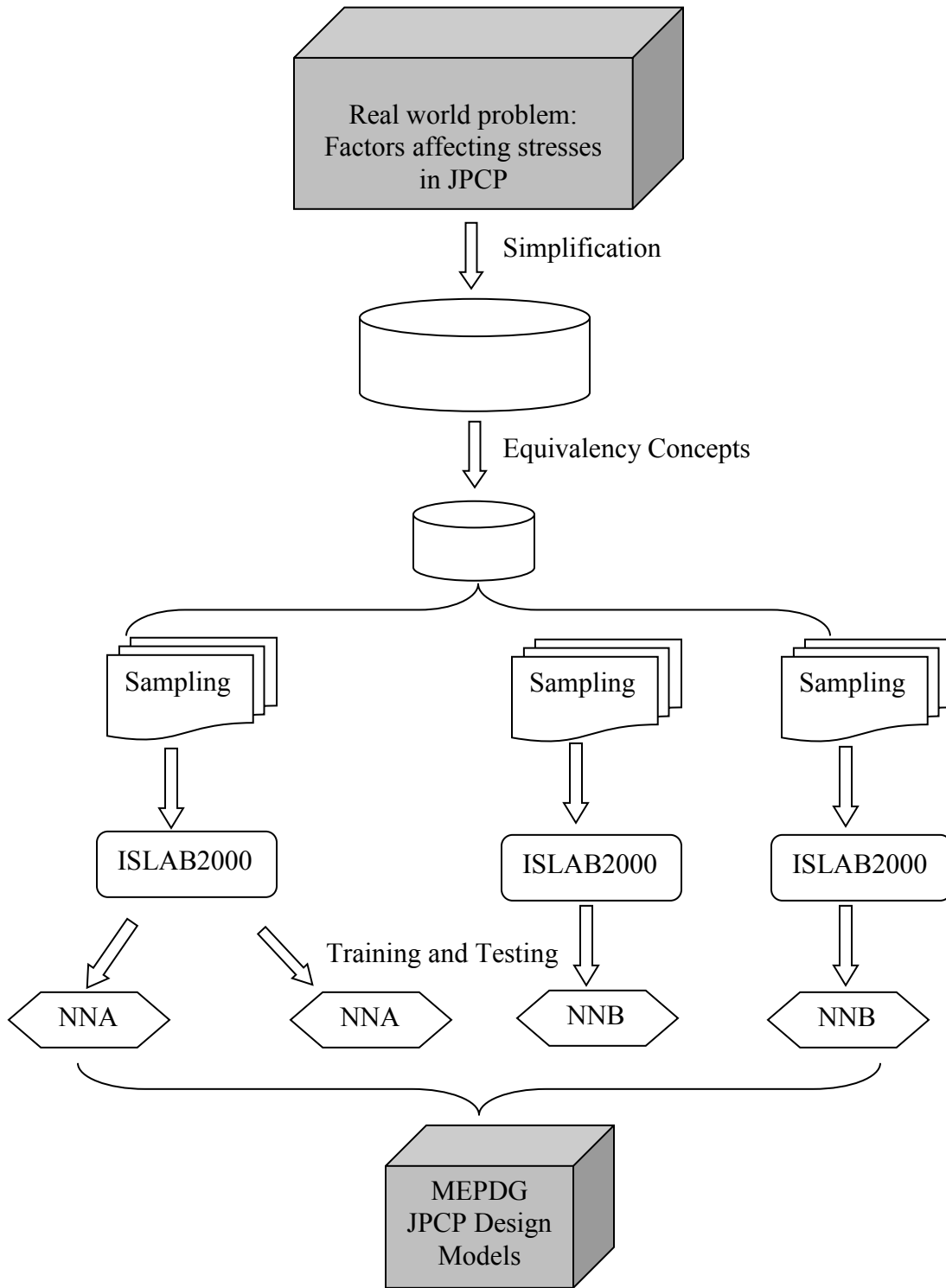


Figure 5.2 Flowchart of Neural Network development for JPCP in NCHRP1-37A

Real world problems were first simplified by minimizing the model size from a comprehensive one to a simple one. For example, the passing lane was found to be negligible, and modeling 3 slabs in longitudinal direction produced the same stress with 5 slabs. After simplification, there were 30 parameters to be considered. However, 30 was still a challenge for modeling. For instance, it would require more than $2 \cdot 10^{14}$ simulations if each parameter was allowed to have just 3 values for the 30 input parameters.

Three equivalent concepts, namely, equivalent thickness, equivalent temperature gradient, and equivalent slab, were introduced to further reduce the number of variables to a manageable scale. Taking the equivalent slab thickness as an example, PCC and base were combined to a single layer with an equivalent thickness defined by

$$h_{eff} = \sqrt{h_{PCC}^3 + \frac{E_{base}}{E_{PCC}} h_{base}^3} \quad (5.1)$$

where

h_{eff} = equivalent slab thickness,

h_{PCC} = PCC slab thickness,

h_{base} = base thickness,

E_{PCC} = PCC modulus of elasticity, and

E_{base} = base modulus of elasticity.

By doing this, four parameters (h_{PCC} , h_{base} , E_{PCC} and E_{base}) were reduced to two parameters (E_{PCC} , h_{eff}). Moreover, MEPDG could be applicable to different structures by using equivalent concepts.

Later, the system was divided into two subsystems: (A) a single slab, and (B) a two-slab system. System A was used for the slab curling analysis. System B was to account for the effect

of tire footprint geometry and shoulder support. When the two systems were combined together, the stresses in a multi-slab system could be obtained.

Finally, four neural networks were developed for modeling JPCP:

- NNA1: predicting the maximum edge stresses at the bottom of a single slab subjected to temperature curling and a single axle loading.
- NNA2: predicting the maximum edge stresses at the bottom of a single slab subjected to temperature curling and a tandem axle loading.
- NNB1: predicting the maximum stresses at the bottom of a two-slab system subjected to a single axle single wheel loading.
- NNB2: predicting the maximum stresses at the bottom of a two-slab system subjected to a single wheel loading.

Samples were prepared based on an experimental design. In total, 104,860 runs of ISLAB2000 were conducted to develop a dataset to train and test the neural networks. The developed surrogate models dramatically reduced the computational time with a high accuracy ($R^2=0.9982$).

Table 5.1 Number of simulations to develop neural networks for rigid pavement design in NCHRP1-37A

	Task	# of simulation	Experimental Design	# of variables
JPCP	Training NNA1, NNA2	14,175*2	5*9*7*9*5	5
	Training NNB1	24,300	5*9*6*6*15	5
	Training NNB2	910	5*14*5*15	4
	Model Testing	2,100		unknown
CRCP	Training	46,800		3
	Model Testing	2,400		unknown
Total runs of ISLAB2000		104,860		

It should be noted that building surrogate models to provide rapid solutions for flexible pavements was tried but did not succeed due to “the complexity of the problem” (6). In current MEPDG software, the multilayer elastic program JULEA was adopted for linear elastic analysis of flexible pavements. If Level 1 inputs of unbound layer materials were used, then finite element analysis was conducted using the 2D finite element program DSC2D.

5.1.2 Response Surface Method

Another approach to model risk is using the Response Surface Method (RSM). RSM is a collection of statistical and mathematical techniques useful for exploring the relationships between independent variables with responses. As an example, Figure 5.3 shows the relationship between the response (expected yield) and two independent variables (temperature and pressure). It is this graphical perspective of the problem environment that has led to the term Response Surface Method (73).

In the context of mechanistic empirical pavement design, the schema proposed in this study is shown in Figure 5.4. Three major factors were considered: climatic influence, traffic load and pavement structure/materials.

Due to the nature of asphalt mixture, climate (temperature and moisture) has a big impact on flexible pavement. Pavement in hot regions like Arizona is prone to rutting problems in the summer; on the contrary, transverse cracking may be an issue for northern states like Minnesota. MEPDG uses dynamic modulus (E^*) to characterize HMA. The dynamic modulus is the ratio of the maximum peak to peak stress over the axial strain during sinusoidal loading. The dynamic modulus is tested according to AASHTO 62-07 over a range of temperatures and loading frequencies. The typical temperatures at which the test is performed are: 14, 40, 70, 100, and 130°F. The frequencies range as follows: 25, 5, 1, 0.5, and 0.1 Hz. To simplify this procedure,

this study adopted the concept of the effective temperature developed by El-Basyouny and Jeong (74). Effective temperature (T_{eff}) was defined as a single test temperature at which an amount of distress would be equivalent to that which occurs from the seasonal temperature fluctuation throughout the annual temperature cycle.

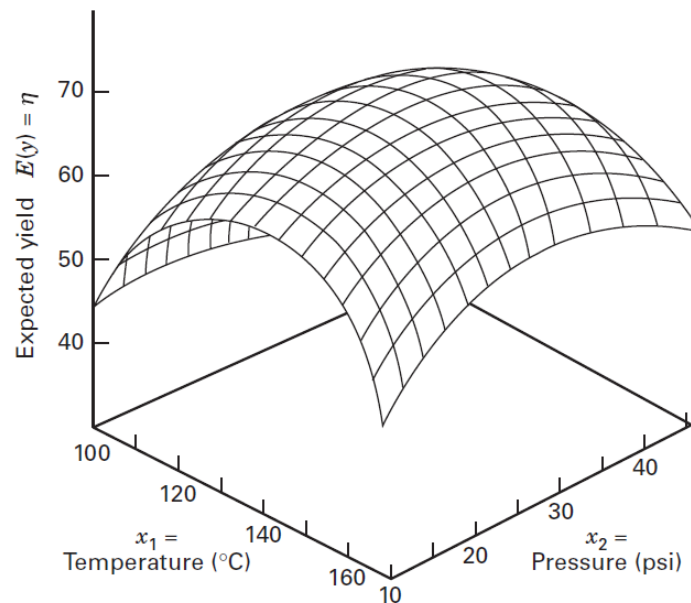


Figure 5.3 A three-dimensional response surface showing the expected yield (η) as a function of temperature (x_1) and pressure (x_2) (75)

MEPDG uses load spectra to characterize traffic loading. Load spectra are composed of traffic volume, vehicle classification and axle weight information. Although it is a scientific advancement, more work is needed to understand and manage it. Nguyen (76) provided a comprehensive study on traffic data for MEPDG. The influence of traffic data variability was also discussed. However, the equivalent single axle load (ESALs) as used in the AASHTO 1993 Guide was selected for this study, because the scope of this study was to understand reliability through Monte Carlo simulation and response surface models. Future efforts on load spectra are highly recommended.

In terms of pavement structure and materials, a three layer typical flexible pavement was used in MEPDG simulations. Modulus and thickness of each layer were probabilistic parameters.

Finally, three response surface models were constructed for the three major performance indexes: alligator cracking, total rutting and smoothness (IRI). The following sections will explain the design of experiment, model construction and validation.

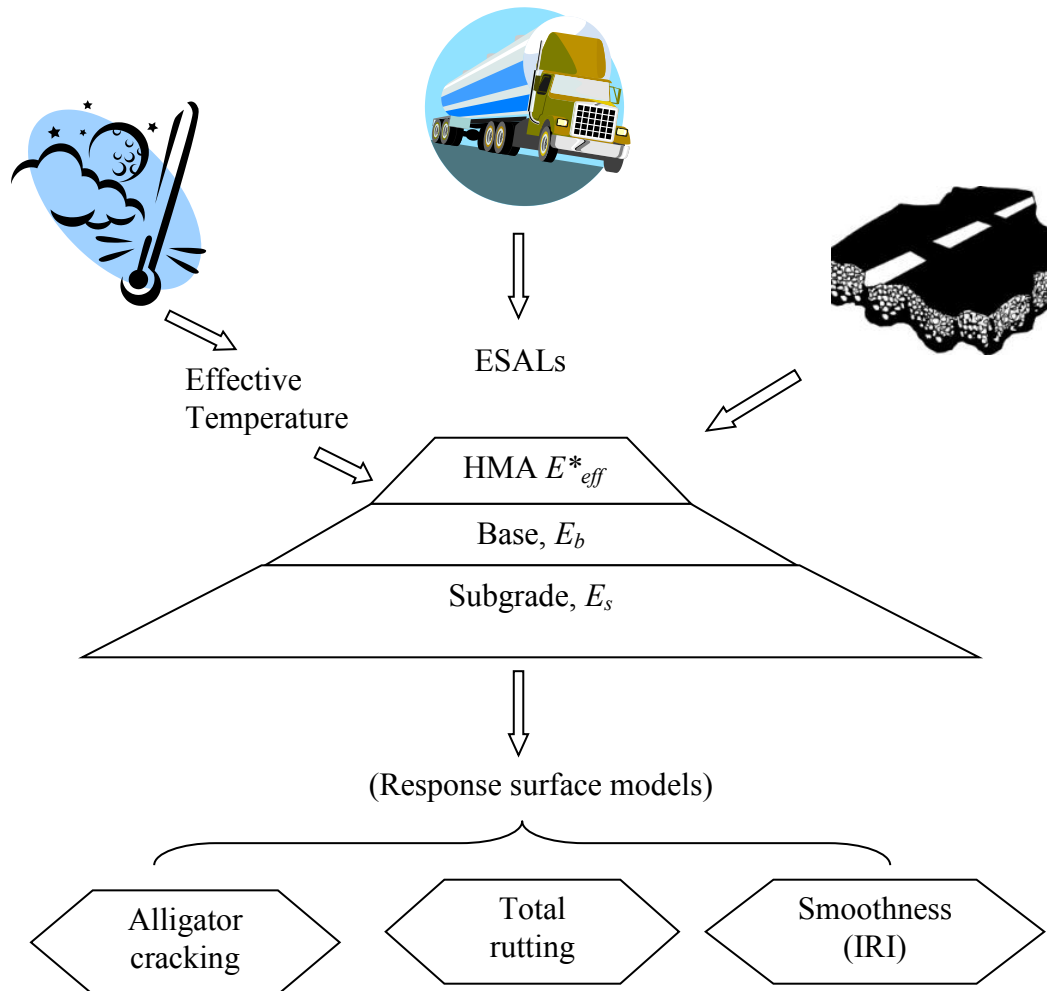


Figure 5.4 Concept of the response surface method for MEPDG



5.2 Design of Experiment

The MEPDG contains a very large number of variables. Although this has been reduced to ten, it was still too many if one applies a full factorial design, which needs $3^{10} = 59,049$ simulations. A variety of experimental design methods, including fractional factorial design, central composite design, Box-Behnken design, random sampling, and Latin Hypercube design (77) were investigated to minimize MEPDG runs to a practical number of runs, while at the same time maintain the model's capability. The following sections discuss the global pavement structure, screening analysis and examples of different experimental design methods.

5.2.1 Global Pavement Structure

A surrogate model focuses on inputs and outputs. By tuning the inputs and observing their corresponding responses, a surrogate model is built and the system is simplified. To achieve this, researchers need to define a global structure first. The global structure will function as the mainframe or motherboard, on which the influence of different factors is simulated. For example, equivalency concepts used in rigid pavement models in MEPDG are means to convert different structures in the real world to the global structure built in the model.

In this study, a three-layer flexible pavement commonly used in Arkansas was selected as the global structure. This structure contained AC surface, Class 7 unbound base, and A-4 subgrade. Based on the results from risk assessment (Chapter 4) and sensitivity analysis from the literature, ten factors were initially considered as necessary to be included in the surrogate model. Other parameters available in MEPDG were set as deterministic factors, using common values in Arkansas or default values in MEPDG.

	Deterministic factors	Probabilistic factors
	Ground water table depth	Climate location
	Traffic growth factor, vehicle class distribution, monthly/hourly adjustment, truck configuration	Initial AADTT, operational speed
Asphalt Concrete	Poisson's ratio, total unit weight, thermal properties, reference temperature, coefficient of thermal contraction	Thickness, gradation, PG grade, voids filled with asphalt (VFA)
Unbound base (Class 7)	Poisson's ratio, gradation, PI, LL, maximum dry unit weight, hydraulic conductivity, optimum water content	Thickness, resilient modulus
Subgrade (A-4)	Poisson's ratio, gradation, PI, LL, maximum dry unit weight, hydraulic conductivity, optimum water content	Resilient modulus

Note: AADTT is Annual Average Daily Truck Traffic; PI is Plasticity Index; LL is Liquid Limit; Class 7 is a category of unbound aggregate base widely used in Arkansas.

Figure 5.5 The global structure and factors considered in this study.

Table 5.2 lists the common values for the ten probabilistic factors in the state of Arkansas. To fully cover the input space, 118,098 simulations were required using a full factorial design. To reduce this impractical number down, further simplification had to be made. Therefore, this study conducted two other screening analyses: one to justify the significance of climate location on pavement design in Arkansas, and the other on operational speed.

Table 5.2 Experimental design for initial interests

Term	Factor	Value	# of values
--	Climate stations	Mountain Home, Fort Smith, Little Rock, Texarkana, Monticello, West Memphis	6
--	Initial AADTT	900, 5450, 10000 (corresponding EASLs: 2.8, 15.4, 30.8 millions)	3
--	Traffic speed (mph)	25, 45, 60	3
h_{ac}	AC thickness (inch)	2, 7, 12	5
--	AC gradation	Fine (1), Regular (2) and Coarse (3)	3
V_a	AC air voids and effective binder content	(4,16); (8,12); (12, 8) (corresponding VFA: 0.8, 0.6, 0.4)	3
--	PG grade	PG64-22, PG70-22, PG76-22	3
h_{base}	Base thickness (inch)	6, 9, 12	3
M_{rb}	Base resilient modulus (ksi)	20, 60, 100	3
M_{rs}	Subgrade resilient modulus (ksi)	5, 15, 25	3
Total runs of a factorial design (10 factors)			118,098

Gradations for the three types of asphalt mixtures are listed in Table 5.3. Other materials properties such as plasticity index, liquid limit, specific gravity and thermal property were MEPDG Level 3 default values. Input values for other deterministic variables are presented in Table 5.4. Traffic data from project TRC-0402 (78) were used to represent the condition of Arkansas. Vehicle classification was in TTC group 6, representing principle arterials that have mixed truck traffic with a higher percentage of single-unit trucks. To understand the difference between MEPDG default and Arkansas' data, Figure 5.6 and 5.7 show the comparison of vehicle classification and hourly distribution. It indicated that TTC6 in Arkansas had slightly more Class 9 vehicle and less Class 5 vehicle than the MEPDG defaults. For hourly distribution, Arkansas

presented higher level of truck traffic in daytime and lower level of trucks in nighttime comparing to the MEPDG default values. Axle load distribution factors were matrix of load bins and vehicle classes. TRC0402 also recommended the statewide load spectra, as shown in Table 5.5 through 5.7. Figure 5.8 through 5.11 give a peek view of the axle load distribution. Using the MEPDG default as a reference, it was found that single axle load in Arkansas was mainly between 8 to 12 kips; the two peaks for tandem axle load were slightly left-shift, indicating that Class 9 trucks could carry slight less weight than the national default. Class 7 trucks, however, could be loaded with more weight than the MEPDG default, and the tridem axle load was concentrated between 42 and 60 kips.

Table 5.3 Gradations for asphalt mixture

	Fine	Regular	Coarse
Cumulative % retained 3/4" sieve	0	6	12
Cumulative % retained 3/8" sieve	18	28	38
Cumulative % retained #4 sieve	47	48.5	50
% Passing #200 sieve	4.5	4.3	4

Table 5.4 Input for deterministic variables

Design Life	5, 10, 15, 20 years
Base/subgrade construction month	August, 2011
Pavement construction month	September, 2011
Traffic open month	October, 2011
Number of lanes in design direction	2
Percent of trucks in design direction	50%
Percent of trucks in design lane	90%
Operational speed	60 mph
Monthly adjustment	1.0 for all classes and all months
Vehicle classification	TTC 6
Traffic growth rate	2% compound growth
Mean wheel location	18 inches
Traffic wander standard deviation	10 inches
Design lane width	12 ft.
Number of axles per truck	MEPDG national default
Axle configuration	MEPDG national default
Wheelbase	MEPDG national default
Depth of water table depth	20 ft.
Thermal cracking	MEPDG Level 3 national default

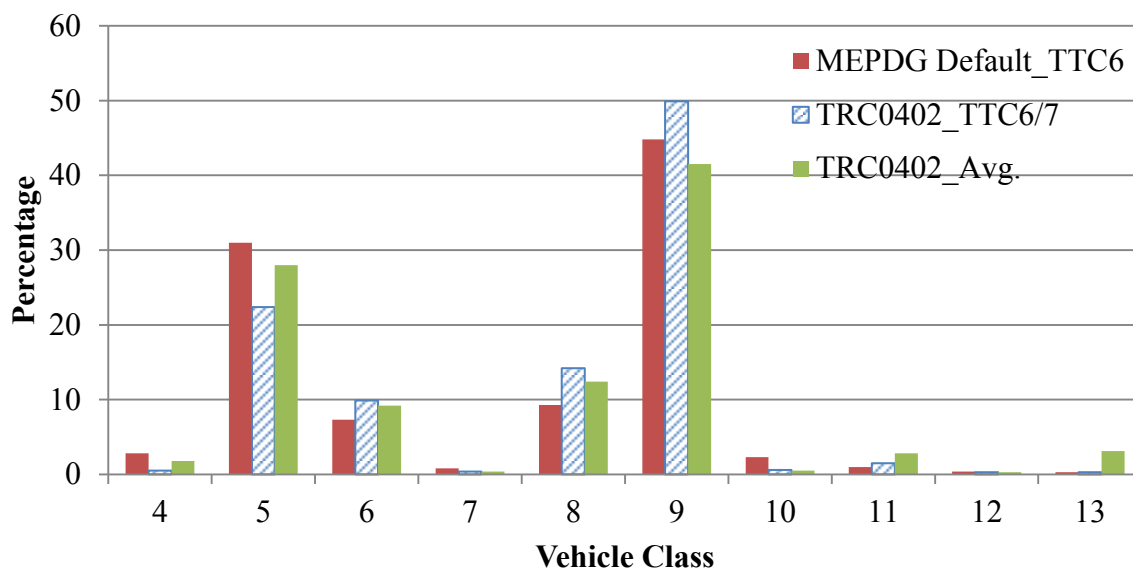


Figure 5.6 Vehicle class distribution.

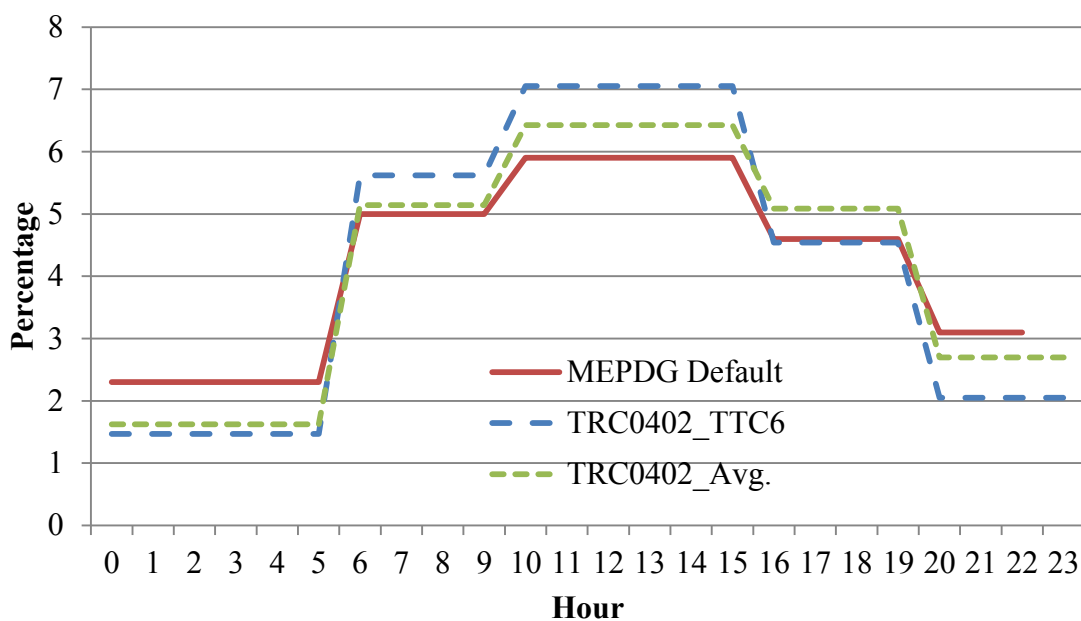


Figure 5.7 Hourly distribution.

Table 5.5 Statewide Single Axle Load Spectra (78)

Ax. Load (lb)	Vehicle Class									
	4	5	6	7	8	9	10	11	12	13
3000	2.641	11.089	1.601	0.119	8.354	0.294	1.058	0.361	0.481	6.155
4000	6.976	29.213	3.982	0.566	19.658	1.313	3.705	1.545	2.602	10.304
5000	4.826	16.709	3.307	0.648	11.548	1.407	3.216	2.874	4.130	5.735
6000	5.517	11.963	4.627	1.542	9.931	2.202	4.082	6.806	10.036	6.908
7000	6.473	7.451	6.378	1.971	7.976	4.240	6.172	9.282	13.239	6.701
8000	6.186	4.667	8.287	2.792	6.091	7.592	8.285	9.211	12.182	6.324
9000	10.021	4.711	15.724	7.054	7.187	18.825	15.948	14.091	16.428	8.673
10000	8.636	2.970	14.774	8.952	5.042	21.041	14.930	10.435	11.665	5.102
11000	11.153	2.868	15.561	14.333	5.166	22.301	16.425	10.618	10.666	7.266
12000	7.798	1.725	8.505	13.091	3.440	10.116	9.422	7.004	5.755	4.097
13000	8.202	1.639	6.580	14.594	3.519	5.909	7.215	7.571	5.254	6.628
14000	5.464	1.014	3.130	10.271	2.271	2.105	3.269	5.018	2.471	3.535
15000	4.888	1.010	2.552	8.441	2.248	1.263	2.389	4.886	1.960	3.578
16000	2.802	0.619	1.346	5.271	1.430	0.529	1.109	2.967	0.999	3.367
17000	2.414	0.617	1.172	3.989	1.447	0.370	0.881	2.774	0.834	3.468
18000	1.422	0.376	0.629	1.807	0.907	0.170	0.438	1.517	0.396	2.493
19000	1.126	0.360	0.546	1.928	0.896	0.124	0.380	1.233	0.337	2.658
20000	0.679	0.221	0.312	0.686	0.569	0.064	0.228	0.614	0.155	1.250
21000	0.651	0.210	0.297	0.654	0.563	0.047	0.197	0.462	0.161	1.205
22000	0.542	0.153	0.191	0.380	0.436	0.030	0.149	0.274	0.069	1.262
23000	0.288	0.091	0.114	0.213	0.277	0.015	0.101	0.148	0.040	0.527
24000	0.325	0.089	0.103	0.170	0.255	0.014	0.089	0.104	0.042	0.588
25000	0.189	0.051	0.060	0.084	0.160	0.008	0.060	0.050	0.017	0.427
26000	0.126	0.051	0.058	0.187	0.155	0.007	0.070	0.048	0.012	0.508
27000	0.107	0.030	0.027	0.081	0.088	0.004	0.030	0.016	0.017	0.181
28000	0.120	0.026	0.030	0.048	0.090	0.004	0.020	0.016	0.008	0.202
29000	0.054	0.015	0.024	0.024	0.057	0.002	0.034	0.008	0.007	0.193
30000	0.062	0.017	0.016	0.031	0.057	0.002	0.037	0.008	0.008	0.149
31000	0.062	0.010	0.014	0.017	0.034	0.001	0.003	0.024	0.003	0.086
32000	0.035	0.009	0.011	0.015	0.040	0.001	0.004	0.011	0.003	0.096
33000	0.059	0.005	0.008	0.004	0.020	0.001	0.014	0.010	0.003	0.024
34000	0.027	0.005	0.009	0.004	0.022	0.000	0.017	0.009	0.010	0.091
35000	0.035	0.004	0.004	0.000	0.016	0.000	0.007	0.001	0.010	0.053
36000	0.039	0.004	0.009	0.017	0.016	0.000	0.001	0.001	0.001	0.051
37000	0.011	0.003	0.005	0.000	0.012	0.000	0.003	0.001	0.001	0.042
38000	0.010	0.002	0.003	0.000	0.006	0.000	0.002	0.001	0.000	0.025
39000	0.035	0.002	0.004	0.013	0.011	0.000	0.008	0.001	0.001	0.009
40000	0.004	0.002	0.002	0.000	0.005	0.000	0.000	0.000	0.000	0.037
41000	0.001	0.001	0.001	0.002	0.003	0.000	0.001	0.000	0.000	0.004

Table 5.6 Statewide Tandem Axle Load Spectra (78)

Ax. Load (lb)	Vehicle Class									
	4	5	6	7	8	9	10	11	12	13
6000	1.048	0.000	2.788	0.000	7.168	1.186	1.267	0.000	0.416	4.488
8000	2.336	0.000	9.477	0.000	13.251	3.940	2.549	0.000	1.800	8.243
10000	1.836	0.000	10.963	0.000	11.831	6.237	2.716	0.000	4.297	6.281
12000	2.538	0.000	10.010	0.000	11.627	8.563	3.814	0.000	10.014	6.847
14000	3.965	0.000	10.456	0.000	10.441	8.924	6.530	0.000	10.447	7.326
16000	3.542	0.000	7.766	0.000	6.841	6.826	7.607	0.000	9.835	6.278
18000	3.973	0.000	6.678	0.000	5.173	5.962	8.315	0.000	10.847	7.332
20000	5.528	0.000	5.739	0.000	4.010	5.439	8.499	0.000	13.733	6.117
22000	7.661	0.000	4.943	0.000	3.314	5.334	7.700	0.000	12.420	5.012
24000	9.697	0.000	4.266	0.000	3.055	5.625	7.933	0.000	9.828	5.152
26000	11.085	0.000	4.004	0.000	3.004	6.098	7.479	0.000	6.669	4.730
28000	11.073	0.000	3.804	0.000	2.908	6.578	6.661	0.000	3.854	5.120
30000	9.557	0.000	3.530	0.000	2.798	6.783	5.882	0.000	2.644	4.538
32000	7.768	0.000	3.042	0.000	2.451	6.253	4.803	0.000	1.366	4.305
34000	6.433	0.000	2.520	0.000	2.095	5.073	4.166	0.000	0.626	3.216
36000	4.286	0.000	2.096	0.000	1.786	3.684	3.360	0.000	0.375	2.648
38000	2.434	0.000	1.756	0.000	1.553	2.489	2.655	0.000	0.228	2.182
40000	1.456	0.000	1.436	0.000	1.281	1.643	2.031	0.000	0.196	2.090
42000	1.043	0.000	1.215	0.000	1.158	1.174	1.684	0.000	0.119	1.819
44000	0.756	0.000	0.815	0.000	0.860	0.680	1.217	0.000	0.073	1.511
46000	0.499	0.000	0.664	0.000	0.705	0.452	0.747	0.000	0.044	1.511
48000	0.282	0.000	0.480	0.000	0.540	0.308	0.562	0.000	0.062	0.729
50000	0.184	0.000	0.365	0.000	0.442	0.213	0.456	0.000	0.045	0.497
52000	0.240	0.000	0.280	0.000	0.361	0.149	0.287	0.000	0.013	0.395
54000	0.081	0.000	0.213	0.000	0.300	0.105	0.217	0.000	0.011	0.513
56000	0.102	0.000	0.150	0.000	0.226	0.078	0.235	0.000	0.008	0.368
58000	0.156	0.000	0.127	0.000	0.174	0.057	0.159	0.000	0.009	0.135
60000	0.074	0.000	0.092	0.000	0.132	0.041	0.143	0.000	0.004	0.120
62000	0.076	0.000	0.073	0.000	0.112	0.030	0.105	0.000	0.002	0.068
64000	0.090	0.000	0.057	0.000	0.092	0.021	0.045	0.000	0.003	0.066
66000	0.130	0.000	0.045	0.000	0.055	0.016	0.045	0.000	0.005	0.066
68000	0.007	0.000	0.033	0.000	0.050	0.012	0.023	0.000	0.005	0.023
70000	0.028	0.000	0.030	0.000	0.041	0.009	0.028	0.000	0.001	0.039
72000	0.002	0.000	0.024	0.000	0.047	0.008	0.017	0.000	0.001	0.017
74000	0.030	0.000	0.023	0.000	0.033	0.005	0.016	0.000	0.000	0.048
76000	0.000	0.000	0.017	0.000	0.035	0.004	0.022	0.000	0.000	0.027
78000	0.007	0.000	0.014	0.000	0.024	0.003	0.020	0.000	0.003	0.016
80000	0.000	0.000	0.008	0.000	0.020	0.002	0.005	0.000	0.000	0.019
82000	0.001	0.000	0.004	0.000	0.009	0.001	0.001	0.000	0.000	0.111

Table 5.7 Statewide Tridem Axle Load Spectra (78)

Ax. Load (lb)	Vehicle Class									
	4	5	6	7	8	9	10	11	12	13
12000	0.000	0.000	0.000	0.157	0.000	0.000	4.717	0.000	0.000	0.000
15000	0.000	0.000	0.000	0.449	0.000	0.000	9.914	0.000	0.000	0.000
18000	0.000	0.000	0.000	0.530	0.000	0.000	9.689	0.000	0.000	0.000
21000	0.000	0.000	0.000	0.655	0.000	0.000	7.746	0.000	0.000	0.000
24000	0.000	0.000	0.000	0.711	0.000	0.000	6.792	0.000	0.000	0.000
27000	0.000	0.000	0.000	1.264	0.000	0.000	7.187	0.000	0.000	0.000
30000	0.000	0.000	0.000	2.015	0.000	0.000	7.184	0.000	0.000	0.000
33000	0.000	0.000	0.000	3.326	0.000	0.000	7.792	0.000	0.000	0.000
36000	0.000	0.000	0.000	6.119	0.000	0.000	7.762	0.000	0.000	0.000
39000	0.000	0.000	0.000	8.980	0.000	0.000	6.188	0.000	0.000	0.000
42000	0.000	0.000	0.000	14.087	0.000	0.000	5.948	0.000	0.000	0.000
45000	0.000	0.000	0.000	14.483	0.000	0.000	4.454	0.000	0.000	0.000
48000	0.000	0.000	0.000	13.647	0.000	0.000	3.698	0.000	0.000	0.000
51000	0.000	0.000	0.000	11.127	0.000	0.000	3.038	0.000	0.000	0.000
54000	0.000	0.000	0.000	7.597	0.000	0.000	1.972	0.000	0.000	0.000
57000	0.000	0.000	0.000	5.083	0.000	0.000	1.733	0.000	0.000	0.000
60000	0.000	0.000	0.000	3.101	0.000	0.000	1.020	0.000	0.000	0.000
63000	0.000	0.000	0.000	2.138	0.000	0.000	0.728	0.000	0.000	0.000
66000	0.000	0.000	0.000	1.491	0.000	0.000	0.619	0.000	0.000	0.000
69000	0.000	0.000	0.000	0.793	0.000	0.000	0.483	0.000	0.000	0.000
72000	0.000	0.000	0.000	0.687	0.000	0.000	0.353	0.000	0.000	0.000
75000	0.000	0.000	0.000	0.436	0.000	0.000	0.242	0.000	0.000	0.000
78000	0.000	0.000	0.000	0.345	0.000	0.000	0.161	0.000	0.000	0.000
81000	0.000	0.000	0.000	0.228	0.000	0.000	0.153	0.000	0.000	0.000
84000	0.000	0.000	0.000	0.194	0.000	0.000	0.100	0.000	0.000	0.000
87000	0.000	0.000	0.000	0.134	0.000	0.000	0.101	0.000	0.000	0.000
90000	0.000	0.000	0.000	0.101	0.000	0.000	0.075	0.000	0.000	0.000
93000	0.000	0.000	0.000	0.075	0.000	0.000	0.063	0.000	0.000	0.000
96000	0.000	0.000	0.000	0.028	0.000	0.000	0.046	0.000	0.000	0.000
99000	0.000	0.000	0.000	0.017	0.000	0.000	0.028	0.000	0.000	0.000
102000	0.000	0.000	0.000	0.005	0.000	0.000	0.016	0.000	0.000	0.000

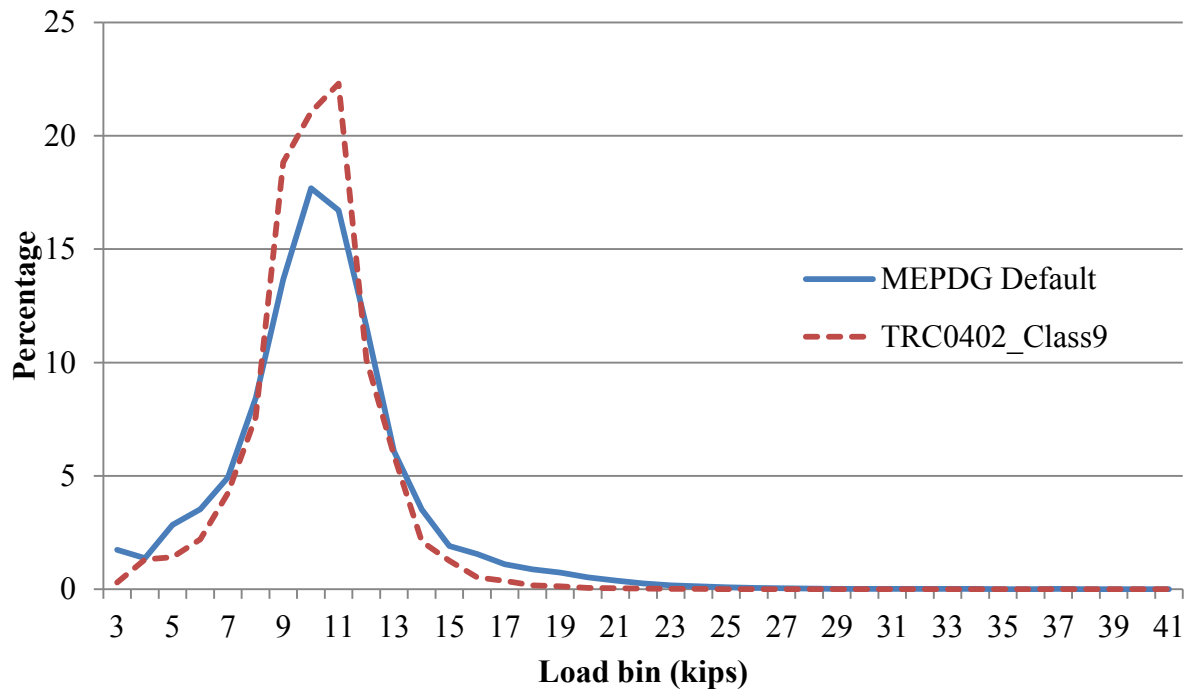


Figure 5.8 Single axle load spectra for Class 9 vehicle.

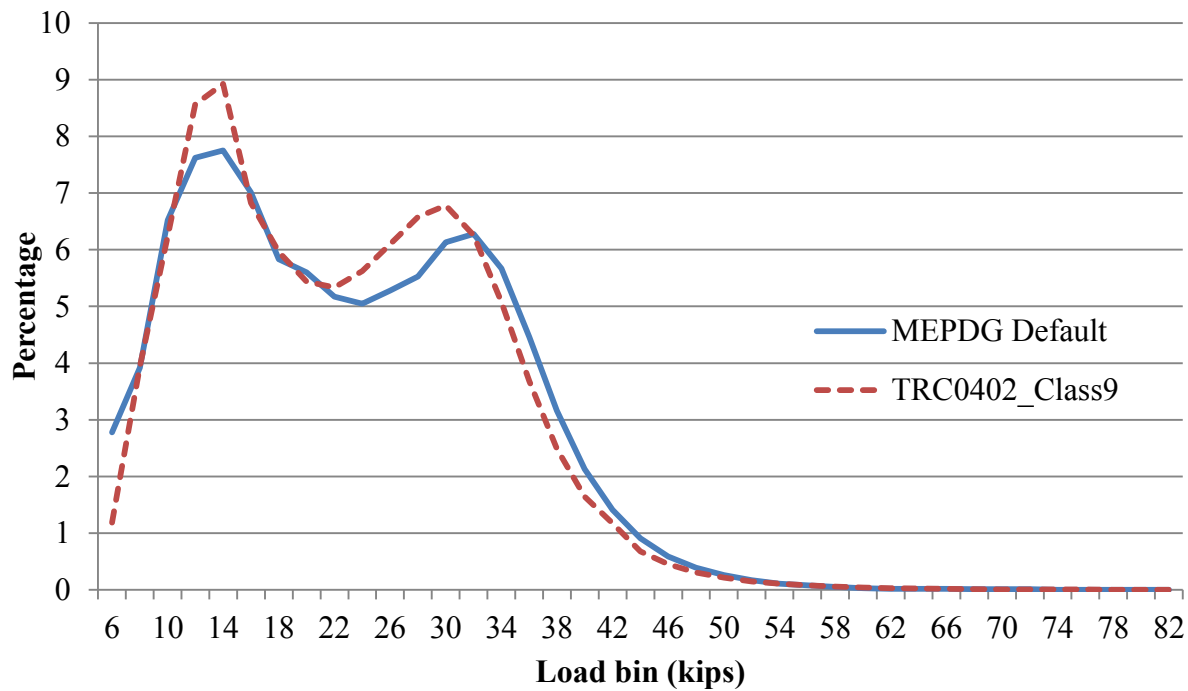


Figure 5.9 Tandem axle load spectra for Class 9 vehicle

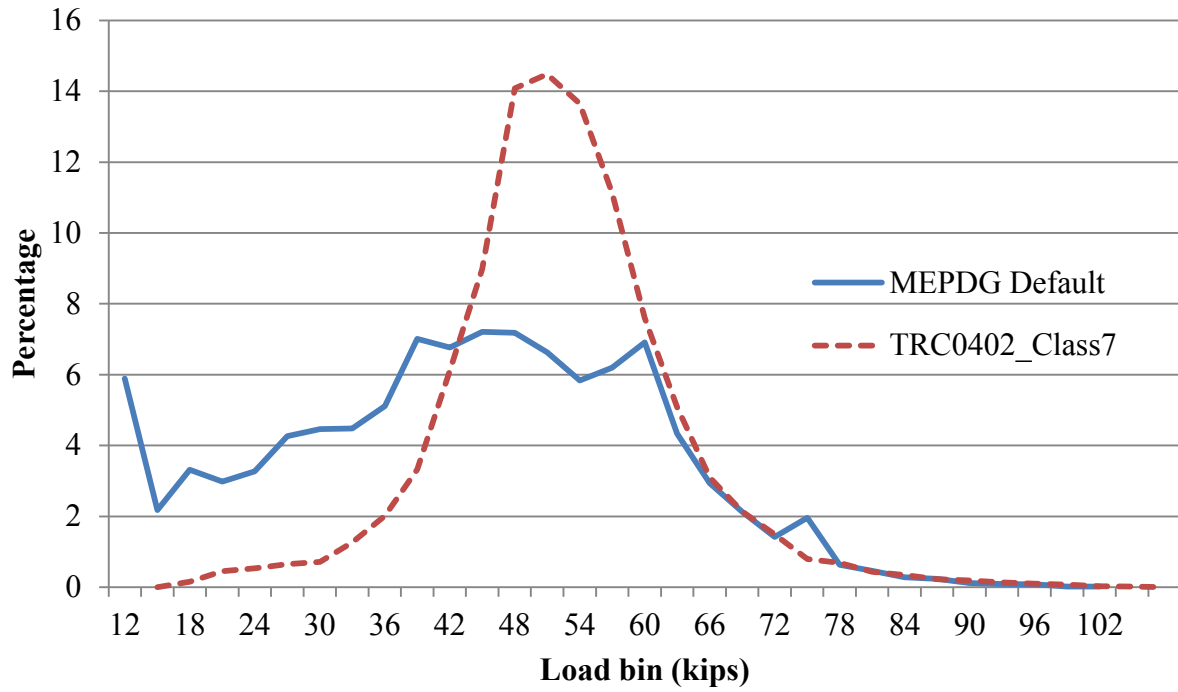


Figure 5.10 Tandem axle load spectra for Class 7 vehicle.

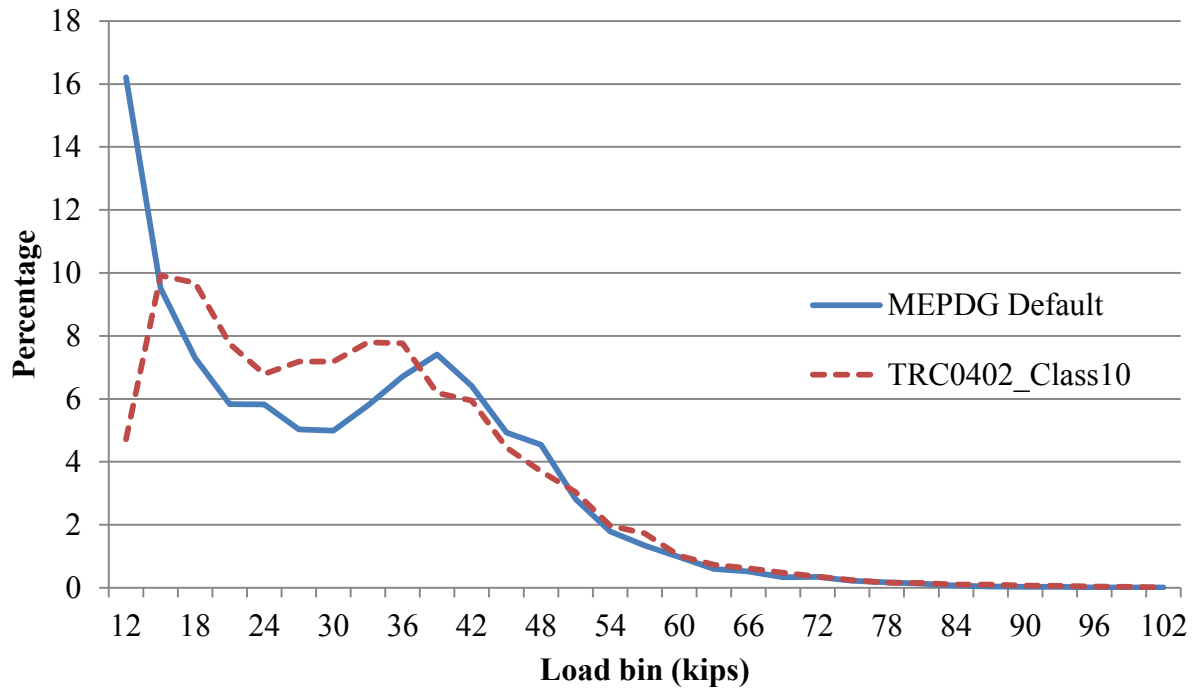


Figure 5.11 Tandem axle load spectra for Class 10 vehicle.

5.2.2 Importance Ranking

Screening analysis is a statistical method that screening out insignificant variables in a system by design experiments. To confirm the selection in Figure 5.5 and further identify the most important factors, a screening analysis with 128 MEPDG simulations was conducted. Three major performance indexes were investigated. The statistical software JMP was used for data analysis. In JMP, the Lenth's t -ratio represents how important a factor is (79). The Lenth's t -ratio is defined as

$$\text{Lenth's } t\text{-ratio} = \frac{\text{Contrast}}{\text{PSE}} \quad (5.2)$$

where *Contrast* is the estimate for the factor. For orthogonal designs, this number is the same as the regression parameter estimate. This is not the case for non-orthogonal designs.

PSE is Lenth's Pseudo-Standard Error.

The results are shown in Table 5.8 and Figure 5.12. It was found that AC thickness, base resilient modulus, VFA and initial AADTT were the most important factors for the three distress indexes. Moreover, all factors except AADTT had a negative t -ratio, which means that, for example, increasing AC thickness will decrease cracking, rutting and IRI. In addition, this analysis showed that climate location, operational speed, binder grade and AC gradation were ranked at the end for most of the cases.

One should note that this study only focused on the state of Arkansas. In other words, climate locations were within the territory of Arkansas. Climate location was found as a significant factor in pavement performance in a nationwide perspective (25).

Table 5.8 Results (Lenth's *t*-ratio) of influence ranking

Variable	Alligator cracking	Total rutting	IRI	Sum(abs())	Ranking
AC Thickness	-237.3	-163.5	-54.45	455.25	1
Base Resilient Modulus	-164.32	-64.52	-48.66	277.5	2
VFA	-200.75	-20.89	-47.59	269.23	3
Initial AADTT	64.45	99.11	43.91	207.47	4
Subgrade Resilient Modulus	-16.99	-82.86	-18.41	118.26	5
Base Thickness	-32.51	-12.6	-15.23	60.34	6
AC Gradation	-10.04	10.34	12.58	32.96	7
Binder PG Grade	0.54	-19.26	-2.38	22.18	8
Operational Speed	-0.16	-13.67	-1.52	15.35	9
Climate Location	0.82	-3.95	-1.69	6.46	10

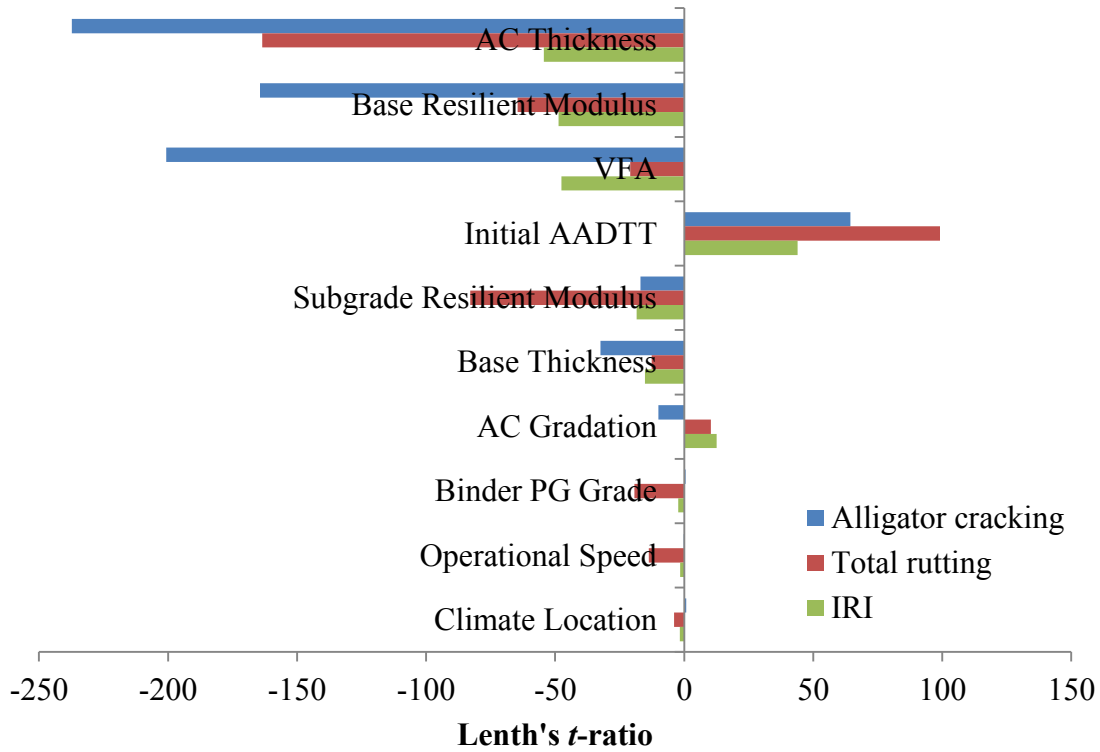


Figure 5.12 Results of screening analysis.

5.2.3 Screening of Climate Location

To further confirm the assumption that climate location is insignificant for Arkansas, a screening analysis which involves 12 climate sites was conducted. Figure 5.13 shows the location of the 12 sites. Other four sites were not included because the climatic files in MEPDG were not complete.

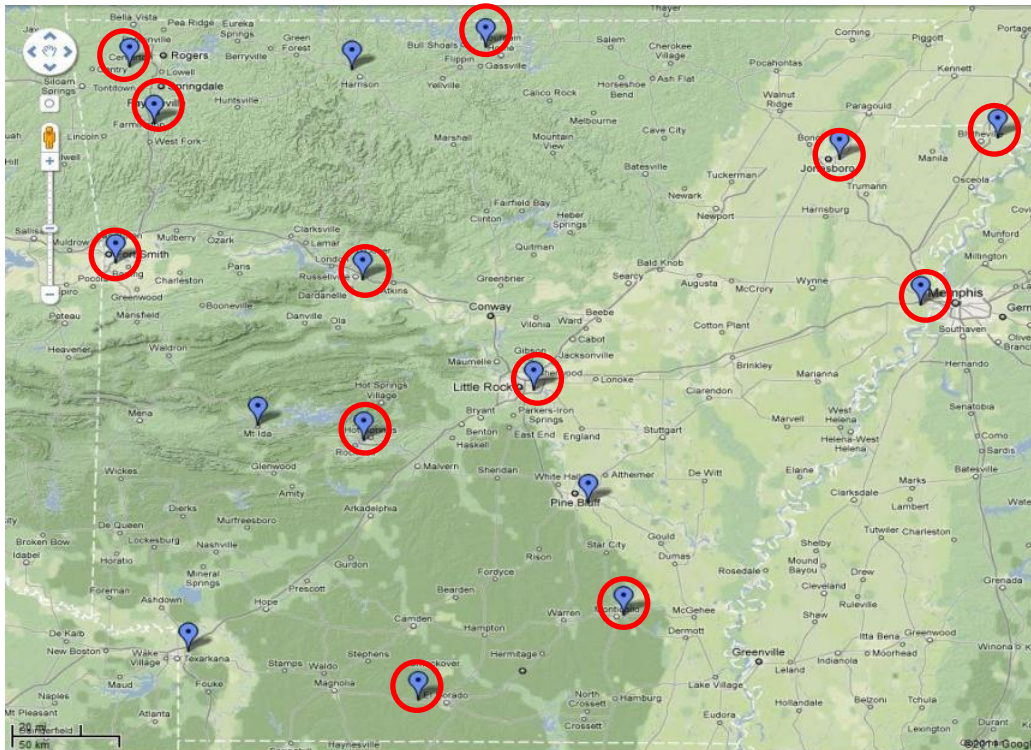


Figure 5.13 Map of Arkansas sites (Google Maps 2011).

Each site was examined under three performance grades commonly used in Arkansas: PG 64-22, PG 70-22, and PG 76-22. All parameters, including traffic, pavement structure and the water table depth, were kept identical while the climatic data was imported from the different site's climate station. Details on inputs can be referred to Byram et al. (80). By doing this, the effects of the climate alone on the pavement performance can be isolated and investigated.

Figure 5.14 through 5.17 are the predicted performance for the 12 stations. Longitudinal cracking, alligator cracking, total rutting and smoothness (IRI) were analyzed. Overall, difference between climate stations was definitely observed for all types of distresses. Climate had more influence on rutting than IRI. In addition, the study found that climate influence was more dramatic for PG64-22 than for PG76-22. This was reasonable considering the definition of the Performance Grade, which was intended to select the right binder than can withstand climatic influences. The higher the grade is, the better the binder resists to rutting under warm temperature.

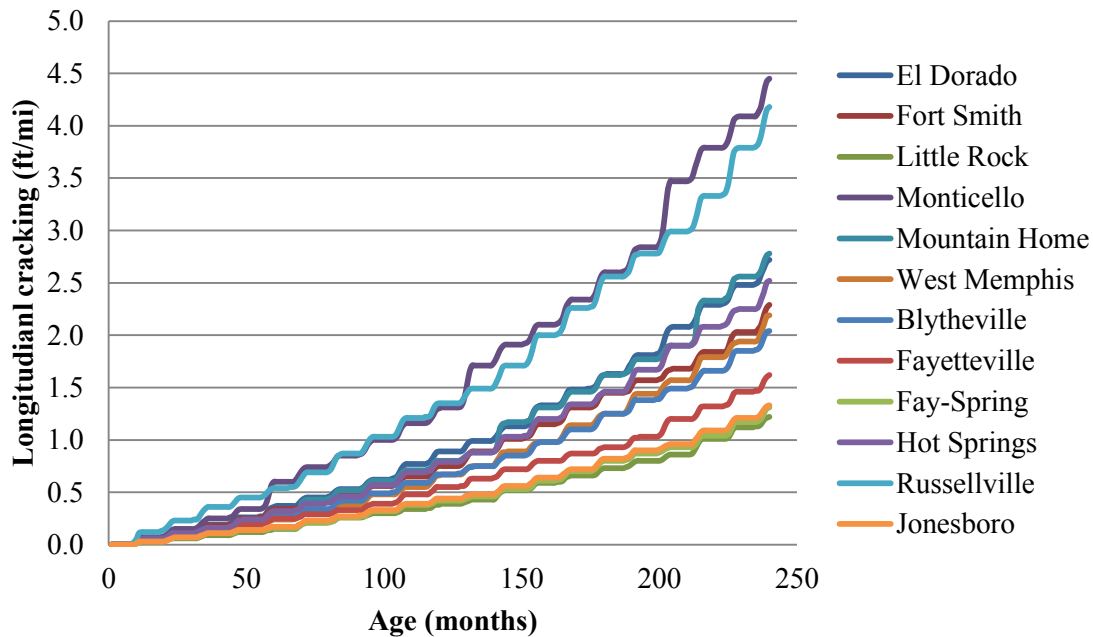


Figure 5.14 Longitudinal cracking predicted for Arkansas sites.

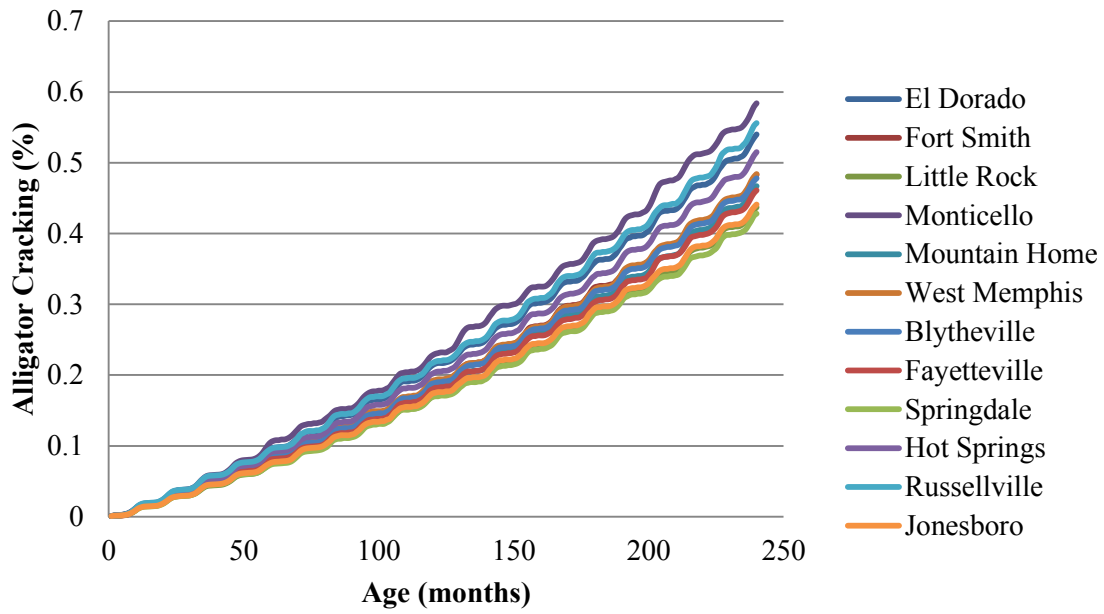


Figure 5.15 Alligator cracking predicted for Arkansas sites.

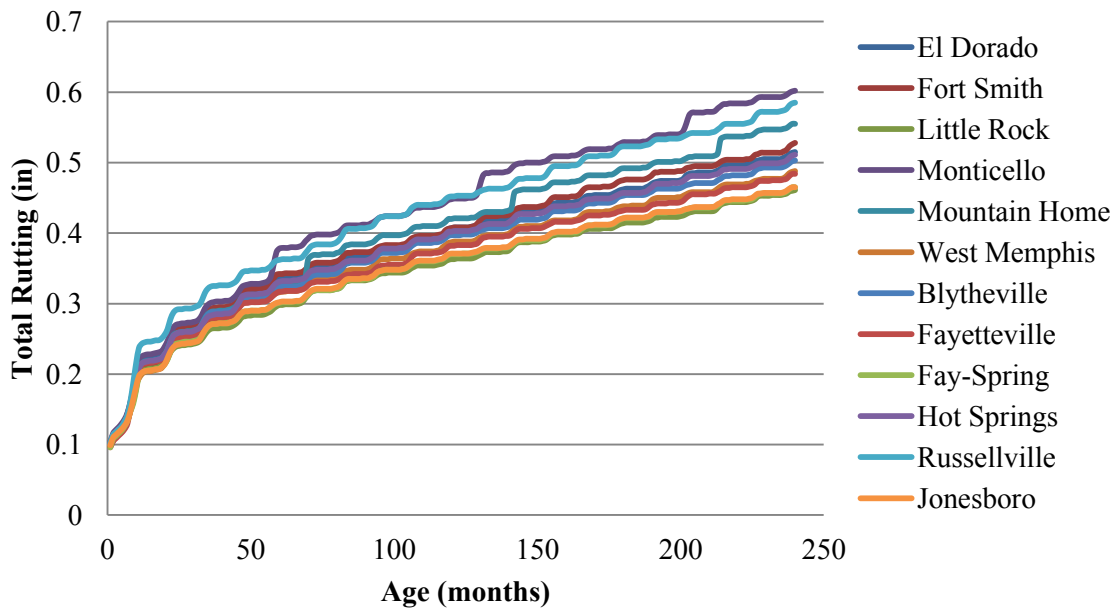


Figure 5.16 Total rutting predicted for Arkansas sites.

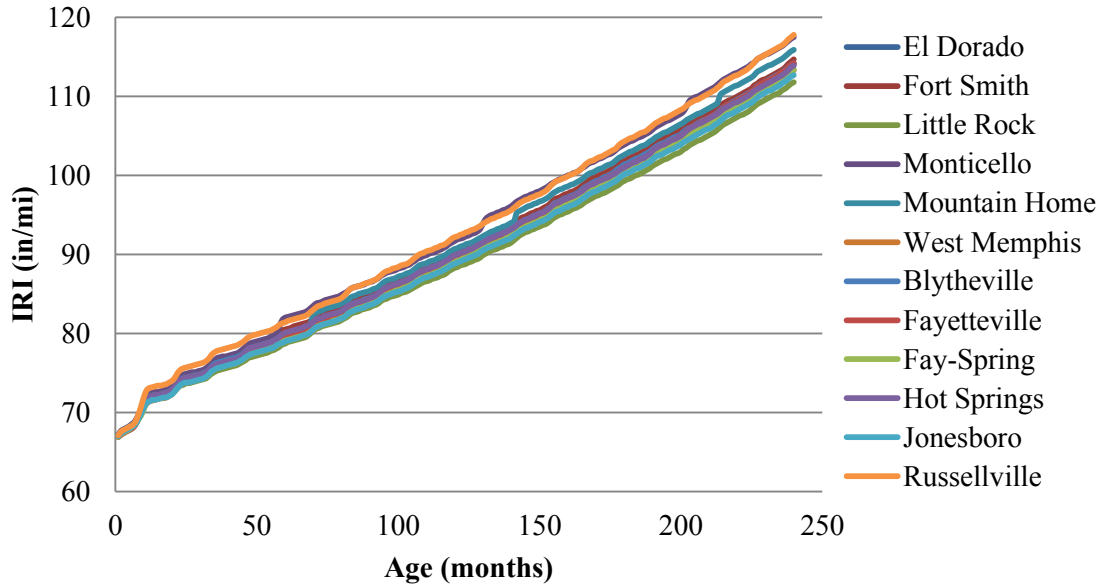


Figure 5.17 IRI predicted for Arkansas sites.

In terms of the extent of influence, however, Figure 5.14 through 5.17 show that the difference was not large for longitudinal cracking, alligator cracking and IRI, especially if one considered that the y axis was far away from the design limits. To quantify this statement, the difference at month 240 (year 20) was compared using Little Rock as the basis. The difference was further normalized to the design limit as recommended by MEPDG. The larger the normalized difference was, the more significant the difference was. The results are presented in Figure 5.18.

$$\Delta_{i,j} = x_{i,j} - x_{i,LR} \quad (5.3)$$

$$\alpha_{i,j} = \frac{x_{i,j} - x_{i,LR}}{L_i} * 100 \quad (5.4)$$

where Δ = difference between climate stations,

i = performance index (longitudinal cracking, alligator cracking, total rutting and IRI),

j = climate stations,

x_{ij} = predicted performance for climate station j ,

LR = the Little Rock station as the basis,

α_{ij} = normalized difference,

L_i = design limit for performance i , longitudinal cracking is 2000 ft/mi, alligator cracking is 25%, total rutting is 0.75 in, IRI is 172 in/mi.

It was found that the difference for longitudinal cracking, alligator cracking and IRI were all less than 5%. Total rutting was slightly sensitive to climatic influence, with an average normalized difference equal to 6%. Monticello had the highest difference. Further analysis found that Monticello was the warmest city and Fayetteville-Springdale was the coldest city among the 12 stations according to the climate record in MEPDG (mean annual air temperature).

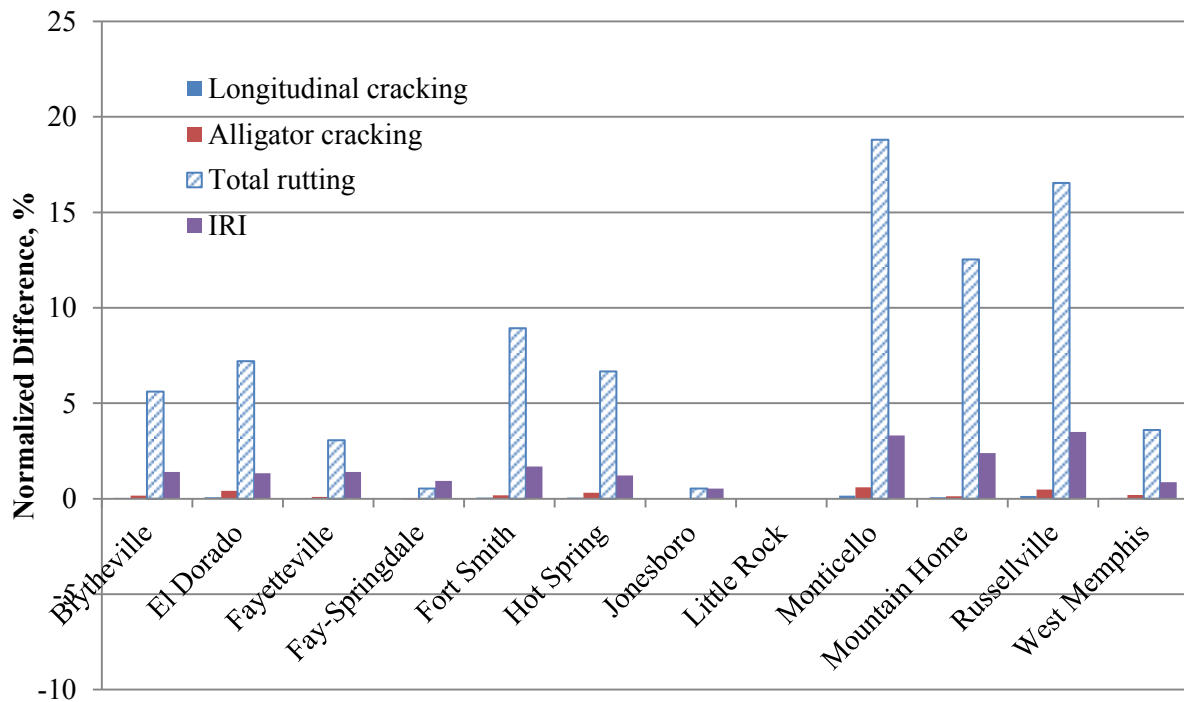


Figure 5.18 Normalized difference for Arkansas sites.

The study also conducted correlation analysis and hierarchical regression analysis to understand what main factors among the several climatic indexes: temperature, rainfall, freeze

index, freeze/thaw, wind speed, sun percentage, number of wet days and forest depth. More analyses were documented in (80). For the purpose of reliability analysis, decision was made in this research to consider climate location as a deterministic factor, using Little Rock as the standard location.

5.2.4 Screening of Operational Speed

The importance ranking showed that operational speed had a slight impact on total rutting. Sumee (81) also reported that operational speed had slight to no impact on pavement performance. But El-Badawy (82) found that operational speed had a big impact on dynamic modulus and therefore on pavement performance. Therefore, a pilot study was conducted to further verify the significance of operational speed.

The study kept all inputs as constant and only changed operational speed from 0.5 mph to 80 mph. Results are shown in Figure 5.19 through 5.21. It was found that the influence of speed was nonlinear: a big influence when the speed was between 0.5 and 5 mph, some influence from 5 to 25 mph, and a slight impact when the speed was over 25 mph. Converting this to practical meaning, that is, flexible pavements performed differently in slow traffic (i.e., in urban street or at traffic signal) and high speed (i.e., on Interstates or major corridors). But there was no dramatic difference after the traffic reached 25 mph.

Since this study mainly focuses on primary roads and freeways, speed was considered as a deterministic factor.

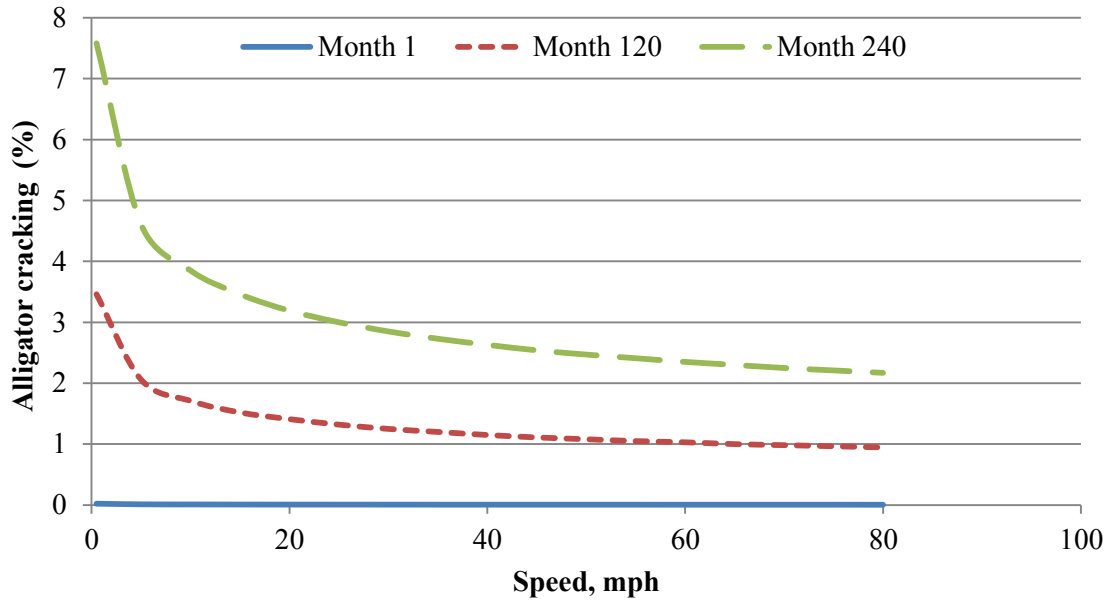


Figure 5.19 Influence of speed on alligator cracking.

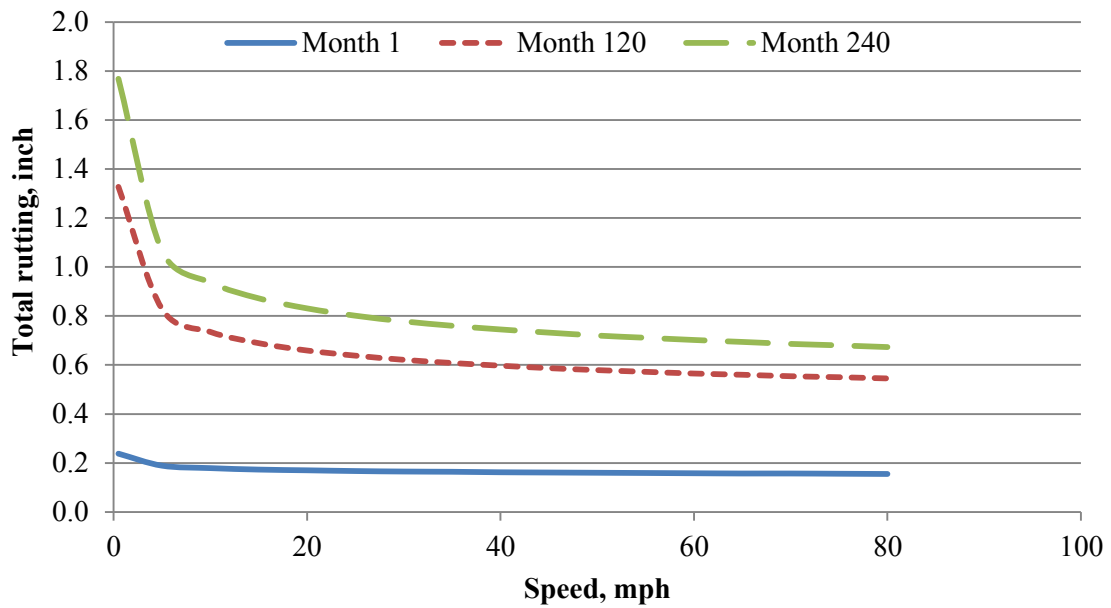


Figure 5.20 Influence of speed on total rutting.

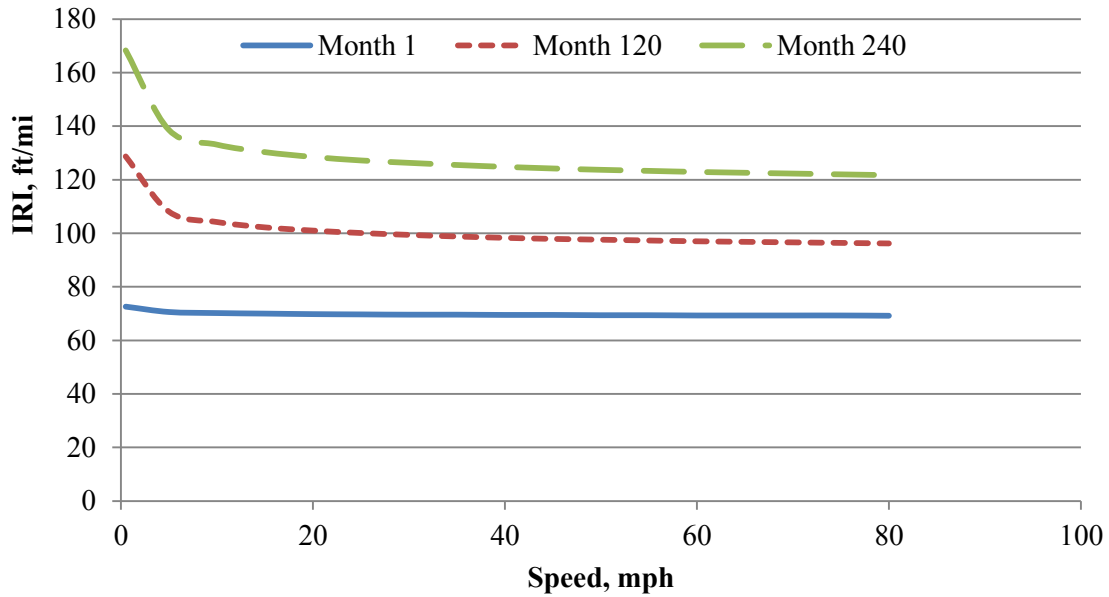


Figure 5.21 Influence of speed on IRI.

5.2.5 Examples of Experimental Design

Based on aforementioned analysis, eight significant factors were selected in this study. The matrix of MEPDG simulations is shown in Table 5.9. Experimental design involved a selection from several methods such as full factorial design, fractional factorial design, Box-Behnken design, central composite design, random sampling, and Latin Hypercube design (77). To illustrate the difference between different methods, two or three factors are shown in the following example for better visualization. Each factor had three levels normalized to -1, 0 and 1. The same concept could be applied to eight factors or more.

Table 5.9 Matrix of MEPDG simulations

Factor	Value	# of values
Climate stations	Little Rock, AR	1
Initial AADTT	900, 5450, 10000 (corresponding EASLs: 2.8, 15.4, 30.8 millions)	3
Traffic speed (mph)	60	1
AC thickness (inch)	2, 7, 12	3
AC gradation	Fine (1), Regular (2) and Coarse (3)	3
AC air voids and effective binder content	(4,16); (8,12); (12, 8) (corresponding VFA: 0.8, 0.6, 0.4)	3
PG grade	PG64-22, PG70-22, PG76-22	3
Base thickness (inch)	6, 9, 12	3
Base resilient modulus (ksi)	20, 60, 100	3
Subgrade resilient modulus (ksi)	5, 15, 25	3

Note: Total runs for factorial design is 6,561; for central composite design is 274.

Full factorial designs measure responses using every treatment, which is defined as combinations of all factors and all levels. For instance, three factors with three levels for each factor require $3*3*3=27$ experimental runs, as shown in Figure 5.22. Therefore, this study with eight variables would require $1*3*1*3*3*3*3*3*3*3=6,561$ MEPDG simulations if a full factorial design was applied. As the amount of factors and levels increase, the number of simulations for a full factorial design increases accordingly. Although full factorial designs provide sufficient data to analyze main effects and interactions, it requires extensive data collection.

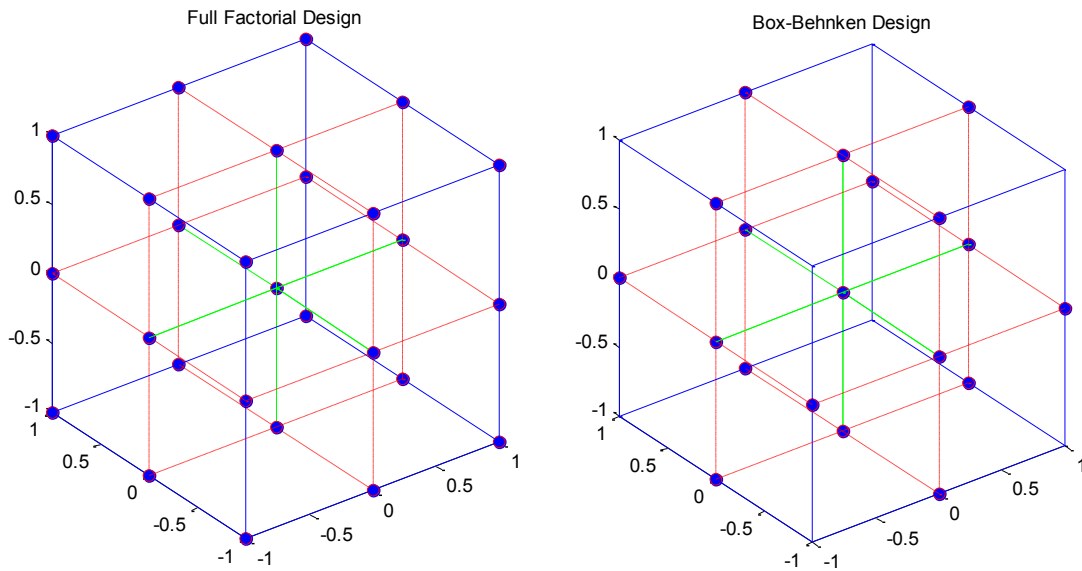


Figure 5.22 (a) Full factorial design; (b) Box-Behnken design

Fractional factorial designs use a fraction of the runs required by full factorial designs. One has to assume some main factors and interactions are aliased to reduce the design requirement.

A Box-Behnken design is able to fit a quadratic response surface. Three levels from each variable are required. Design points are located at the middle of edges and at the center of the design space. Hence, combinations of extreme values are not included. As shown in Figure 5.23 and Table 5.10, 15 experiments with 12 on edges and 3 in the center are needed for three variables using Box-Behnken design.

Central Composite Design, also known as Box-Wilson designs, is also widely used to construct response surface models. It uses three or five levels of each variable to estimate second-order effects. According to the location of the star (center) points, central composite design has three types: circumscribed, inscribed, and faced. Figure 5.23 shows the faced and circumscribed design. For faced design, center points are located on the face of the design cubic;

therefore, each factor needs only three levels. The center points are located in the circumference of the circle centered at the cubic center; hence five levels are involved. As listed in Table 5.10, 25 experiments are designed for the three variables (8 at corners of the cubic, 6 at the center of each surface, and 10 at the center of the cubic). The two types of central composite design (faced and circumscribed) are the same except the 6 experiments at the center of each surface.

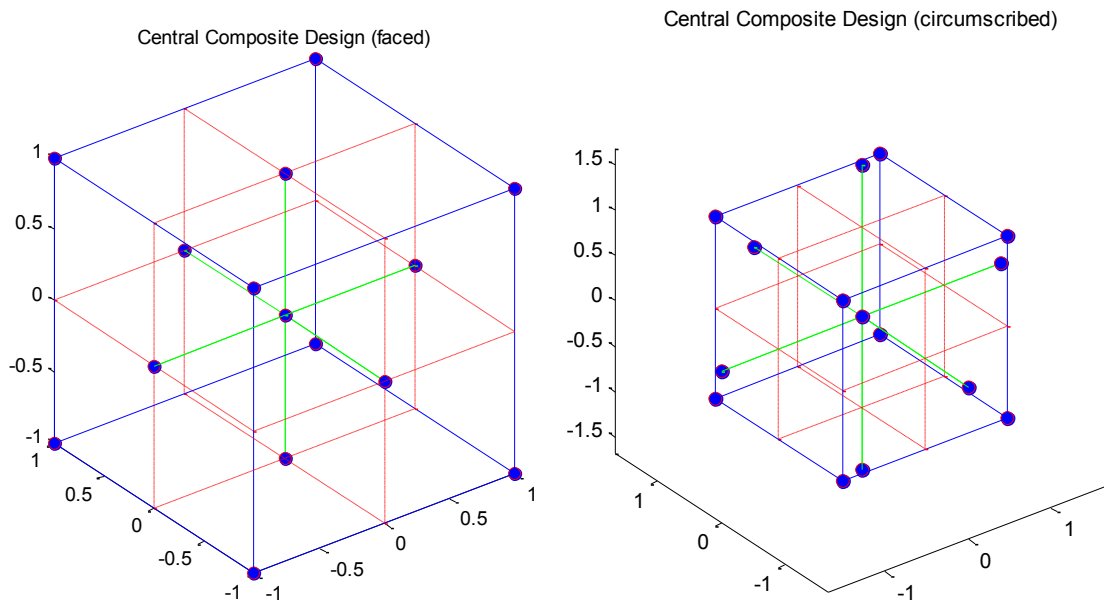


Figure 5.23 Central composite design (a) faced, (b) circumscribed.

Table 5.10 Example of experimental design for three factors with three levels

Run	Full Factorial			Central Composite (Faced)			Central Composite (Circumscribed)			Box-Behnken		
	x_1	x_2	x_3	x_1	x_2	x_3	x_1	x_2	x_3	x_1	x_2	x_3
1	-1	-1	-1	-1	-1	-1	-1	-1	-1	-1	-1	0
2	0	-1	-1	-1	-1	1	-1	-1	1	-1	1	0
3	1	-1	-1	-1	1	-1	-1	1	-1	1	-1	0
4	-1	0	-1	-1	1	1	-1	1	1	1	1	0
5	0	0	-1	1	-1	-1	1	-1	-1	-1	0	-1
6	1	0	-1	1	-1	1	1	-1	1	-1	0	1
7	-1	1	-1	1	1	-1	1	1	-1	1	0	-1
8	0	1	-1	1	1	1	1	1	1	1	0	1
9	1	1	-1	-1	0	0	-1.68	0	0	0	-1	-1
10	-1	-1	0	1	0	0	1.68	0	0	0	-1	1
11	0	-1	0	0	-1	0	0	-1.68	0	0	1	-1
12	1	-1	0	0	1	0	0	1.68	0	0	1	1
13	-1	0	0	0	0	-1	0	0	-1.68	0	0	0
14	0	0	0	0	0	1	0	0	1.68	0	0	0
15	1	0	0	0	0	0	0	0	0	0	0	0
16	-1	1	0	0	0	0	0	0	0	0	0	0
17	0	1	0	0	0	0	0	0	0	0	0	0
18	1	1	0	0	0	0	0	0	0	0	0	0
19	-1	-1	1	0	0	0	0	0	0	0	0	0
20	0	-1	1	0	0	0	0	0	0	0	0	0
21	1	-1	1	0	0	0	0	0	0	0	0	0
22	-1	0	1	0	0	0	0	0	0	0	0	0
23	0	0	1	0	0	0	0	0	0	0	0	0
24	1	0	1	0	0	0	0	0	0	0	0	0
25	-1	1	1									
26	0	1	1									
27	1	1	1									

Random sampling selects samples randomly from the population using random numbers. Therefore, samples are independent from each other. However, there are chances that two or more samples are clustered in one region of the sample space. It is not guaranteed that all regions are covered.

Latin Hypercube sampling, however, provides better coverage by dividing the design space into square grids and then assigning random samples into each grid. To achieve this, one must remember what row and column the sample point is assigned to. In other words, samples are dependently drawn to assure only one sample occupies one row and one column. The result of Latin Hypercube sampling is a better coverage with no additional samples.

Figure 5.24 gives an example of six experiments for two variables (X_1 and X_2) from uniform distribution ranging at $[-3, 3]$ and standard normal distribution $X_i \sim N(0, 1)$. The difference for the uniform distribution is more obvious than it is for the normal distribution. It is found that five out of the six experiments located between -1 and 0. No experiment is assigned to X_1 between -3 and -2, -2 and -1, 1 and 2, as well as X_2 between -3 and -2, 1 and 2, 2 and 3. On the contrary, Latin Hypercube assigns at least one number to the predefined interval. Hence, six experiments cover the six intervals for this example.

The same pattern is observed for the normal distribution example. Using random sampling, the number of experiments assigned for X_1 in the range of $[-2,-1]$, $[-1,0]$, $[0,1]$, $[1,2]$ are 2, 1, 3, 0, respectively. This is not normally distributed though. More experiments should be assigned to the range of $[-1, 0]$ and $[0, 1]$ than the outside ranges, if a normal distribution is followed. Using Latin Hypercube sampling method, the expected distribution is achieved. The number of experiments assigned for X_1 in the four ranges is 1, 2, 2, 1, respectively.

In summary, Latin Hypercube sampling provides better coverage to the full design space.

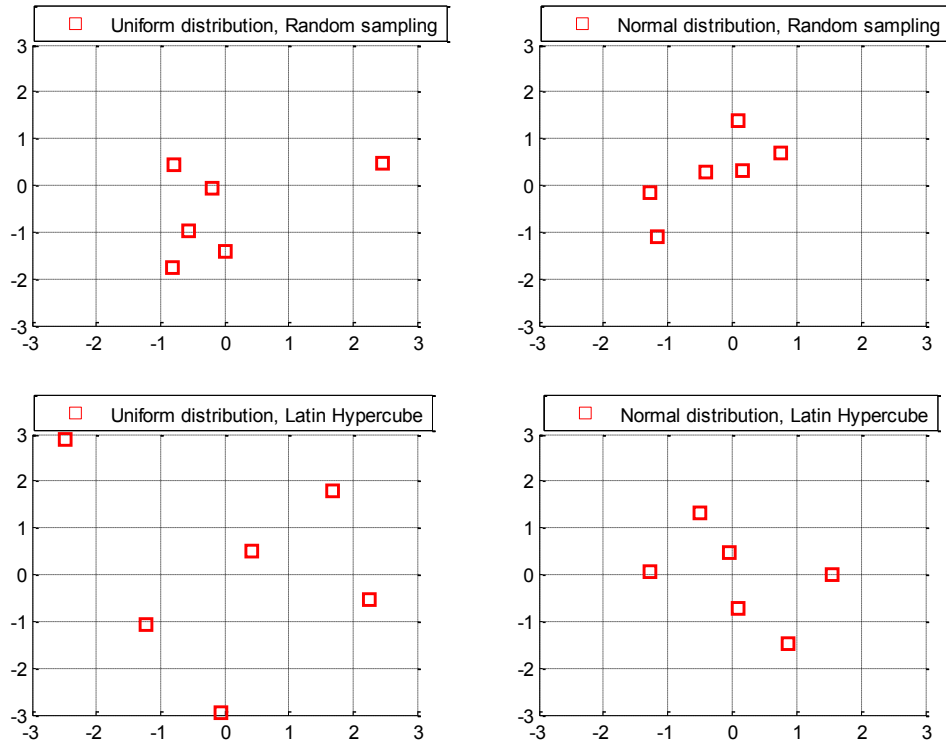


Figure 5.24 Example of random and Latin Hypercube sampling

Based on the aforementioned analysis, a central composite design was selected since it was a cost-effective method to build a quadratic model for the response without using a full three-level factorial design. By using a central composite design, the number of simulation was reduced from 6,561, the case of a full factorial design, to 274, which was a manageable 137 hours of simulation time. The range of each variable based on Arkansas' condition and practice is listed in Table 5.9. In addition, another 100 experiments, using Latin Hypercube random sampling method, were conducted to cover other untouched regions in the design space. Overall, the experimental design provided a good sample of the full design space. For example, Figure 5.25 shows the traffic levels (represented by the ESALs) included in the experiment. The three points in the central composite design (CCD) are shown as three dashed lines that set at the

bottom, middle and top of the design space. Other simulations spread between the bottom and top range (30 million to 3 million).

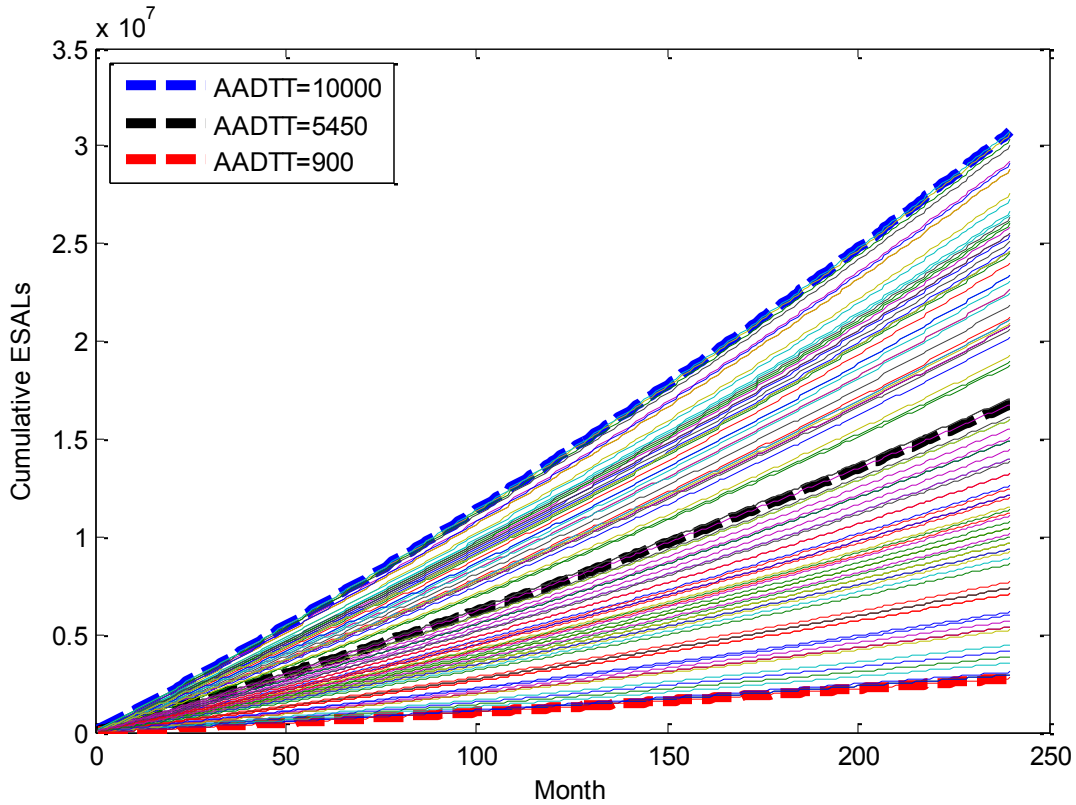


Figure 5.25 Traffic levels considered in the experimental design

5.3 Model construction

MEPDG simulations following the experimental design were conducted manually in this study. Predicted performance from MEPDG in Excel format were retrieved and stored in a single file for further analyses such as descriptive statistics, outlier test and regression analysis.

5.3.1 Parameters Preparation

Table 5.9 lists the range of each variable based on Arkansas' condition and practice. Other inputs were also mainly statewide data that were based on past research (83). For example, three typical

gradations for HMA are listed in Table 5.3 according to (84). Traffic inputs including directional distribution, lane distribution, vehicle class distribution, and axle load distribution factors were statewide data collected from project TRC-0402 (78). MEPDG defaults were also used for some inputs that did not have state-specific data, such as the viscosity parameters (A and VTS) for binders.

Table 5.11 Viscosity parameters for binders

High temperature grade	Low temperature grade (-22)	
	VTS	A
64	-3.680	10.980
70	-3.426	10.299
76	-3.208	9.715

Past research showed that alligator cracking was a type of load-related distress on which the dynamic modulus of HMA had a big impact. This study used the concept of effective dynamic modulus proposed by El-Badawy, Jeong and El-Basyouny (82). The effective AC dynamic modulus (E_{eff}^*) was defined as the single dynamic modulus at which the amount of predicted bottom-up fatigue damage equals the bottom-up fatigue damage that would occur with variable (seasonal) dynamic modulus values, which change in response to temperature and frequency change. Effective temperature in this study was based on the climate in Little Rock.

$$\log E_{eff}^* = -1.249937 + 0.029232p_{200} - 0.001767(p_{200})^2 - 0.002841p_4 - 0.058097V_a - 0.8022 \frac{V_{beff}}{V_{beff} + V_a} + \frac{3.87197 - 0.0021p_4 + 0.003958p_{38} - 0.000017(p_{38})^2 + 0.00547p_{34}}{1 + e^{(-0.603313 - 0.31333\log(f) - 0.393532\log(\eta))}} \quad (5.5)$$

where E_{eff}^* = asphalt mix dynamic modulus, 10^5 psi;

η = bitumen viscosity, 10^6 poise;

f_{eff} = effective loading frequency, Hz;

V_a = air voids in the mix, by volume, %;

Vb_{eff} = effective binder content, by volume, %;

$p_{34}, p_{38}, p_4, p_{200}$ = aggregate gradation of asphalt mix, %.

Among these factors, the bitumen viscosity is directly related to temperature.

$$\log \log \eta = A + VTS \log T \quad (5.6)$$

Where η = bitumen viscosity, Cp

A, VTS are constant related to binder grade

T = temperature in Rankine scale, $^{\circ}R = ^{\circ}F + 459.67$

Effective loading frequency is given by

$$f_{eff} = \frac{1}{t} \quad (5.7)$$

t is the time of loading

$$t = \frac{2(a + h_{ac})}{17.6v} \quad (5.8)$$

Effective temperature is calculated by

$$T_{eff} = -2.3316\sqrt{f_{eff}} - 13.9951 + 1.0056(MAAT) + 0.8755(\sigma_{MMAT}) - 1.1861(wind) + 0.5489(sun) + 0.0706(rain) \quad (5.9)$$

where $MAAT$ = mean annual air temperature, $^{\circ}F$

σ_{MMAT} = standard deviation of mean monthly air temperature in a given year, $^{\circ}F$

$wind$ = mean annual wind speed, mph

sun = mean annual sunshine, %

$rain$ = mean cumulative rainfall depth, in

Although state specific load spectra were used in MEPDG simulations, this study used the traditional ESALs as a representative of traffic in response surface models. Among all traffic inputs, only initial AADTT was a probabilistic variable. A relationship between initial AADTT and ESALs in the design life was established using the dataset in this study, as shown in Figure 5.26. The x axis is initial AADTT and y axis is the cumulative ESALs at the end of year 5, 10, 15 and 20. It was found that the two factors had a perfect linear relation when other traffic inputs are constant. Linear relationships $f_i(AADTT)$ of at year 5, 10, 15 and 20 were created using regression analysis. It should be strengthened that the linear relationship between initial AADTT and total ESALs was only valid when other traffic variables were held constant.

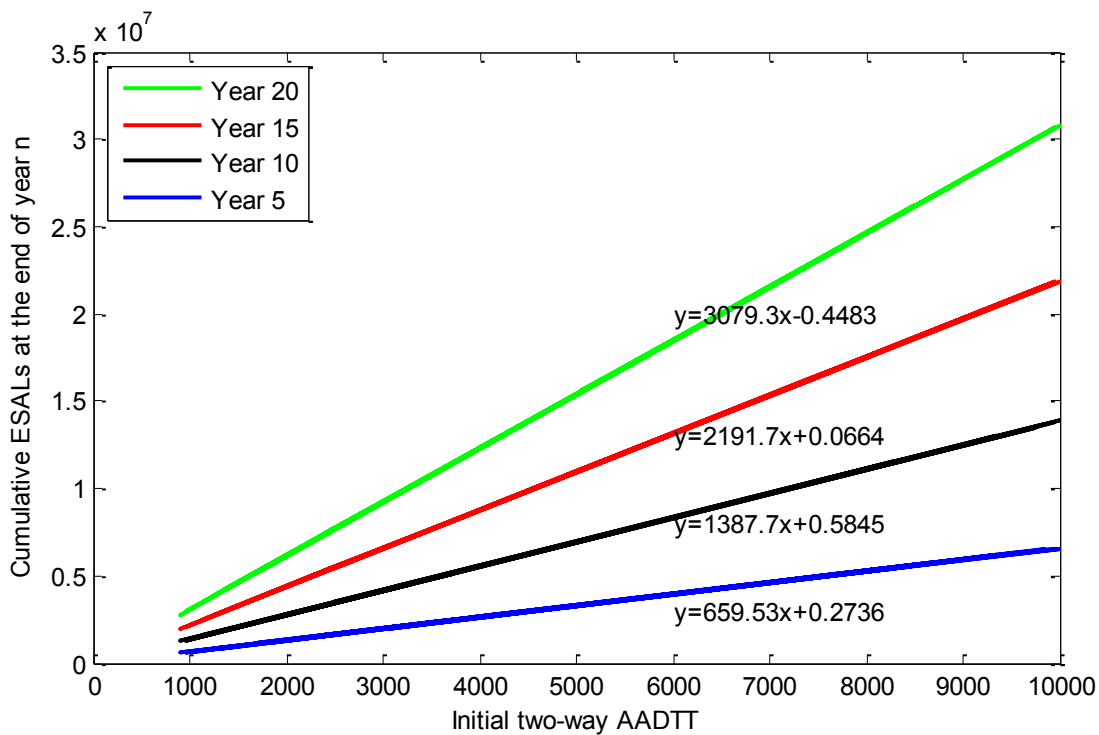


Figure 5.26 Relationship between initial AADTT and ESALs

One of MEPDG's advancements is that it provides a time series performance prediction.

For traffic, it estimates a cumulative ESALs curve. Since this study simplified the load spectra to

one probabilistic variable, initial AADTT, an effort was made to predict the traffic growth in this research.

Data from the 374 simulations were analyzed. The overall time series traffic is presented in Figure 5.27. It was found that the growth rate, comparing to the final ESALs at year 20, was constant for all cases, although the final ESALs were different for different AADTT levels. If a parameter named growth ratio is defined by

$$GR_i = \frac{ESAL_i}{ESAL_{240}} \quad (5.10)$$

where month $i=1$ to 240,

$ESAL_i$ = the cumulative ESALs at the end of month i ,

$ESAL_{240}$ = the cumulative ESALs at the end of month 240.

Then, the growth ratio of all cases in Figure 5.27 is indeed one single curve as shown in Figure 5.26. By definition, the growth ratio is between 0 and 1. Now given an initial AADTT, the time series traffic in ESALs can be calculated using

$$ESAL_i = GR_i * ESAL_{20} = GR_i * f_{20}(AADTT) \quad (5.11)$$

where month $i=1$ to 240,

$f_{20}(AADTT)$ is the relationship between $ESAL_{20}$ and AADTT as shown in Figure 5.25.

Figure 5.28 presents an example, also a test, of the aforementioned method. Giving the initial AADTT=5450, a time series ESALs is available. The growth curve from MEPDG matched exactly with the estimation from this study. This method will be used in comparing the reliability design between this study and MEPDG in Chapter 6. One should note that the linear relationship between ESALs and AADTT was only valid when other traffic parameters were held constant.

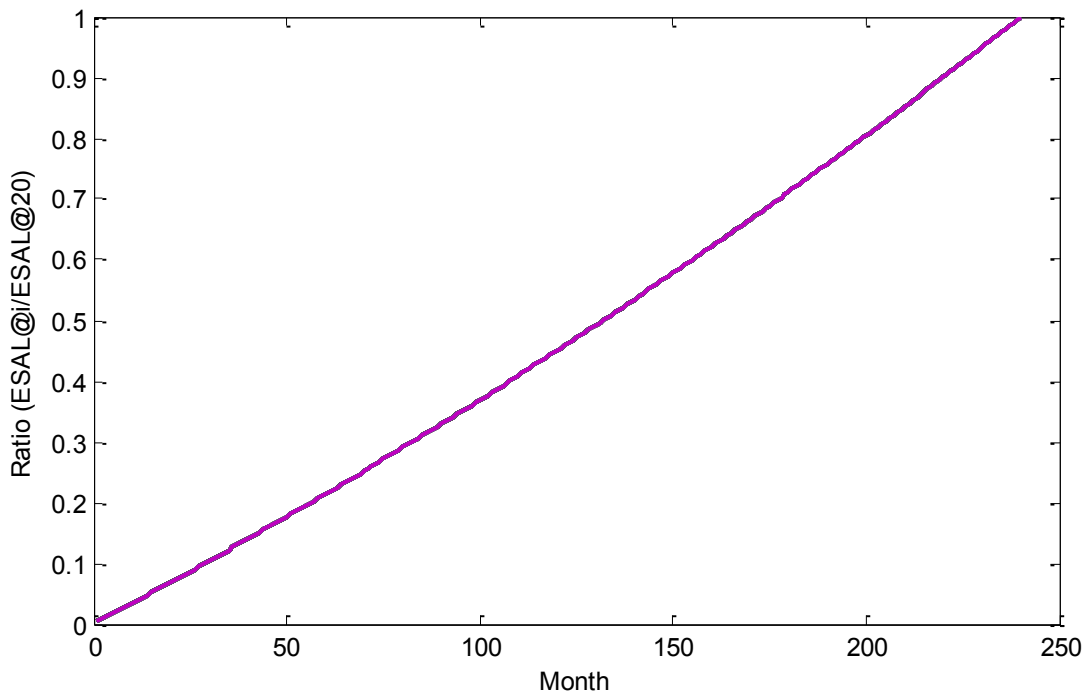


Figure 5.27 Growth ratio of ESALs

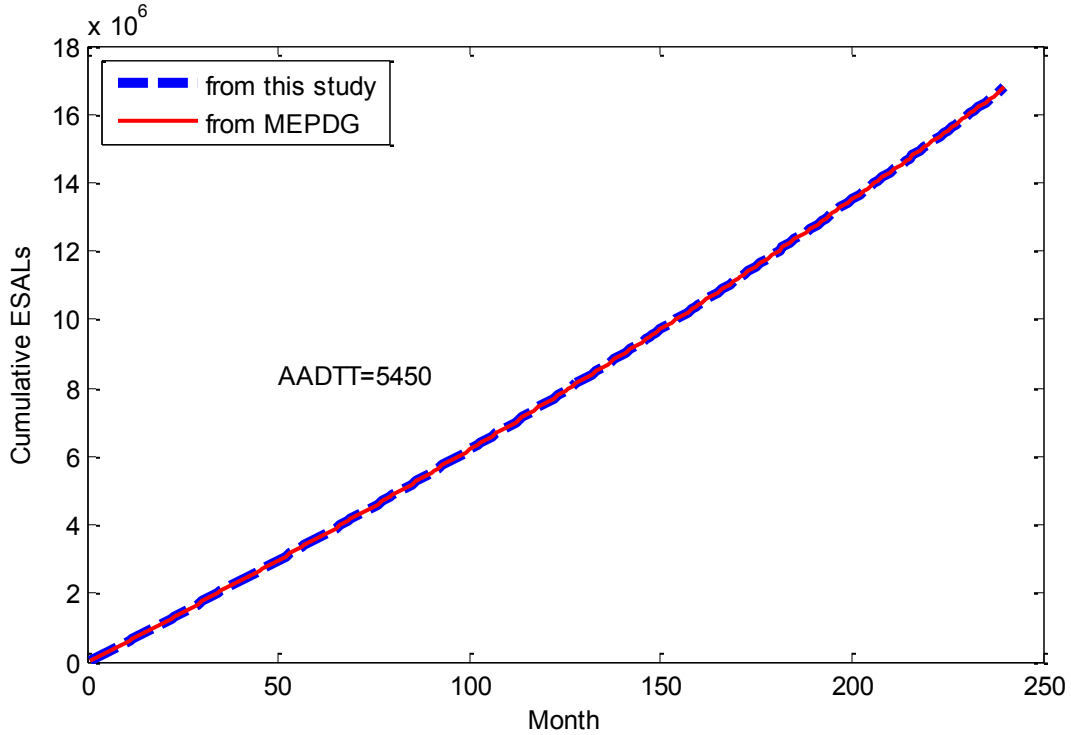


Figure 5.28 An example of predicting time series ESALs using AADTT

The procedure to estimate alligator cracking is the same as the MEPDG model, which is based on the cumulative damage concept, given by

$$D = \sum_{i=1}^T \frac{n_i}{N_{fi}} \quad (5.12)$$

where D = damage;

T = total number of computational periods;

n_i = actual traffic for period i ;

N_{fi} = allowable failure repetitions in period i .

Damage is then used to estimate the alligator fatigue cracking according to the transfer function given by

$$FC = \left(\frac{6000}{1 + e^{(C_1 * C_1' + C_2 * C_2' * \log(D))}} \right) * \left(\frac{1}{60} \right) \quad (5.13)$$

where FC = fatigue cracking, %;

C_1, C_2 are calibration coefficients;

$C_1' = -C_2'$

$C_2' = -2.40874 - 39.748 * (1 + h_{ac})^{-2.856}$

Therefore, the alligator cracking model is indeed a model of N_f , the allowable number of traffic repetitions until failure. In addition, one should expect different model statistics (i.e. R^2) for the two related models (N_f and FC) because it is not a linear relationship.

5.3.2 Outlier Test

Initial data analysis revealed that some abnormal data points needed to be excluded in model construction. For example, the second simulation (Run #2) had abnormal performance (total rutting 3.09'', alligator cracking 100%, IRI 3893.1 ft/mi). This simulation was corresponding to

AADTT=10,000 vehicle per day, ESALs = 30 million, AC thickness = 2'', base thickness = 6'', and subgrade resilient modulus = 5,000 psi, which should not exist in the real world. Although central composite design gave comprehensive coverage of the design space, those impractical simulations should not be used to build a model for engineering's application.

In statistics, an outlier is defined as an outlying observation that appears to deviate markedly from other members of the sample in which it occurs (85). Some approaches can be used to identify outliers, such as box plot, Grubbs' test, Cook's distance, and Dixon's Q test. However, there is no rigid mathematical definition for an outlier; instead, it is a subjective matter mainly based on its application.

In this study, an outlier was defined as the simulation with excessive performances but unreasonable pavement structure (i.e., thin layer thickness, low strength material, extremely high traffic load). Box plot of alligator cracking, total rutting and IRI were first plotted separately. Then, relationships between inputs (i.e. AADTT, AC thickness, base thickness, subgrade resilient modulus) and performances were investigated for any abnormality. Finally criteria in accordance to engineering experience were set up to identify outliers from the dataset.

Figure 5.29 is the box plot of alligator cracking from the raw data. The predicted alligator cracking was dominated by slight cracks, with a mean of 0.876%. The data was skewed to the lower side. Cracking over 24.399% was considered as outliers according to the definition of box plot (an outlier is a value that is more than 1.5 times the interquartile range away from the top or bottom of the box).

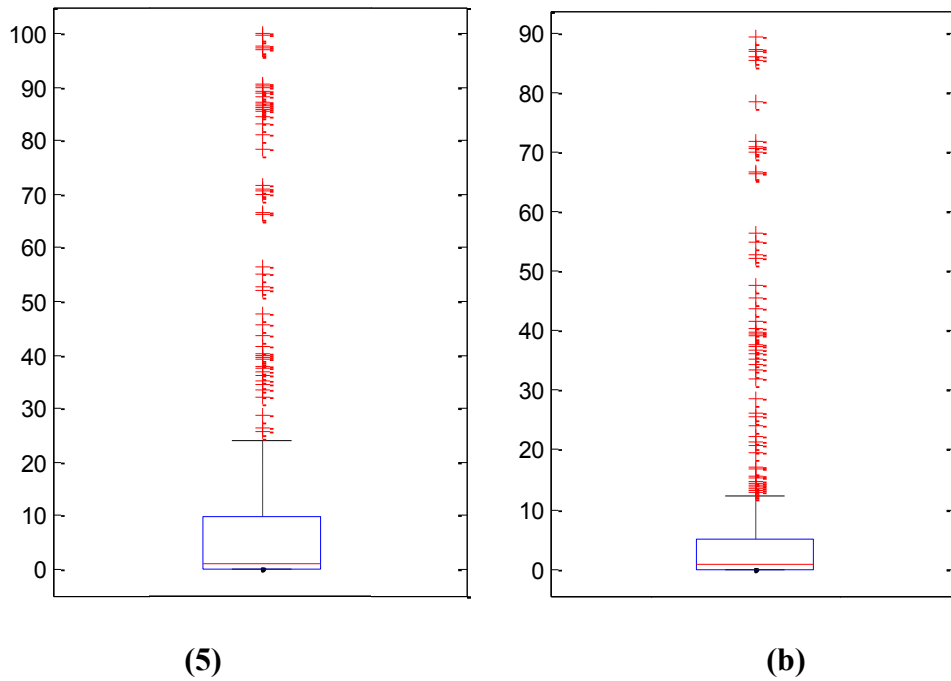


Figure 5.29 Box plot of alligator cracking (a) before and (b) after outliers are removed.

Engineering experience tells us the trend for alligator cracking should be: the more traffic, the weaker structure and material, so the more alligator cracking. Based on this premise, abnormal data points with low traffic, thick AC thickness and strong subgrade, but extreme alligator cracking (over 80%) were identified as outliers. This conservative criterion retained some of the outliers identified by statistical box plot in order to preserve a wide input space. Figure 5.30 shows the comparison of alligator cracking before and after outlier exclusion.

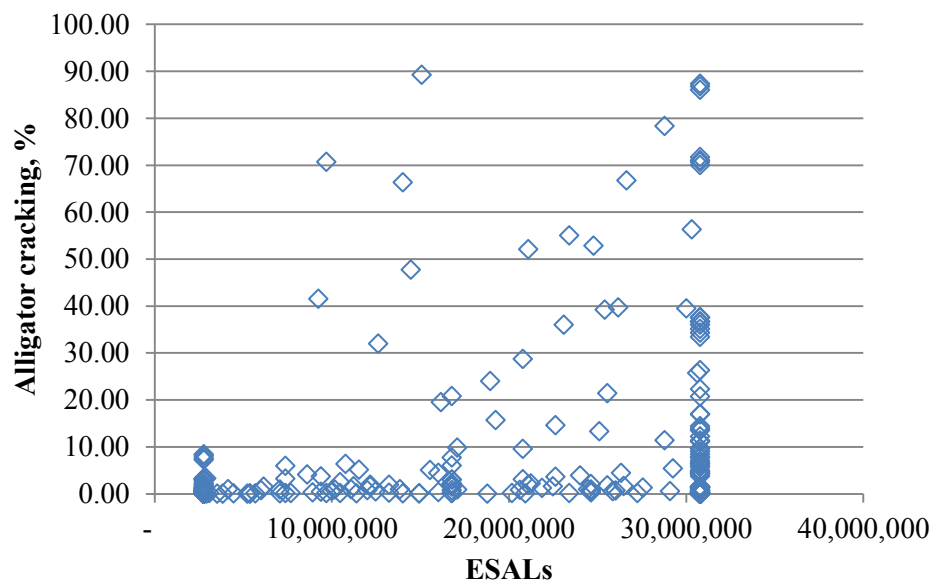
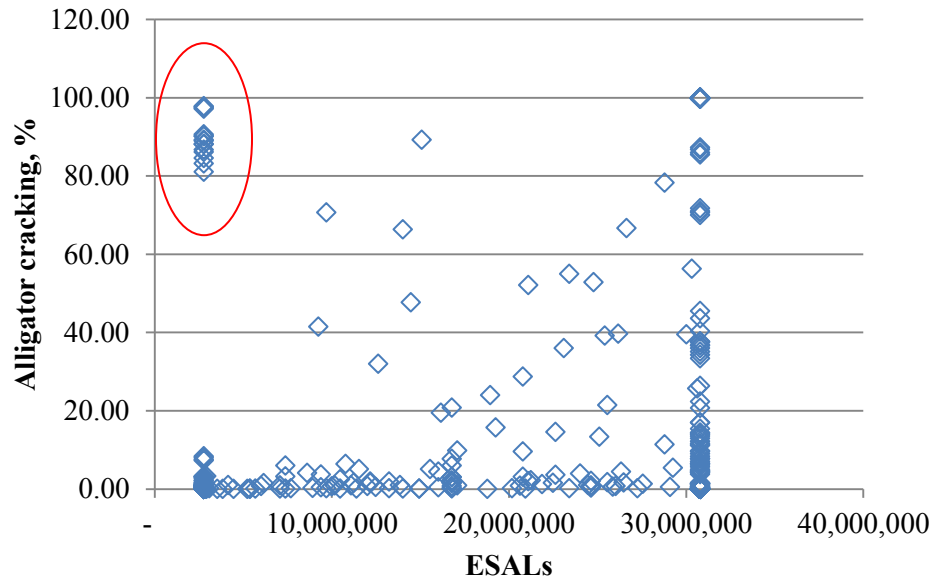


Figure 5.30 Alligator cracking (a) before and (b) after outliers are excluded.

A box plot of AC rutting, base rutting, subgrade rutting and total rutting is plotted in Figure 5.31. All means were nearly centered between the 25th percentile and the 75th percentile with a few outliers of extreme rutting. The mean AC rutting was 0.301''; the mean subgrade

rutting was 0.178". Base had the least rutting (the mean is 0.059"). The mean total rutting was 0.578". Total rutting over 1.342" was considered as outliers statistically.

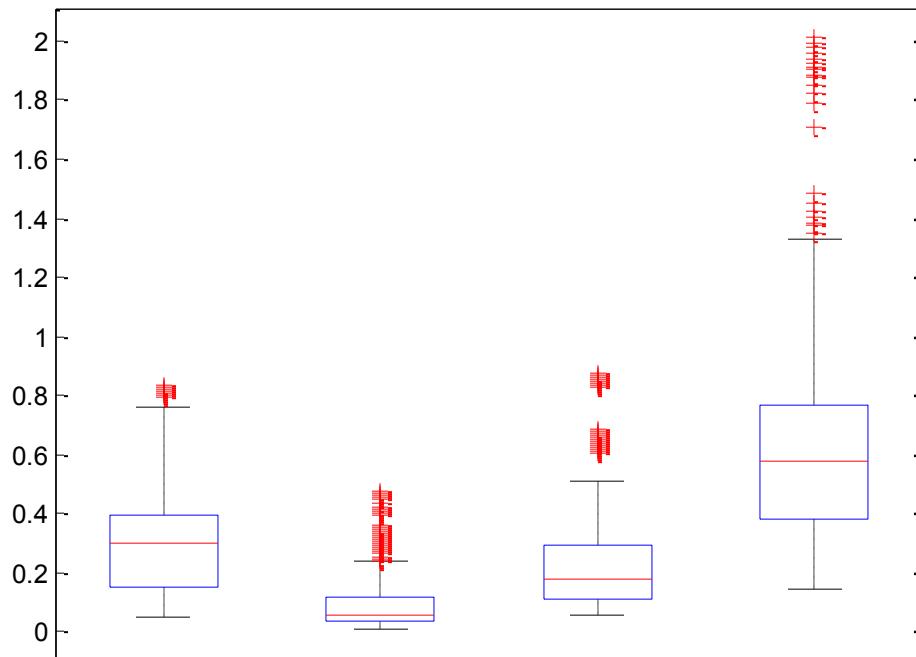


Figure 5.31 Box plot of rutting shows possible outliers.

From engineering's perspective, total rutting should follow the similar trend as alligator cracking: the more traffic, the weaker structure and materials, the more rutting. Overall the total rutting followed this trend; except for some cases with 2" AC layer but over 1.6" predicted rutting. After deleting these outliers, a better trend was revealed, as shown in Figure 5.32.

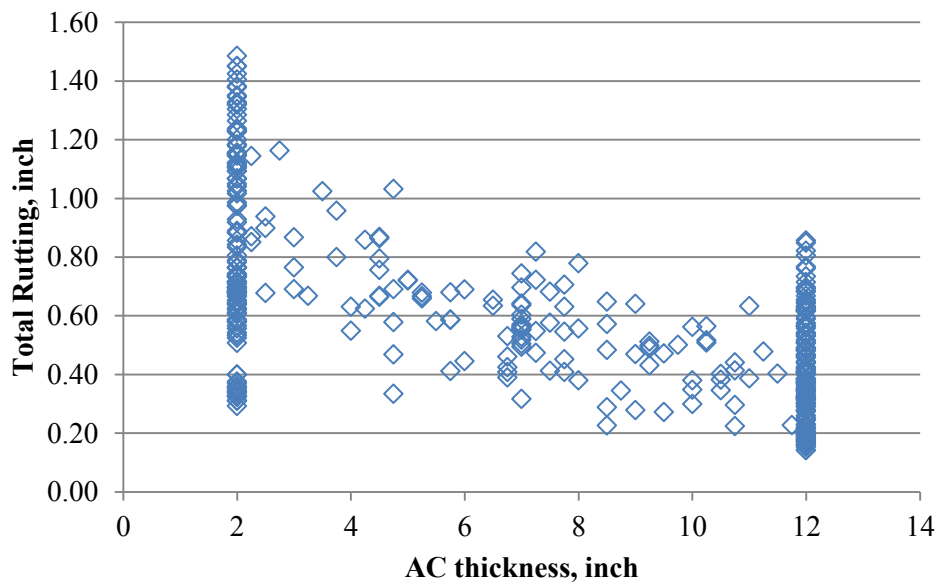
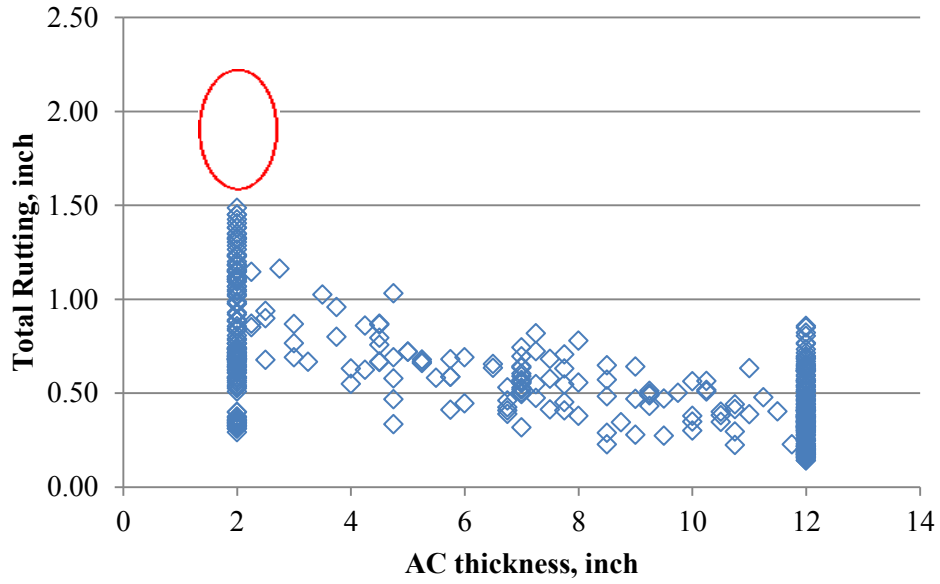


Figure 5.32 Total rutting (a) before and (b) after outliers are excluded.

Extreme large IRI was found in the raw data, as shown in Figure 5.33. The mean was 128.95 ft/mi, and IRI over 216.90 ft/mi should be regarded as statistical outliers.

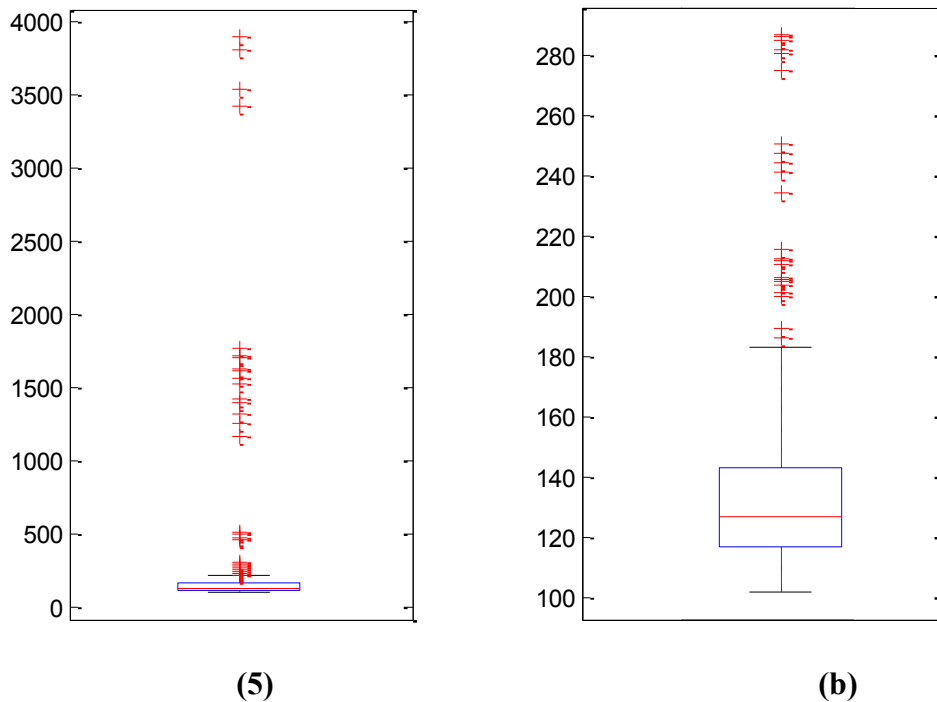


Figure 5.33 Box plot of IRI shows (a) before and (b) after outliers are removed.

The trend for IRI was normal in general. High IRI was related to thin layer thickness, weak material and heavy traffic. But some extremely severe IRI (over 1000 ft/mi) were questionable. It was found that simulations corresponding to $IRI > 1000$ ft/mi were cases with heavy traffic (AADTT=10,000), thin AC layer thickness (2''), low voids filled by asphalt (VFA=0.4), and weak base (MrBase=20,000 psi). Therefore, those impractical simulations were deleted from the dataset. Figure 5.34 shows the comparison of raw data and data after outliers were deleted.

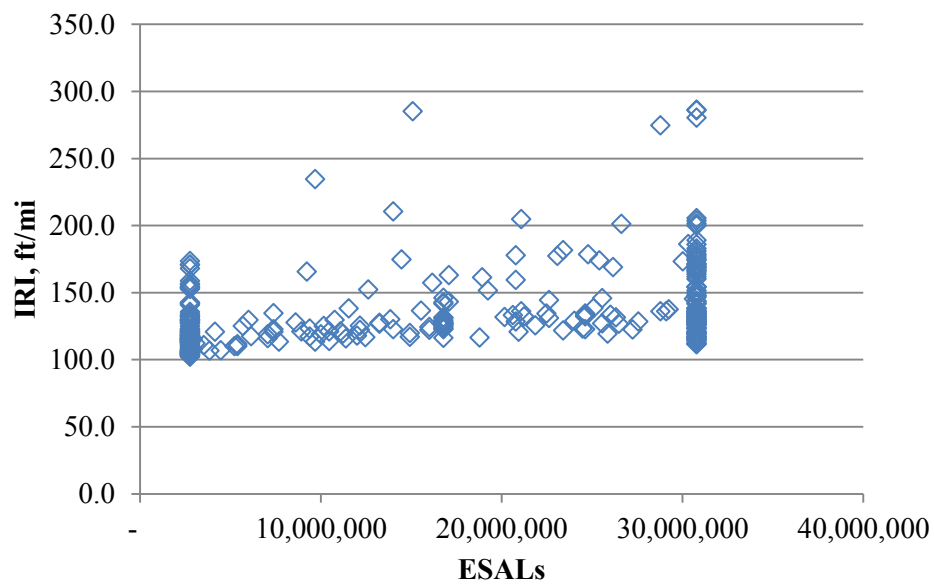
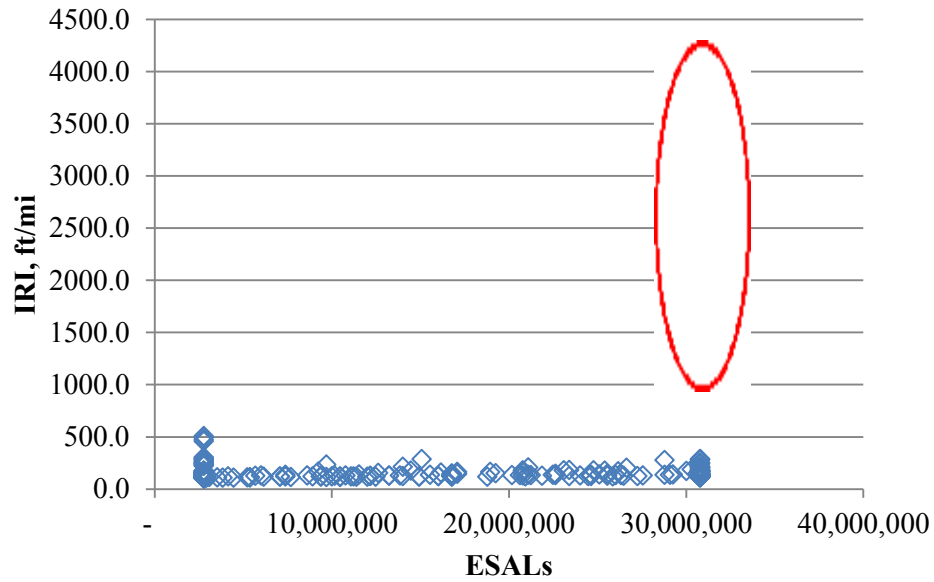


Figure 5.34 IRI (a) before and (b) after outliers are excluded.

After all outliers were identified and excluded, 342 simulations were remained for further analysis.

5.3.3 Regression Analysis

Response surface methodology (RSM) is a collection of statistical and mathematical techniques used for developing, improving, and optimizing process (86). RSM develops surrogate models using specially designed experiments so that engineers can investigate the relationship between inputs and outputs in the full design space. In this study, a second-order response surface model is adopted to cover the nonlinear relationship between design parameters and pavement performances.

$$y = \beta_0 + \sum_{i=1}^k \beta_i x_i + \sum_{i=1}^k \beta_{ii} x_i^2 + \sum_{i < j=2}^k \beta_{ij} x_i x_j + \varepsilon \quad (5.14)$$

where y = pavement performance

x_i = selected design parameters

β_i = model coefficients

ε = random error

Based on aforementioned analysis, eight significant factors were selected in this study.

The matrix of MEPDG simulations is shown in Table 5.9. By using central composite design, the number of simulation was reduced from 6,561, the case of a full factorial design, to 274, which was manageable with a 137 hour computation time. Table 5.9 lists the range of each variable based on Arkansas' condition and practice. Other inputs were also mainly statewide data that are based on past research (83). For example, traffic inputs including directional distribution, lane distribution, vehicle class distribution, and axle load distribution factors were statewide data collected from project TRC-0402 (78). Additionally, another 100 simulations using random sampling were conducted to cover other unknown areas in the design space. In total, response surface models were based on 374 MEPDG simulations.

In this study, MEPDG input files were manually prepared and the batch mode was used to execute the simulations. All data analysis and response surface models were conducted using MATLAB[®] software. Models for alligator cracking, total rutting, and smoothness (IRI) are as follows.

Building the response surface model was a trial and error process. First, an initial model was proposed, incorporating all significant factors based on engineering experience as detailed in the Risk Identification section. Adequacy of the model was then assessed using adjusted R^2 , residual plots (residuals versus predictions and normal probability plot of residuals), goodness of fit test, and analysis of variance. Other models with more variables, less variables, or changed variables were then built and compared with the initial model. During the process, transformation (i.e. logarithm) of some variables could be necessary. Finally, a response surface model with satisfactory performance was determined for further analysis. Equation 5.15 is the response surface model for alligator cracking (N_f). The model has 28 coefficients.

$$\begin{aligned}
 \log N_f = & -53.591 + [0.007h_{ac}^2 + 0.321h_{ac} - 0.005h_{ac}VFA + 0.040h_{ac} \log E_{eff}^* \\
 & - 0.002h_{ac}h_b - 0.127h_{ac} \log M_{rb} + 0.045h_{ac} \log M_{rs}] + [1.327VFA^2 + 1.345VFA \\
 & + 0.419VFA \log E_{eff}^* + 0.000VFAh_b - 0.091VFA \log M_{rb} - 0.020VFA \log M_{rs}] \\
 & + [-0.519(\log E_{eff}^*)^2 + 11.044 \log E_{eff}^* - 0.018 \log E_{eff}^* h_b - 1.391 \log E_{eff}^* \log M_{rb} \\
 & + 0.479 \log E_{eff}^* \log M_{rs}] + [-0.003h_b^2 + 0.147h_b + 0.065h_b \log M_{rb} - 0.053h_b \log M_{rs}] \\
 & + [0.276(\log M_{rb})^2 + 8.9821 \log M_{rb} - 0.274 \log M_{rb} \log M_{rs}] \\
 & + [0.086(\log M_{rs})^2 - 1.725 \log M_{rs}]
 \end{aligned} \tag{5.15}$$

where N_f = allowable number of traffic repetitions to failure;

h_{ac} = layer thickness of AC surface, inch;

VFA = voids filled with asphalt, %;

h_b = thickness of base layer, inch;

M_{rb} = resilient modulus of base, psi;

M_{rs} = resilient modulus of subgrade, psi;

E_{eff}^* = effective asphalt concrete dynamic modulus given by Equation 5.5, psi.

This model looks complicated, but it is indeed a basic second-order response surface model just as Equation 5.14. To better understand this model, it is presented in a different way as shown in Table 5.12. The response ($\log N_f$) is at the top left corner. Column headers are the model variables while the numbers in the table are model coefficients corresponding to the row variable multiply by the column variable.

Figure 5.35 (a) and (b) show the comparison of $\log N_f$ and alligator cracking between the MEPDG and the response surface model. As the model statistics show, the model accuracy was high ($R^2=0.997$ for $\log N_f$ and $R^2=0.978$ for alligator cracking).

Table 5.12 Model Coefficients for Alligator Cracking

$\log N_f$	I	h_{ac}	VFA	E_{eff}^*	h_b	$\log M_{rb}$	$\log M_{rs}$
I	-53.591						
h_{ac}	0.321	0.007					
VFA	1.345	-0.005	1.327				
E_{eff}^*	11.044	0.040	0.419	-0.519			
h_b	0.147	-0.002	0.000	-0.018	-0.003		
$\log M_{rb}$	8.982	-0.127	-0.091	-1.391	0.065	0.276	
$\log M_{rs}$	-1.725	0.045	-0.020	0.479	-0.053	-0.274	0.086

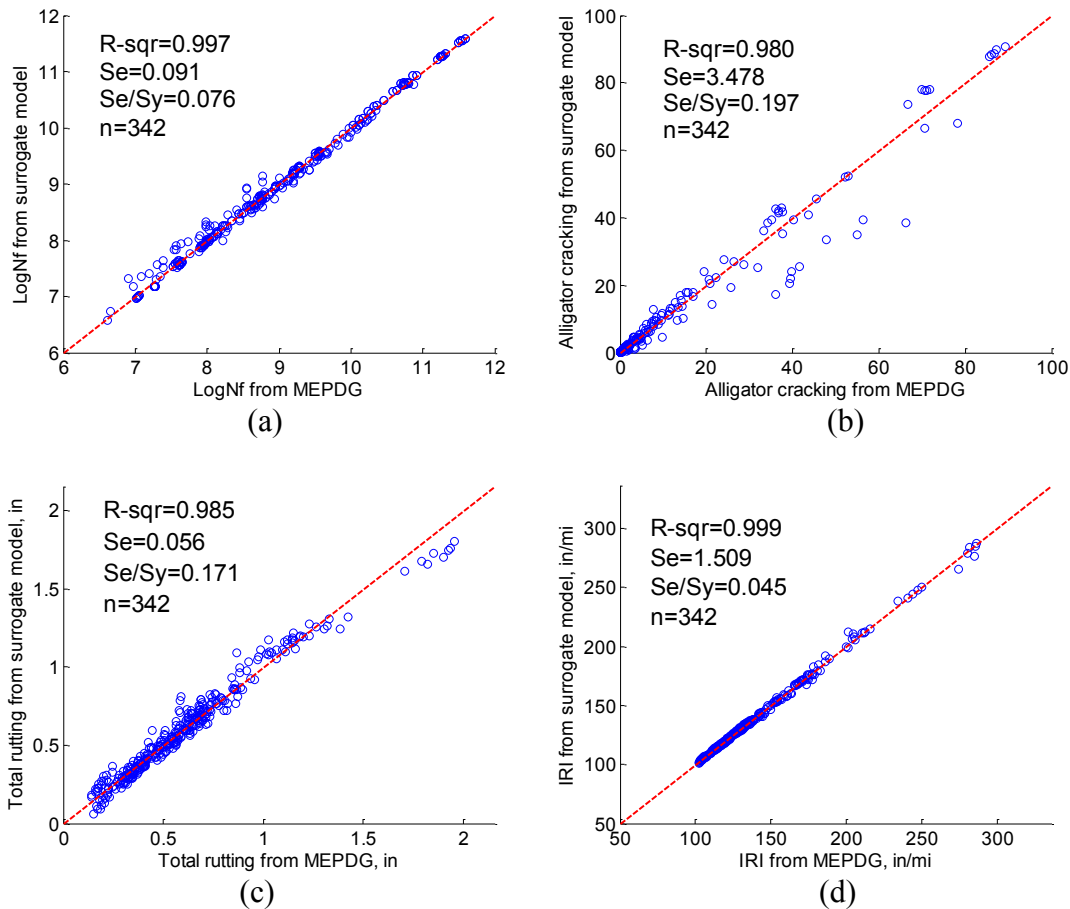


Figure 5.35 Response surface models for: (a) $\text{Log}N_f$, (b) alligator cracking, (c) total rutting, and (d) IRI.

Similar models were built for total rutting (Table 5.13), which had 28 coefficients, and smoothness IRI (Table 5.14), which had 55 coefficients. The comparison between the prediction from MEPDG and surrogate models is shown in Figure 5.35 (c) and (d). Models for total rutting and IRI had better accuracy than the alligator cracking model. This could be due to the complexity of estimating alligator cracking, and the nonlinearity of alligator cracking. It was not surprising that the R^2 for IRI model was over 0.99, giving that IRI model in MEPDG was also a regression model of other distresses and site adjustment. Rutting and alligator cracking were the main contributors to pavement roughness.

Table 5.13 Model Coefficients for Total Rutting

<i>TotRut</i>	<i>l</i>	<i>h_{ac}</i>	<i>logEASL</i>	<i>E_{eff}[*]</i>	<i>h_b</i>	<i>logM_{rb}</i>	<i>logM_{rs}</i>
<i>l</i>	24.612						
<i>h_{ac}</i>	-0.387	0.001					
<i>logEASL</i>	2.185	-0.029	0.140				
<i>E_{eff}[*]</i>	-3.621	0.003	-0.411	0.533			
<i>h_b</i>	0.043	0.001	0.001	-0.012	-0.002		
<i>logM_{rb}</i>	-4.623	0.078	-0.159	-0.028	-0.008	0.456	
<i>logM_{rs}</i>	-3.050	0.029	-0.078	-0.108	0.021	0.193	0.318

Table 5.14 Model Coefficients for Smoothness (IRI)

<i>IRI</i>	<i>l</i>	<i>h_{ac}</i>	<i>VFA</i>	<i>E_{eff}[*]</i>	<i>h_b</i>	<i>logM_{rb}</i>	<i>logM_{rs}</i>	<i>logESAL</i>	<i>AlliCrk</i>	<i>TotRut</i>
<i>l</i>	-1049.74									
<i>h_{ac}</i>	13.05	-0.04								
<i>VFA</i>	159.36	-0.02	1.59							
<i>E_{eff}[*]</i>	360.83	-2.27	-25.84	-30.34						
<i>h_b</i>	-0.68	0.01	0.62	-0.43	0.08					
<i>logM_{rb}</i>	75.37	-0.60	-1.07	-7.11	0.05	-3.09				
<i>logM_{rs}</i>	60.37	-0.39	-11.06	-9.79	0.08	-2.72	-1.21			
<i>logESAL</i>	-116.47	1.01	8.27	19.81	0.13	3.01	4.53	-4.42		
<i>AlliCrk</i>	-0.67	0.07	-1.06	0.56	0.05	0.08	0.23	-0.66	0.02	
<i>TotRut</i>	267.11	-2.90	-52.44	-20.33	-1.15	-18.10	-14.07	20.35	0.59	-14.71

Overall, based on model statistics and checking residual plots, these surrogate models had sufficient accuracy to be used for performance prediction. It should also be noted that the complexity of these models will be solved by coding them into a software toolkit.

5.4 Validation and Sensitivity Analysis

It was necessary to validate the response surface models with new datasets. 100 MEPDG simulations were conducted for this purpose. Random sampling was used in order to test any possible locations in the design space. Figure 5.36 shows the comparison between MEPDG and the surrogate models. Analysis of variance and residuals were also checked. In general, the response surface models provided reasonable estimates of results generated by the MEPDG. The alligator cracking model may need further investigation for higher level of accuracy. Within the context of this research, the models could be suitable for generating probability distributions of performance predictions through Monte Carlo simulation.

Now that four surrogate models ($\log N_f$, alligator cracking, total rutting and IRI) are built to reduce the computing time of MEPDG, it is necessary to conduct a sensitivity analysis of the eight probabilistic variables in the surrogate models. This will assure the well-known relationships from MEPDG have been carried on to the new models, and no abnormal relationship is developed possibly due to simplification and error accumulation.

The structure proposed for Bella Vista Bypass was used as the base structure. Details on the Bypass project are described in section 6.4.2. The eight variables were analyzed in four groups. The full range as listed in Table 5.9 for each variable was investigated. Using surrogate models, thousands of design combinations were executed in a short amount of time.

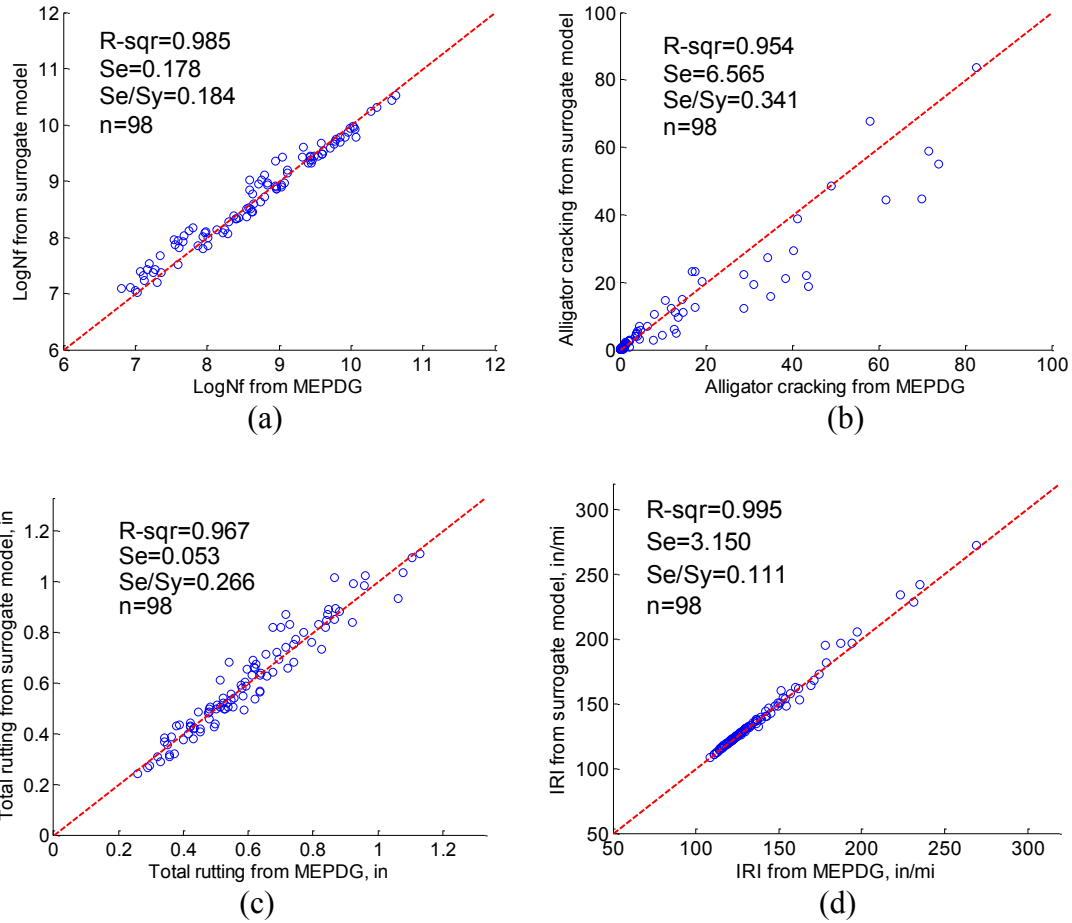


Figure 5.36 Validation of response surface models: (a) $LogN_f$, (b) alligator cracking, (c) total rutting, and (d) IRI.

The relationship between initial AADTT and asphalt layer thickness is presented in Figure 5.37. Figure 5.38 is the corresponding contour plot. Since $LogN_f$, as defined in Equation 5.15, represents the structural ability of a pavement structure, it is a parameter that is unrelated to the applied traffic loading. $LogN_f$ is the amount of traffic that a pavement theoretically could withstand, not the traffic that it carries in real. Figure 5.37 shows this trend. For pavement performance (cracking, rutting, IRI), there is no doubt that a thin road under heavy traffic performs worse than a thick road under light traffic. This is observed in Figure 5.37, in which red

color represents worse performance (large values) and blue color is better performance (small values).

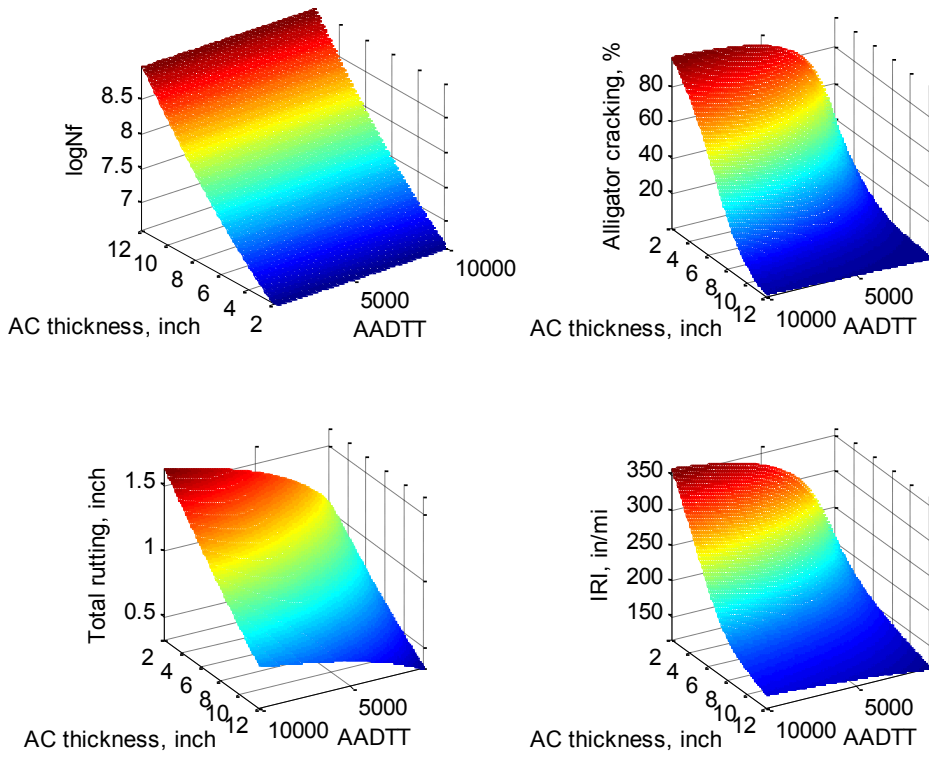


Figure 5.37 Sensitivity analysis of AADTT and AC thickness (3D mesh plot)

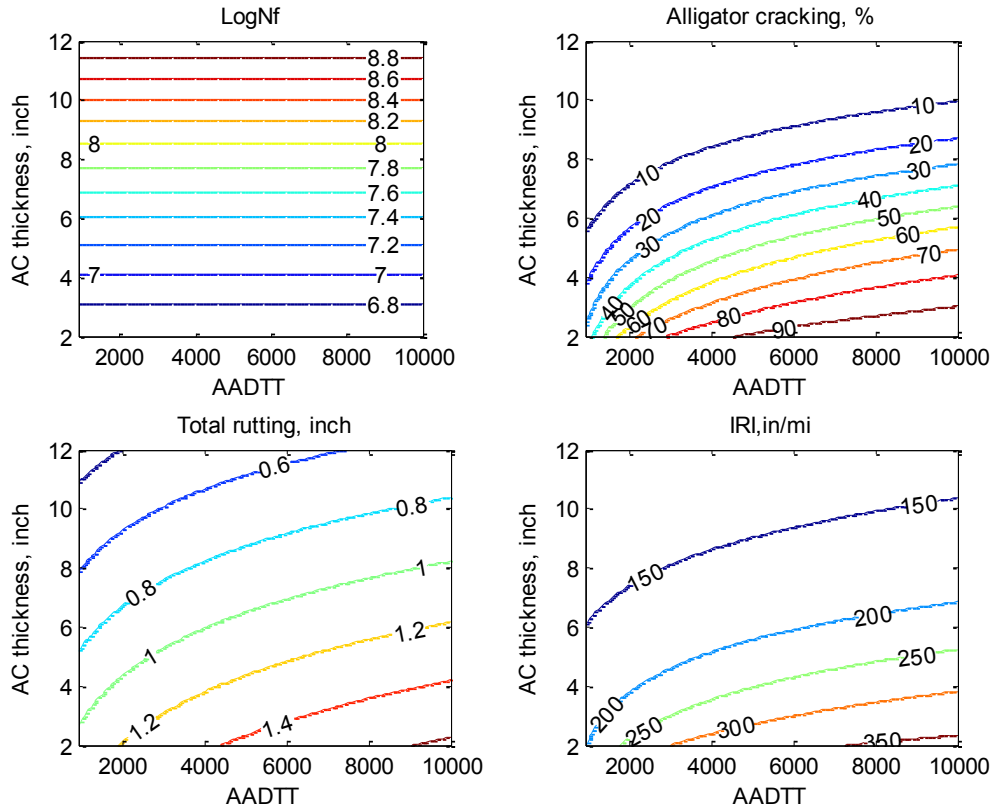


Figure 5.38 Sensitivity analysis of AADTT and AC thickness (contour plot)

The influence of air voids, effective binder content and thickness of the base layer is presented in Figure 5.39 and 5.40. Clearly that alligator cracking and IRI get worse when base is thin and VFA is low (binder is not sufficient). When these two distresses are at low level, the influence of base thickness is not as dramatic as the influence when VFA is low and distress level is high. On the contrary, notice that rutting has a different trend: total rutting increases as VFA increases. In other words, the more binder in the voids, the more chance to expect rutting.

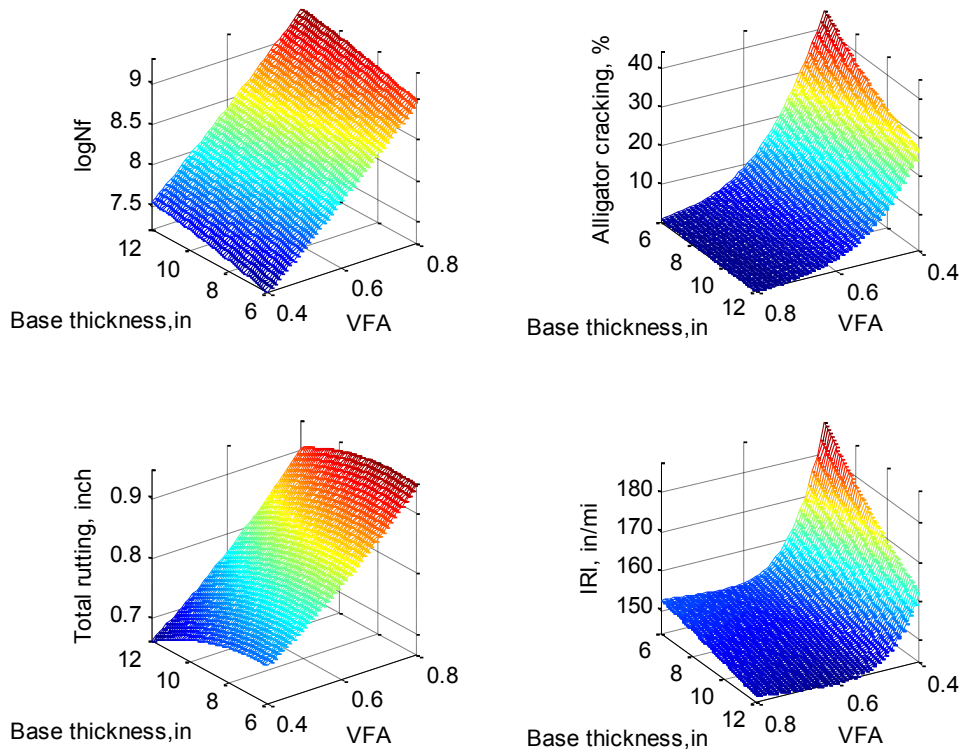


Figure 5.39 Sensitivity analysis VFA and base thickness (3D mesh plot)

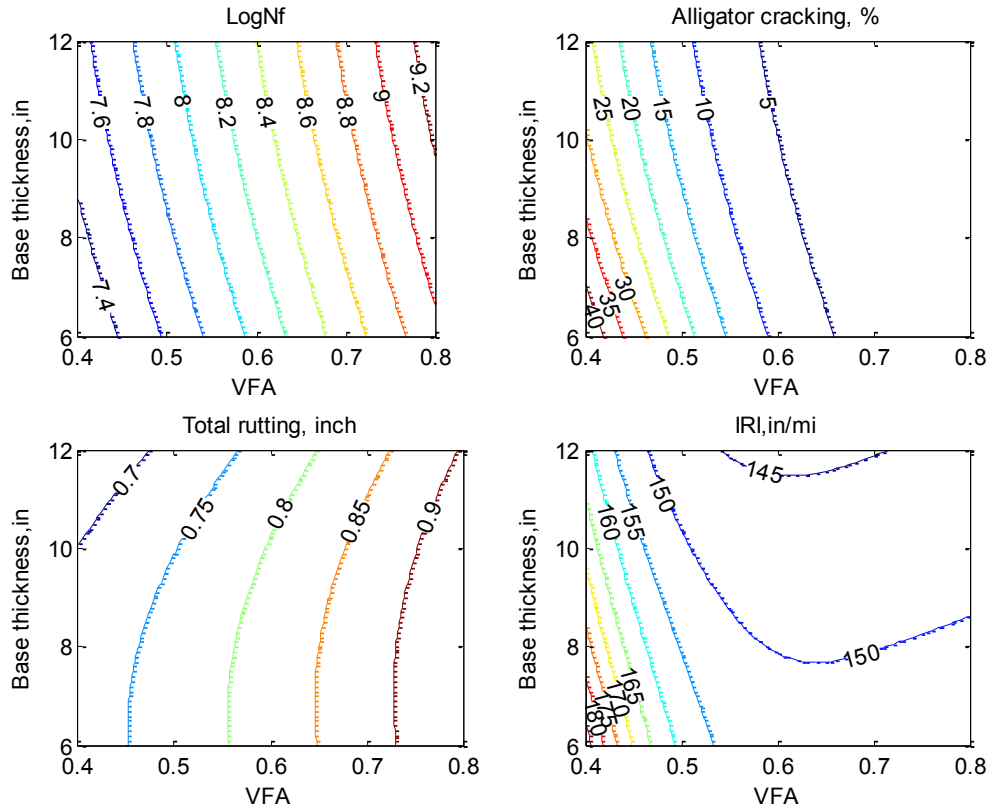


Figure 5.40 Sensitivity analysis of VFA and base thickness (contour plot)

The influence of base and subgrade strength (resilient modulus) is given in Figure 5.41 and 5.42. As expected, Figure 5.41 shows that a strong base and subgrade provide more strength ability to carry more traffic ($\log N_f$). On the contrary, a weak base and subgrade lead to worse performance (more cracking, rutting and IRI). A nonlinear relationship is also observed. One should be aware that the x axis and y axis in the 3D plots are not constant. In favor of a better view angle, the direction of axis may have been changed.

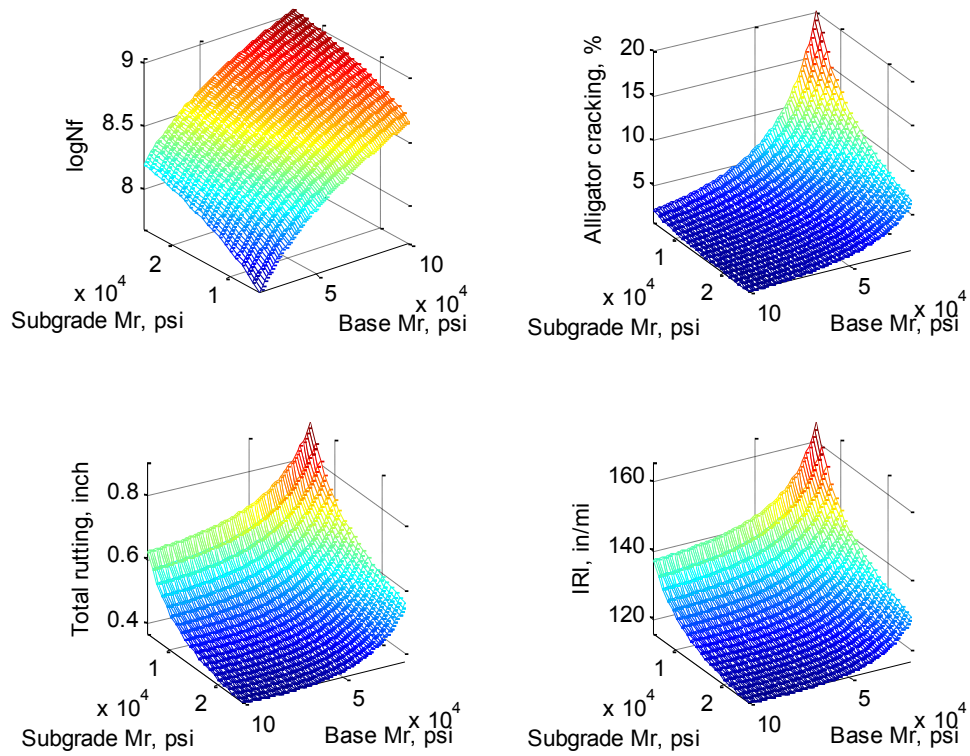


Figure 5.41 Sensitivity analysis of resilient modulus of base and subgrade (mesh plot)

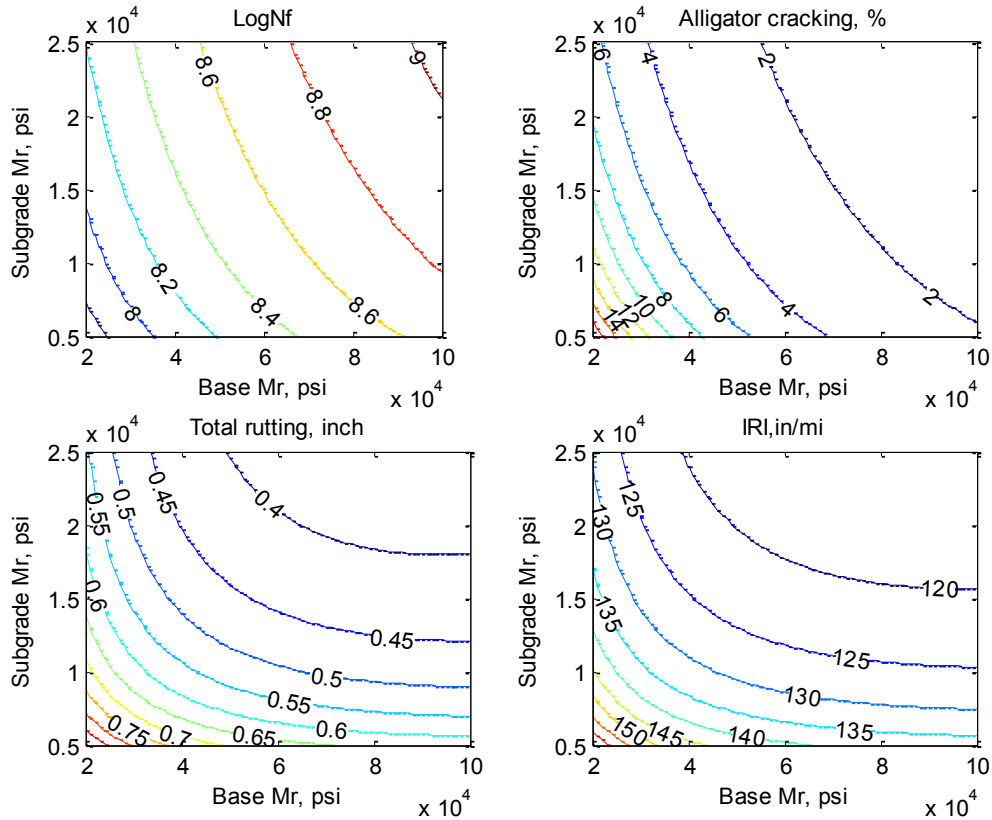


Figure 5.42 Sensitivity analysis of resilient modulus of base and subgrade (contour plot)

5.5 Summary

This chapter was to develop models in aim to analyze risk and variation. Neural network and Response Surface Methodology (RSM) were introduced. Experiment design that reduces the simulations numbers was explained in detail. Climate and operation speed were further investigated and screened out of this study. Model construction and validation were addressed. Some important findings include

- Neural Network, one type of surrogate model, had already been applied in the MEPDG to reduce the computing time for rigid pavement analysis.
- In total ten probabilistic factors were initially selected. After screening out the climate and operation speed, eight factors were included in response surface models.

- Using Central Composite Design, experiment numbers were reduced to 274. Plus additional 100 random sampling, 374 simulations were conducted for model construction.
- Besides statistical methods to identify outliers, this study reduced impractical data such as those had extremely high traffic volume but extremely thin pavement. In total 32 cases were reduced.
- The developed alligator cracking model and total rutting model had 28 coefficients. The IRI model had 55 coefficients. R square for all models was over 0.95 in both model construction and model validation.

CHAPTER 6 RELIABILITY IMPROVEMENT

6.1 Introduction

The proposed method to improve reliability consideration relies on the Monte Carlo Simulation, which is widely accepted as an effective reliability analysis method. The obstacle of conducting Monte Carlo simulation on the MEPDG, as indicated by (6), was the extensive computation time. With the surrogate models developed in Chapter 5, this constraint was eliminated.

The new procedure is illustrated in Figure 6.1.

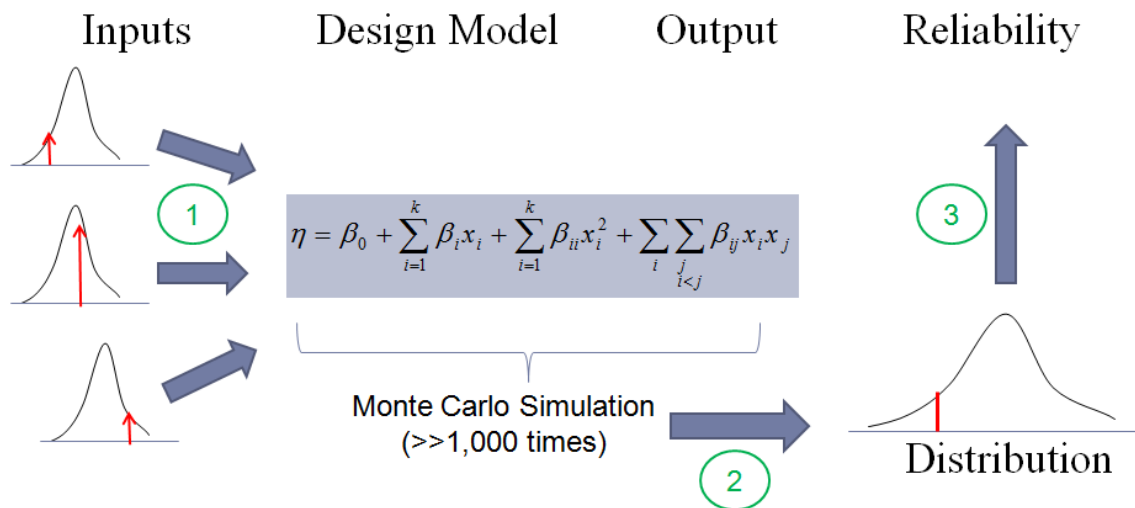


Figure 6.1 Flowchart of the proposed reliability improvement procedure

Step 1. Input not only the mean value but also the distribution of the significant variables identified in Chapter 4. Then a set of inputs was prepared by random sampling from the distribution. A simulation using surrogate models was conducted with that set of inputs. Using Monte Carlo Simulation, the same procedure was repeated tens of thousands of times.

Step 2. By recording the output from each simulation, the distribution of predicted performance was available. The distribution, of the most importance, was used for statistical

analysis and design check. Separate distribution was developed for each distress such as alligator cracking, total rutting and IRI.

Step 3. When the user-defined design criterion was plotted in the distribution, the reliability of that design was determined. This reliability was the true reliability since it was based on the distribution rather than an empirical relationship such as the one being used in the current MEPDG.

The concept of Monte Carlo method is straightforward. However, it should be used carefully and it does not work everywhere. The success of this procedure depends on the following assumptions:

- The probabilistic distribution of each input variable is well defined using the right distribution type and characteristics.
- Surrogate models on which Monte Carlo Simulation operates predict the same results as the raw model (MEPDG in this study) does.
- Sampling method and simulation runs are sufficient to cover the full design space, so that the full distribution of output could be captured.

This chapter is to discuss the proposed procedure in detail and explain the validity of this method.

6.2 Monte Carlo Simulation

Monte Carlo Simulation was developed based on a simple idea that in many complex situations it was not necessary to consider all possible trajectories but only to look at a large random sampling of them (87). But the practice of this idea, or the origin of Monte Carlo method, was not possible until the electronic computer was invented in 1946 so that a large number of random sampling could be done in a practically acceptable timeframe.

Technically, when doing a Monte Carlo problem, attention should be given to:

- “random sampling”: generating sample values of the random variables, which may follow different probability distributions.
- “a large number”: determine the required simulation number to achieve a specified accuracy. This also includes designing and using variance reduction techniques that could maintain the same accuracy with reduced number of simulation.
- “model”: choose the probability process or establish the probability model.

The first two topics are discussed in the following section. The topic of model has already been elaborated in Chapter 5.

6.2.1 Generation of Random Numbers

Due to the importance of sampling, it is worth explaining how a random point is generated in a way that the full distribution is represented in a Monte Carlo Simulation.

First of all, generate uniformly distributed random numbers. This is not a complicated process any more in today’s digital world. But one may wonder how a random number is used to guide the sampling of a non-uniformly distributed variable. Although there are many methods such as inverse transformation, composition method, function-based method, discrete variables, and jointly distributed variables, the concept will be illustrated by the inverse transformation approach (88).

In the inverse transformation approach, first a uniformly distributed random number r_i in the range $[0, 1]$ is generated. Since the cumulative density function of $y=F_X(x)$ also has a range of $[0, 1]$, a counterpart relationship is established as shown in Figure 6.2. Hence, the desired random number x_i can be calculated by solving the equation

$$F_X(x_i) = R_i = F_R(r_i) \quad (6.1)$$

Or by simply solving the inverse CDF given by

$$x_i = F_X^{-1}(R_i) \quad (6.2)$$

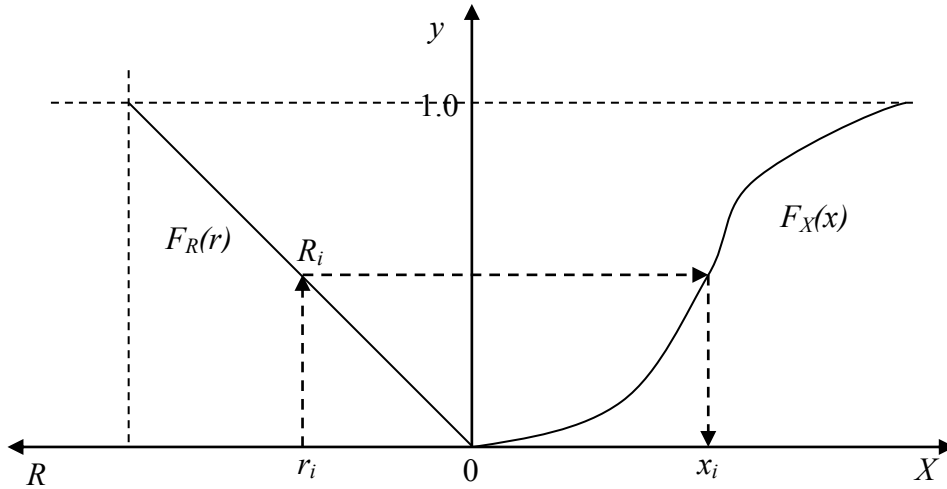


Figure 6.2 Determination of random number x with desired distribution from uniformly distributed random number r (88)

In MATLAB, a library of functions to generate random numbers is available. Most common distributions are included, such as binomial random numbers, Gamma random numbers, normal random numbers, Student's t random numbers, Weibull random numbers, and Latin hypercube samples from a normal distribution (89).

The following is a simple example considering only two variables, the layer thickness of asphalt concrete and the air voids of HMA. Set the truth as Table 6.1.

Table 6.1 Example of variable distributions

Distribution	AC thickness	Air voids
Uniform	Mean 6'', range [5,7]	Mean 8%, range [6,10]
Normal	Mean 6'', standard deviation 0.5''	Mean 8%, standard deviation 1%
Lognormal	Mean 6'', standard deviation 1''	Mean 8%, standard deviation 1%
Gamma	Shape parameter $k=3$, scale parameter $\theta=2$	

Apply the corresponding functions in MATLAB and generate 10,000 samples. For example, the code to generate normal distributed samples is

$$x_i = \text{normrnd}(6,0.5) \quad (6.3)$$

where x_i is a random sample of a normal distribution that has mean $\mu=6$ and standard deviation $\sigma=0.5$.

Figure 6.3 shows the histogram plot of the generated samples of AC layer thickness. For visualization purpose, a fitted normal distribution curve is plotted in all of the graphs. It shows clearly that the generated sample meets the truth as set in Table 6.1. The uniform distribution ranges from 5'' to 7''. The normal distribution centers at 6'' and mainly range from 5'' to 7'' too. The lognormal distribution is skewed to the left, or has a long right tail. The Gamma distribution is also left skewed with a long range from 0 to 20.

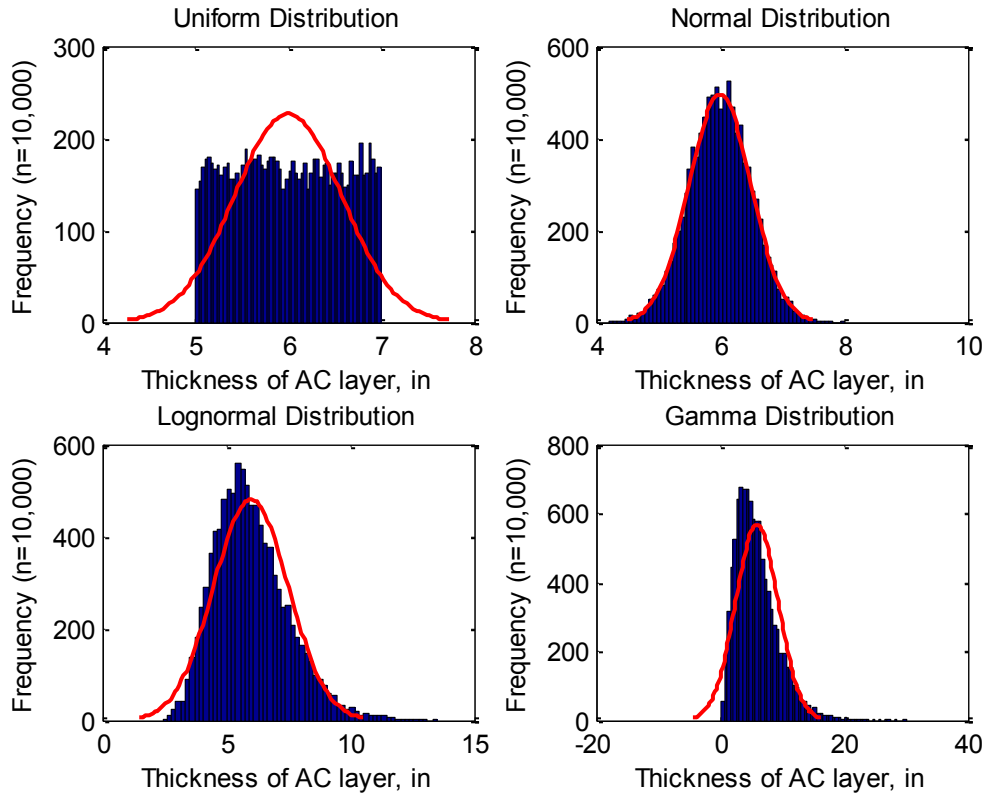
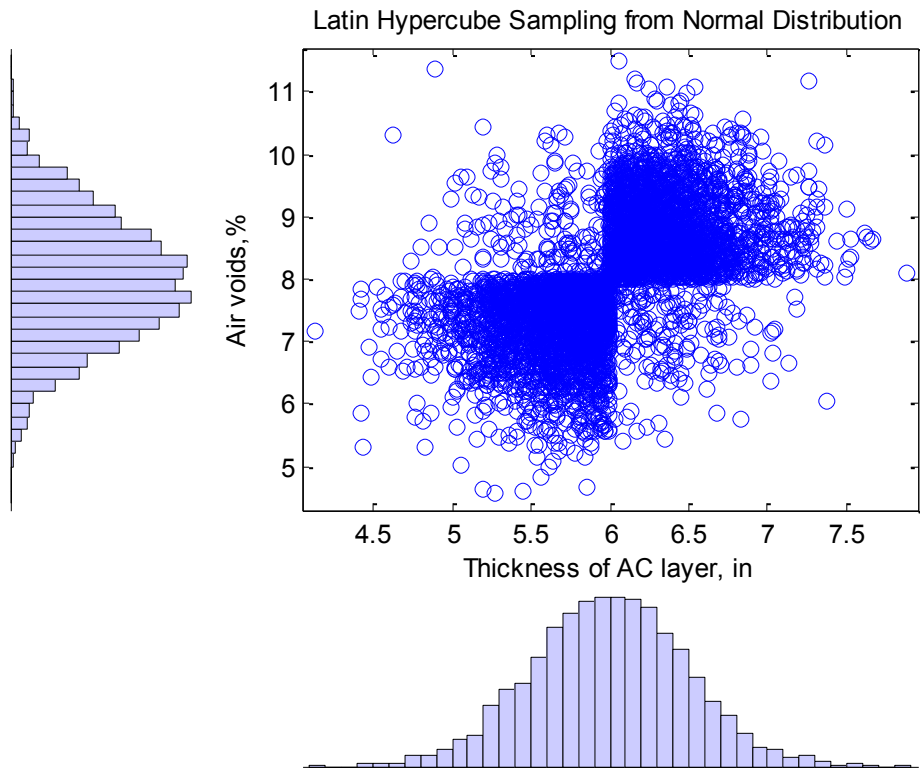


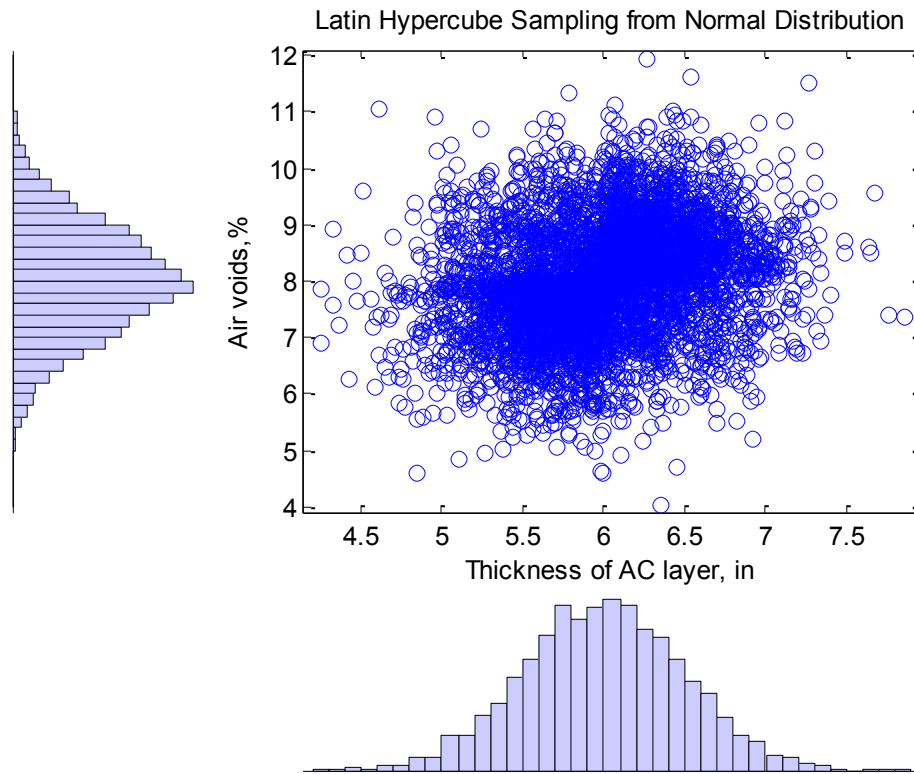
Figure 6.3 Histogram of generated random samples

As shown in Chapter 5, the Latin Hypercube Sampling method only applies to multivariate distribution. Using two normal distribution as example, Figure 6.4 shows the generated random samples of layer thickness and air voids, assuming the covariance is 0.49, which means that AC thickness increases when air voids is high (or the HMA is not well compacted). The trend is clearly observed in Figure 6.4. Although in general AC thickness is normal distributed with mean at 6'' and a range from 4.5'' to 7.5'', the likelihood of a pavement with thick layer and small air voids is much smaller than the chance of a thick layer and large air voids. The covariance has a significant role on multivariate distribution. For instance, if the covariance is reduced from 0.49 to 0.30, the interaction between layer thickness and air voids is reduced, as shown in Figure 6.5.



Note: For a clear visualization, sample size $n=1,000$ is used.

Figure 6.4 Histogram of generated random samples (covariance=0.49)



Note: For a clear visualization, sample size $n=1,000$ is used.

Figure 6.5 Histogram of generated random samples (covariance=0.30)

In summary, examples show that random numbers could be easily generated using MATLAB to meet a variety of probabilistic distributions for the purpose of Monte Carlo Simulation.

6.2.2 Simulation Numbers

It is given in statistics that the exact mean value of a trial can be obtained only when the number of sampling reaches the population, or infinite (which is impossible). For example,

$$P_f = \lim_{n \rightarrow \infty} \frac{m}{n} \quad (6.4)$$

where P_f is the failure probability, m is the number of failures and n is the total number of trials.

Therefore, the accuracy of Monte Carlo simulation is directly related to the number of simulations. Based on the central limit theorem, the sum of samples will be approximately normal if N is sufficiently large. If the mean of the random variable ξ is m , and the variance is b^2 , Sobol (90) explained that the mean and the error of the Monte Carlo method can be calculated using

$$P\left\{\left|\frac{1}{N}\sum_{j=1}^n\xi_j - m\right| < \frac{3b}{\sqrt{N}}\right\} \approx 0.997 \quad (6.5)$$

To test the influence of simulation numbers, a pilot study was conducted. The input data as shown in Figure 6.11 was used. Monte Carlo simulation was executed using a run number from 100 to 15,000 in the interval of 100. Figure 6.6 and 6.7 are the result for a high reliability and a low reliability, respectively. The mean, mean plus standard deviation and mean minus standard deviation are also plotted. As expected, the result fluctuates at the beginning when the sample size is small. Then it reaches a stable range within mean plus/minus one standard deviation when the simulation is more than 4,000. Although it is never stabilized at the mean value, the variation range is less than 2%, which is practically acceptable considering that reliability of pavement design is widely measured with an interval of 5%.

Since the computing time of a Monte Carlo simulation with 10,000 samples was less than one minute in this research, the simulation number was determined to be 10,000.

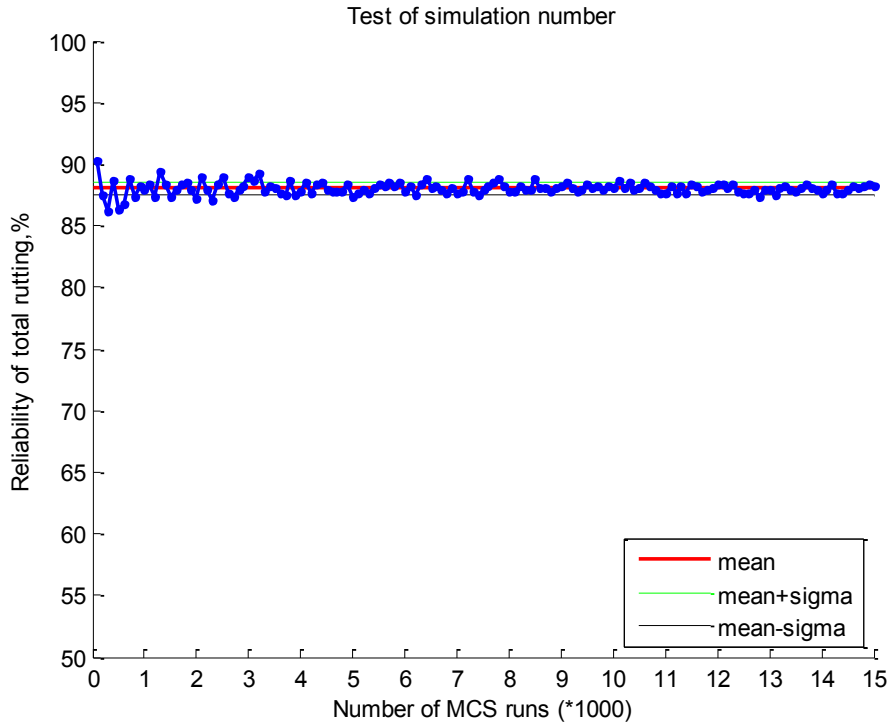


Figure 6.6 Test of simulation numbers ($h_{ac}=11''$)

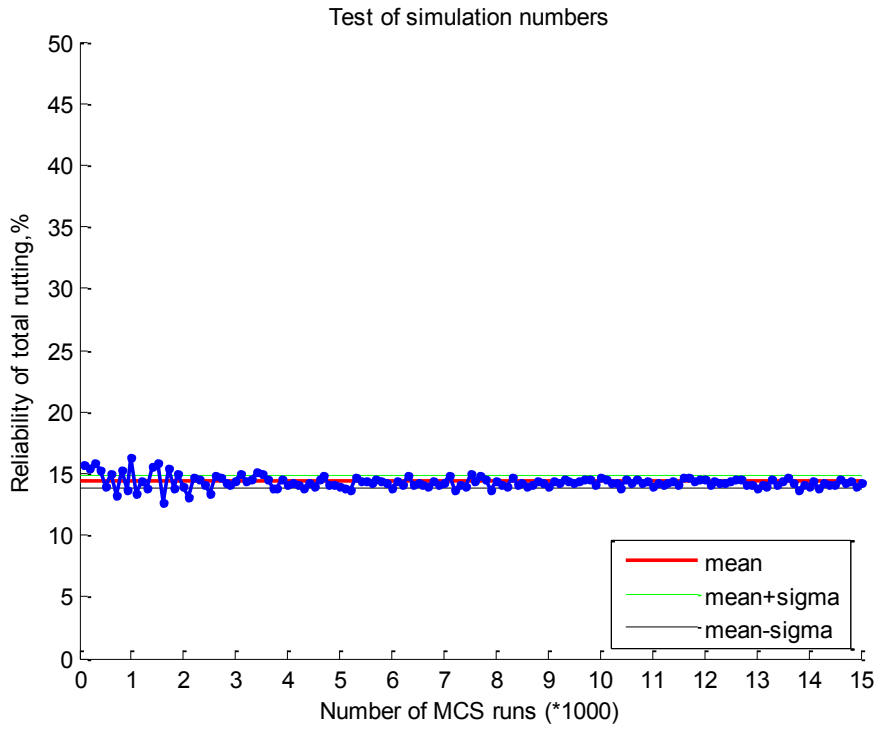


Figure 6.7 Test of simulation numbers ($h_{ac}=8''$)

6.2.3 Determine the Reliability

One should note that the result from a Monte Carlo simulation of the MEPDG is not the reliability of the design, but the predicted performance including alligator cracking percentage, total rutting in inches, and IRI in in/mi. By comparing the predicted performance with the user-defined design criteria (i.e. 0.75' for total rutting), the reliability of the design can be calculated using two methods:

- The “Hit-or-Miss” method, and
- The normal fit method.

The “Hit-or-Miss” method is the basis for Monte Carlo integration. If the output space, from one dimension to multiple dimensions, is separated by the design criteria to two regions: success region and failure region. Any sample will produce a result either with the success region or the failure region. By counting the total number in the two regions, the reliability R is calculated by

$$\mathfrak{R} = \frac{N_{success}}{N_{total}} = \frac{N_{success}}{N_{success} + N_{failure}} \quad (6.6)$$

where \mathfrak{R} = the reliability of the design;

$N_{success}$ = the total number of trials in the success region;

$N_{failure}$ = the total number of trials in the failure region;

N_{total} = the total number of trials.

If the predicted performance is normally distributed, the normal fitting method could be applied. First, the results are fit to a normal distribution; the corresponding mean μ and standard deviation σ are estimated. Then the reliability of the design is calculated at the design criteria level using the estimated normal distribution.

$$\mathfrak{R} = F(x | \mu, \sigma) = \frac{1}{\sigma\sqrt{2\pi}} \int_{-\infty}^x e^{-\frac{(t-\mu)^2}{2\sigma^2}} dt \quad (6.7)$$

where \mathfrak{R} = the reliability of the design;

F = the cumulative distribution function of a normal distribution;

x = the user-specified performance criteria;

μ = the mean of the predicted performance;

σ = the standard deviation of the predicted performance.

Figure 6.8 shows an example of the predicted total rutting for a design shown in Figure 6.11. It is a histogram of the results from MCS fit to a normal distribution (the bell curve in red). The design criterion is shown as the red dotted line, which divides the output space into two regions: a success region in the left and a failure region in the right. Using the “Hit-or-Miss” method, the reliability is 90.7%. Since it is a normal distribution for this example, the normal fit method is viable, which gives a reliability of 90.9%. The two methods provide similar result. Figure 6.9 presents the CDF plot of the fitted normal distribution of Figure 6.8. The red dotted line is the design criteria.

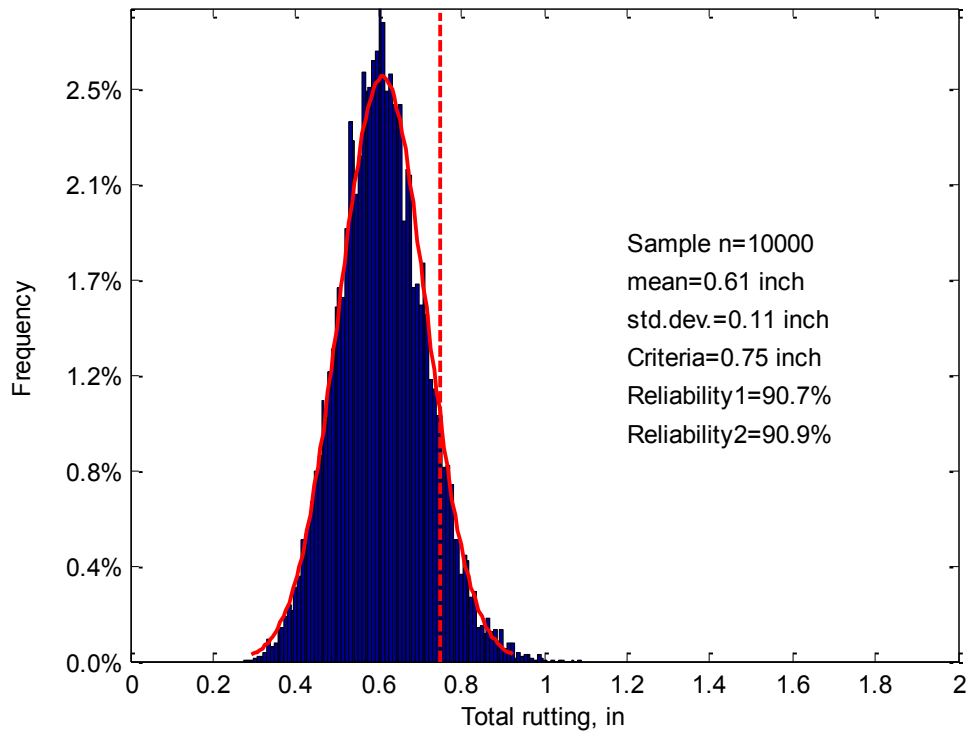


Figure 6.8 Example of estimating the reliability level in a histogram plot

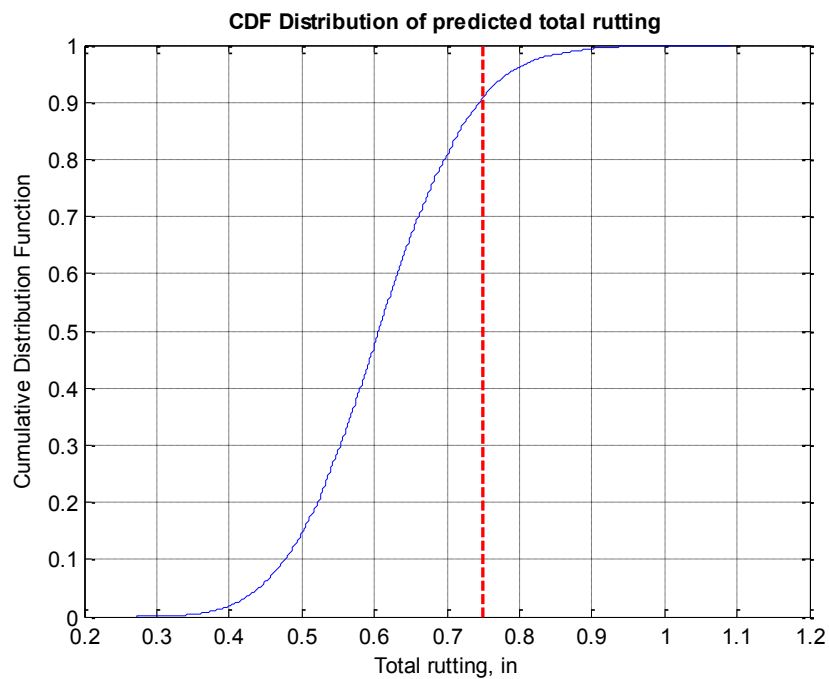


Figure 6.9 Example of estimating the reliability level in a CDF plot

6.3 Development of *ReliME*

The proposed reliability improvement through Monte Carlo simulation could be placed on two platforms: one is Excel and the other is MATLAB. Since none of them have a developed library for Monte Carlo simulation (in other words, users have to create their own spreadsheet or code), a decision was made to continue using MATLAB. Some other pros and cons are also considered:

- Excel is widely available and familiar to users. MATLAB is used mainly for research. Fortunately, it is possible to convert MATLAB files to a stand-alone executable file, which will be easy to transfer and used in the same way as an Excel spreadsheet.
- There is a size limit for Excel (65,536 rows and 256 columns for the 2003 version). But MATLAB does not impose a limit on the dimensions and size of matrices. It is only determined by the hardware memory and disk size. Moreover, a large file may dramatically slow the speed of Excel; but MATLAB is relatively dynamic.
- The surrogate models were built and verified in MATLAB. It is easier for data transfer when the same tool is used.
- MATLAB provides a Graphical User Interface (GUI) tool on which a user-friendly screen could be created. With another tool called MATLAB Compiler™, the whole process could be delivered as a self-sustained executable package.

Therefore, it was decided to build a software tool that contains all the information presented in this research using MATLAB. The software is named *ReliME*, standing for Reliability improvement for Mechanistic-Empirical pavement design. In addition, due to the importance of local calibration, it is envisioned that *ReliME* shall be state specific (because calibration coefficients will be most likely different from state to state). Hence, the tool in this study will be

called *ReliME-AR* for the state of Arkansas only. Other tools such as *ReliME-TX* and *ReliME-OK* can be developed using the same procedure.

6.3.1 Procedures

The development of *ReliME* involves the following steps, as shown in Figure 6.10:

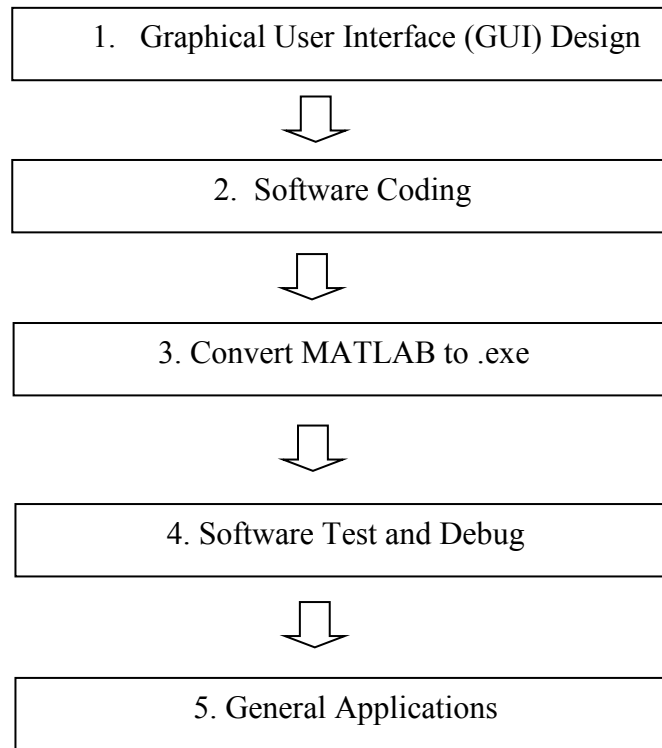


Figure 6.10 Steps to develop *ReliME*

Step 1. Design the users interface or the screen. A user-friendly screen shall be well organized, intuitive and aesthetically beautiful. Input and output shall be easy to use and operate. This process was completed in the GUI Design Environment (GUIDE) in MATLAB. The product from this step is a file named *ReliME.fig*

Step 2. Code all functions, including data preparation, data check and reduction, Monte Carlo simulation and reliability calculation, using MATLAB. Detail on this step will be discussed later. The product from this step is a file named *ReliME.m*

Step 3. Convert the MATLAB m file developed in Step 2 to an executable stand-alone file. This was completed using the MATLAB compiler. The product from this step is a file named *ReliME.exe*

Step 4. Test the reasonableness of the developed software tool in Step 3. Debug the code if necessary.

Step 5. Apply the tool on real problems. In particular, comparison with the reliability method in the AASHTO 1993 Guide and the MEPDG is of great interest. Three case studies will be presented at the end of this chapter.

The interface of *ReliME* is divided into two main regions, Input and Output. Figure 6.11 is a screenshot. At the top, user will have the option to choose the state, which acts like a switch being tied to the specific model calibrated to that state. The Input side contains all required variables, including traffic, climate, structure, materials and performance criteria. The nominal value and variance are required for probabilistic variables. For deterministic variables, only the nominal value is needed. The current version assumes a normal distribution which is characterized using the mean value and the coefficient of variation. Other distribution types could also be incorporated in the future. In the Input area, users have an option to select at which year the analysis is. A “Run Analysis” button is distinctively located at the bottom of the Input side. User starts the analysis by click this button after all required inputs are completed. The Output side contains three histogram plots of the three performance index, alligator cracking, total rutting and smoothness (IRI). Mean and standard deviation of the three parameters are also presented besides the histogram. Cumulative traffic load represented by ESALs is shown as well. The mean, upper bound and bottom bound of traffic load are included. The bound is related to

the variance of AADTT. Finally, the calculated reliability is displayed at the bottom of the Output area.

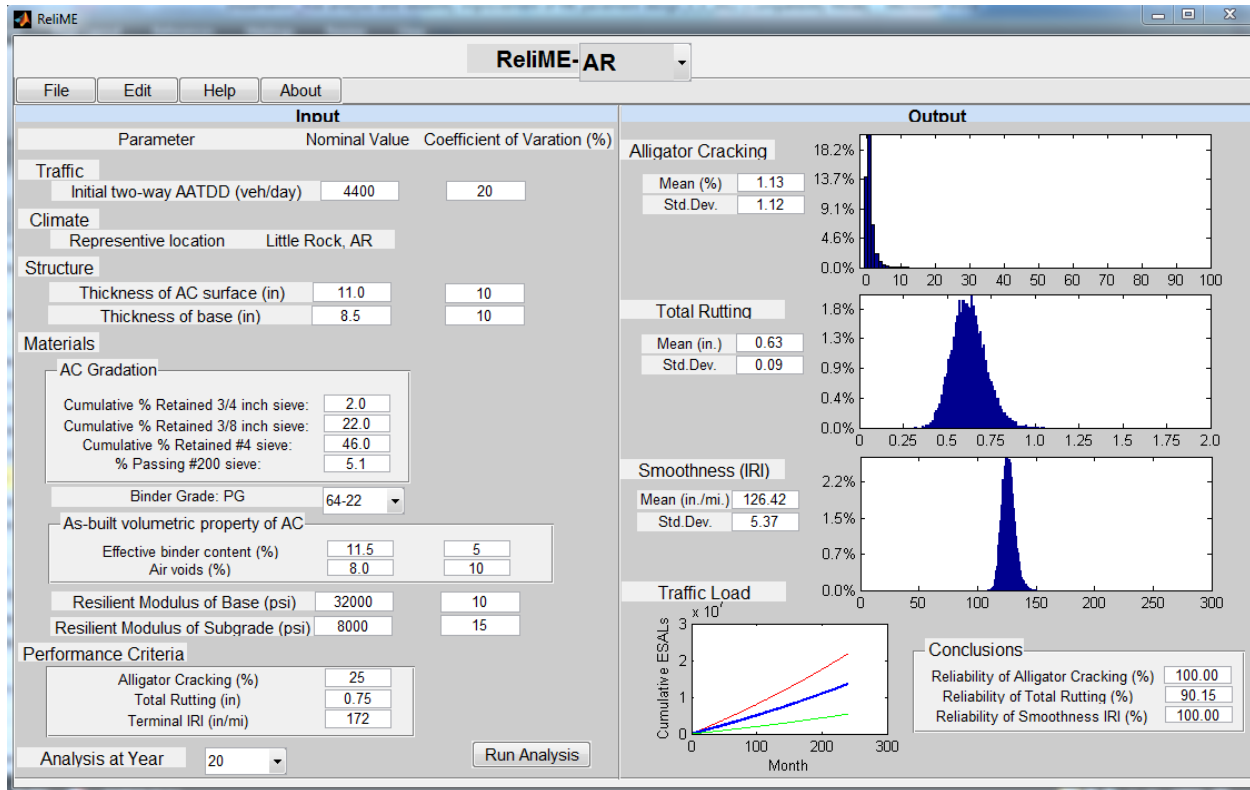


Figure 6.11 Screenshot of *ReliME-AR*.

6.3.2 Software Coding

The flowchart of *ReliME* is shown in Figure 6.12. The software first interprets the required inputs from the GUI interface. Nominal value and variance are then fed to the random number generator as discussed before. A single sample is picked from each variable and gathered together to form a set of inputs. Then some intermediate variables such as the dynamic modulus using the Witczak model are calculated. The software also loads model coefficients from a file which is the final product from Chapter 5. Now all inputs are ready and a simulation is ready to run. The output from such a simulation is the predicted alligator cracking in percentage, total rutting in inches, and IRI in in./mi.

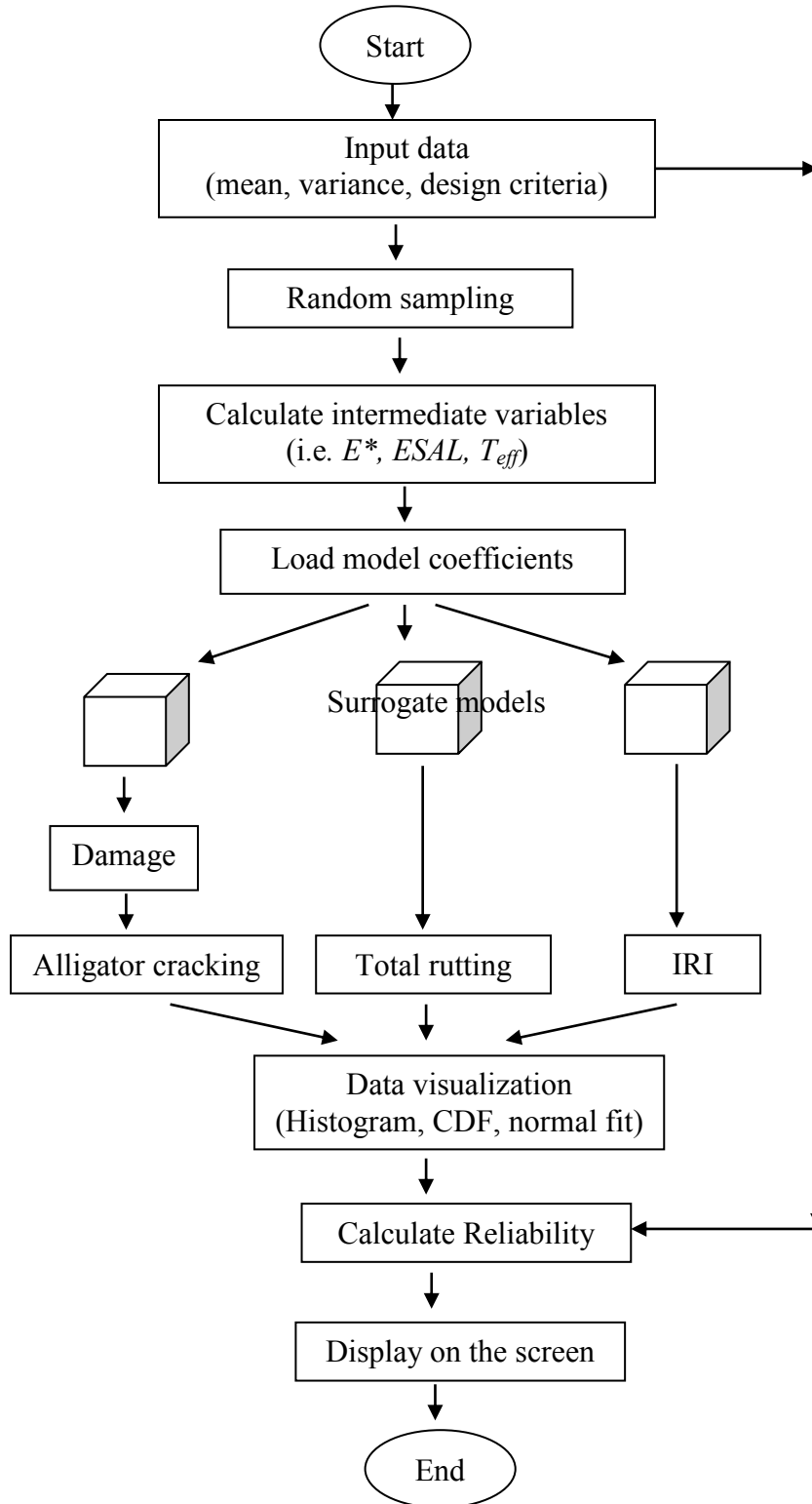


Figure 6.12 Example of estimating the reliability level

Note that the concept of damage and Miner's law as used in MEPDG is used in this study to calculate alligator cracking. This simulation will be repeated using different set of inputs. Finally, after tens of thousands of simulations, a large number of predicted performances are available for data visualization and further analysis. Histogram plots will be displayed on the GUI screen. Normal fit is conducted for normal distributed outputs, and by comparing to the user-defined design criteria, the reliability of a design is calculated. The ultimate result, reliability level, is then shown on the screen.

All details about each single step have been elaborated before. The MATLAB code for the software tool is presented in Appendix E.

The next step is to convert the MATLAB code into a standalone executable file. MATLAB provides a tool called CompilerTM which can accomplish this task. This transformation enables the MATLAB application could be run outside the MATLAB environment.

Two executable packages are developed. One named *ReliME_pkg4MATLAB.exe*, which is designed for users who have a MATLAB software installed on his/her computer. This is a small file measured only 374 kB. The other package named *ReliME_pkg.exe* is intended for users who don't have the MATLAB software. This is a relatively large file measured as 175 MB. The reason for the dramatic difference is that a file named *MCRInstaller.exe* is included in the package for applications outside the MATLAB environment. The MATLAB Compiler Runtime (MCR) is a standalone set of shared libraries that enable the execution of MATLAB files, even on computers without an installed version of MATLAB. When users open the package for the first time, a MCR installation wizard which will automatically install the MCR on that computer will be initiated. After one step or two steps simple operation, the final product, a file named

ReliME.exe, will be generated in the same folder. Then the software tool is ready for use by double click the .exe file. To assist the installation, a text file named *UsersGuide.txt* is also included in the package.

6.3.3 Software Test

To test the performance of *ReliME*, a verification study was conducted using 100 samples which were also used to construct surrogate models in Chapter 5. Ideally, *ReliME* shall predict the same distress as MEPDG does, if there was no model error. Since variance is required in *ReliME* and zero is not allowed, all coefficient of variance are set to one in the study, as shown in Figure 6.13. As expected, the predicted performance has nearly no variation. This is particularly obvious in the traffic load plot, in which the upper bound and lower bound set on top of the mean curve. The 100 samples were manually evaluated in *ReliME*. Predicted mean alligator cracking, total rutting and IRI were recorded. Comparison between *ReliME* and MEPDG was then conducted and presented in Figure 6.14. It is found that the rutting model performs the best. Alligator cracking and IRI model are good at low values but has a larger variance at high values. Note that Figure 6.14 is similar but not the same as Figure 5.35. Figure 5.35 compares the prediction from MEPDG and from surrogate models, which are deterministic response surface models. But Figure 6.14 compares the result from MEPDG and from *ReliME*, which is a Monte Carlo Simulation. The data presented in Figure 6.14 from *ReliME* is the mean value of 10,000 simulations of surrogate models. It is because of this difference, Figure 6.14 and 5.35 are slight different. Otherwise, they should be the same by definition. Overall, a wide range is covered by *ReliME*.

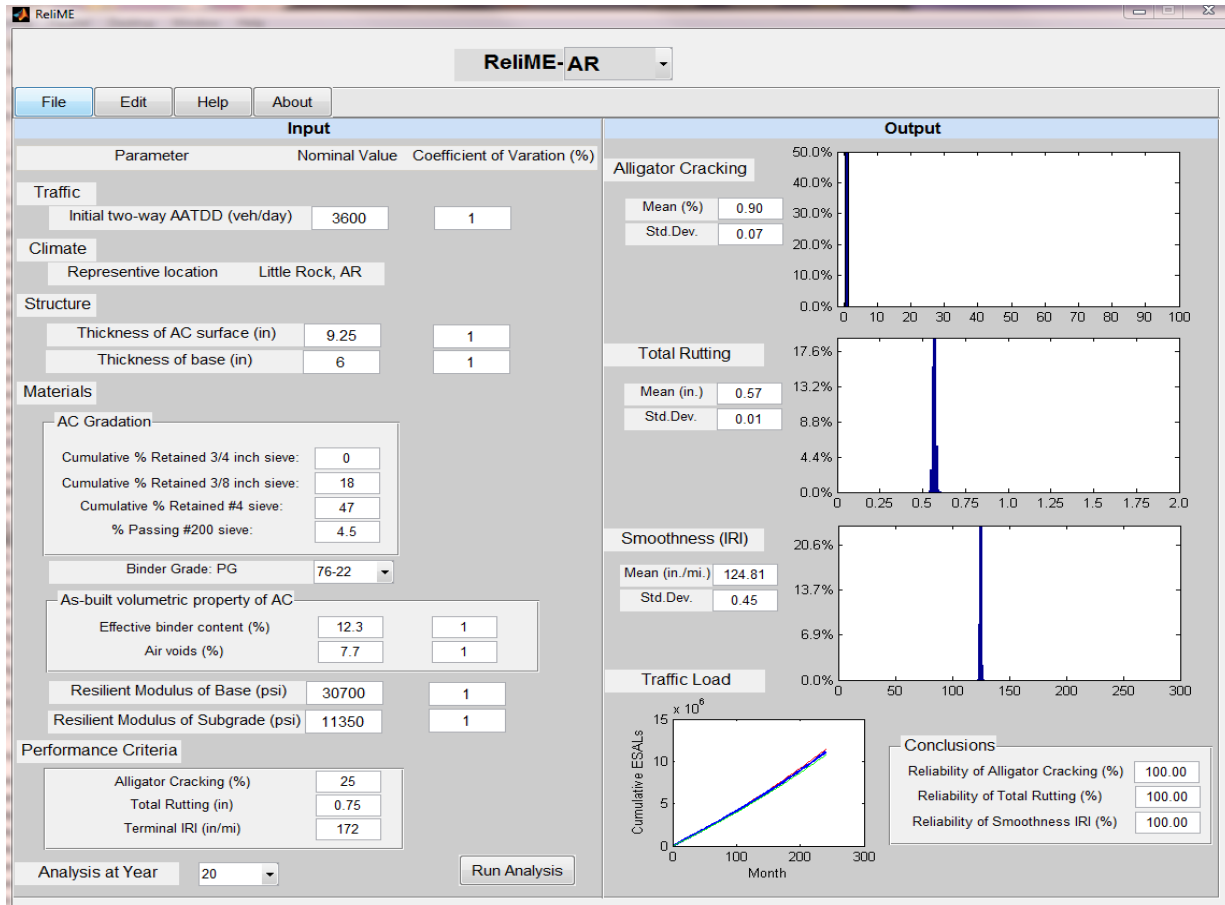
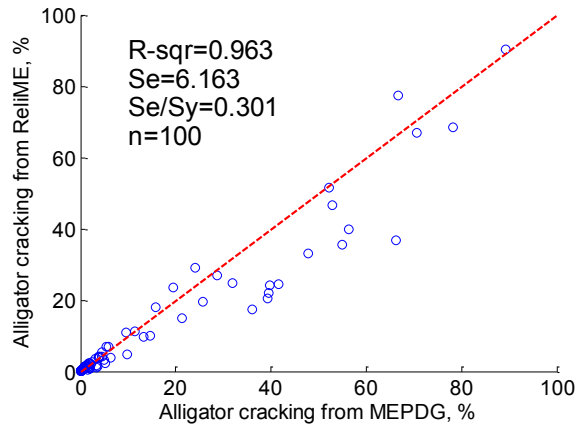
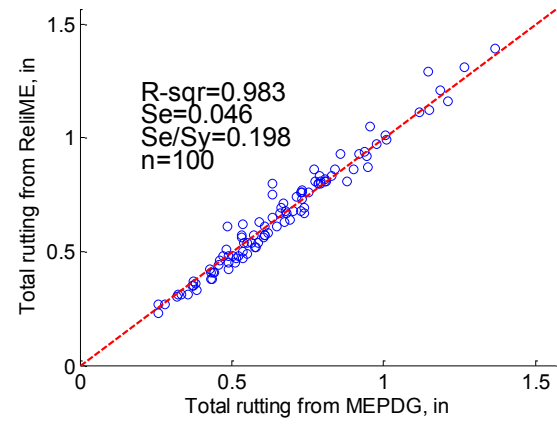


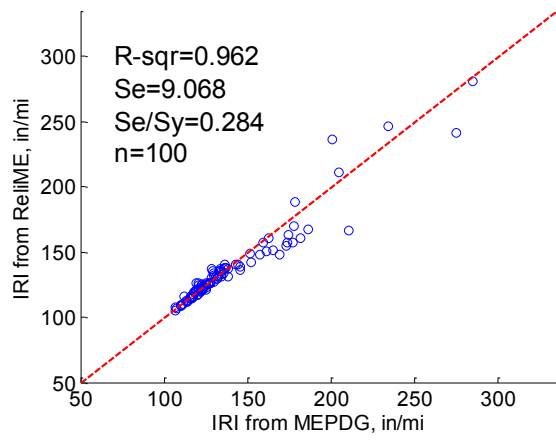
Figure 6.13 Screenshot of *ReliME* with COV=1



(a)



(b)



(c)

Figure 6.14 Verification of *ReliME* using 100 random samples: (a) alligator cracking, (b) total rutting, and (c) IRI.

6.4 Case Studies

ReliME provides a simple-to-use tool for pavement design, especially when the reliability and uncertainty are of user's interest. This section presents three case studies showing how *ReliME* performs in real world projects. Comparisons between the AASHTO 1993 Guide, MEPDG and *ReliME* are discussed in detail.

As discussed in Chapter 2.2, the reliability model in MEPDG is an empirical relationship derived from the national calibration. Standard error of each distress is related to the predicted

mean distress. In addition, standard error has an overall increasing trend. That is, more severe distress may have a larger standard error; and vice versa. The closed-form relationship between the predicted mean distress and the corresponding standard error is as following (13)

$$Se_{AC} = 0.5 + \frac{12}{1 + e^{1.308 - 2.949 \log D}} \quad (6.8)$$

where Se_{AC} = standard error of estimate for bottom up alligator cracking

D = predicted damage for bottom up fatigue cracking

$$Se_{PDAC} = 0.1587 PD_{AC}^{0.4579} \quad (6.9)$$

where Se_{PDAC} = standard error for AC permanent deformation

PD_{AC} = predicted AC permanent deformation, inches

$$Se_{PDGB} = 0.1169 PD_{GB}^{0.6303} \quad (6.10)$$

where Se_{PDGB} = standard error for granular base permanent deformation

PD_{GB} = predicted granular permanent deformation, inches

$$Se_{PD SG} = 0.1724 PD_{SG}^{0.5516} \quad (6.11)$$

where $Se_{PD SG}$ = standard error for subgrade permanent deformation

PD_{SG} = predicted subgrade permanent deformation, inches

$$Se_{TR} = \sqrt{(Se_{PDAC})^2 + (Se_{PDGB})^2 + (Se_{PD SG})^2} \quad (6.12)$$

where Se_{TR} = standard error for the total rutting.

$$Se_{IRI} = -4.3370^{-4} IRI^2 + 0.3040 IRI + 2.4817 \quad (6.13)$$

where Se_{IRI} = standard error for IRI,

IRI = predicted IRI, in/mi.

Note that the IRI model is not transparent to users because intermediate parameters are not reported by MEPDG. Therefore, the standard error equation in this study is an empirical relationship derived from data in this study. It should not be used for other purposes. The equation is valid here because it is a relationship between the predicted distress at 50% and the predicted distress at 90%.

To compare different possible variations, four coefficient of variance levels were simulated using *ReliME*. Table 6.2 shows the three levels: low, medium and high. Note that the medium level is set as close as possible with the AASHTO 1993 Design Guide, as presented in Table 2.2.

Table 6.2 Coefficient of variance simulated in *ReliME*

Variables	Low variance (1)	Medium variance (2)	High variance (3)	Extra high variance (4)
AADTT	10	15	20	30
AC thickness, h_{ac}	5	10	15	20
Base thickness, h_{base}	5	10	15	20
Effective binder content, p_{beff}	5	7.5	10	20
Air voids, V_a	5	7.5	10	20
Base resilient modulus, M_{rb}	10	15	20	30
Subgrade resilient modulus, M_{rs}	10	15	20	30

6.4.1 *Bella Vista Bypass*

The construction of the Bella Vista Bypass in northwest Arkansas has long been considered a high priority for the development of the transportation system in this region of the United States. The current facility through Bella Vista is congested with the nine signalized intersections, which will continue to create a bottleneck to the entire corridor, hampering future economic opportunities for the entire Midwest. The proposed 18.9-mile, Highway 71 Bella Vista Bypass

(BVB) project consists of completing the construction of a new, four-lane, Interstate-type facility from the Highway 71/Highway 71 Business interchange south of Bella Vista, Arkansas to Highway 71 south of Pineville, Missouri. The cross-section will consist of a 60-foot depressed median, paved four-foot inside shoulder and 10-foot outside shoulder.

As shown in Figure 61, this project will complete a critical link in the Future Interstate 49 (I-49) corridor connecting the Port of New Orleans, Interstates 10, 20, 30, 40, 44, and 70, thereby allowing for the seamless movement of people and goods from the Gulf of Mexico to the Great Lakes area and Winnipeg, Canada. Upon completion of the Bypass, the Highway 71 corridor from I-40 to I-44 will be constructed to Interstate standards which will allow this segment of the corridor to ultimately be designated as Future I-49. Highway 71 between Highway 540 south of Bella Vista, Arkansas to I-44 in Joplin, Missouri is one of the few remaining gaps in an Interstate quality system between I-40 in Fort Smith, Arkansas and I-44 in Joplin, Missouri.

The proposed Interstate 49 is intended to complement the existing Interstate system, integrate regions of the country, facilitate safer and more efficient travel between Mexico and Canada, improve safety and efficiency of travel and commerce, and promote economic development. It will also improve intra-regional accessibility to alternative education and training, employment, recreation and medical facilities.



Figure 6.15 Location of Bella Vista Bypass

6.4.1.1 Pavement Design

Currently Arkansas Highway and Transportation Department (AHTD) is using the 1993 AASHTO Pavement Design Guide for pavement design. The design inputs for the Bella Vista bypass are summarized in Table 6.2. Considering the availability of material, equipment in Arkansas, and AHTD’s current pavement construction practices, the recommended flexible pavement structure based on the 1993 AASHTO Pavement Design Guide is shown in Figure 6.16.

Table 6.3 Inputs for flexible pavement design

2008 ADT	40,000
2028 ADT	56,000
Percent trucks	11%
ESALs (flexible)	13,008,600
Initial PSI	4.5
Terminal PSI	2.5
Reliability	90%
Overall standard deviation (flexible)	0.45
Subgrade R value	20
Subgrade resilient modulus	4,305 psi
Required SN (flexible)	5.85

In addition to design using AASHTO 1993 Guide, MEPDG was applied to this case study. Table 6.3 lists properties of main materials used for MEPDG analysis. A virtual climate station is interpreted from nearby weather station in Joplin regional airport and Northwest Arkansas regional airport. The mean annual air temperature is 57.7 °F; mean annual rainfall is 42.5 inch; and there are 61 freeze/thaw cycles every year in average. Using statewide traffic data, the study conducted in 2011 by Li and Xiao (91) optimized the pavement design. The results are listed in Figure 6.16 accompanying with the corresponding the AASHTO 1993 design. It was found that AASHTO 1993 was more conservative than MEPDG. About one inch material was saved according to MEPDG.

Table 6.4 Inputs for MEPDG analysis

	HMA Surface	HMA binder	HMA base	Aggregate base
3/4" (% retained)	0	2	12	
3/8" (% retained)	12	22	33	
#4 (% retained)	39	46	48	
#200 (% passing)	6.7	5.1	6.5	
Binder grade (PG)	76-22	70-22	70-22	
P _{beff} (%)	11.5	10.3	9.7	
Air voids (%)	8	8	8	
Resilient modulus (psi)				30,000
R-value of subgrade				20

AASHTO 1993	MEPDG
HMA Surface 2''	HMA Surface 2''
HMA Binder 3''	HMA Binder 3''
HMA Base (NMAS 1 1/2'') 8''	HMA Base (NMAS 1 1/2'') 6.5''
Aggregate base (Class 7) 6''	Aggregate base (Class 7) 6''
Subgrade A-4 (R value = 20)	

Figure 6.16 Recommended pavement structures

6.4.1.2 Results Analysis

Reliability of the four scenarios is presented as cumulative density functions. The x axis is the predicted distress and the y axis is the reliability level. Distresses of alligator cracking, total rutting and IRI are shown in Figure 6.17, 6.18 and 6.19, respectively. This design would pass the alligator cracking criteria, if it was set at 25%. As expected, higher variance leads to lower reliability. ReliME1 has a steeper slope than ReliME2; ReliME2 has a higher slope than ReliME3, and so on. ReliME4 has the most flat slope which represents its large variance. According to the slope of the CDF curve, the variance of the alligator cracking model built in MEPDG is most likely close to the variance of ReliME3.

It is worthwhile explaining the inconsistency of the mean predictions. Although it may be natural to think that no matter what variance level it is, the mean prediction (at 50% reliability) should be the same for all scenarios; one has to remember that the prediction from *ReliME* is based on Monte Carlo Simulation. Only if the relationship between alligator cracking (and other distresses) and individual input variables was linear, the predicted distress would have the same mean value (Equation 2.4 through 2.16). Referring to Figure 6.17, the mean prediction is close for case ReliME1, ReliME2 and MEPDG, but further away for ReliME3 and ReliME4. This implies that the alligator cracking model was a nonlinear relationship and the nonlinear character presents clearly when variances are high.

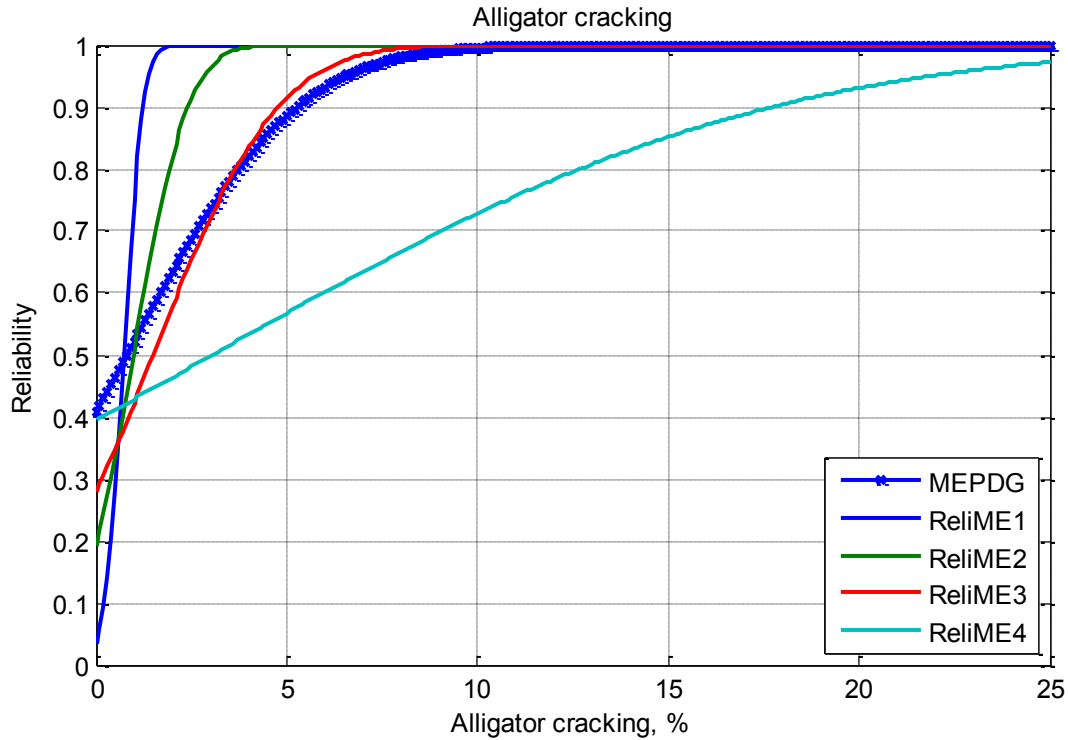


Figure 6.17 Reliability of alligator cracking for Bella Vista Bypass

Figure 6.18 provides the reliability comparison for total rutting. It is found that MEPDG predicts slightly more rutting than *ReliME* does in this case. In addition, this design would pass the design criteria if the total rutting criteria was 0.75 inches. One may question that *ReliME* was designed to function as a surrogate model of MEPDG, how could the two predict differently? The answer is that data in this case study are from real project; some of them, and most likely, a combination of them may be out of the design space that was used to build *ReliME*. For example, the gradation of HMA is different. On the other hand, as shown in section 6.3.3, *ReliME* matches well with the mean value for any random samples within the design space. Nevertheless it should be pointed out that the purpose of *ReliME* is to analyze uncertainty/variance and reliability. Model error between MEPDG and *ReliME* could be considered in the development of *ReliME* so that the deterministic mean prediction shall match, as presented in Section 6.3.3.

The slope change due to variance changes is observed but not as dramatical as the alligator cracking model does. Based on the slope of the CDF curve, the variance in MEPDG is close to the variance in ReliME2, or the AASHTO 1993 Guide.

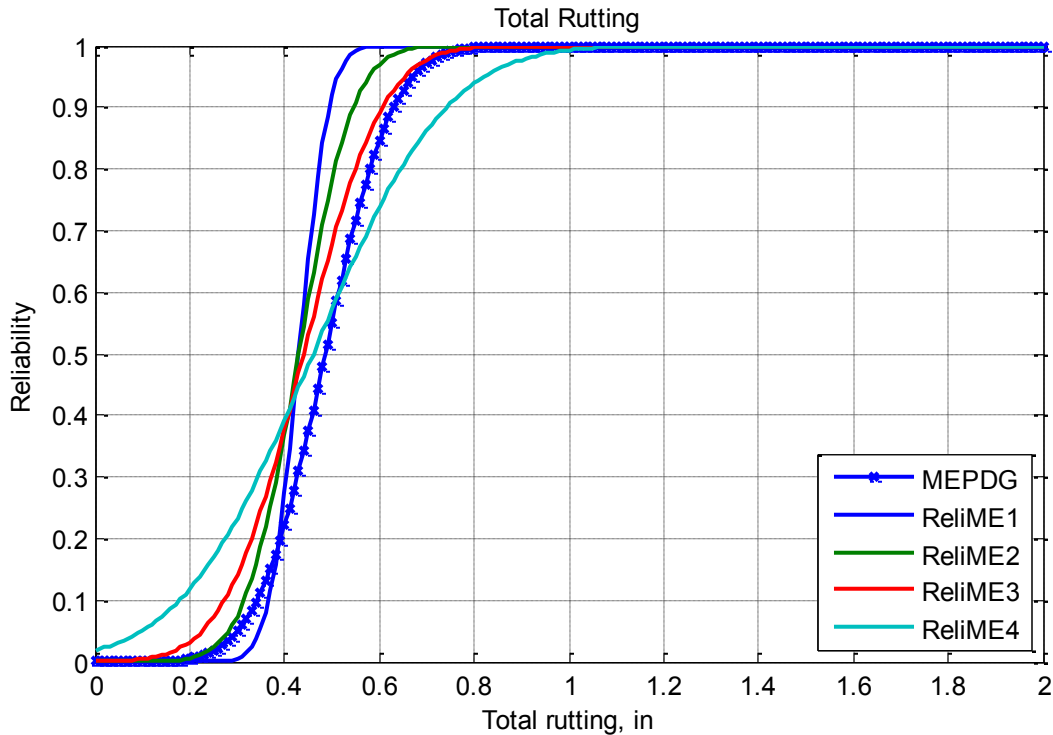


Figure 6.18 Reliability of total rutting for Bella Vista Bypass

The reliability of IRI is shown in Figure 6.19. Setting the criteria at the national default, 172 in/mi, this design is 90% for MEPDG, and 100% for *ReliME* except for the extra high variance case. It is found that the range, or variance, of IRI is larger in MEPDG than that in *ReliME*. This may be due to the fact that the IRI model in *ReliME* is an empirical model which was derived using less data and fewer variables than the national IRI model in MEPDG. It also should be noted that the comparison is at year 20. The reliability model in MEPDG assumes that variance increases as distress level and age increases. Another explanation is that the variance built in MEPDG for IRI is extremely high, closer to ReliME4.

Figure 6.19 proves the inconsistency of the mean prediction in Figure 6.17 and 6.18. Considering the IRI model in MEPDG is a linear relationship of other distresses and site factor, therefore the mean IRI of all scenarios matches well.

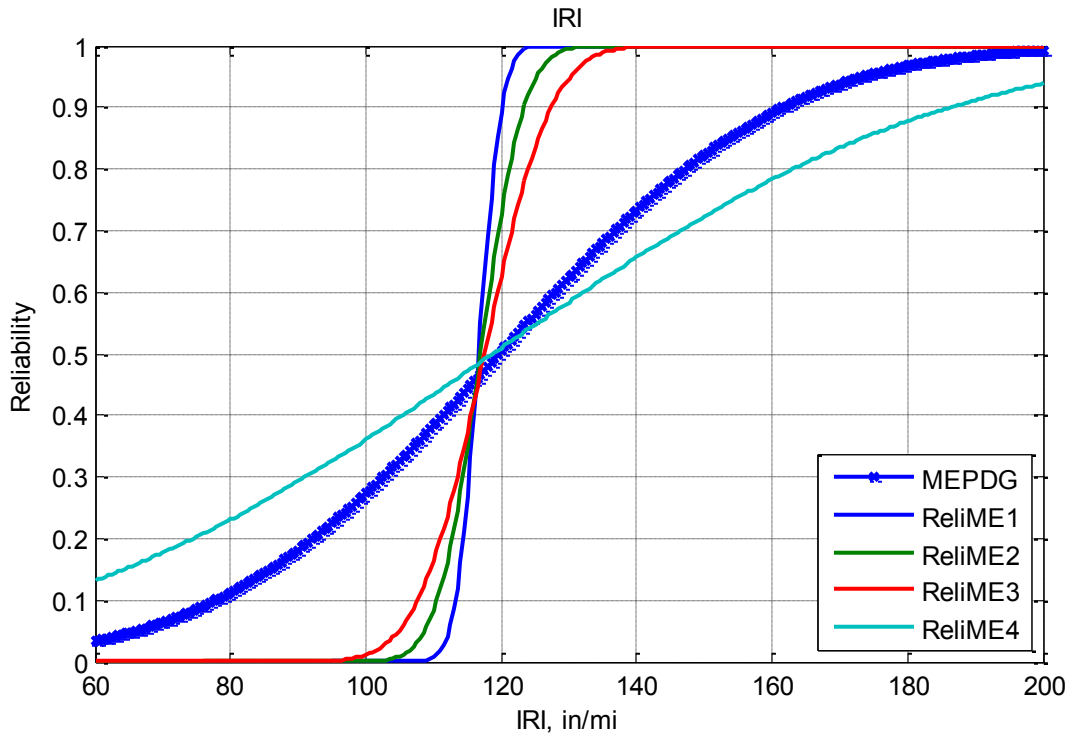


Figure 6.19 Reliability of IRI for Bella Vista Bypass

6.4.2 Pleasant Plains Bypass

Job R50084, one of the projects used in the local calibration, is selected as another example. The project was a new construction on US highway 167, section 17, close to Pleasant Plains, AR. Figure 6.20 illustrates the location and the zoom-in map. Figure 6.21 is the aerial map of the same location in 1994 and 2001. The new road is clearly visible from the air. The right of way view is presented in Figure 6.22 through 6.24. It is a five-lane road with two lanes in each direction and a Two Way Left Turn Lane (TWLTL). The lane width is 12 ft, with 6 ft shoulder on the left and right. The road was resurfaced in 2010.

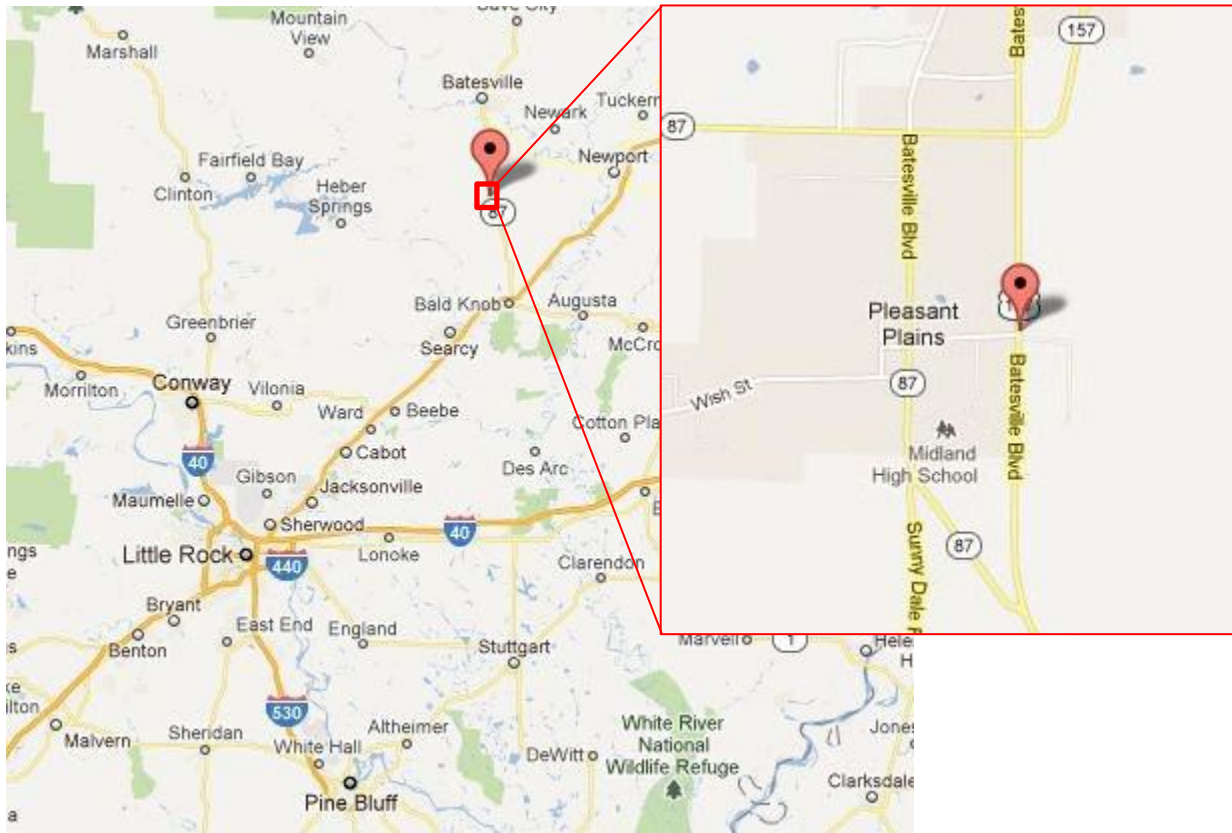


Figure 6.20 Location of Job R50084



(a)

(b)

Figure 6.21 Aerial map of Pleasant Plains by Google Earth (a) 1994, (b) 2001



Figure 6.22 ROW of R50084 when first constructed in 2001



Figure 6.23 ROW of R50084 in April 2010



Figure 6.24 ROW of R50084 after resurfacing in September 2010

6.4.2.1 Pavement Design

The function class is 2. The measured ADT is shown in Figure 6.25. Steady growth was observed from 1986 to 1999. The “outlier” in 2000 and 2001 are because the road was under construction. One should note that the project was a “new location”, which means the ADT was measured differently before and after construction of the new road. As shown in the aerial map, traffic was on the left road (old road) before the opening of the right road. It is obvious that about 70% (5,000 among the 7,000 ADT) traffic was attracted to the new road. The other 30% traffic may be drivers from and to the town keeping using the old road. The growth of traffic is also obvious from Figure 6.25. The linear growth rate is 1.8%; the compound growth rate is 1.6%. The difference between the two methods is negligible though. Figure 6.26 shows the truck percentage and AADTT of the project. Although slight growth is present, this study uses the

average, 16.5%, as the truck percentage. In short, the initial AADTT is 729 in 2002 with a linear growth rate 1.8% in the 20 years design life.

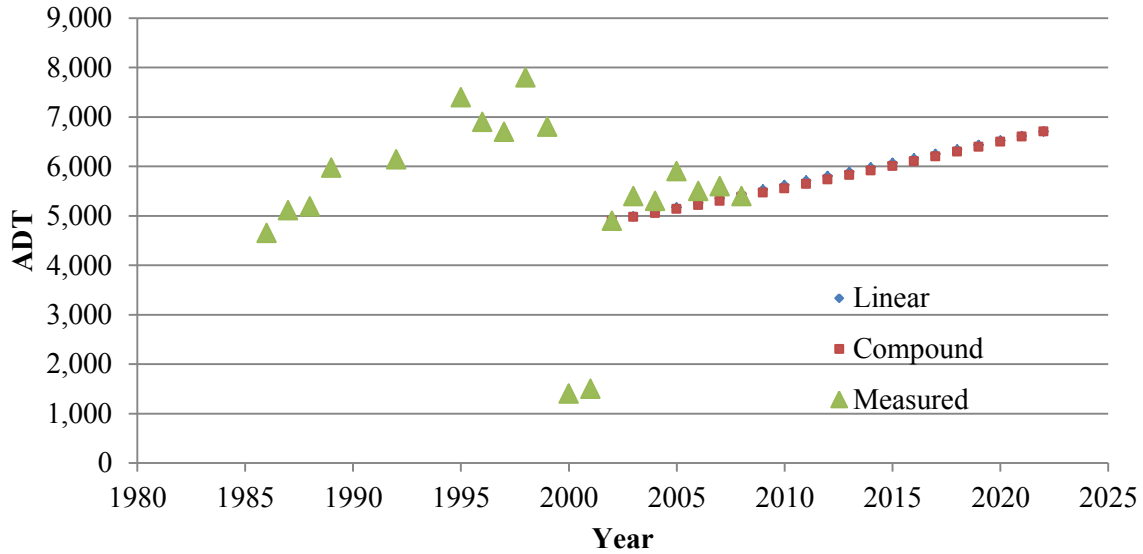


Figure 6.25 Measured and predicted ADT of R50084

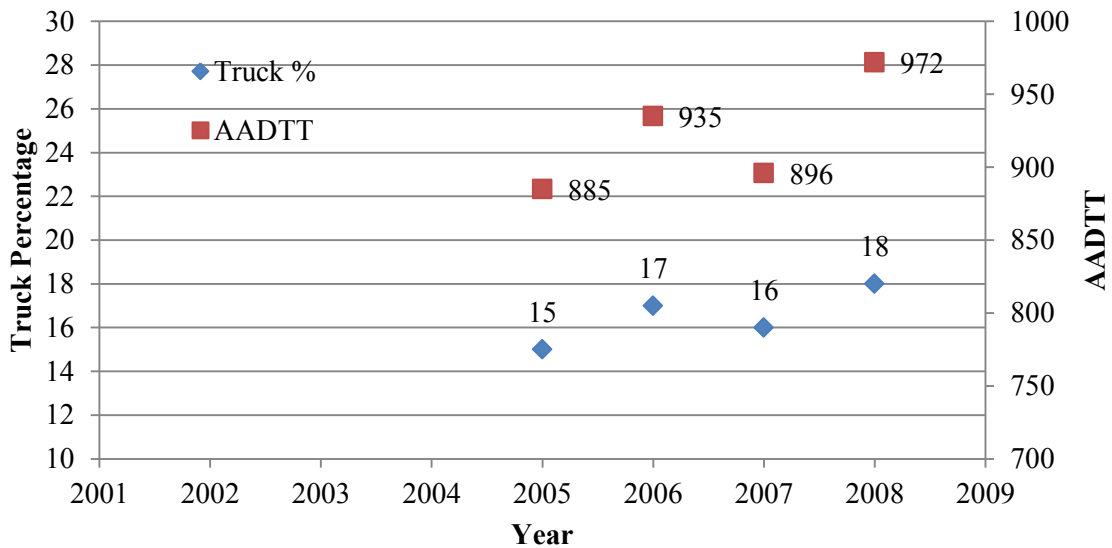


Figure 6.26 Truck percentage of AADTT of R50084

Table 6.5 lists the input for the pavement structure design using AASHTO 1993 guide. The designed structure is 7'' HMA surface on top of 11'' Class 7 aggregate base. PG64-22 was used as the binder. The posted speed limit is 55 mph. The same materials as used in the Bella Vista Bypass are used in the MEPDG analysis for this project. The structure designed from both AASHTO 1993 and MEPDG is shown in Figure 6.27. Specially note that the structure from AASHTO 1993 does not pass the MEPDG design criteria. In other words, AASHTO 1993 did not provide sufficient structure for the traffic condition in the 20 years according to MEPDG. Therefore, the proposed structure from MEPGD is 2'' HMA surface, 3'' HMA binder and 6.5'' HMA base course on top of a 6'' aggregate base layer. Although it is commonly understood that AASHTO 1993 Guide provides conservative designs, even the “conservative” design fails early for this project. This is true considering the project was overlaid in 2010 after 10 years of service, instead of the designed 20 years.

Table 6.5 Inputs for flexible pavement design

1997 ADT	4,050
2017 ADT	6,090
Percent trucks	18%
ESALs (flexible)	2,289,280
Initial PSI	4.5
Terminal PSI	2.5
Reliability	90%
Overall standard deviation (flexible)	0.45
Subgrade resilient modulus	4,400 psi
Required SN (flexible)	4.59

Table 6.6 Inputs for MEPDG analysis

	HMA Surface	HMA binder	Unbound base/subgrade
3/4" (% retained)	0	16	
3/8" (% retained)	19	52	
#4 (% retained)	48	69	
#200 (% passing)	6.6	4.7	
Binder grade (PG)	64-22	64-22	
Pb_{eff} (%)	10.9	8.4	
Air voids (%)	8	8	
Resilient modulus (psi)			30,000
Subgrade type			A-6
Subgrade resilient modulus (psi)			4,400

AASHTO 1993	MEPDG
HMA Surface 2''	HMA Surface 2''
HMA Binder 5''	HMA Binder 3''
Aggregate base (Class 7) 11''	HMA Base (NMAS 1 1/2'') 6.5''
	Aggregate base (Class 7) 6''
Subgrade A-4 ($M_R = 4400$ psi)	

Figure 6.27 Recommended pavement structures for job R50084

6.4.2.2 Results Analysis

Reliability of alligator cracking is shown in Figure 6.28. For a 25% criterion, this design would survive the alligator cracking distress at 93% in 20 years design life according to MEPDG, and 100% per *ReliME*. *ReliME4* has the widest range among the three *ReliME* variance

scenarios, but MEPDG surpasses all of them. In addition, the five curves have a single tie at about 35% reliability with 2% alligator cracking.

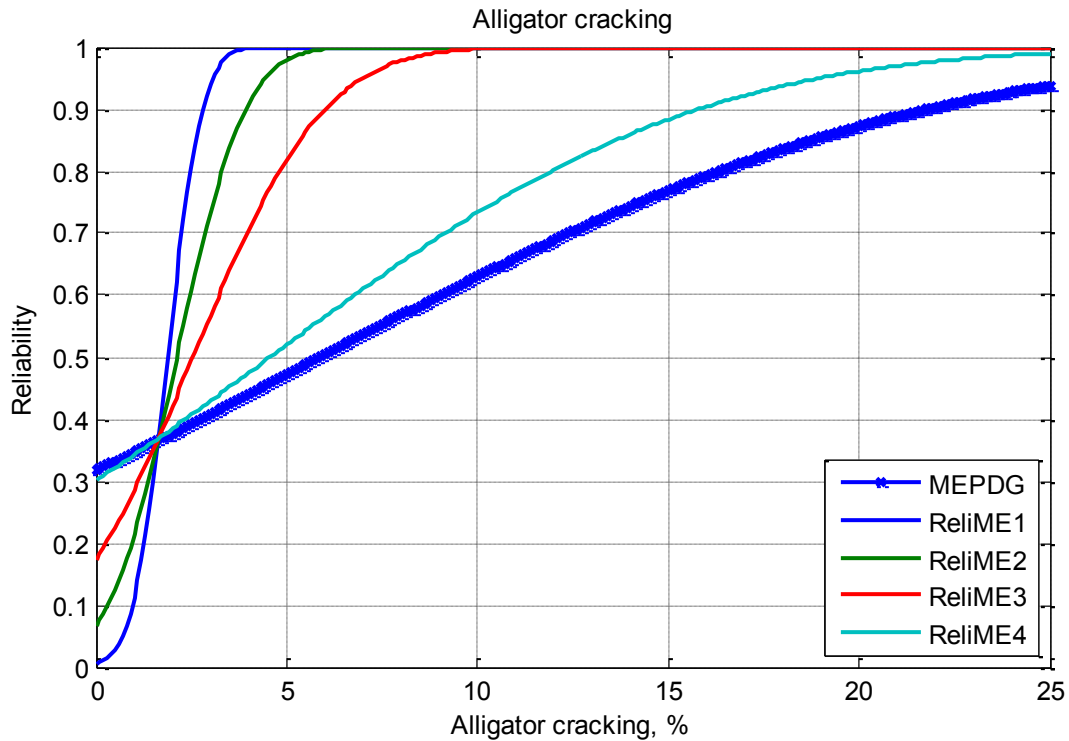


Figure 6.28 Reliability of alligator cracking for Pleasant Plain Bypass

Figure 6.29 is the total rutting reliability. First of all, it is found that the MEPDG curve matches with the ReliME3 curve. This means MEPDG has the same variation as ReliME3 simulates. However, this design could not withstand the intended traffic in 20 years (reliability=31.18%).

Figure 6.30 is the comparison of IRI for the Pleasant Plain Bypass. MEPDG does not pass the 172 in/mi criteria, but *ReliME* gives a level of 100% reliability for the design in variance level 1, 2 and 3. MEPDG has the widest variance/coverage among the five cases. Again it is found that MEPDG has extremely high variance for the IRI model. ReliME4 is the closest case to the MEPDG prediction.

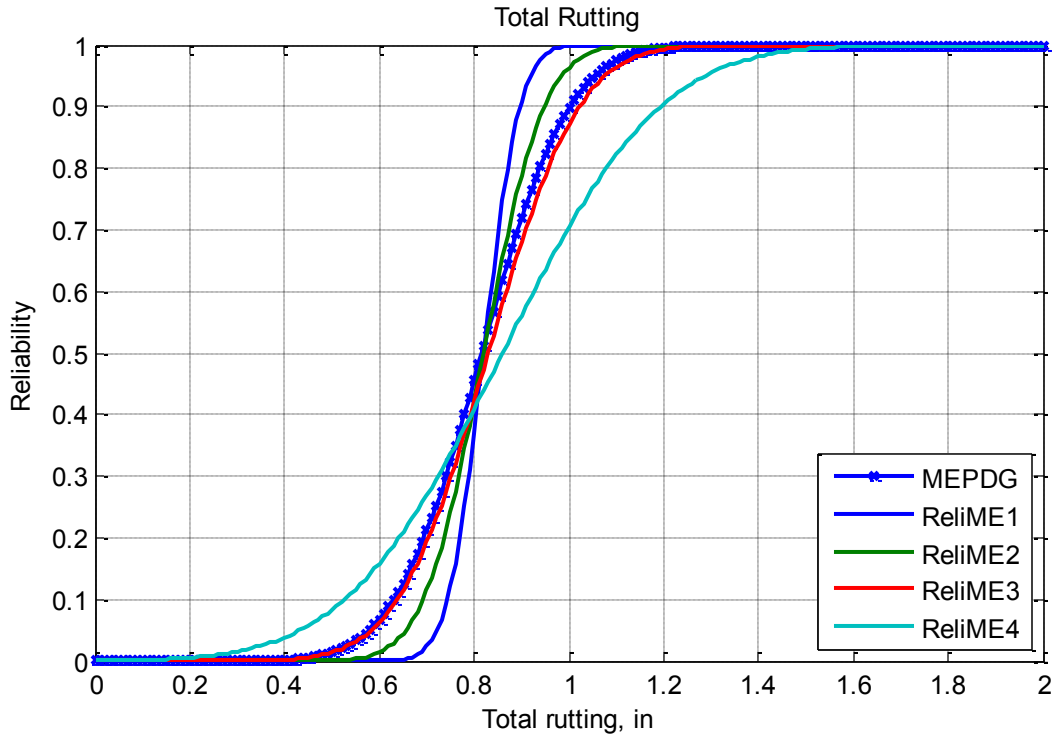


Figure 6.29 Reliability of total rutting for Pleasant Plain Bypass

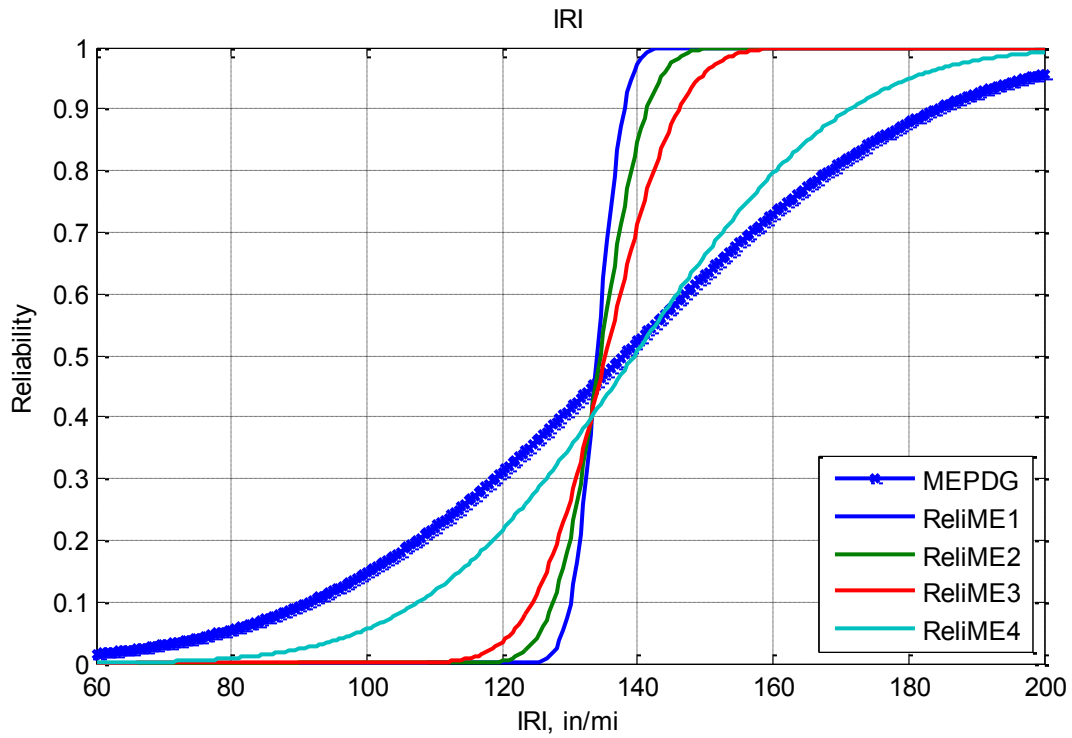


Figure 6.30 Reliability of IRI for Pleasant Plain Bypass

6.4.3 Sheridan Bypass

A bypass on Highway 167 near Sheridan, AR (Job number 020464) is in plan. The location is shown in Figure 6.31. The City of Sheridan is located in the center of Grant County and is approximately 32 miles South of Little Rock. The population had a +18.1% growth since 2000, reached 4,572 in July 2008.

6.4.3.1 Pavement Design

General information, soil survey and traffic record are prepared by the corresponding section in AHTD. As listed in Table 6.7, the planned four-lane road will carry 11,300 vehicles daily, in which 15% are trucks. The estimated compound growth rate is 1.7%. Using the AASHTO 1993 method, the design ESAL is about 4.4 million in 20 years. A R-value of 12 was suggested by Materials Division for pavement design. In addition, AHTD conducted resilient modulus test on subgrade soils. The average resilient modulus is 8,496 psi.

Table 6.7 Main Design Information for Job 020464

Parameter	Value	Station	Resilient Modulus (psi)
Initial ADT (2010)	11,300	148+00	8,641
Trucks	15%	220+00	8,125
Design ADT (2030)	15,820	237+00	9,534
Design speed	60 mph	382+00	4,863
Design ESALs (for flexible pavement)	4,365,400	428+00	8,590
Initial serviceability	4.5	475+00	9,686
Terminal serviceability	2.5	510+00	10,178
Reliability level	90%	average	8,517
Overall standard deviation	0.45		
Subgrade	R-value =12		
Design structural number	5.51		

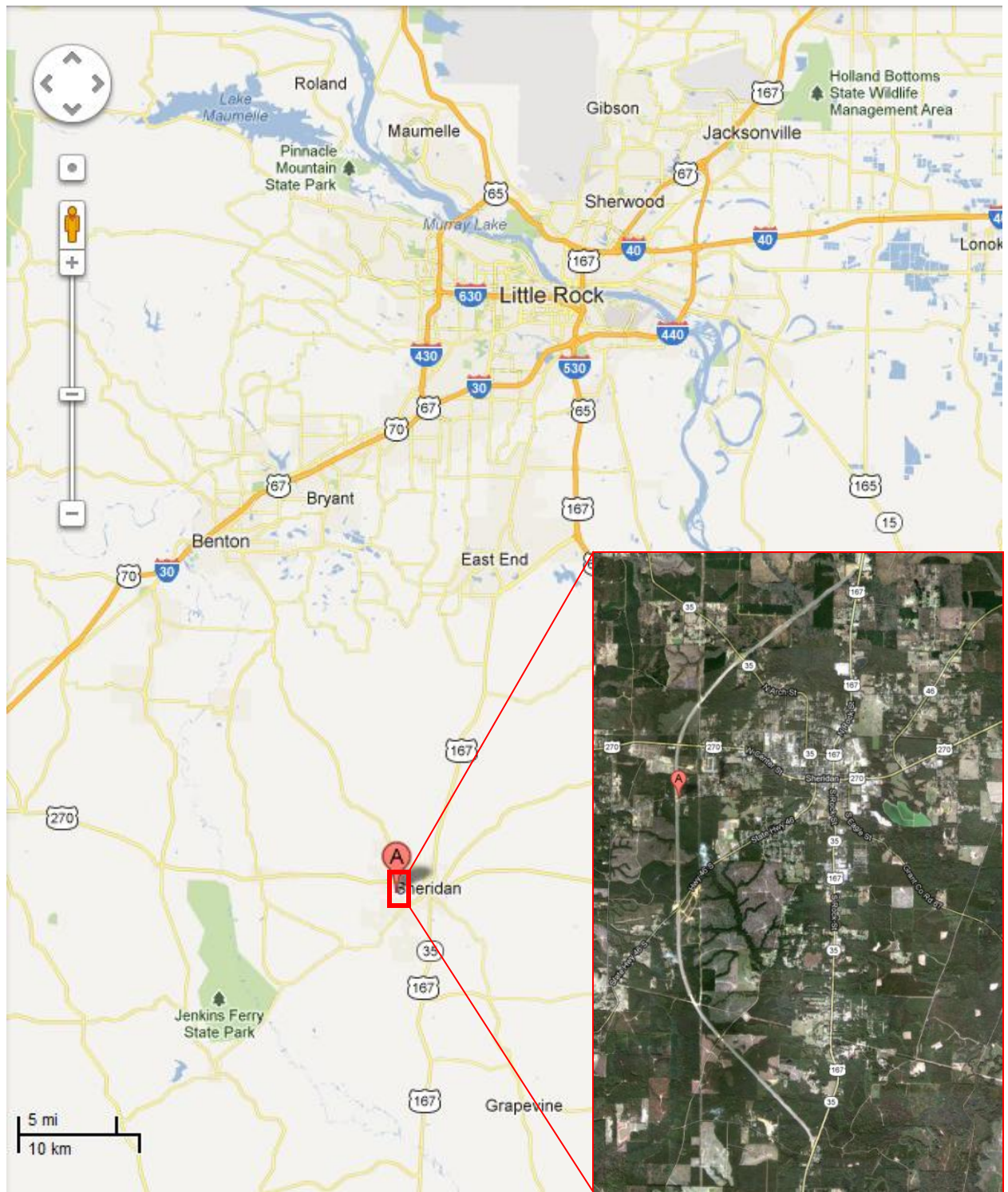


Figure 6.31 Location of the Sheridan Bypass

Three mix designs were approved for this job in 2012. Table 6.8 shows the mix design data as required by MEPDG. Note that this is a project-level input for this case study. In general design process, project-level mix design is not available. Designers have to rely on a material library built on historical mix design data. Currently the Department does not conduct Level 1 dynamic modulus test on asphalt mixtures, because a study found that the Witczak model prediction fits well with the Level 1 measurement of common mixtures in Arkansas (92).

Table 6.8 Mix Design for Job 020464

Layer	3/4" retained	3/8" retained	#4 retained	#200 passing	Binder grade	Binder content	Air voids	VMA
Surface	0	18	44	5.6	PG70-22	5.4	4.5	15.0
Binder	18	35	56	4.6	PG70-22	4.4	4.5	13.2
Base	23	38	56	4.6	PG70-22	4.0	4.5	12.4

Design volume of traffic was obtained from the comprehensive traffic count program operated by AHTD. For this project, a nearby station (ID: 270017) with vehicle classification data was determined to be representative for the section under design. Figure 6.35 shows the vehicle class distribution of this station. Comparing to the definition of Truck Traffic Classification (TTC) (13), this station belongs to TTC-1, which has more than 75% Class 9 trucks. Statewide axle load spectra was produced using *PrepME*, a software that conducts quality check on traffic data from Weigh-in-Motion stations and generates traffic input for MEPDG (93).

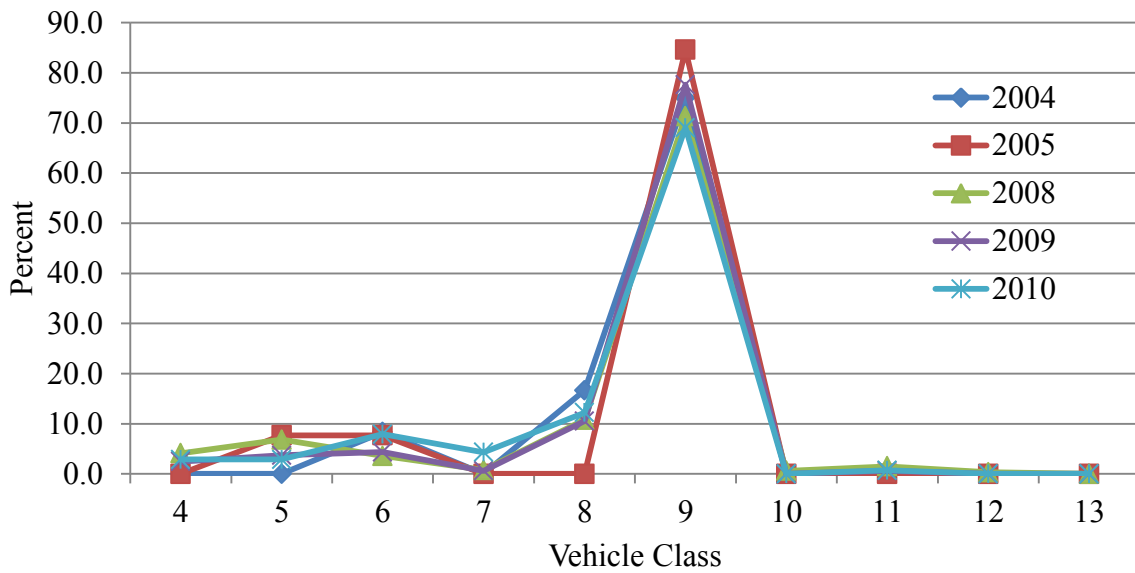


Figure 6.32 Truck classification of station 270017 for Job 020464.

Climate data was generated by interpolation of nearby climate stations (Hot Spring, Little Rock and Pine Bluff). The default performance criteria were used. The production-ready software of MEPDG, DARWin-ME, was deployed to complete the analysis.

The design procedure starts from the pavement structure proposed by using the *AASHTO 1993 Guide*. Then multiple trial-and-error processes based on engineering experience were conducted. Figure 6.36 shows the proposed structure that passes all performance criteria. For comparison purpose, the original design was also presented. In total MEPDG reduces one inch (1”) asphalt mixture. Referring to the average material cost in 2011, the one inch difference could save the Department about \$336,621 for this 2.77-mile project.

AASHTO 1993	MEPDG
HMA surface 4''	HMA surface 2''
HMA binder 3''	HMA binder 3.5''
HMA base 4.5''	HMA base 5''
Aggregate base (Class 7) 6''	Aggregate base (Class 7, Mr=30,000 psi) 6''
Lime treated subgrade 6''	Lime treated subgrade (Mr=45,000 psi) 6''
Subgrade A-6 (R-value=12)	Subgrade A-6 (Mr=8,500 psi)

Figure 6.33 Proposed pavement structure by AASHTO 1993 and MEPDG (not to scale).

6.4.3.2 Results Analysis

The MEPDG design was modeled in *ReliME* with four variation levels as shown in Table 6.4.

The relationship between reliability and the predicted mean alligator cracking is shown in Figure 6.34. All of the five scenarios pass the alligator cracking criteria, 25%. The predicted mean alligator cracking is about 1%. The variation of MEPDG is larger than the variation of ReliME3 but less than ReliME4, according to this simulation.

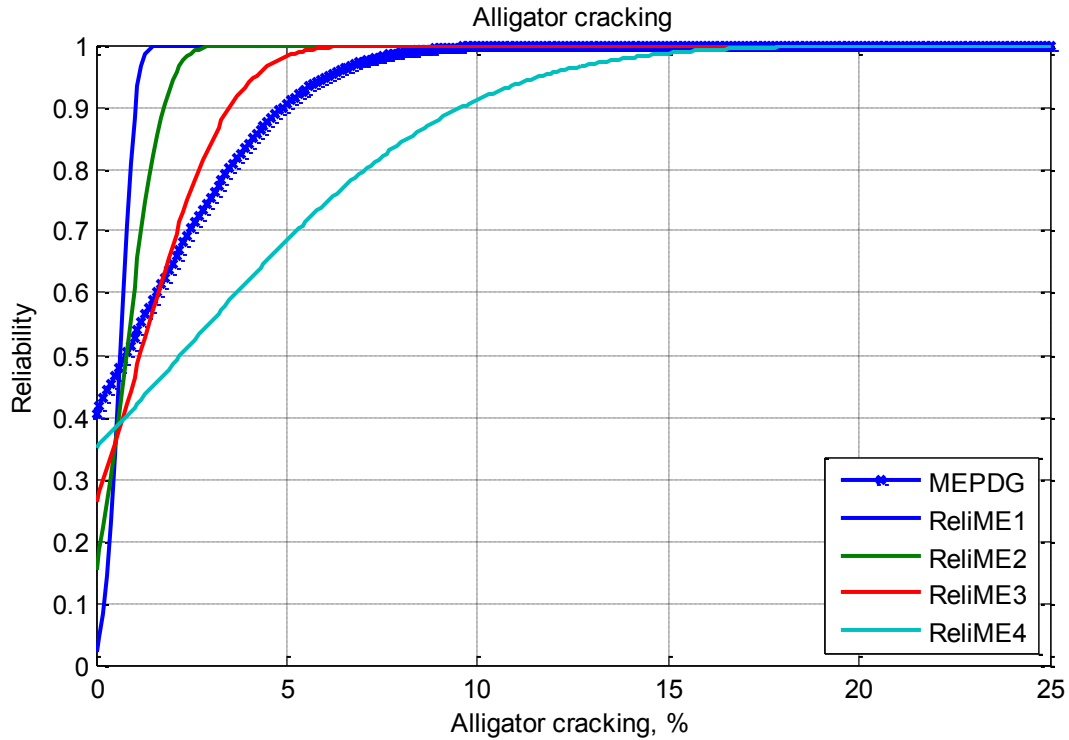


Figure 6.34 Reliability of alligator cracking for Sheridan Bypass

Figure 6.35 presents the reliability comparison of total rutting. It is found that the CDF for the five cases are very similar. In particular, MEPDG matches closely with the ReliME2 and ReliME3. The mean prediction is about 0.45". If the design criterion was 0.75", this design for ReliME1 would be 100% reliability and 92% reliability for ReliME4.

Comparison of IRI is presented in Figure 6.36. Again, it shows that MEPDG has a much larger variation than the simulated cases in *ReliME*. The slope of MEPDG is even flatter than it of ReliME4. In other words, the variance in MEPDG for IRI is larger than the extra high variance in Table 6.2. The mean prediction is 117 in/mi. The three variation levels do not cause dramatic reliability difference. This design passes the IRI criterion if it was set at 172 in/mi.

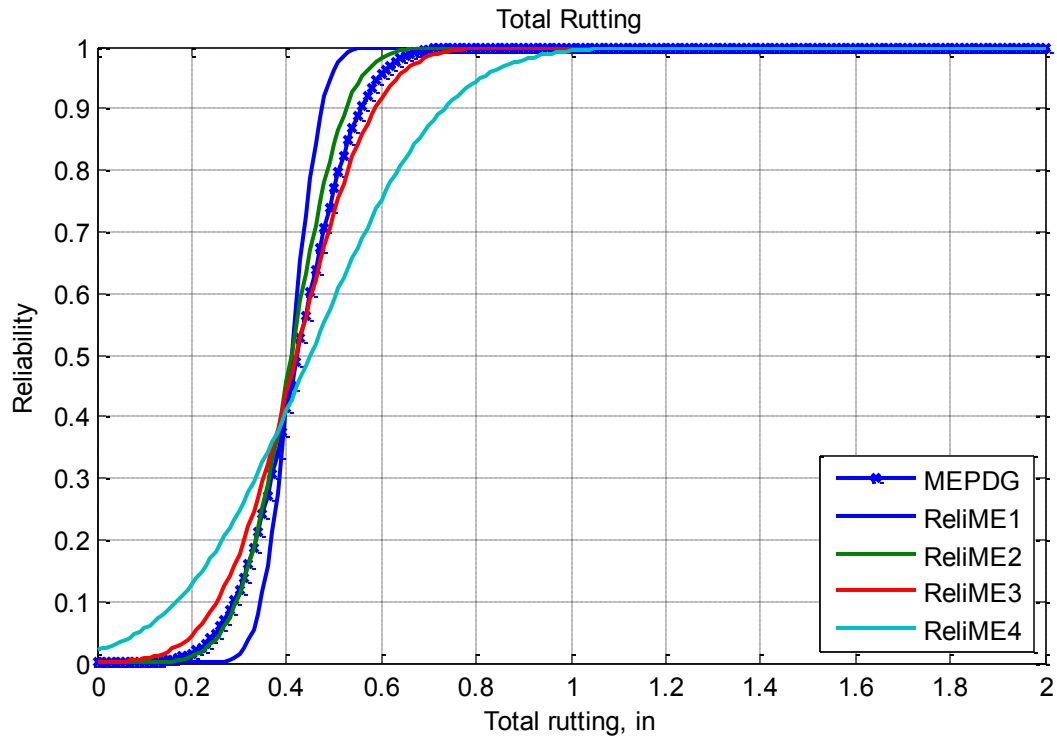


Figure 6.35 Reliability of total rutting for Sheridan Bypass

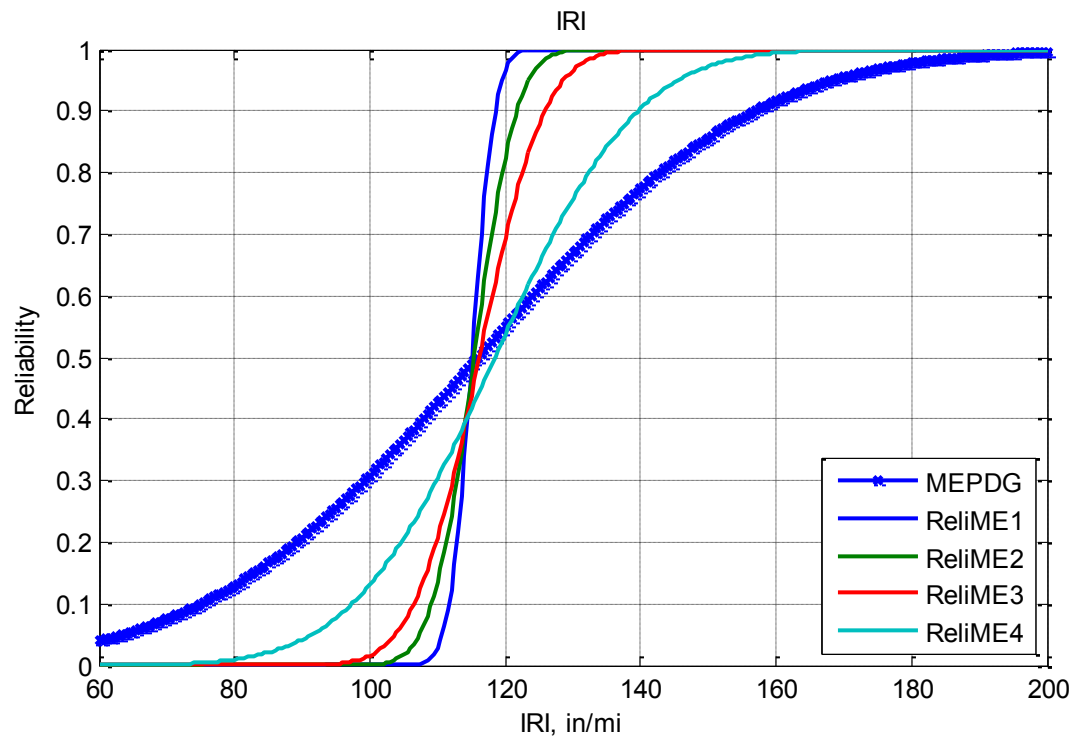


Figure 6.36 Reliability of IRI for Sheridan Bypass

6.5 Summary

The proposed reliability analysis method is illustrated in the development and application of *ReliME*, which provides designers a statistically sound estimate of design reliability for each flexible pavement distress prediction, based on user-supplied estimates of the mean value and variability of critical design inputs. The procedure of Monte Carlo simulation, software coding, testing are presented in this chapter.

The *ReliME* analysis is dynamic; the user may change the mean value and/or variation of any design variable and see the effect on design reliability almost instantaneously. This allows the designer to manually optimize a given design with respect to the reliability of each of the distress predictions. It also allows the designer to gauge the effect of changes – i.e. differences in pavement properties stemming from construction, compared to design values – on design reliability. As intended for the hierarchical input system, Level 1 inputs provide a higher reliability than Level 3 inputs do because the variation is reduced by conducting site-specific tests. Therefore, *ReliME* may also provide a powerful communication tool to demonstrate to designers, materials engineers, and construction personnel the effect of variability on design reliability.

Three case studies on the Bella Vista Bypass, Pleasant Plains Bypass and Sheridan Bypass using AASHTO 1993, MEPDG and *ReliME* are conducted. By simulating the MEPDG and four variance levels in *ReliME*, the cumulative density distribution of reliability is compared. As summarized in Table 6.9, the variation of alligator cracking and total rutting in MEPDG is mostly between the medium level and high level of variation. The smoothness IRI model in MEPDG, however, has an extremely large variance. Overall the total rutting model of MEPDG has the smallest variation and matches well with the *ReliME* estimation.

Table 6.9 Summary of Variance Comparison

Cases	ESALs	Alligator Cracking	Total Rutting	IRI
Bella Vista Bypass	15,748,053	ReliME3 ~ ReliME4	ReliME2	ReliME3 ~ ReliME4
Pleasant Plains Bypass	5,330,612	ReliME4 +	ReliME3	ReliME4 +
Sheridan Bypass	6,516,969	ReliME3 ~ ReliME4	ReliME2 ~ ReliME3	ReliME4 +

One should note that the development of *ReliME* is not intended to replace MEPDG for pavement design. The prediction on alligator cracking and IRI does not match well with the MEPDG. This limitation is due to the model construction and limited sampling. The purpose of *ReliME* is to illustrate the possibility of using Monte Carlo Simulation for true reliability analysis. As computing technology advances, it will be possible to conduct MCS without developing surrogate models. The result will most likely surpass the current MEPDG and the *ReliME*.

CHAPTER 7 CONCLUSIONS AND RECOMMENDATIONS

7.1 Conclusions

This research proposed a framework to improve the reliability model for probabilistic pavement design. The following conclusions were reached:

- 1) Local calibration was not only recommended by MEPDG to reduce bias and variation, it could also be the basis for building state-specific reliability models. The procedure for local calibration of the MEPDG using LTPP and PMS data in Arkansas was established. Alligator cracking model and total rutting model were calibrated to Arkansas' condition. Longitudinal cracking and thermal cracking were rarely predicted by MEPDG but some observations existed. For this reason, longitudinal cracking and thermal cracking model were not calibrated at this time.
- 2) Risk analysis and assessment could be applied to understand uncertainty in pavement design, and then increase the reliability of the design process. Using Holographic Hierarchical Modeling (HHM) and Analytical Hierarchical Process (AHP), pavement design was inspected in a great detail. In total 75 factors were compared and ranked to identify critical parameters. It was worthwhile strengthening the difference between this study and sensitivity analysis: risk assessment was a subjective examination out of the design software; however, sensitivity analysis was to understand how the software reacts to a change of input.
- 3) In the context of current technology, surrogate models such as neural network and response surface models can be a viable method to bypass the hinder for extensive computing time. In general, second-order response surface models had a good accuracy

for alligator cracking, total rutting and smoothness. Among these, the alligator cracking model required more attention due to its extreme nonlinearity.

- 4) Using central composite design and random sampling, 6,561 experiments for factorial design were reduced to 374 experiments to develop a database to build surrogate models which involved seven probabilistic variables: initial AADTT, HMA layer thickness, effective binder content, air voids, base layer thickness, resilient modulus of base material, and resilient modulus of subgrade. Climate location was found not sensitive to the climatic difference across Arkansas. Traffic speed was insignificant for arterial highways because MEPDG was not sensitive to speed if it was over 25 mph.
- 5) In short, the proposed reliability method was “probabilistic design based on Monte Carlo simulation of response surface models”. This concept was illustrated by developing a software tool named *ReliME* which included collecting inputs, generating random samples, conducting MCS, and calculating reliability. With a user interface, designers could easily evaluate a preliminary design and, particularly, investigate the influence of individual variation on pavement design.
- 6) Comparison of AASHTO 1993, MEPDG and *ReliME* revealed that the alligator cracking and rutting model in MEPDG had a moderate level of variability. But the smoothness IRI model had an extremely high level of variability. In other words, based on this study, MEPDG was more conservative than *ReliME* was.
- 7) The framework of *ReliME* could be easily applied to other states since it only required several hundred MEPDG simulations. However, it was not intended to replace MEPDG for pavement design. Limitations of *ReliME* included the limited number of

probabilistic variables, possible loss of accuracy due to surrogate models, and the difficulty of benchmarking with MEPDG variation assumptions.

- 8) It must be noted that *ReliME* was a state specific toolkit based on locally-calibrated MEPDG simulations. The framework illustrated in this study was promising for other states (i.e. *ReliME-TX*) because it only took about 500 MEPDG runs to build and validate, which was practically tangible. On the national level, this study demonstrated the feasibility of probability design using Monte Carlo simulation. This could be an option to be incorporated into future mechanistic empirical pavement design software.

7.2 Recommendations

Probabilistic mechanistic empirical pavement design that considers uncertainty, variability and other risks had been a challenge for pavement engineers. This research along with other studies such as Darter (6), Timm (20), Thyagarajan (94) and Retherford (95) were only preliminary trials in this direction. Limitations of this study, lessons learned during this dissertation and suggestions for future research are as follows:

- 1) The availability and quality of design, materials, construction, and performance data are critical for local calibration. It is likely that states like Arkansas will need to establish additional calibration sites to supplement available LTPP and PMS data. Another possible direction may be to redefine PMS, which is traditionally designed for network level management, to also serve the purpose of project level management. This will demand more specific data collection, storage and analysis. Fortunately this should be viable if the construction data for quality control and quality assurance purposes were included in future PMS. Future PMS may also be designed with calibration application

in mind. By doing this, an interface might be available to “plug” the data into design models and update the calibration coefficients for local conditions.

- 2) The difference in defining transverse cracking between the MEPDG and LTPP may be critical in terms of data collection and identification. Thermal cracking should be specifically identified in a transverse cracking survey to calibrate the transverse cracking model in MEPDG. Considering the difficulty of distress survey with mechanism included, this may remain a challenge for many years to come.
- 3) Local calibration is a straightforward but time consuming process. Integration of databases from different divisions in a state highway agency using advanced information technology and Geographic Information System (GIS) is highly recommended to reduce the effort for data preparation.
- 4) The risk assessment based on pairwise comparison might provide important information from experts and engineers. However it is a very time consuming process. This study was only based on limited respondents. A wider range survey and analysis is recommended to better justify the ranking of critical factors and avoid personal bias. Such a successful national survey might incubate a new generation pavement design method.
- 5) The main reason to develop surrogate models in this research was to bypass the extensive computing time of conducting Monte Carlo simulation on the MEPDG software. However, there is another solution without sacrificing the accuracy of MEPDG. That is to use a supercomputer or parallel computing, which has been widely used in other fields such as physics, climate research, structural analysis and molecular modeling. A trial to run MEPDG on a supercomputer was made but failed in this study

due to the fact that the MEPDG software was not coded for parallel computing. In the meantime, finite element analysis software such as ABAQUS and ANSYS are capable of running on supercomputers. As the computer technology advances, the era of using parallel computing in a state highway agency and a design company is in the foreseeable future. The future development of mechanistic empirical pavement design software shall be aware of the potential of computing power, just as how the born of ENIAC, the first electronic computer, triggered the invention of the Monte Carlo method.

6) Limitations of *ReliME* include

- (1) a limited number of probabilistic variable. Future research could explore other approaches (i.e. artificial neural network) that can build surrogate models with more inputs.
- (2) design space only works for projects within the space. Some projects may not perform very well due to extrapolation.
- (3) possible accuracy loss due to surrogate models.
- (4) traffic is represented by ESALs, which is a aggregated value of load spectra.

Investigating the detail of traffic inputs is another challenging work.

7) To use *ReliME*, both the nominal value and the variation of each design parameter are required. However, variation has only been slightly used in quality control and assurance so far. Research on collecting, documenting and analyzing variation data for probabilistic design is needed.

7.3 Byproducts

Pavement design heavily relies on modeling in the mechanistic-empirical era. Pavement modeling however is a complicated process because it integrates most, if not all, of the aspects in pavement engineering. During this research, some other related studies were also conducted, which are summarized here as four byproducts.

7.3.1 Distress Classification

The predicted distress did not match well with measured distress in the local calibration of MEPDG for Arkansas. This intrigued this study to investigate closely on the definition of each distress type in MEPDG, and its corresponding definition in LTPP.

During this study, different distress protocols were reviewed, especially LTPP and MEPDG. Issues about definition mismatch between MEPDG and LTPP were identified and discussed. It was found that LTPP was designed for general pavement management purposes, without consideration of the mechanism of each distress. On the contrary, MEPDG had to rely on mechanism of distresses to predict pavement performance. This could be an important factor that led to the mismatch of distress definitions.

It was suggested to consider longitudinal cracking in wheelpath as the beginning phase of alligator cracking. A new category of longitudinal cracking called between wheelpath longitudinal cracking was recommended for future LTPP data collection. Current data of longitudinal cracking out of wheelpath could not be used to calibrate the longitudinal cracking in MEPDG.

No strong evidence was found to vote for or against the weighting of low, medium and high severity distresses to calibrate alligator cracking, longitudinal cracking and transverse cracking. Expert judgment can be hold as true.

The influence of wheelpath width and location was suggested to be investigated in the future.

7.3.2 Arkansas' Long Term Pavement Performance Program

Project named the TOP 25, which was initiated in March 2002 to validate the SuperPave[®] mix design method in Arkansas, provided an important database for engineers to understand not only the new mix design method but also other issues related to pavement technologies in Arkansas. Moreover, the database served as the backbone to conduct the local calibration of the MEPDG.

In the era of mechanistic-empirical design, it is anticipated that national models will be updated and calibrated from time to time. Therefore, a statewide long term pavement performance program is of great importance. Such a program will also be beneficial for other purposes including validating new materials, new construction techniques, pilot study of new data collection equipment, evaluation of pavement management systems, etc.

The new project, following the TOP 25 project, is named the NEXT 25. In total 25 pavement sections will selected to cover all climatic districts, and contain all main pavement structures and materials used in Arkansas. Each section is 500 ft long to be consistent with LTPP. Only new flexible pavements are investigated in this project. Rehabilitations (i.e. overlay) will be studied separately under another project in the future.

In the new project, guidelines and manuals will be developed to guide the collection and storage of data in a uniform and consistent way. The data collection will be guided by the requirement of MEPDG, and the new production-level software DARWin-ME.

7.3.3 Accuracy Requirement for Thickness Estimation

Accurate estimates of existing pavement layer thickness are considered critical for pavement evaluation. Layer thickness data is used in assessments throughout the life-cycle of the pavement

structure, including construction quality control/quality assurance (QC/QA), prediction of remaining life, network-level pavement management, backcalculation of layer moduli, and overlay design. Inevitably, a constructed pavement layer will vary in thickness.

Layer thickness is traditionally assessed by drilling cores from the pavement, which is destructive, slow, expensive, and provides only limited coverage of the project or network. Nondestructive testing (NDT) techniques have been developed to replace coring, such as ultrasonic gauge, ground penetrating radar (GPR), and spectral analysis of seismic waves (SASW). However, the accuracy of these methods can be variable. For example, the accuracy of GPR is reported as being 3-5% for new asphalt pavement, 5-10% for existing asphalt pavement, 5-10% for concrete and 8-15% for the granular base (96). Accuracy may even be project or site-specific.

Although it is always worthy pursuing a higher accuracy level, a question was asked during the analysis of uncertainty and variation: what level of accuracy of the estimated layer thickness is needed for a particular application, regardless of the NDT technique being used? Or, is it necessary to invest heavily to achieve a 1% accuracy increase? What is the influence of measurement accuracy on pavement reliability? To illustrate this concept, four typical applications requiring layer thickness were discussed: construction QC/QA, pavement layer moduli backcalculation, determination of remaining life, and overlay design. Table 7.1 summarizes the observations related to these applications.

A prime topic for discussion within any pavement agency considering implementation of NDT-based pavement thickness estimation equipment and techniques must center on their application. Certainly, a tendency is to obtain the ‘best’ (i.e. most accurate, perhaps implying the

most expensive) system available; however, given the economic conditions faced by most agencies, the most accurate system may not be the ‘best’ system for the agency.

Table 7.1 Summary of Findings/Observations for layer thickness accuracy requirement

Application	Degree of Sensitivity to Pavement Layer Thickness (%)	Comments
Construction Quality Control / Quality Assurance	HIGH Desired Accuracy: 2.5 – 5 %	Final pavement thickness is typically a pay item for construction; increased accuracy is required to limit risk to both agency and contractor.
Pavement Layer Modulus Estimation	MODERATE Desired Accuracy: ~ 5%	Variations in layer thickness result in variations in backcalculated moduli. The ‘final’ effect is a function of the system used to forward-calculate stress/strain (using the estimated moduli) and the specific transfer functions to relate stress/strain to pavement performance.
Estimation of Remaining Service Life	LOW Desired Accuracy: ~ 10% (?)	Current AASHTO-based remaining life estimation procedures are not sensitive to the thickness of the existing pavement.
Overlay Design	LOW Desired Accuracy: ~ 10% (?)	Current empirical and mechanistic-empirical overlay design procedures do not show significant sensitivity to the thickness of the existing pavement. As overlay design procedures continue to evolve, however, the issue should be revisited.

7.3.4 Integration of Pavement Management and Design

Traditionally, the primary goal of pavement management is to monitor the condition of pavement and to provide recommendations for maintenance scheduling. Meanwhile, pavement design is based on representative material properties and empirical design equations. Division of pavement management and division of design in a state highway agency rarely shared information. This

dilemma can be changed after implementing the Mechanistic Empirical Pavement Design Guide (MEPDG), through which pavement design and management are integrated.

As shown in Figure 7.1, white arrows represent the current state of practice. Different divisions in a state highway agency take charge of their assigned responsibility in the assembly line. Every individual division has its own internal management (IM) which may involve administrative records and/or database. The output from Plan Division is submitted to Design Division. The output from Design Division is then submitted to Construction Division. After a road is completed and opened to traffic, Maintenance Division takes over. During this time, Management Division may conduct performance monitoring from time to time. Maintenance Division may request recommendations for maintenance schedule from Management Division, or maintenance operation may only rely on engineer's judgment and experience.

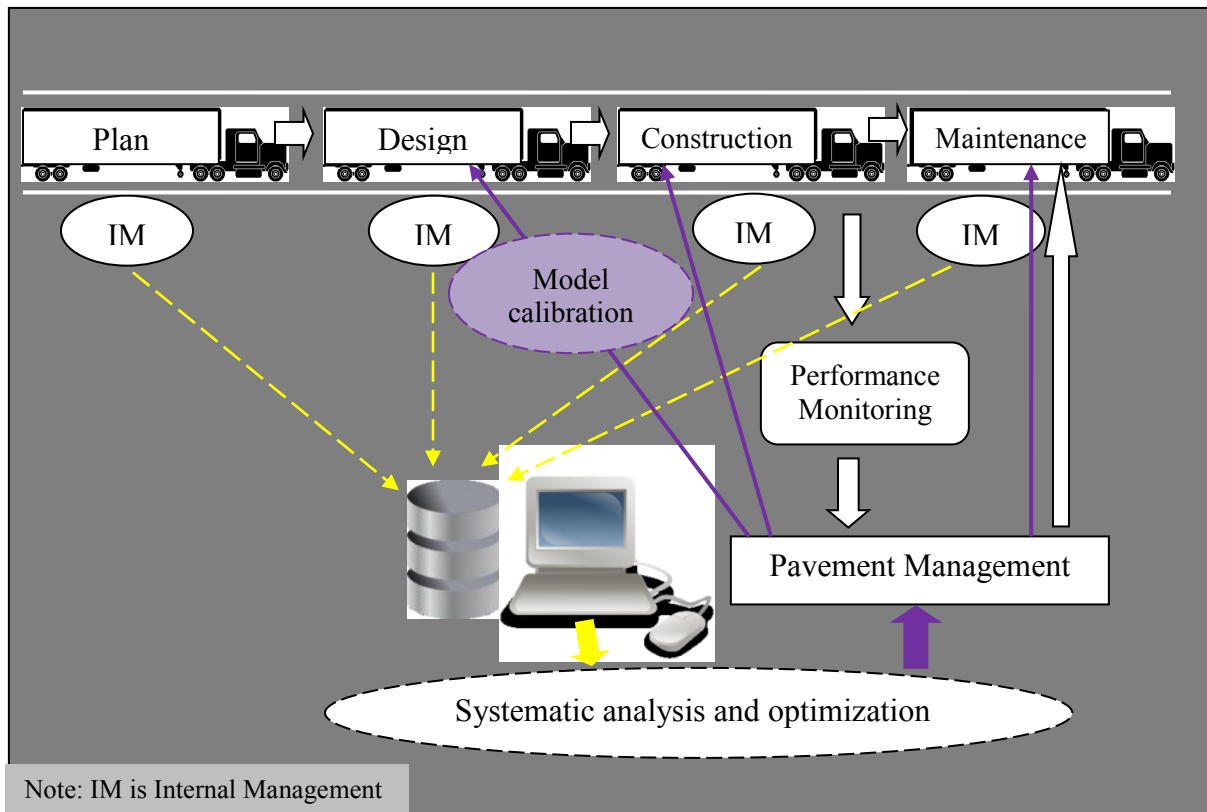


Figure 7.1 Integration of management and design.

Arrows in yellow and purple color are proposed future improvements. First of all, data from individual divisions should be shared with pavement management. Engineers should understand that pavement management is not only performance monitoring but also project-level data management and systematic analysis. Only are complete and accurate data available, could pavement management develop valuable and reliable recommendations. Fortunately, the need for data share has already been advocated, and state highway agencies are starting the integration of different database into one platform. There are also vendor-developed software solutions for systematic analysis and optimization using advanced mathematical methods. Quantum growth is expected when such a pavement management system is populated with reliable data.

The other solution to integrate management and design is by model development and/or calibration. To most extent, design is a process that applies successful experience on new cases. Design methods are mainly, if not all, derived from historical observations, which are the Pavement Management System. Therefore, development and calibration of models using data from management systems are naturally straightforward.

REFERENCES

1. Ceylan, H., Coree, B. J. and Gopalakrishnan, K. Evaluation of the Mechanistic-Empirical Pavement Design Guide for Implementation in Iowa. *Baltic Journal of Road and Bridge Engineering*, Volume 4, Issue 1, 2009, pp. 5-12.
2. Mehta, Y. A., Sauber, R. W., Owad, J., Krause, J. *Lessons Learned During Implementation of Mechanistic-Empirical Pavement Design Guide*. Transportation Research Board Annual Meeting. Washington D.C.: Transportation Research Board, 2008.
3. Wang, K., Hall, K., Li, Q., Nguyen, V. and Gong, W. *Database Support for the Mechanistic-Empirical Pavement Design Guide (MEPDG)*. Fayetteville, AR: University of Arkansas, 2009.
4. Von Quintus, H. L. and Moulthrop, J. S. *Mechanistic-Empirical Pavement Design Guide Flexible Pavement Performance Prediction Models*. Montana Department of Transportation, Helena MT., 2007.
5. ARA, Inc., ERES Consultants Division. *Guide for Mechanistic-Empirical Design of New and Rehabilitated Pavement Structures. Final Report. Part 1. Introduction. Chapter 1. Background, Scope and Overview*. Washington D.C. : National Cooperative Highway Research Program, 2004. pp. 12.
6. Darter, M., Khazanovich, L., Yu, T. and Mallela, J. Reliability Analysis of Cracking and Faulting Prediction in the New Mechanistic-Empirical Pavement Design Procedure. In *Transportation Research Record: Journal of the Transportation Research Board* No.1936, Transportation Research Board of the National Academies, Washington, D.C., 2005, pp. 150-160.
7. AASHTO. *AASHTO Guide for Design of Pavement Structures*. American Association for State Highway and Transportation Officials, Washington D.C., 1993.
8. Federal Highway Administration (FHWA). Design Guide Implementation Survey. <http://www.fhwa.dot.gov/pavement/dgit/dgitsurv.cfm>. Accessed April 1, 2011.
9. Tompson, M. R. Mechanistic-Empirical Flexible Pavement Design: An Overview. In *Transportation Research Record: Journal of the Transportation Research Board*, No. 1539, Transportation Research Board of the National Academies, Washington, D.C., 1996, pp. 1-5.
10. Mechanistic Pavement Design. *Supplement to Section 7 of the Illinois Department of Transportation Design Manual*. Springfield, IL., 1989.
11. WSDOT. WSDOT Pavement Guide. <http://training.ce.washington.edu/WSDOT/>. Accessed April 1, 2011.

12. MnDOT. MnPave Home. <http://www.dot.state.mn.us/app/mnpave/index.html>. Accessed April 1, 2011.
13. ARA, Inc., ERES Consultants Diviison. MEPDG Guide. *NCHRP 1-37A Design Guide*. <http://onlinepubs.trb.org/onlinepubs/archive/mepdg/guide.htm>. Accessed Sep. 12, 2009.
14. ARA, Inc., ERES Division. *Guide for Mechanistic-Empirical Design of New and Rehabilitated Pavement Structures. Appendix BB: Design Reliability*. Washington D.C. : National Cooperative Highway Research Program, 2003.
15. Huang, Yang H. *Pavement Analysis and Design*. Prentice Hall, Upper Saddle River, NJ., 1993.
16. Von Quintus, H. L., Darter, M. and Mallela, J. *Recommended Practice for Local Calibration of the ME Pavement Design Guide*. Applied Research Associates, Inc.- Transportation Sector, Round Rock, Texas, 2009.
17. Kher, R. K. and Darter, M. I. Probabilistic concepts and their applications to AASHTO interim guide for design of rigid pavements. *Highway Research Record 466*. 1973, pp. 20-36.
18. Darter, M. I., McCullough, B. F. and Brown, J. L. Statistical variations of flexible pavement properties an their consideration in design. *Association of Asphalt Paving technologists*. 1973, pp. 589-613.
19. Jiang, Y. J., Selezneva, O., Mladenovic, G., Aref, S. and Darter, M. Estimation of pavement layer thickness variability for reliability-based design. In *Transportation Research Record: Journal of the Transportation Research Board*, No. 1849, Transportation Research Board of the National Academies, Washington, D.C., 2003, pp. 156-165.
20. Timm, D. H., Newcomb, D. E. and Galambos, T. V. Incorporation of reliability into Mechanistic-Empirical pavement design. In *Transportation Research Record: Journal of the Transportation Research Board*, No. 1730, Transportation Research Board of the National Academies, Washington, D.C., 2000, pp. 73-80.
21. Collop, Andrew, Armitage, Robert and Thom, Nicholas. Assessing variability of in situ pavement material stiffness moduli. *Journal of Transportation Engineering*, Vol. 127, No. 1, 2001, pp. 74 - 81.
22. Tayabji, S. and Wu, C. Variability of concrete materials data in Long-Term Pavement Performance program. In *Transportation Research Record: Journal of the Transportation Research Board*, No. 1813. Transportation Research Board of the National Academies, Washington, D.C., 2002, pp. 181 - 190.

23. Turochy, R., Baker, S. M. and Timm, D. Spatial and Temporal Variations in Axle Load Spectra and Impacts on Pavement Design. *Journal of Transportation Engineering*. Vol. 131, 2005, pp. 802-808.
24. Tan, W. and Von Quintus, H. Use of Long-Term Pavement Performance Data to Develop Traffic Defaults in Support of Mechanistic– Empirical Pavement Design Procedures. In *Transportation Research Record: Journal of the Transportation Research Board*, No.1855. Transportation Research Board of the National Academies, Washington, D.C., 2003, pp. 176–182.
25. Johanneck, L. and Khazanovich, L. Comprehensive Evaluation of Effect of Climate in Mechanistic-Empirical Pavement Design Guide Predictions. In *Transportation Research Record: Journal of the Transportation Research Board*, No. 2170, Transportation Research Board of the National Academies, Washington, D.C., 2010, pp. 45-55.
26. Li, Q., Mills, L. and McNeil, S. *The Implications of Climate Change on Pavement Performance and Design*. Newark, DE : University of Delaware University Transportation Center, 2011.
27. Rada, G., Wu, C., Elkins, G., Bhandari, R. and Bellinger, W. Update of Long-Term Pavement Performance Manual Distress Data Variability: Bias and Precision. In *Transportation Research Record: Journal of the Transportation Research Board*, No. 1643, Transportation Research Board of the National Academies, Washington, D.C., 1998, pp. 71-79.
28. Selezneva, O., Darter, M., Zollinger, D. and Shoukry, S. Characterization of Transverse Cracking Spatial Variability: Use of Long-Term Pavement Performance Data for Continuously Reinforced Concrete Pavement Design. In *Transportation Research Record: Journal of the Transportation Research Board*, No. 1849. Transportation Research Board of the National Academies, Washington, D.C., 2003, pp. 147-155.
29. Kohler, E. and Roesler, J. Nondestructive Testing for Crack Width and Variability on Continuously Reinforced Concrete Pavements. *Transportation Research Record: Journal of the Transportation Research Board*, No. 1974, Transportation Research Board of the National Academies, Washington, D.C., 2006, pp. 89–96.
30. Ramakumar, R. *Engineering reliability: fundamentals and applications*. Prentice-Hall, Inc., Englewood Cliffs, New Jersey, 1993.
31. Harr, M. E. *Reliability-based design in civil engineering*. McGraw-Hill, Inc., New York, 1987.
32. Carter, A.D.S. *Mechanical Reliability and Design*. John Wiley & Sons, Inc., New York, 1997.

33. Zhang, Z. and Damjanovic, I. Applying method of moments to model reliability of pavements infrastructure. *Journal of Transportation Engineering*. Vol. 132, No. 5, 2006, pp. 416-424.
34. Ayyub, B. M. and Klir, G. J. *Uncertainty Modeling and Analysis in Engineering and the Sciences*. Chapman & Hall/CRC, Boca Raton, FL., 2006.
35. Metropolis, N. The Beginning of the Monte Carlo Method. *Los Alamos Science Special Issue*. 1987, pp. 125-130.
36. Metropolis, N. and Ulam, S. The Monte Carlo Method. *Journal of the American Statistical Association*, 1949, pp. 335-341.
37. Rubinstein, R. *Simulation and the Monte Carlo method*. John Wiley & Sons, Inc., New York, 1981.
38. Kang, M. and Adams, T. M. *Local calibration for fatigue cracking models used in the Mechanistic-Empirical Pavement Design Guide*. Proceedings of the 2007 Mid-Continent Transportation Research Symposium. Ames, Iowa : Iowa State University, 2007.
39. Fernando, E., Oh, J. and Ryu, D. *Phase I of MEPDG Program Implementation in Florida*. Florida Department of Transportation, Tallahassee, FL., 2007.
40. Muthadi, N. R. and Kim, R. Y. Local Calibration of Mechanistic–Empirical Pavement Design Guide for Flexible Pavement Design. In *Transportation Research Record: Journal of the Transportation Research Board*, No. 2087, Transportation Research Board of the National Academies, Washington, D.C., 2008, pp. 131–141.
41. Banerjee, A., Aguiar-Moya, J. P. and Prozzi, J. A. *Texas experience using LTPP for calibration of the MEPDG permanent deformation models*. Transportation Research Board Annual Meeting. Washington D.C., 2009.
42. Velasquez, R., Hoegh, K., Yut, I., Funk, N., Cochran, G., Marasteanu, M. and Khazanovich, L. *Implementation of the MEPDG for New and Rehabilitated Pavement Structures for Design of Concrete and Asphalt Pavements in Minnesota*. Minnesota Department of Transportation, St. Paul, Minnesota, 2009.
43. Mallela, J., Glover, L. T., Darter, M. I., Von Quintus, H., Gotlif, A., Stanley, M. and Sadasivam, S. *Guidelines for Implementing NCHRP 1-37A M-E Design Procedures in Ohio: Volume 1— Summary of Findings, Implementation Plan, and Next Steps*. Ohio Department of Transportation, Columbus, Ohio, 2009.
44. ARA, Inc., ERES Division. *Guide for Mechanistic-Empirical Design of new and rehabilitated pavement structures, Appendix II: Calibration of fatigue cracking models for flexible pavements*. Washington D.C. : National Cooperative Highway Research Program, 2004. pp. 50.

45. Rada, G. R., Bhandari, R. K., Elkins, G. E and; Bellinger, W. Y. Assessment of Long-Term Pavement Performance Program Manual Distress Data Variability: Bias and Precision. In *Transportation Research Record: Journal of the Transportation Research Board*, No. 1592, Transportation Research Board of the National Academies, Washington, D.C., 1997, pp. 151-168.
46. Schwartz, C. W. Implications of Uncertainty in Distress Measurement for Calibration of Mechanistic–Empirical Performance Models. In *Transportation Research Record: Journal of the Transportation Research Board*, No. 2037, Transportation Research Board of the National Academies, Washington, D.C., 2007, pp. 136–142.
47. Wang, K., Hou, Z. and Williams, S. Precision Test of Cracking Surveys with the Automated Distress Analyzer. *Journal of Transportation Engineering*, Vol. 137, No. 8, 2011, pp. 571–579.
48. Miller, J. S. and Bellinger, W. Y. *Distress Identification Manual for the Long-Term Pavement Performance Program*. Washington D.C.: Federal Highway Administration, 2003.
49. Federal Highway Administration. Status of the Nation's Highways, Bridges, and Transit: Conditions and Performance. <http://www.fhwa.dot.gov/policy/2008cpr/es.htm#c3a>. Accessed Nov. 22, 2010.
50. Flyvbjerg, B., Holm, M. S. and Buhl, S. Underestimating costs in public works projects: Error or lie? *Journal of the American Planning Association*, 2002, pp. 279-295.
51. Molenaar, K., Anderson, S. and Schexnayder, C. *NCHRP Report 658: Guidebook on Risk Analysis Tools and Management Practices to Control Transportation Project Costs*. Transportation Research Board, Washington D.C., 2008.
52. Modarres, M. *Risk Analysis in Engineering: Techniques, Tools, and Trends*. Taylor & Francis Group, Boca Raton, FL., 2006.
53. Elias, A. M. and Herbsman, Z. J. Risk Analysis Techniques for Safety Evaluation of Highway Work Zones. In *Transportation Research Record: Journal of Transportation Research Board*, No. 1715, Transportation Research Board of the National Academies, Washington, D.C., 2000, pp. 10-17.
54. Walls, J. and Smith, M. R. *Life-Cycle Cost Analysis in Pavement Design -Interim Technical Bulletin*. Federal Highway Administration, Washington, D.C., 1998.
55. Caltrans. *Project Risk Management Handbook: Threats and Opportunities*. Office of Statewide Project Management Improvement, Sacramento, CA., 2007.

56. Damnjanovic, I. and Zhang, Z.. Risk-Based Model for Valuation of Performance-Specified Pavement Maintenance Contracts. *Journal of Construction Engineering and Management*, 2008, pp. 492-500.
57. Kim, S., Ceylan, H. and Heitzman, M. *Sensitivity Study of Design Input Parameters for Two Flexible Pavement Systems Using the Mechanistic-Empirical Pavement Design Guide*. Proceedings of the 2005 Mid-Continent Transportation Research Symposium. Ames, Iowa : Iowa State University, 2005.
58. Graves, R. C. and Mahboub, K. C. Pilot Study in Sampling-Based Sensitivity Analysis of NCHRP Design Guide for Flexible Pavements. In *Transportation Research Record: Journal of the Transportation Research Board*, No.1947. Transportation Research Board of the National Academies, Washington, D.C., 2006, pp. 123-135.
59. Tran, N. and Hall, K. D. Development and influence of statewide axle load spectra an flexible pavement performance. In *Transportation Research Record: Journal of the Transportation Research Board*, No. 2037, Transportation Research Board of the National Academies, Washington, D.C., 2007, pp. 106-114.
60. Sayyady, F., Stone, J. R., Taylor, K. L., Jadoun, F. M. and Kim, Y. R. Clustering Analysis to Characterize Mechanistic–Empirical Pavement Design Guide Traffic Data in North Carolina. In *Transportation Research Record: Journal of the Transportation Research Board*, No. 2160, Transportation Research Board of the National Academies, Washington, D.C., 2010, pp. 118–127.
61. Li, J., Pierce, L. M., Hallenbeck, M. E. and Uhlmeyer, J. Sensitivity of Axle Load Spectra in the Mechanistic–Empirical Pavement Design Guide for Washington State. In *Transportation Research Record: Journal of the Transportation Research Board*, No. 2093, Transportation Research Board of the National Academies, Washington, D.C., 2009, pp. 50–56.
62. Buch, N., Chatti, K., Haider, S. W. and Manik, A. *Evaluation of the I-37A Design Process for New and Rehabilitated JPCP and HMA Pavements*. Michigan Department of Transportation, Lansing, MI., 2008.
63. Maher, A. and Bennert, T. *Evaluation of Poisson’s Ratio for Use in the Mechanistic Empirical Pavement Design Guide (MEPDG)*. New Jersey Department of Transportation, Trenton, NJ., 2008.
64. Schwartz, C. W., Li, R., Kim, S. H. and Ceylan, H. *NCHRP 1-47 Final Report: Sensitivity Evaluation of MEPDG Performance Prediction*. Transportation Research Board, Washington D.C., 2011.
65. Haimes, Y. Y. *Risk Modeling, Assessment, and Management*. John Wiley & Sons, Inc., New York, 1998.

66. Saaty, T. L. *The Analytic Hierarchy Process*. McGraw-Hill, New York, 1980.
67. Smith, J. T. and Tighe, S. L. Analytic Hierarchy Process as a Tool for Infrastructure Management. In *Transportation Research Record: Journal of the Transportation Research Board*, No. 1974, Transportation Research Board of the National Academies, Washington, D.C., 2006, pp. 3-9.
68. Wu, Z., Flintsch, G. W. and Chowdhury, T. Hybrid Multiobjective Optimization Model for Regional Pavement-Preservation Resource Allocation. In *Transportation Research Record: Journal of the Transportation Research Board*, No. 2084, Transportation Research Board of the National Academies, Washington, D.C., 2008, pp. 28-37.
69. Farhan, J. and Fwa, T. F. Pavement Maintenance Prioritization Using Analytic Hierarchy Process. In *Transportation Research Record: Journal of the Transportation Research Board*, No. 2093, Transportation Research Board of the National Academies, Washington, D.C., 2009, pp. 12-24.
70. Guo, D., Zhou, W., Sha, A. and Bai, R. Application of Uncertainty Analytic Hierarchy Process Method for Asphalt Pavement Construction Quality Control in China. In *Transportation Research Record: Journal of the Transportation Research Board*, No. 2098, Transportation Research Board of the National Academies, Washington, D.C., 2009, pp. 43-50.
71. Orobio, A. *Sensitivity Analysis of Flexible Pavement Performance Parameters in the Mechanistic-Empirical Design Guide*. PhD Dissertation. Morgantown, WV: West Virginia University, 2010.
72. ARA, Inc., ERES Division. *Guide for Mechanistic-Empirical Design of new and rehabilitated pavement structures, Appendix QQ: structural response models for rigid pavements*. Champaign, IL: National Cooperative Highway Research Program, 2003. pp. 37-73.
73. Myers, R. H., Montgomery, D. C. and Anderson-Cook, C. M. *Response Surface Methodology: Process and Product Optimization Using Designed Experiments, Third Edition*. John Wiley & Sons, Inc., Hoboken, NJ., 2009.
74. El-Basyouny, M. and Jeong, M. G. Effective Temperature for Analysis of Permanent Deformation and Fatigue Distress on Asphalt Mixtures. In *Transportation Research Record: Journal of the Transportation Research Board*, No. 2127, Transportation Research Board of the National Academies, Washington, D.C., 2009, pp. 155-163.
75. Montgomery, D. C. *Design and Analysis of Experiments (7th Edition)*. John Wiley & Sons, Inc., Hoboken, NJ., 2009.
76. Nguyen, V. *Traffic Data Modeling for Pavement Design*. PhD Dissertation. Fayetteville, AR: University of Arkansas, 2011.

77. Thyagarajan, S, Muhunthan, B., Sivaneswaran, N. and Petros, K. Efficient simulation Techniques for Reliability Analysis of Flexible Pavements using the Mechanistic-Empirical Pavement Design Guide. *Journal of Transportation Engineering*, Vol. 137, 2011, pp. 796-804.
78. Tran, N. H. and Hall, K. D. *Projected Traffic Loading for Mechanistic-Empirical Pavement Design Guide, TRC-0402 Final Report*. Fayetteville, Arkansas: University of Arkansas, 2006.
79. SAS Institute Inc. *JMP 9 Modeling and Multivariate Methods*. Cary, NC., 2009.
80. Byram, D., Xiao, D., Wang, K. and Hall, K. *Sensitivity Analysis of Climatic Influence on MEPDG Flexible Pavement Performance Predictions*. Transportation Research Board Annual Meeting. Washington D.C., 2012.
81. Sumeet, N. *Sensitivity of MEPDG Using Advanced Statistical Analyses*, Master Thesis. Albuquerque, New Mexico: University of New Mexico, 2010.
82. El-Badawy, S. M., Jeong, M. G. and El-Basyouny, M. Methodology to Predict Alligator Fatigue Cracking Distress Based on Asphalt Concrete Dynamic Modulus. In *Transportation Research Record: Journal of the Transportation Research Board*, No. 2095, Transportation Research Board of the National Academies, Washington, D.C., 2009, pp. 115-124.
83. Li, Q., Xiao, D., Wang, K., Hall, K. D. and Qiu, Y. Mechanistic-empirical pavement design guide (MEPDG): a bird's-eye view. *Journal of Modern Transportation*, Vol. 19, 2011, pp. 114-133.
84. Li, Q., Xiao, D. and Hall, K. D. Mechanistic–Empirical Pavement Design Guide –Based Pavement Design Catalog for Low-Volume Roads in Arkansas. In *Transportation Research Record: Journal of the Transportation Research Board*, No. 2203, Transportation Research Board of the National Academies, Washington, D.C., 2011, pp. 169–177.
85. Grubbs, F.E. Procedures for detecting outlying observations in samples. *Technometrics* Vol. 11, 1969, pp. 1-21.
86. Myers, R. H., Montgomery, D. C. and Anderson-Cook, C. M. *Response Surface Methodology: Process and Product Optimization Using Designed Experiments, Third Edition*. John Wiley & Sons, Inc., Hoboken, NJ., 2009.
87. Rosenbluth, M. N. Genesis of the Monte Carlo Algorithm for Statistical Mechanics. James E. G. *The Monte Carlo Method in the Physical Sciences*. Danvers, MA: American Institute of Physics, 2003, pp. 22-30.
88. Singh, V., Jain, S. and Tyagi, A. *Risk and reliability analysis: a handbook for civil and environmental engineers*. American Society of Civil Engineers, Reston, Virginia, 2007.

89. MathWorks Inc. *MATLAB Product Help*. The MathWorks Inc., Natick, MA., 2010.
90. Sobol, I. M. *A primer for the Monte Carlo method*. CRC Press, Inc., Boca Raton, 1994.
91. Li, Q., Xiao, D., McNeil, S. and Wang, K. *Benchmarking Sustainable Mechanistic-Empirical Based Pavement Design Alternatives Using Data Envelopment Analysis (DEA)*. The 8th International Conference on Managing Pavement Assets. Santiago, Chile, 2011.
92. Tran, N. H. *Characterizing and predicting dynamic modulus of hot-mix asphalt for mechanistic-empirical design guide*. PhD Dissertation. Fayetteville, AR : University of Arkansas, 2005.
93. Wang, K, Li, Q., Hall, K. D., Nguyen, V., Gong, W. and Hou, Z. Database Support for the New Mechanistic-Empirical Pavement Design Guide. In *Transportation Research Record: Journal of the Transportation Research Board*, No. 2087, Transportation Research Board of the National Academies, Washington, D.C., 2008, pp. 109-119.
94. Thyagarajan, S. *Improvements to strain computation and reliability analysis of flexible pavements in the mechanistic-empirical pavement design guide*. PhD Dissertation. Pullman, WA: Washington State University, 2009.
95. Retherford, J. *Management of Uncertainty for Flexible Pavement Design Utilizing Analytical and Probabilistic Methods*. PhD Dissertation. Nashville, TN: Vanderbilt University, 2012.
96. Daniels, D. J. *Ground Penetrating Radar 2nd Edition*. The Institution of Electrical Engineers, London, United Kingdom, 2004.

APPENDIX A Screenshot of the AHP Pairwise Comparison Survey Sheet

Instructions

	A	B	C	D	E	F	G	H	I	J	K	L
1	Thank you for conducting this Analytical Hierachical Process (AHP) survey.											
2												
3	Please keep in mind that you are weighing the importance of a factor upon										Your Name	
4	"A safe, long-lasting, cost-effective flexible pavement".										Your email	
5												
6	The format is Row:Column. For example, Traffic:Climate=7 means "Traffic is very strongly preferred comparing to Climate". On the contrary, Climate:Structure=1/7 means "Structure is very strongly preferred comparing to Climate".											
7												
8												
9	Please don't write in black-colored area.											
10												
11												
12												
13	With sincere appreciation,											
14												
15	Danny Xiao											
16	xxiao@uark.edu											
17	479.799.7686											
18												

L2

	A	B	C	D	E	F
1		Traffic	Climate	Structure	Material	Reliability
2	Traffic	1				
3	Climate		1			
4	Structure			1		
5	Material				1	
6	Reliability					1
7						
8	Numerical Rating		Definition			
9	9		Extremely preferred			
10	7		Very strongly preferred			
11	5		Strongly preferred			
12	3		Moderately preferred			
13	1		Equally preferred			

L3 Traffic

	A	B	C	D	E	F	G	H	I	J	K	L	M	N
1		Initial AADTT	Direction distribution	Lane distribution	Operational speed	Vehicle class distribution	Axle load distribution	Growth factor	Monthly adjustment	Hourly adjustment	Traffic wander	Axles per truck	Axle configuration	Wheelbase
2		1												
3			1											
4				1										
5					1									
6						1								
7							1							
8								1						
9									1					
10										1				
11											1			
12												1		
13													1	
14														1
15					Numerical Rating		Definition							
16					9		Extremely preferred							
17					7		Very strongly preferred							
18					5		Strongly preferred							
19					3		Moderately preferred							
20					1		Equally preferred							
21														

L3 Climate

	A	B	C	D	E	F	G	H	I	J	K
1		Elevation	Precipitation	Water table depth	Humidity	Temperature	Wind speed	Sunshine	UV level	Base/subgrade construction time	Pavement construction time
2		1									
3			1								
4				1							
5					1						
6						1					
7							1				
8								1			
9									1		
10										1	
11											1
12				Numerical Rating		Definition					
13				9		Extremely preferred					
14				7		Very strongly preferred					
15				5		Strongly preferred					
16				3		Moderately preferred					
17				1		Equally preferred					
18											

L3 Structure

	A	B	C	D	E	F	G	H	I	J	K	L
1		Material types	Surface layer thickness	Base layer thickness	Dynamic modulus of HMA	Resilient modulus of base	Resilient modulus of subgrade	Interface bond	Edge support	Water infiltration	Cross-slope	Drainage path length
2	Material types	1										
3	Surface layer thickness		1									
4	Base layer thickness			1								
5	Dynamic modulus of HMA				1							
6	Resilient modulus of base					1						
7	Resilient modulus of subgrade						1					
8	Interface bond							1				
9	Edge support								1			
10	Water infiltration									1		
11	Cross-slope										1	
12	Drainage path length											1
13			Numerical Rating		Definition							
14			9	Extremely preferred								
15			7	Very strongly preferred								
16			5	Strongly preferred								
17			3	Moderately preferred								
18			1	Equally preferred								
19												

L3 Materials

	A	B	C	D	E	F
1		Asphalt mixture	Stabilized base	Geotextile	Unbound base	Subgrade
2	Asphalt mixture	1				
3	Stabilized base		1			
4	Geotextile			1		
5	Unbound base				1	
6	Subgrade					1
7						
8		Numerical Rating		Definition		
9		9	Extremely preferred			
10		7	Very strongly preferred			
11		5	Strongly preferred			
12		3	Moderately preferred			
13		1	Equally preferred			
14						

L3 Reliability

	A	B	C	D	E	F
1		Reliability level	Traffic uncertainty	Climate uncertainty	Material variation	Construction variation
2	Reliability level	1				
3	Traffic uncertainty		1			
4	Climate uncertainty			1		
5	Material variation				1	
6	Construction variation					1
7						
8		Numerical Rating		Definition		
9		9		Extremely preferred		
10		7		Very strongly preferred		
11		5		Strongly preferred		
12		3		Moderately preferred		
13		1		Equally preferred		
14						

L4 HMA

	A	B	C	D	E	F	G	H	I	J
1		Gradation	Binder grade	Effective binder content	Air voids	Unit weight	Poisson's ratio	Dynamic modulus	Thermal conductivity	Heat capacity
2	Gradation	1								
3	Binder grade		1							
4	Effective binder content			1						
5	Air voids				1					
6	Unit weight					1				
7	Poisson's ratio						1			
8	Dynamic modulus							1		
9	Thermal conductivity								1	
10	Heat capacity									1
11										
12		Numerical Rating		Definition						
13		9		Extremely preferred						
14		7		Very strongly preferred						
15		5		Strongly preferred						
16		3		Moderately preferred						
17		1		Equally preferred						

L4 Stabilized Base

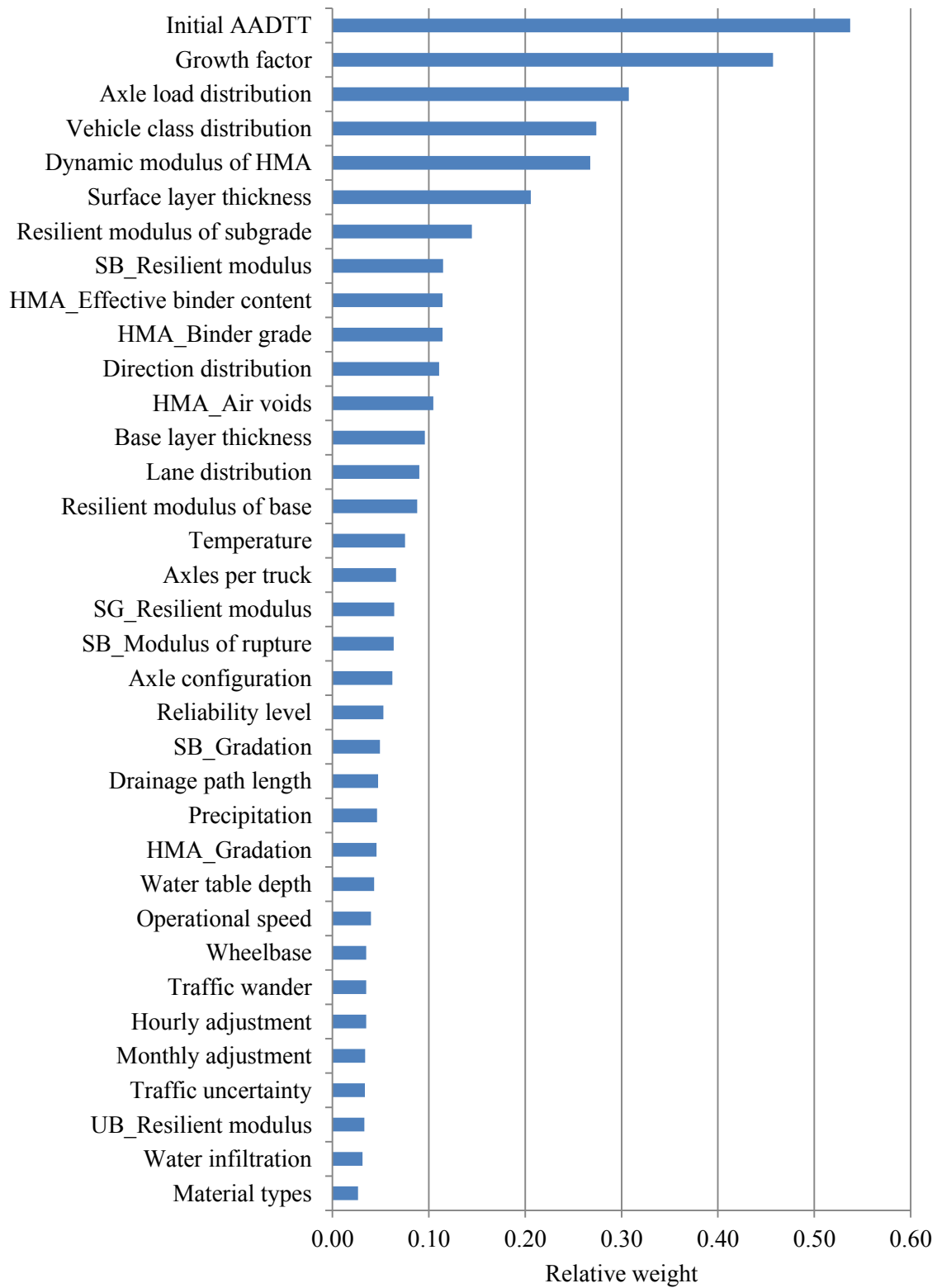
	A	B	C	D	E	F	G	H
1		Gradation	Unit weight	Poisson's ratio	Resilient modulus	Modulus of rupture	Thermal conductivity	Heat capacity
2	Gradation	1						
3	Unit weight		1					
4	Poisson's ratio			1				
5	Resilient modulus				1			
6	Modulus of rupture					1		
7	Thermal conductivity						1	
8	Heat capacity							1
9		Numerical Rating		Definition				
10		9		Extremely preferred				
11		7		Very strongly preferred				
12		5		Strongly preferred				
13		3		Moderately preferred				
14		1		Equally preferred				
15								

L4 Unbound

	A	B	C	D	E	F	G	H	I	J	K
1		Resilient modulus	Poisson's ratio	Coefficient of lateral pressure	Gradation	Plasticity Index	Liquid limit	Max. unit weight	Specific gravity	Hydraulic conductivity	Optimum water content
2	Resilient modulus	1									
3	Poisson's ratio		1								
4	Coefficient of lateral pressure			1							
5	Gradation				1						
6	Plasticity Index					1					
7	Liquid limit						1				
8	Max. unit weight							1			
9	Specific gravity								1		
10	Hydraulic conductivity									1	
11	Optimum water content										1
12		Numerical Rating		Definition							
13		9		Extremely preferred							
14		7		Very strongly preferred							
15		5		Strongly preferred							
16		3		Moderately preferred							
17		1		Equally preferred							
18											

APPENDIX B Overall Ranking of All Factors Influencing Flexible Pavement Design

Overall Ranking of All Factors Influencing Flexible Pavement Design (Rank 1-40)



Overall Ranking of All Factors Influencing Flexible Pavement Design (Rank 41-75)



APPENDIX C DESIGN OF EXPERIMENT FOR IMPORTANCE RANKING

Run	Pattern	Block	AADTT	Speed	h_{ac}	VFA	h_{bs}	Mr_{bs}	Mr_{sub}	Climate	Gradation	PG
1	---++++---	2	900	25	20	(8,12)	12	120	25	Mountain Home	Fine	76-22
2	-----	2	900	25	2	(8,12)	6	20	5	Mountain Home	Fine	64-22
3	---++++---	4	900	25	20	(16,4)	12	120	5	Mountain Home	Fine	76-22
4	---++++---	4	900	25	2	(16,4)	6	20	25	Mountain Home	Fine	64-22
5	-----	6	900	25	2	(8,12)	12	20	25	Mountain Home	Fine	64-22
6	---++++---	6	900	25	20	(8,12)	6	120	5	Mountain Home	Fine	76-22
7	---++++---	8	900	25	2	(16,4)	12	20	5	Mountain Home	Fine	64-22
8	---++++---	8	900	25	20	(16,4)	6	120	25	Mountain Home	Fine	76-22
9	-----	10	900	25	2	(8,12)	6	120	25	Mountain Home	Fine	64-22
10	---++++---	10	900	25	20	(8,12)	12	20	5	Mountain Home	Fine	76-22
11	---++++---	12	900	25	20	(16,4)	12	20	25	Mountain Home	Fine	76-22
12	---++++---	12	900	25	2	(16,4)	6	120	5	Mountain Home	Fine	64-22
13	---++++---	14	900	25	20	(8,12)	6	20	25	Mountain Home	Fine	76-22
14	-----	14	900	25	2	(8,12)	12	120	5	Mountain Home	Fine	64-22
15	---++++---	16	900	25	20	(16,4)	6	20	5	Mountain Home	Fine	76-22
16	---++++---	16	900	25	2	(16,4)	12	120	25	Mountain Home	Fine	64-22
17	+++++---	2	10000	25	20	(16,4)	6	120	5	Mountain Home	Coarse	64-22
18	+++++---	2	10000	25	2	(16,4)	12	20	25	Mountain Home	Coarse	76-22
19	+++++---	4	10000	25	20	(8,12)	6	120	25	Mountain Home	Coarse	64-22
20	+++++---	4	10000	25	2	(8,12)	12	20	5	Mountain Home	Coarse	76-22
21	+++++---	6	10000	25	20	(16,4)	12	120	25	Mountain Home	Coarse	64-22
22	+++++---	6	10000	25	2	(16,4)	6	20	5	Mountain Home	Coarse	76-22
23	+++++---	8	10000	25	20	(8,12)	12	120	5	Mountain Home	Coarse	64-22
24	+++++---	8	10000	25	2	(8,12)	6	20	25	Mountain Home	Coarse	76-22
25	+++++---	10	10000	25	20	(16,4)	6	20	25	Mountain Home	Coarse	64-22
26	+++++---	10	10000	25	2	(16,4)	12	120	5	Mountain Home	Coarse	76-22

Run	Pattern	Block	AADTT	Speed	h _{ac}	VFA	h _{bs}	Mr _{bs}	Mr _{sub}	Climate	Gradation	PG
27	+++-----+	12	10000	25	20	(8,12)	6	20	5	Mountain Home	Coarse	64-22
28	+++++++	12	10000	25	2	(8,12)	12	120	25	Mountain Home	Coarse	76-22
29	+++-----+	14	10000	25	2	(16,4)	6	120	25	Mountain Home	Coarse	76-22
30	++++-----+	14	10000	25	20	(16,4)	12	20	5	Mountain Home	Coarse	64-22
31	++++-----+	16	10000	25	2	(8,12)	6	120	5	Mountain Home	Coarse	76-22
32	++++-----+	16	10000	25	20	(8,12)	12	20	25	Mountain Home	Coarse	64-22
33	+++-----+	1	900	60	2	(8,12)	12	20	5	Mountain Home	Coarse	64-22
34	+++-----+	1	900	60	20	(8,12)	6	120	25	Mountain Home	Coarse	76-22
35	++++-----+	3	900	60	20	(16,4)	6	120	5	Mountain Home	Coarse	76-22
36	+++-----+	3	900	60	2	(16,4)	12	20	25	Mountain Home	Coarse	64-22
37	+++-----+	5	900	60	2	(8,12)	6	20	25	Mountain Home	Coarse	64-22
38	+++-----+	5	900	60	20	(8,12)	12	120	5	Mountain Home	Coarse	76-22
39	+++-----+	7	900	60	2	(16,4)	6	20	5	Mountain Home	Coarse	64-22
40	++++-----+	7	900	60	20	(16,4)	12	120	25	Mountain Home	Coarse	76-22
41	+++-----+	9	900	60	20	(8,12)	6	20	5	Mountain Home	Coarse	76-22
42	+++-----+	9	900	60	2	(8,12)	12	120	25	Mountain Home	Coarse	64-22
43	+++-----+	11	900	60	2	(16,4)	12	120	5	Mountain Home	Coarse	64-22
44	++++-----+	11	900	60	20	(16,4)	6	20	25	Mountain Home	Coarse	76-22
45	+++-----+	13	900	60	2	(8,12)	6	120	5	Mountain Home	Coarse	64-22
46	+++-----+	13	900	60	20	(8,12)	12	20	25	Mountain Home	Coarse	76-22
47	+++-----+	15	900	60	2	(16,4)	6	120	25	Mountain Home	Coarse	64-22
48	++++-----+	15	900	60	20	(16,4)	12	20	5	Mountain Home	Coarse	76-22
49	+++-----+	1	10000	60	2	(16,4)	6	20	25	Mountain Home	Fine	76-22
50	++++-----	1	10000	60	20	(16,4)	12	120	5	Mountain Home	Fine	64-22
51	+++-----+	3	10000	60	2	(8,12)	6	20	5	Mountain Home	Fine	76-22
52	++++-----	3	10000	60	20	(8,12)	12	120	25	Mountain Home	Fine	64-22
53	+++-----+	5	10000	60	2	(16,4)	12	20	5	Mountain Home	Fine	76-22
54	++++-----	5	10000	60	20	(16,4)	6	120	25	Mountain Home	Fine	64-22
55	+++-----+	7	10000	60	2	(8,12)	12	20	25	Mountain Home	Fine	76-22

Run	Pattern	Block	AADTT	Speed	h _{ac}	VFA	h _{bs}	Mr _{bs}	Mr _{sub}	Climate	Gradation	PG
56	+++----	7	10000	60	20	(8,12)	6	120	5	Mountain Home	Fine	64-22
57	+++++----	9	10000	60	20	(16,4)	12	20	25	Mountain Home	Fine	64-22
58	++-++-+-	9	10000	60	2	(16,4)	6	120	5	Mountain Home	Fine	76-22
59	+-+---+-	11	10000	60	2	(8,12)	6	120	25	Mountain Home	Fine	76-22
60	+++----	11	10000	60	20	(8,12)	12	20	5	Mountain Home	Fine	64-22
61	++++-----	13	10000	60	20	(16,4)	6	20	5	Mountain Home	Fine	64-22
62	+-+----+-	13	10000	60	2	(16,4)	12	120	25	Mountain Home	Fine	76-22
63	+-+----+-	15	10000	60	2	(8,12)	12	120	5	Mountain Home	Fine	76-22
64	+++----+-	15	10000	60	20	(8,12)	6	20	25	Mountain Home	Fine	64-22
65	----+++++	1	900	25	2	(16,4)	12	120	5	Monticello	Coarse	76-22
66	---+----+	1	900	25	20	(16,4)	6	20	25	Monticello	Coarse	64-22
67	---+----+	3	900	25	20	(8,12)	6	20	5	Monticello	Coarse	64-22
68	----+++++	3	900	25	2	(8,12)	12	120	25	Monticello	Coarse	76-22
69	----+++++	5	900	25	2	(16,4)	6	120	25	Monticello	Coarse	76-22
70	---+----+	5	900	25	20	(16,4)	12	20	5	Monticello	Coarse	64-22
71	----+++++	7	900	25	2	(8,12)	6	120	5	Monticello	Coarse	76-22
72	---+----+	7	900	25	20	(8,12)	12	20	25	Monticello	Coarse	64-22
73	----+++++	9	900	25	2	(16,4)	12	20	25	Monticello	Coarse	76-22
74	---+----+	9	900	25	20	(16,4)	6	120	5	Monticello	Coarse	64-22
75	----+++++	11	900	25	2	(8,12)	12	20	5	Monticello	Coarse	76-22
76	---+----+	11	900	25	20	(8,12)	6	120	25	Monticello	Coarse	64-22
77	---+----+	13	900	25	20	(16,4)	12	120	25	Monticello	Coarse	64-22
78	----+++++	13	900	25	2	(16,4)	6	20	5	Monticello	Coarse	76-22
79	---+----+	15	900	25	20	(8,12)	12	120	5	Monticello	Coarse	64-22
80	----+++++	15	900	25	2	(8,12)	6	20	25	Monticello	Coarse	76-22
81	++-++-+-	1	10000	25	20	(8,12)	12	20	5	Monticello	Fine	76-22
82	+-----	1	10000	25	2	(8,12)	6	120	25	Monticello	Fine	64-22
83	++-++-+-	3	10000	25	20	(16,4)	12	20	25	Monticello	Fine	76-22
84	+-----	3	10000	25	2	(16,4)	6	120	5	Monticello	Fine	64-22

Run	Pattern	Block	AADTT	Speed	h _{ac}	VFA	h _{bs}	Mr _{bs}	Mr _{sub}	Climate	Gradation	PG
85	+++-----++	5	10000	25	20	(8,12)	6	20	25	Monticello	Fine	76-22
86	-----++	5	10000	25	2	(8,12)	12	120	5	Monticello	Fine	64-22
87	+++-----++	7	10000	25	20	(16,4)	6	20	5	Monticello	Fine	76-22
88	-----++	7	10000	25	2	(16,4)	12	120	25	Monticello	Fine	64-22
89	+++-----++	9	10000	25	20	(8,12)	12	120	25	Monticello	Fine	76-22
90	-----++	9	10000	25	2	(8,12)	6	20	5	Monticello	Fine	64-22
91	+++-----++	11	10000	25	20	(16,4)	12	120	5	Monticello	Fine	76-22
92	-----++	11	10000	25	2	(16,4)	6	20	25	Monticello	Fine	64-22
93	-----++	13	10000	25	2	(8,12)	12	20	25	Monticello	Fine	64-22
94	+++-----++	13	10000	25	20	(8,12)	6	120	5	Monticello	Fine	76-22
95	-----++	15	10000	25	2	(16,4)	12	20	5	Monticello	Fine	64-22
96	+++-----++	15	10000	25	20	(16,4)	6	120	25	Monticello	Fine	76-22
97	-----++	2	900	60	2	(16,4)	6	120	5	Monticello	Fine	76-22
98	-----++	2	900	60	20	(16,4)	12	20	25	Monticello	Fine	64-22
99	-----++	4	900	60	2	(8,12)	6	120	25	Monticello	Fine	76-22
100	-----++	4	900	60	20	(8,12)	12	20	5	Monticello	Fine	64-22
101	-----++	6	900	60	2	(16,4)	12	120	25	Monticello	Fine	76-22
102	-----++	6	900	60	20	(16,4)	6	20	5	Monticello	Fine	64-22
103	-----++	8	900	60	2	(8,12)	12	120	5	Monticello	Fine	76-22
104	-----++	8	900	60	20	(8,12)	6	20	25	Monticello	Fine	64-22
105	-----++	10	900	60	2	(16,4)	6	20	25	Monticello	Fine	76-22
106	-----++	10	900	60	20	(16,4)	12	120	5	Monticello	Fine	64-22
107	-----++	12	900	60	20	(8,12)	12	120	25	Monticello	Fine	64-22
108	-----++	12	900	60	2	(8,12)	6	20	5	Monticello	Fine	76-22
109	-----++	14	900	60	20	(16,4)	6	120	25	Monticello	Fine	64-22
110	-----++	14	900	60	2	(16,4)	12	20	5	Monticello	Fine	76-22
111	-----++	16	900	60	2	(8,12)	12	20	25	Monticello	Fine	76-22
112	-----++	16	900	60	20	(8,12)	6	120	5	Monticello	Fine	64-22
113	-----++	2	10000	60	2	(8,12)	12	120	25	Monticello	Coarse	64-22

Run	Pattern	Block	AADTT	Speed	h_{ac}	VFA	h_{bs}	Mr_{bs}	Mr_{sub}	Climate	Gradation	PG
114	+++-----+++	2	10000	60	20	(8,12)	6	20	5	Monticello	Coarse	76-22
115	++++-----+	4	10000	60	20	(16,4)	6	20	25	Monticello	Coarse	76-22
116	++-++++-+-	4	10000	60	2	(16,4)	12	120	5	Monticello	Coarse	64-22
117	++-----+--	6	10000	60	2	(8,12)	6	120	5	Monticello	Coarse	64-22
118	+++-----+	6	10000	60	20	(8,12)	12	20	25	Monticello	Coarse	76-22
119	++-----+--	8	10000	60	2	(16,4)	6	120	25	Monticello	Coarse	64-22
120	++++-----+	8	10000	60	20	(16,4)	12	20	5	Monticello	Coarse	76-22
121	+++-----+	10	10000	60	20	(8,12)	6	120	25	Monticello	Coarse	76-22
122	++-----+--	10	10000	60	2	(8,12)	12	20	5	Monticello	Coarse	64-22
123	++++-----+	12	10000	60	20	(16,4)	6	120	5	Monticello	Coarse	76-22
124	++-----+--	12	10000	60	2	(16,4)	12	20	25	Monticello	Coarse	64-22
125	++-----+--	14	10000	60	2	(8,12)	6	20	25	Monticello	Coarse	64-22
126	+++-----+	14	10000	60	20	(8,12)	12	120	5	Monticello	Coarse	76-22
127	++-----+--	16	10000	60	2	(16,4)	6	20	5	Monticello	Coarse	64-22
128	++++-----+	16	10000	60	20	(16,4)	12	120	25	Monticello	Coarse	76-22

APPENDIX D CENTRAL COMPOSITE DESIGN (CCD) FOR MODEL CONSTRUCTION

Run	Pattern	AADTT	h_{ac}	Gradation	VFA	Va	Pb_{eff}	PG	h_{bs}	Mr_{bs}	Mr_{sub}
1	-----	900	2	Fine	0.4	12	8	64-22	6	20	5
2	+-----	10000	2	Fine	0.4	12	8	64-22	6	20	5
3	--+-----	900	12	Fine	0.4	12	8	64-22	6	20	5
4	++-----	10000	12	Fine	0.4	12	8	64-22	6	20	5
5	---+-----	900	2	Coarse	0.4	12	8	64-22	6	20	5
6	+++-----	10000	2	Coarse	0.4	12	8	64-22	6	20	5
7	--++-----	900	12	Coarse	0.4	12	8	64-22	6	20	5
8	+++-----	10000	12	Coarse	0.4	12	8	64-22	6	20	5
9	----+-----	900	2	Fine	0.8	4	16	64-22	6	20	5
10	++++-----	10000	2	Fine	0.8	4	16	64-22	6	20	5
11	---++-----	900	12	Fine	0.8	4	16	64-22	6	20	5
12	++++-----	10000	12	Fine	0.8	4	16	64-22	6	20	5
13	---++-----	900	2	Coarse	0.8	4	16	64-22	6	20	5
14	++++-----	10000	2	Coarse	0.8	4	16	64-22	6	20	5
15	---++-----	900	12	Coarse	0.8	4	16	64-22	6	20	5
16	++++-----	10000	12	Coarse	0.8	4	16	64-22	6	20	5
17	----+-----	900	2	Fine	0.4	12	8	76-22	6	20	5
18	+----+-----	10000	2	Fine	0.4	12	8	76-22	6	20	5
19	--++-----	900	12	Fine	0.4	12	8	76-22	6	20	5
20	+++-----	10000	12	Fine	0.4	12	8	76-22	6	20	5
21	---++-----	900	2	Coarse	0.4	12	8	76-22	6	20	5
22	++++-----	10000	2	Coarse	0.4	12	8	76-22	6	20	5
23	--++-----	900	12	Coarse	0.4	12	8	76-22	6	20	5
24	+++-----	10000	12	Coarse	0.4	12	8	76-22	6	20	5
25	----+-----	900	2	Fine	0.8	4	16	76-22	6	20	5
26	+----+-----	10000	2	Fine	0.8	4	16	76-22	6	20	5

Run	Pattern	AADTT	h_{ac}	Gradation	VFA	Va	Pb_{eff}	PG	h_{bs}	Mr_{bs}	Mr_{sub}
27	--++++--	900	12	Fine	0.8	4	16	76-22	6	20	5
28	++++--	10000	12	Fine	0.8	4	16	76-22	6	20	5
29	---+++--	900	2	Coarse	0.8	4	16	76-22	6	20	5
30	++++--	10000	2	Coarse	0.8	4	16	76-22	6	20	5
31	---+++--	900	12	Coarse	0.8	4	16	76-22	6	20	5
32	++++--	10000	12	Coarse	0.8	4	16	76-22	6	20	5
33	-----+--	900	2	Fine	0.4	12	8	64-22	12	20	5
34	+-----+--	10000	2	Fine	0.4	12	8	64-22	12	20	5
35	--+---+--	900	12	Fine	0.4	12	8	64-22	12	20	5
36	++---+--	10000	12	Fine	0.4	12	8	64-22	12	20	5
37	---+---+--	900	2	Coarse	0.4	12	8	64-22	12	20	5
38	++---+--	10000	2	Coarse	0.4	12	8	64-22	12	20	5
39	--+---+--	900	12	Coarse	0.4	12	8	64-22	12	20	5
40	+++---+--	10000	12	Coarse	0.4	12	8	64-22	12	20	5
41	----+++--	900	2	Fine	0.8	4	16	64-22	12	20	5
42	+---+++--	10000	2	Fine	0.8	4	16	64-22	12	20	5
43	--++++--	900	12	Fine	0.8	4	16	64-22	12	20	5
44	++++--	10000	12	Fine	0.8	4	16	64-22	12	20	5
45	---+++--	900	2	Coarse	0.8	4	16	64-22	12	20	5
46	++++--	10000	2	Coarse	0.8	4	16	64-22	12	20	5
47	---+++--	900	12	Coarse	0.8	4	16	64-22	12	20	5
48	++++--	10000	12	Coarse	0.8	4	16	64-22	12	20	5
49	-----+--	900	2	Fine	0.4	12	8	76-22	12	20	5
50	+-----+--	10000	2	Fine	0.4	12	8	76-22	12	20	5
51	--+---+--	900	12	Fine	0.4	12	8	76-22	12	20	5
52	++---+--	10000	12	Fine	0.4	12	8	76-22	12	20	5
53	---+++--	900	2	Coarse	0.4	12	8	76-22	12	20	5
54	++---+--	10000	2	Coarse	0.4	12	8	76-22	12	20	5
55	--+---+--	900	12	Coarse	0.4	12	8	76-22	12	20	5

Run	Pattern	AADTT	h_{ac}	Gradation	VFA	Va	Pb_{eff}	PG	h_{bs}	Mr_{bs}	Mr_{sub}
56	+++++---	10000	12	Coarse	0.4	12	8	76-22	12	20	5
57	-----+++	900	2	Fine	0.8	4	16	76-22	12	20	5
58	+-----+	10000	2	Fine	0.8	4	16	76-22	12	20	5
59	--++++-	900	12	Fine	0.8	4	16	76-22	12	20	5
60	+++++---	10000	12	Fine	0.8	4	16	76-22	12	20	5
61	-----+++	900	2	Coarse	0.8	4	16	76-22	12	20	5
62	+-----+	10000	2	Coarse	0.8	4	16	76-22	12	20	5
63	-----+++	900	12	Coarse	0.8	4	16	76-22	12	20	5
64	+++++---	10000	12	Coarse	0.8	4	16	76-22	12	20	5
65	0000000a	5450	7	Regular	0.6	8	12	70-22	9	60	5
66	-----++	900	2	Fine	0.4	12	8	64-22	6	100	5
67	+-----++	10000	2	Fine	0.4	12	8	64-22	6	100	5
68	--++++-	900	12	Fine	0.4	12	8	64-22	6	100	5
69	++-----+	10000	12	Fine	0.4	12	8	64-22	6	100	5
70	---+---++	900	2	Coarse	0.4	12	8	64-22	6	100	5
71	++-----+	10000	2	Coarse	0.4	12	8	64-22	6	100	5
72	--++++-	900	12	Coarse	0.4	12	8	64-22	6	100	5
73	+++-----+	10000	12	Coarse	0.4	12	8	64-22	6	100	5
74	---+---++	900	2	Fine	0.8	4	16	64-22	6	100	5
75	+-----++	10000	2	Fine	0.8	4	16	64-22	6	100	5
76	--++++-	900	12	Fine	0.8	4	16	64-22	6	100	5
77	+++-----+	10000	12	Fine	0.8	4	16	64-22	6	100	5
78	---+---++	900	2	Coarse	0.8	4	16	64-22	6	100	5
79	++++-----+	10000	2	Coarse	0.8	4	16	64-22	6	100	5
80	---+---++	900	12	Coarse	0.8	4	16	64-22	6	100	5
81	++++-----+	10000	12	Coarse	0.8	4	16	64-22	6	100	5
82	-----+++	900	2	Fine	0.4	12	8	76-22	6	100	5
83	+-----++	10000	2	Fine	0.4	12	8	76-22	6	100	5
84	--++++-	900	12	Fine	0.4	12	8	76-22	6	100	5

Run	Pattern	AADTT	h_{ac}	Gradation	VFA	Va	$P_{b_{eff}}$	PG	h_{bs}	Mr_{bs}	Mr_{sub}
85	+++----	10000	12	Fine	0.4	12	8	76-22	6	100	5
86	---++++	900	2	Coarse	0.4	12	8	76-22	6	100	5
87	+++----	10000	2	Coarse	0.4	12	8	76-22	6	100	5
88	---++++	900	12	Coarse	0.4	12	8	76-22	6	100	5
89	+++----	10000	12	Coarse	0.4	12	8	76-22	6	100	5
90	----++++	900	2	Fine	0.8	4	16	76-22	6	100	5
91	+----+++	10000	2	Fine	0.8	4	16	76-22	6	100	5
92	---++++	900	12	Fine	0.8	4	16	76-22	6	100	5
93	+++----	10000	12	Fine	0.8	4	16	76-22	6	100	5
94	---++++	900	2	Coarse	0.8	4	16	76-22	6	100	5
95	++++----	10000	2	Coarse	0.8	4	16	76-22	6	100	5
96	---++++	900	12	Coarse	0.8	4	16	76-22	6	100	5
97	++++----	10000	12	Coarse	0.8	4	16	76-22	6	100	5
98	-----++	900	2	Fine	0.4	12	8	64-22	12	100	5
99	+-----+	10000	2	Fine	0.4	12	8	64-22	12	100	5
100	--++++	900	12	Fine	0.4	12	8	64-22	12	100	5
101	++++---	10000	12	Fine	0.4	12	8	64-22	12	100	5
102	---++++	900	2	Coarse	0.4	12	8	64-22	12	100	5
103	+++----	10000	2	Coarse	0.4	12	8	64-22	12	100	5
104	---++++	900	12	Coarse	0.4	12	8	64-22	12	100	5
105	+++----	10000	12	Coarse	0.4	12	8	64-22	12	100	5
106	----++++	900	2	Fine	0.8	4	16	64-22	12	100	5
107	+----+++	10000	2	Fine	0.8	4	16	64-22	12	100	5
108	---++++	900	12	Fine	0.8	4	16	64-22	12	100	5
109	+++----	10000	12	Fine	0.8	4	16	64-22	12	100	5
110	---++++	900	2	Coarse	0.8	4	16	64-22	12	100	5
111	++++---	10000	2	Coarse	0.8	4	16	64-22	12	100	5
112	---++++	900	12	Coarse	0.8	4	16	64-22	12	100	5
113	++++---	10000	12	Coarse	0.8	4	16	64-22	12	100	5

Run	Pattern	AADTT	h_{ac}	Gradation	VFA	Va	Pb_{eff}	PG	h_{bs}	Mr_{bs}	Mr_{sub}
114	-----++-	900	2	Fine	0.4	12	8	76-22	12	100	5
115	+-----++-	10000	2	Fine	0.4	12	8	76-22	12	100	5
116	--+-----++-	900	12	Fine	0.4	12	8	76-22	12	100	5
117	++-+-----++-	10000	12	Fine	0.4	12	8	76-22	12	100	5
118	---+-----++-	900	2	Coarse	0.4	12	8	76-22	12	100	5
119	+++-----++-	10000	2	Coarse	0.4	12	8	76-22	12	100	5
120	--++-----++-	900	12	Coarse	0.4	12	8	76-22	12	100	5
121	+++-----++-	10000	12	Coarse	0.4	12	8	76-22	12	100	5
122	----++++-	900	2	Fine	0.8	4	16	76-22	12	100	5
123	+---++++-	10000	2	Fine	0.8	4	16	76-22	12	100	5
124	--++++-	900	12	Fine	0.8	4	16	76-22	12	100	5
125	++++++-	10000	12	Fine	0.8	4	16	76-22	12	100	5
126	---++++-	900	2	Coarse	0.8	4	16	76-22	12	100	5
127	+-----++-	10000	2	Coarse	0.8	4	16	76-22	12	100	5
128	--++++-	900	12	Coarse	0.8	4	16	76-22	12	100	5
129	+++++--	10000	12	Coarse	0.8	4	16	76-22	12	100	5
130	000000a0	5450	7	Regular	0.6	8	12	70-22	9	20	15
131	00000a00	5450	7	Regular	0.6	8	12	70-22	6	60	15
132	0000a000	5450	7	Regular	0.6	8	12	64-22	9	60	15
133	000a0000	5450	7	Regular	0.4	12	8	70-22	9	60	15
134	00a00000	5450	7	Fine	0.6	8	12	70-22	9	60	15
135	0a000000	5450	2	Regular	0.6	8	12	70-22	9	60	15
136	a0000000	900	7	Regular	0.6	8	12	70-22	9	60	15
137	00000000	5450	7	Regular	0.6	8	12	70-22	9	60	15
138	00000000	5450	7	Regular	0.6	8	12	70-22	9	60	15
139	A0000000	10000	7	Regular	0.6	8	12	70-22	9	60	15
140	0A000000	5450	12	Regular	0.6	8	12	70-22	9	60	15
141	00A00000	5450	7	Coarse	0.6	8	12	70-22	9	60	15
142	000A0000	5450	7	Regular	0.8	4	16	70-22	9	60	15

Run	Pattern	AADTT	h_{ac}	Gradation	VFA	Va	Pb_{eff}	PG	h_{bs}	Mr_{bs}	Mr_{sub}
143	0000A000	5450	7	Regular	0.6	8	12	76-22	9	60	15
144	00000A00	5450	7	Regular	0.6	8	12	70-22	12	60	15
145	000000A0	5450	7	Regular	0.6	8	12	70-22	9	100	15
146	-----+	900	2	Fine	0.4	12	8	64-22	6	20	25
147	+-----+	10000	2	Fine	0.4	12	8	64-22	6	20	25
148	--+-----+	900	12	Fine	0.4	12	8	64-22	6	20	25
149	++-----+	10000	12	Fine	0.4	12	8	64-22	6	20	25
150	---+-----+	900	2	Coarse	0.4	12	8	64-22	6	20	25
151	+++-----+	10000	2	Coarse	0.4	12	8	64-22	6	20	25
152	--++-----+	900	12	Coarse	0.4	12	8	64-22	6	20	25
153	++++-----+	10000	12	Coarse	0.4	12	8	64-22	6	20	25
154	----+-----+	900	2	Fine	0.8	4	16	64-22	6	20	25
155	---++-----+	10000	2	Fine	0.8	4	16	64-22	6	20	25
156	--+++-----+	900	12	Fine	0.8	4	16	64-22	6	20	25
157	++++-----+	10000	12	Fine	0.8	4	16	64-22	6	20	25
158	---+++-----+	900	2	Coarse	0.8	4	16	64-22	6	20	25
159	++++-----+	10000	2	Coarse	0.8	4	16	64-22	6	20	25
160	---+++-----+	900	12	Coarse	0.8	4	16	64-22	6	20	25
161	++++-----+	10000	12	Coarse	0.8	4	16	64-22	6	20	25
162	----+-----+	900	2	Fine	0.4	12	8	76-22	6	20	25
163	+----+-----+	10000	2	Fine	0.4	12	8	76-22	6	20	25
164	--++-----+	900	12	Fine	0.4	12	8	76-22	6	20	25
165	++++-----+	10000	12	Fine	0.4	12	8	76-22	6	20	25
166	---++-----+	900	2	Coarse	0.4	12	8	76-22	6	20	25
167	++++-----+	10000	2	Coarse	0.4	12	8	76-22	6	20	25
168	--++-----+	900	12	Coarse	0.4	12	8	76-22	6	20	25
169	++++-----+	10000	12	Coarse	0.4	12	8	76-22	6	20	25
170	----+-----+	900	2	Fine	0.8	4	16	76-22	6	20	25
171	---+++-----+	10000	2	Fine	0.8	4	16	76-22	6	20	25

Run	Pattern	AADTT	h _{ac}	Gradation	VFA	V _a	P _b _{eff}	PG	h _{bs}	Mr _{bs}	Mr _{sub}
172	--++++--	900	12	Fine	0.8	4	16	76-22	6	20	25
173	++++--	10000	12	Fine	0.8	4	16	76-22	6	20	25
174	---++++	900	2	Coarse	0.8	4	16	76-22	6	20	25
175	++++--	10000	2	Coarse	0.8	4	16	76-22	6	20	25
176	---++++	900	12	Coarse	0.8	4	16	76-22	6	20	25
177	++++--	10000	12	Coarse	0.8	4	16	76-22	6	20	25
178	-----++	900	2	Fine	0.4	12	8	64-22	12	20	25
179	+-----++	10000	2	Fine	0.4	12	8	64-22	12	20	25
180	--++++	900	12	Fine	0.4	12	8	64-22	12	20	25
181	++----	10000	12	Fine	0.4	12	8	64-22	12	20	25
182	---++++	900	2	Coarse	0.4	12	8	64-22	12	20	25
183	++----	10000	2	Coarse	0.4	12	8	64-22	12	20	25
184	---++++	900	12	Coarse	0.4	12	8	64-22	12	20	25
185	+++----	10000	12	Coarse	0.4	12	8	64-22	12	20	25
186	----++++	900	2	Fine	0.8	4	16	64-22	12	20	25
187	+----++	10000	2	Fine	0.8	4	16	64-22	12	20	25
188	---++++	900	12	Fine	0.8	4	16	64-22	12	20	25
189	++++--	10000	12	Fine	0.8	4	16	64-22	12	20	25
190	---++++	900	2	Coarse	0.8	4	16	64-22	12	20	25
191	++++--	10000	2	Coarse	0.8	4	16	64-22	12	20	25
192	---++++	900	12	Coarse	0.8	4	16	64-22	12	20	25
193	++++--	10000	12	Coarse	0.8	4	16	64-22	12	20	25
194	-----++	900	2	Fine	0.4	12	8	76-22	12	20	25
195	+-----++	10000	2	Fine	0.4	12	8	76-22	12	20	25
196	---++++	900	12	Fine	0.4	12	8	76-22	12	20	25
197	++----	10000	12	Fine	0.4	12	8	76-22	12	20	25
198	---++++	900	2	Coarse	0.4	12	8	76-22	12	20	25
199	++----	10000	2	Coarse	0.4	12	8	76-22	12	20	25
200	---++++	900	12	Coarse	0.4	12	8	76-22	12	20	25

Run	Pattern	AADTT	h _{ac}	Gradation	VFA	V _a	P _b _{eff}	PG	h _{bs}	Mr _{bs}	Mr _{sub}
201	+++----+	10000	12	Coarse	0.4	12	8	76-22	12	20	25
202	----++++	900	2	Fine	0.8	4	16	76-22	12	20	25
203	+----+++	10000	2	Fine	0.8	4	16	76-22	12	20	25
204	--+++++	900	12	Fine	0.8	4	16	76-22	12	20	25
205	+++++++	10000	12	Fine	0.8	4	16	76-22	12	20	25
206	-----+	900	2	Coarse	0.8	4	16	76-22	12	20	25
207	+-----+	10000	2	Coarse	0.8	4	16	76-22	12	20	25
208	-----+	900	12	Coarse	0.8	4	16	76-22	12	20	25
209	+++++++	10000	12	Coarse	0.8	4	16	76-22	12	20	25
210	000000A	5450	7	Regular	0.6	8	12	70-22	9	60	25
211	-----++	900	2	Fine	0.4	12	8	64-22	6	100	25
212	+-----++	10000	2	Fine	0.4	12	8	64-22	6	100	25
213	--+-----	900	12	Fine	0.4	12	8	64-22	6	100	25
214	++-----	10000	12	Fine	0.4	12	8	64-22	6	100	25
215	---+-----	900	2	Coarse	0.4	12	8	64-22	6	100	25
216	+++-----	10000	2	Coarse	0.4	12	8	64-22	6	100	25
217	--+-----	900	12	Coarse	0.4	12	8	64-22	6	100	25
218	+++-----	10000	12	Coarse	0.4	12	8	64-22	6	100	25
219	----+-----	900	2	Fine	0.8	4	16	64-22	6	100	25
220	+----+-----	10000	2	Fine	0.8	4	16	64-22	6	100	25
221	--++-----	900	12	Fine	0.8	4	16	64-22	6	100	25
222	+++-----	10000	12	Fine	0.8	4	16	64-22	6	100	25
223	-----++	900	2	Coarse	0.8	4	16	64-22	6	100	25
224	++++-----	10000	2	Coarse	0.8	4	16	64-22	6	100	25
225	-----++	900	12	Coarse	0.8	4	16	64-22	6	100	25
226	++++-----	10000	12	Coarse	0.8	4	16	64-22	6	100	25
227	-----+++	900	2	Fine	0.4	12	8	76-22	6	100	25
228	+----+-----	10000	2	Fine	0.4	12	8	76-22	6	100	25
229	--++-----	900	12	Fine	0.4	12	8	76-22	6	100	25

Run	Pattern	AADTT	h_{ac}	Gradation	VFA	Va	Pb_{eff}	PG	h_{bs}	Mr_{bs}	Mr_{sub}
230	+++----++	10000	12	Fine	0.4	12	8	76-22	6	100	25
231	---++----++	900	2	Coarse	0.4	12	8	76-22	6	100	25
232	+++----++	10000	2	Coarse	0.4	12	8	76-22	6	100	25
233	---++----++	900	12	Coarse	0.4	12	8	76-22	6	100	25
234	+++----++	10000	12	Coarse	0.4	12	8	76-22	6	100	25
235	----++----++	900	2	Fine	0.8	4	16	76-22	6	100	25
236	+----++----++	10000	2	Fine	0.8	4	16	76-22	6	100	25
237	---++----++	900	12	Fine	0.8	4	16	76-22	6	100	25
238	+++----++	10000	12	Fine	0.8	4	16	76-22	6	100	25
239	---++----++	900	2	Coarse	0.8	4	16	76-22	6	100	25
240	++++----++	10000	2	Coarse	0.8	4	16	76-22	6	100	25
241	---++----++	900	12	Coarse	0.8	4	16	76-22	6	100	25
242	++++----++	10000	12	Coarse	0.8	4	16	76-22	6	100	25
243	-----++	900	2	Fine	0.4	12	8	64-22	12	100	25
244	+-----++	10000	2	Fine	0.4	12	8	64-22	12	100	25
245	---++----++	900	12	Fine	0.4	12	8	64-22	12	100	25
246	+++----++	10000	12	Fine	0.4	12	8	64-22	12	100	25
247	---++----++	900	2	Coarse	0.4	12	8	64-22	12	100	25
248	+++----++	10000	2	Coarse	0.4	12	8	64-22	12	100	25
249	---++----++	900	12	Coarse	0.4	12	8	64-22	12	100	25
250	+++----++	10000	12	Coarse	0.4	12	8	64-22	12	100	25
251	---++----++	900	2	Fine	0.8	4	16	64-22	12	100	25
252	+----++----++	10000	2	Fine	0.8	4	16	64-22	12	100	25
253	---++----++	900	12	Fine	0.8	4	16	64-22	12	100	25
254	+++----++	10000	12	Fine	0.8	4	16	64-22	12	100	25
255	---++----++	900	2	Coarse	0.8	4	16	64-22	12	100	25
256	+++----++	10000	2	Coarse	0.8	4	16	64-22	12	100	25
257	---++----++	900	12	Coarse	0.8	4	16	64-22	12	100	25
258	++++----++	10000	12	Coarse	0.8	4	16	64-22	12	100	25

Run	Pattern	AADTT	h_{ac}	Gradation	VFA	Va	Pb_{eff}	PG	h_{bs}	Mr_{bs}	Mr_{sub}
259	----++++	900	2	Fine	0.4	12	8	76-22	12	100	25
260	+----++++	10000	2	Fine	0.4	12	8	76-22	12	100	25
261	--++-----	900	12	Fine	0.4	12	8	76-22	12	100	25
262	++--++++	10000	12	Fine	0.4	12	8	76-22	12	100	25
263	---+-----	900	2	Coarse	0.4	12	8	76-22	12	100	25
264	+++-----	10000	2	Coarse	0.4	12	8	76-22	12	100	25
265	--++-----	900	12	Coarse	0.4	12	8	76-22	12	100	25
266	+++-----	10000	12	Coarse	0.4	12	8	76-22	12	100	25
267	----++++	900	2	Fine	0.8	4	16	76-22	12	100	25
268	+--++++	10000	2	Fine	0.8	4	16	76-22	12	100	25
269	--++-----	900	12	Fine	0.8	4	16	76-22	12	100	25
270	++-----	10000	12	Fine	0.8	4	16	76-22	12	100	25
271	---+-----	900	2	Coarse	0.8	4	16	76-22	12	100	25
272	+-----	10000	2	Coarse	0.8	4	16	76-22	12	100	25
273	---+-----	900	12	Coarse	0.8	4	16	76-22	12	100	25
274	++++-----	10000	12	Coarse	0.8	4	16	76-22	12	100	25

APPENDIX E DESIGN OF EXPERIMENT FOR MODEL CONSTRUCTION: RANDOM SELECTION

Run	AADTT	h_{ac}	Gradation	p38	p34	p4	p200	PG	Pb_{eff}	Va	VFA	h_{bs}	Mr_{bs}	Mrs_{ub}
1	1,750	9.00	Coarse	12	38	50	4	70-22	13.6	6.4	0.7	8	44,750	22,600
2	6,100	10.50	Regular	6	28	48.5	4.3	76-22	15.4	4.6	0.8	9.75	97,200	12,900
3	6,900	5.75	Regular	6	28	48.5	4.3	64-22	13.7	6.3	0.7	11.5	48,950	20,200
4	7,600	10.25	Coarse	12	38	50	4	64-22	11.9	8.1	0.6	8.75	92,850	24,150
5	4,900	2.25	Fine	0	18	47	4.5	76-22	8.1	11.9	0.4	7	45,650	22,250
6	7,350	4.25	Fine	0	18	47	4.5	76-22	13.6	6.4	0.7	9.5	79,150	21,000
7	8,150	5.25	Coarse	12	38	50	4	70-22	9.8	10.2	0.5	10.75	84,750	21,750
8	4,850	9.50	Regular	6	28	48.5	4.3	64-22	13.8	6.2	0.7	11.5	83,550	19,000
9	950	4.75	Regular	6	28	48.5	4.3	70-22	10.0	10.0	0.5	6.5	83,250	24,850
10	3,950	4.00	Coarse	12	38	50	4	64-22	13.0	7.0	0.7	11.25	90,700	22,900
11	5,200	9.75	Regular	6	28	48.5	4.3	70-22	8.7	11.3	0.4	8.75	42,050	17,800
12	7,350	5.00	Regular	6	28	48.5	4.3	70-22	11.1	8.9	0.6	7.5	76,650	13,000
13	8,950	8.50	Coarse	12	38	50	4	70-22	13.0	7.0	0.7	7.5	44,900	11,800
14	6,750	2.75	Fine	0	18	47	4.5	64-22	13.7	6.3	0.7	8.5	26,850	17,950
15	8,050	6.00	Coarse	12	38	50	4	76-22	8.3	11.7	0.4	9	43,600	11,600
16	3,150	10.50	Regular	6	28	48.5	4.3	70-22	11.2	8.8	0.6	8.5	75,050	23,200
17	2,400	10.75	Fine	0	18	47	4.5	70-22	14.8	5.2	0.7	6.75	21,750	6,350
18	8,000	4.00	Regular	6	28	48.5	4.3	76-22	14.9	5.1	0.7	7.5	92,600	13,900
19	4,300	7.50	Fine	0	18	47	4.5	64-22	14.6	5.4	0.7	7.75	81,400	12,100
20	3,000	4.50	Coarse	12	38	50	4	70-22	8.9	11.1	0.4	6.5	73,250	8,100
21	2,400	7.50	Regular	6	28	48.5	4.3	76-22	8.5	11.5	0.4	9.5	50,700	16,250
22	1,000	10.75	Regular	6	28	48.5	4.3	70-22	11.9	8.1	0.6	9.5	21,550	11,150
23	3,250	11.50	Coarse	12	38	50	4	70-22	8.5	11.5	0.4	7.5	92,750	8,850
24	4,300	8.00	Fine	0	18	47	4.5	70-22	10.2	9.8	0.5	8.25	79,400	14,150
25	4,550	3.75	Fine	0	18	47	4.5	70-22	9.0	11.0	0.4	6.5	74,750	10,650
26	8,400	7.75	Coarse	12	38	50	4	76-22	13.7	6.3	0.7	8.75	51,800	24,950

27	3,750	3.00	Fine	0	18	47	4.5	70-22	12.4	7.6	0.6	10.25	68,300	12,800
28	2,400	3.25	Regular	6	28	48.5	4.3	64-22	14.1	5.9	0.7	11	42,550	13,750
29	3,950	4.75	Coarse	12	38	50	4	76-22	13.2	6.8	0.7	10	67,300	17,350
30	4,850	7.75	Regular	6	28	48.5	4.3	70-22	15.6	4.4	0.8	6.25	83,600	24,700
31	8,000	11.25	Coarse	12	38	50	4	70-22	13.1	6.9	0.7	9.5	33,050	10,000
32	8,850	9.25	Coarse	12	38	50	4	64-22	15.2	4.8	0.8	7	51,850	22,300
33	8,300	5.00	Regular	6	28	48.5	4.3	70-22	10.4	9.6	0.5	9.75	64,050	23,600
34	5,200	9.25	Regular	6	28	48.5	4.3	70-22	11.1	8.9	0.6	11.5	85,050	14,450
35	7,100	10.25	Regular	6	28	48.5	4.3	70-22	8.4	11.6	0.4	11.25	92,400	16,400
36	8,250	3.00	Coarse	12	38	50	4	70-22	9.0	11.0	0.5	11.75	93,950	7,700
37	1,250	10.75	Regular	6	28	48.5	4.3	70-22	14.6	5.4	0.7	8.75	43,250	24,650
38	2,300	11.00	Regular	6	28	48.5	4.3	70-22	12.8	7.2	0.6	6.75	63,800	7,400
39	1,150	8.50	Regular	6	28	48.5	4.3	64-22	16.0	4.0	0.8	8.75	50,100	19,250
40	9,500	7.75	Regular	6	28	48.5	4.3	70-22	11.4	8.6	0.6	9.75	44,050	10,900
41	9,950	5.25	Coarse	12	38	50	4	76-22	9.6	10.4	0.5	11.25	65,850	22,900
42	6,750	5.75	Regular	6	28	48.5	4.3	70-22	14.7	5.3	0.7	7.75	25,350	21,800
43	4,100	5.25	Fine	0	18	47	4.5	70-22	9.1	10.9	0.5	8.75	53,450	14,900
44	7,950	10.25	Coarse	12	38	50	4	70-22	10.4	9.6	0.5	11.25	54,450	15,900
45	9,350	4.75	Regular	6	28	48.5	4.3	70-22	9.1	10.9	0.5	10.75	38,200	7,350
46	8,600	5.75	Regular	6	28	48.5	4.3	76-22	12.5	7.5	0.6	12	88,100	21,850
47	4,700	4.50	Fine	0	18	47	4.5	70-22	10.8	9.2	0.5	7	39,150	13,300
48	3,150	4.50	Coarse	12	38	50	4	76-22	10.1	9.9	0.5	7	22,750	5,600
49	8,300	10.00	Regular	6	28	48.5	4.3	70-22	10.8	9.2	0.5	7	50,300	14,150
50	1,950	7.75	Fine	0	18	47	4.5	70-22	11.7	8.3	0.6	8.25	66,700	5,550
51	3,700	8.00	Coarse	12	38	50	4	70-22	16.0	4.0	0.8	10.75	53,750	17,000
52	2,300	10.00	Regular	6	28	48.5	4.3	70-22	10.1	9.9	0.5	11.25	28,200	16,150
53	2,900	10.75	Coarse	12	38	50	4	70-22	13.0	7.0	0.6	6.25	31,400	7,100
54	3,300	6.75	Regular	6	28	48.5	4.3	64-22	11.6	8.4	0.6	7.25	98,450	15,000
55	3,400	6.75	Regular	6	28	48.5	4.3	70-22	10.1	9.9	0.5	6.75	90,950	24,600
56	5,550	3.50	Coarse	12	38	50	4	76-22	15.6	4.4	0.8	11.25	23,900	5,850

57	1,350	6.75	Fine	0	18	47	4.5	70-22	13.2	6.8	0.7	7	30,850	11,150
58	6,150	2.50	Coarse	12	38	50	4	64-22	11.7	8.3	0.6	8.5	43,500	21,950
59	7,800	5.50	Coarse	12	38	50	4	70-22	14.5	5.5	0.7	6.25	31,400	22,600
60	7,300	7.25	Fine	0	18	47	4.5	64-22	12.2	7.8	0.6	9.5	69,400	18,200
61	6,850	2.25	Fine	0	18	47	4.5	70-22	11.1	8.9	0.6	9	47,500	6,800
62	6,250	8.00	Regular	6	28	48.5	4.3	70-22	8.4	11.6	0.4	6.25	82,800	5,300
63	9,750	4.25	Coarse	12	38	50	4	70-22	10.4	9.6	0.5	7.75	84,400	8,950
64	950	8.50	Regular	6	28	48.5	4.3	76-22	15.9	4.1	0.8	8.25	42,450	19,450
65	8,500	4.50	Regular	6	28	48.5	4.3	64-22	9.8	10.2	0.5	8	75,050	20,550
66	3,900	6.75	Regular	6	28	48.5	4.3	76-22	12.9	7.1	0.6	6.75	71,800	20,750
67	7,500	3.75	Coarse	12	38	50	4	64-22	11.4	8.6	0.6	7.25	73,500	7,500
68	4,550	9.00	Fine	0	18	47	4.5	76-22	14.0	6.0	0.7	8	94,550	8,900
69	3,050	8.50	Fine	0	18	47	4.5	70-22	8.3	11.7	0.4	7	75,750	18,050
70	5,250	2.25	Fine	0	18	47	4.5	64-22	10.2	9.8	0.5	11.25	60,600	20,700
71	7,600	3.00	Fine	0	18	47	4.5	76-22	9.4	10.6	0.5	9.25	72,750	24,700
72	8,450	9.00	Coarse	12	38	50	4	64-22	14.8	5.2	0.7	6.5	29,700	8,300
73	2,500	8.75	Regular	6	28	48.5	4.3	70-22	12.6	7.4	0.6	8.75	66,150	23,350
74	8,650	2.00	Fine	0	18	47	4.5	76-22	9.6	10.4	0.5	9.25	56,100	19,000
75	1,850	7.25	Coarse	12	38	50	4	70-22	13.9	6.1	0.7	9.25	98,700	5,250
76	9,350	6.50	Regular	6	28	48.5	4.3	76-22	9.9	10.1	0.5	6.75	85,050	18,050
77	6,700	2.50	Fine	0	18	47	4.5	70-22	13.2	6.8	0.7	8.75	96,850	21,750
78	6,550	8.50	Fine	0	18	47	4.5	64-22	15.1	4.9	0.8	9	76,100	9,750
79	3,400	10.00	Regular	6	28	48.5	4.3	70-22	13.1	6.9	0.7	6	61,550	22,100
80	1,750	10.00	Regular	6	28	48.5	4.3	70-22	15.1	4.9	0.8	11.25	40,500	15,050
81	1,450	11.75	Fine	0	18	47	4.5	76-22	10.8	9.2	0.5	8.25	86,500	23,100
82	6,750	2.50	Regular	6	28	48.5	4.3	64-22	9.9	10.1	0.5	10	99,900	7,100
83	1,700	9.50	Fine	0	18	47	4.5	76-22	15.6	4.4	0.8	9	39,000	18,850
84	8,550	7.75	Coarse	12	38	50	4	70-22	10.3	9.7	0.5	10.75	60,350	14,650
85	3,050	6.75	Coarse	12	38	50	4	76-22	12.6	7.4	0.6	9.75	77,950	14,700
86	3,500	4.75	Regular	6	28	48.5	4.3	64-22	11.8	8.2	0.6	9.5	57,600	23,150

87	3,650	6.00	Regular	6	28	48.5	4.3	76-22	13.8	6.2	0.7	11.75	27,350	23,500
88	6,850	4.50	Coarse	12	38	50	4	70-22	15.0	5.0	0.7	6.5	83,800	10,400
89	5,050	4.75	Regular	6	28	48.5	4.3	64-22	14.7	5.3	0.7	7.75	33,650	15,400
90	6,800	9.25	Coarse	12	38	50	4	64-22	14.9	5.1	0.7	10.75	66,100	20,150
91	4,500	2.00	Regular	6	28	48.5	4.3	70-22	10.9	9.1	0.5	11	99,000	16,150
92	9,450	7.50	Coarse	12	38	50	4	70-22	14.4	5.6	0.7	9.25	71,950	6,700
93	9,850	4.50	Coarse	12	38	50	4	70-22	9.7	10.3	0.5	10.25	51,000	22,650
94	4,050	10.50	Coarse	12	38	50	4	70-22	9.3	10.7	0.5	11	77,600	17,600
95	8,000	6.50	Regular	6	28	48.5	4.3	76-22	13.8	6.2	0.7	10.5	92,200	6,800
96	3,600	9.25	Fine	0	18	47	4.5	76-22	12.3	7.7	0.6	6	30,700	11,350
97	8,000	11.00	Regular	6	28	48.5	4.3	64-22	11.7	8.3	0.6	6.75	54,300	8,100
98	5,550	7.25	Fine	0	18	47	4.5	64-22	11.8	8.2	0.6	10.5	95,550	5,700
99	2,000	5.75	Regular	6	28	48.5	4.3	70-22	10.2	9.8	0.5	11.5	89,250	23,600
100	2,800	7.25	Fine	0	18	47	4.5	70-22	8.1	11.9	0.4	8.75	99,000	12,300

APPENDIX F DESIGN OF EXPERIMENT FOR MODEL VALIDATION

Run	AADTT	h_{ac}	Gradation	p38	p34	p4	p200	PG	Pb_{eff}	Va	VFA	h_{bs}	Mr_{bs}	Mrs_{ub}
1	9,700	2.50	Fine	0	18	47	4.5	70-22	8.5	11.5	0.4	8	66,000	10,200
2	2,900	7.50	Regular	6	28	48.5	4.3	70-22	10.2	9.8	0.5	10.5	35,350	22,700
3	7,250	6.50	Fine	0	18	47	4.5	70-22	10.8	9.2	0.5	10.5	50,150	6,650
4	1,800	9.00	Fine	0	18	47	4.5	70-22	9.4	10.6	0.5	6.25	80,000	13,150
5	1,800	8.75	Coarse	12	38	50	4	64-22	13.2	6.8	0.7	12	49,900	22,400
6	5,000	3.25	Regular	6	28	48.5	4.3	76-22	11.8	8.2	0.6	9	72,350	19,000
7	7,100	4.50	Coarse	12	38	50	4	70-22	9.0	11.0	0.4	9.75	53,400	13,300
8	6,400	2.50	Coarse	12	38	50	4	70-22	12.6	7.4	0.6	8.25	95,750	6,150
9	2,000	8.25	Coarse	12	38	50	4	70-22	11.1	8.9	0.6	9.5	29,450	14,350
10	6,000	8.00	Regular	6	28	48.5	4.3	70-22	13.9	6.1	0.7	9.75	48,200	17,000
11	9,100	3.75	Regular	6	28	48.5	4.3	64-22	9.0	11.0	0.5	11.25	98,350	7,200
12	9,200	6.00	Coarse	12	38	50	4	70-22	14.7	5.3	0.7	8	57,350	13,750
13	8,850	3.75	Regular	6	28	48.5	4.3	76-22	11.5	8.5	0.6	10.25	64,750	16,800
14	1,500	3.75	Fine	0	18	47	4.5	76-22	15.3	4.7	0.8	10	93,900	8,100
15	4,150	5.25	Coarse	12	38	50	4	70-22	12.6	7.4	0.6	10	95,900	10,050
16	5,700	8.75	Regular	6	28	48.5	4.3	76-22	8.0	12.0	0.4	10.5	90,350	12,500
17	7,050	10.00	Regular	6	28	48.5	4.3	64-22	15.1	4.9	0.8	7.25	93,500	18,550
18	2,000	4.25	Regular	6	28	48.5	4.3	70-22	11.8	8.2	0.6	6.5	25,150	5,400
19	3,400	10.00	Coarse	12	38	50	4	64-22	10.0	10.0	0.5	11	51,250	10,150
20	1,750	11.00	Regular	6	28	48.5	4.3	70-22	10.6	9.4	0.5	10	24,200	15,450
21	1,500	9.00	Fine	0	18	47	4.5	70-22	15.2	4.8	0.8	7.75	46,000	19,800
22	9,600	3.25	Fine	0	18	47	4.5	70-22	10.6	9.4	0.5	10	52,850	8,250
23	9,650	9.75	Fine	0	18	47	4.5	64-22	13.3	6.7	0.7	10.75	73,650	25,000
24	7,600	7.25	Fine	0	18	47	4.5	70-22	10.6	9.4	0.5	9.25	23,550	23,000
25	8,000	8.25	Fine	0	18	47	4.5	70-22	14.9	5.1	0.7	6.25	60,550	24,400
26	9,600	5.00	Fine	0	18	47	4.5	76-22	14.8	5.2	0.7	8	44,200	15,750

27	2,450	9.00	Coarse	12	38	50	4	64-22	10.5	9.5	0.5	8.5	79,900	10,550
28	6,250	8.00	Regular	6	28	48.5	4.3	70-22	11.0	9.0	0.6	11.25	47,750	23,950
29	6,650	3.50	Regular	6	28	48.5	4.3	76-22	14.1	5.9	0.7	11.25	79,750	24,550
30	6,000	4.25	Regular	6	28	48.5	4.3	76-22	15.6	4.4	0.8	11.75	68,050	23,100
31	6,050	4.75	Regular	6	28	48.5	4.3	76-22	15.5	4.5	0.8	11.75	83,750	12,400
32	2,750	9.00	Fine	0	18	47	4.5	70-22	13.7	6.3	0.7	6.25	94,600	5,600
33	3,900	5.75	Regular	6	28	48.5	4.3	76-22	15.2	4.8	0.8	7.25	74,900	17,600
34	9,800	2.50	Fine	0	18	47	4.5	70-22	13.9	6.1	0.7	7.5	65,050	19,200
35	2,850	12.00	Regular	6	28	48.5	4.3	76-22	10.9	9.1	0.5	10	24,650	18,200
36	6,750	3.50	Fine	0	18	47	4.5	70-22	11.9	8.1	0.6	7	25,550	7,350
37	2,700	3.00	Coarse	12	38	50	4	70-22	14.7	5.3	0.7	9.5	73,600	10,150
38	7,950	10.75	Regular	6	28	48.5	4.3	64-22	14.2	5.8	0.7	12	67,500	8,750
39	6,600	6.25	Fine	0	18	47	4.5	70-22	10.6	9.4	0.5	8.25	50,300	13,800
40	6,350	7.75	Coarse	12	38	50	4	70-22	15.1	4.9	0.8	11.25	67,800	21,800
41	9,200	10.75	Regular	6	28	48.5	4.3	64-22	10.1	9.9	0.5	8	25,000	14,700
42	3,300	6.25	Coarse	12	38	50	4	70-22	15.0	5.0	0.8	6.25	88,050	13,550
43	5,350	9.00	Fine	0	18	47	4.5	76-22	10.0	10.0	0.5	6.75	88,500	18,850
44	8,000	3.25	Regular	6	28	48.5	4.3	64-22	10.4	9.6	0.5	8.25	92,800	12,200
45	1,750	5.75	Regular	6	28	48.5	4.3	76-22	14.6	5.4	0.7	9.75	59,350	14,300
46	7,100	6.50	Regular	6	28	48.5	4.3	64-22	8.0	12.0	0.4	11	38,600	15,000
47	1,850	8.50	Regular	6	28	48.5	4.3	70-22	11.7	8.3	0.6	12	92,450	14,200
48	3,150	7.25	Fine	0	18	47	4.5	76-22	11.3	8.7	0.6	9	86,350	17,550
49	5,200	10.75	Fine	0	18	47	4.5	64-22	9.3	10.7	0.5	7.75	36,350	6,900
50	8,100	3.75	Fine	0	18	47	4.5	70-22	12.9	7.1	0.6	11.25	33,150	13,850
51	9,250	2.50	Fine	0	18	47	4.5	70-22	13.7	6.3	0.7	6.5	41,050	17,000
52	9,750	7.25	Regular	6	28	48.5	4.3	64-22	14.4	5.6	0.7	8.25	71,800	11,500
53	7,100	3.00	Regular	6	28	48.5	4.3	64-22	15.9	4.1	0.8	10.75	59,350	18,150
54	2,300	2.75	Regular	6	28	48.5	4.3	70-22	9.1	10.9	0.5	10	60,100	8,000
55	7,850	10.75	Regular	6	28	48.5	4.3	76-22	10.4	9.6	0.5	10	78,500	8,500
56	3,700	3.00	Regular	6	28	48.5	4.3	70-22	10.0	10.0	0.5	10.5	89,700	8,950

57	8,350	2.75	Coarse	12	38	50	4	64-22	10.2	9.8	0.5	11.75	93,550	18,200
58	6,950	6.50	Regular	6	28	48.5	4.3	64-22	11.4	8.6	0.6	9.75	22,050	21,800
59	9,550	3.00	Regular	6	28	48.5	4.3	70-22	11.2	8.8	0.6	8	26,200	8,750
60	3,100	3.25	Regular	6	28	48.5	4.3	76-22	10.4	9.6	0.5	7.75	49,700	17,000
61	6,350	2.25	Regular	6	28	48.5	4.3	70-22	13.8	6.2	0.7	10	77,500	9,700
62	1,200	6.25	Fine	0	18	47	4.5	64-22	14.9	5.1	0.7	11.75	78,950	16,500
63	8,250	8.00	Fine	0	18	47	4.5	76-22	15.5	4.5	0.8	7	81,300	6,800
64	8,950	11.25	Fine	0	18	47	4.5	70-22	8.4	11.6	0.4	10.25	25,450	20,400
65	2,100	3.75	Coarse	12	38	50	4	70-22	10.9	9.1	0.5	7.75	85,700	12,650
66	4,100	9.75	Fine	0	18	47	4.5	70-22	8.7	11.3	0.4	9.5	36,050	23,150
67	1,050	9.00	Regular	6	28	48.5	4.3	70-22	14.3	5.7	0.7	9.75	40,150	19,900
68	6,500	5.50	Fine	0	18	47	4.5	70-22	10.2	9.8	0.5	10.75	69,000	6,400
69	5,250	10.25	Regular	6	28	48.5	4.3	76-22	14.2	5.8	0.7	8.25	25,800	14,050
70	6,550	10.25	Regular	6	28	48.5	4.3	64-22	15.6	4.4	0.8	11.25	22,350	5,950
71	7,250	10.00	Regular	6	28	48.5	4.3	64-22	8.7	11.3	0.4	7	25,750	17,200
72	3,250	5.00	Coarse	12	38	50	4	70-22	9.5	10.5	0.5	7.25	50,250	8,500
73	5,000	6.50	Fine	0	18	47	4.5	70-22	8.2	11.8	0.4	10.75	81,150	10,650
74	7,850	9.75	Regular	6	28	48.5	4.3	70-22	10.3	9.7	0.5	10.75	26,000	12,100
75	1,650	4.50	Coarse	12	38	50	4	70-22	11.2	8.8	0.6	11	25,750	13,150
76	1,200	7.75	Fine	0	18	47	4.5	76-22	14.5	5.5	0.7	6.5	90,800	8,600
77	4,200	8.25	Regular	6	28	48.5	4.3	76-22	14.9	5.1	0.7	6.5	76,500	7,000
78	9,300	4.50	Fine	0	18	47	4.5	70-22	10.2	9.8	0.5	9.25	34,100	19,300
79	7,800	2.00	Fine	0	18	47	4.5	70-22	11.0	9.0	0.5	7	45,300	21,950
80	5,350	2.75	Regular	6	28	48.5	4.3	76-22	14.3	5.7	0.7	11.25	85,750	8,350
81	4,450	3.00	Regular	6	28	48.5	4.3	70-22	15.1	4.9	0.8	7	93,700	15,450
82	1,100	4.50	Fine	0	18	47	4.5	70-22	8.9	11.1	0.4	11	65,850	21,550
83	7,400	3.00	Regular	6	28	48.5	4.3	76-22	13.4	6.6	0.7	6.25	32,900	24,700
84	9,150	8.00	Fine	0	18	47	4.5	70-22	14.4	5.6	0.7	7	98,400	10,600
85	8,550	8.00	Coarse	12	38	50	4	64-22	12.3	7.7	0.6	10.5	73,850	23,850
86	3,500	11.25	Fine	0	18	47	4.5	70-22	13.9	6.1	0.7	11.25	64,650	7,450

87	1,100	8.25	Regular	6	28	48.5	4.3	70-22	10.8	9.2	0.5	6.25	27,750	13,200
88	7,700	8.25	Regular	6	28	48.5	4.3	70-22	12.3	7.7	0.6	6.75	50,050	23,250
89	1,450	4.75	Coarse	12	38	50	4	70-22	14.2	5.8	0.7	8.25	74,350	10,800
90	2,150	8.00	Coarse	12	38	50	4	70-22	11.6	8.4	0.6	6	30,950	21,850
91	4,000	10.50	Regular	6	28	48.5	4.3	70-22	14.8	5.2	0.7	10	77,850	17,200
92	9,150	10.00	Regular	6	28	48.5	4.3	70-22	13.9	6.1	0.7	11.25	35,600	19,700
93	2,850	2.25	Regular	6	28	48.5	4.3	70-22	12.3	7.7	0.6	11.5	35,300	12,500
94	8,600	9.75	Fine	0	18	47	4.5	70-22	10.3	9.7	0.5	7.75	50,450	24,900
95	4,750	3.50	Coarse	12	38	50	4	76-22	10.0	10.0	0.5	10.75	29,650	20,900
96	2,100	6.50	Coarse	12	38	50	4	70-22	10.8	9.2	0.5	10.25	50,950	14,800
97	6,050	8.00	Coarse	12	38	50	4	70-22	13.9	6.1	0.7	8.5	49,150	15,300
98	9,650	9.50	Coarse	12	38	50	4	64-22	13.7	6.3	0.7	8	100,000	9,600
99	7,050	11.75	Fine	0	18	47	4.5	64-22	11.2	8.8	0.6	12	82,700	12,550
100	2,400	5.50	Regular	6	28	48.5	4.3	70-22	8.2	11.8	0.4	8.75	32,100	22,100

VITAE

Xingqiang “Danny” XIAO (pronounced as Shing-Chung Shaw) was born in Mianyang, Sichuan Province, China on May 18, 1982. He studied Highway and Transportation Engineering in Southwest Petroleum University, and Highway and Railway Engineering in Southwest Jiaotong University. During his internship at the Department of Transportation of Sichuan Province in 2005, he conducted a network- level (1,100 miles) pavement condition evaluation of all major highways in Sichuan Province. He came to the University of Arkansas in August 2007 and started research on the Mechanistic Empirical Pavement Design Guide (MEPDG). During his time in Arkansas, he has worked on several projects including local calibration of MEPDG, pavement evaluation using Ground Penetrating Radar, automatic distress evaluation, long term pavement performance monitoring, traffic data analysis and pavement management. When interned at the Arkansas State Highway and Transportation Department in 2012, his primary task was to implement the MEPDG in Arkansas. His research is presented in seven journal articles and 13 conference publications. In his spare time, he likes to stay with his family and friends, running, hiking and playing guitar.